ATMOSPHERIC FACTORS AFFECTING THE CORROSION OF ENGINEERING METALS

S. K. Coburn, *editor*

STP 646

AMERICAN SOCIETY FOR TESTING AND MATERIALS

ATMOSPHERIC FACTORS AFFECTING THE CORROSION OF ENGINEERING METALS

Proceedings of the
Golden Anniversary Symposium
Commemorating 50 Years'
Atmospheric Exposure Testing

A symposium sponsored by
Committee A-5 on
Metallic-Coated Iron and Steel Products
and Committee G-1 on
Corrosion of Metals
AMERICAN SOCIETY FOR TESTING
AND MATERIALS
Pennsylvania State University
State College, Pa., 18–19 May 1976

ASTM SPECIAL TECHNICAL PUBLICATION 646
S. K. Coburn, editor
United States Steel Corporation

04-646000-27

AMERICAN SOCIETY FOR TESTING AND MATERIALS
1916 Race Street, Philadelphia, Pa. 19103

Library of Congress Catalog Card Number: 77-93113
ISBN 0-8031-0286-0

Printed in Baltimore, Md.
June 1978
Second Printing, Mars, Pa.
March 1985

Dedication

Vincent Paul Pearson
12 April 1916 to 15 October 1977

This volume, recording the activities of the Golden Anniversary Symposium, and serving as a permanent record of contributions to the field of atmospheric corrosion, is hereby dedicated as a living memorial to our professional colleague and close personal friend—Vincent Paul Pearson, Senior Research Engineer, Research Department, Inland Steel Company, East Chicago, Indiana, who passed away on 15 October 1977, at the age of 61 years.

Vince was born in Chicago, Illinois, and attended its public schools and the University of Illinois. He completed the requirements for the B.S. degree at Roosevelt University in 1940. He began his career in the Research Laboratory of the Inland Steel Company in 1940 in the field of steel pickling inhibitors. He spent the period 1942 to 1945, during World War II, in the United States Army Armored Artillery where he achieved the rank of Colonel.

Upon his return to Inland Steel, he became engaged in corrosion activities beginning in 1948 and continuing to 1968. He had responsibilities in the area of corrosion control. During this period, he was granted three patents in the field of tinplating. Beginning in 1968, he supervised programs in atmospheric corrosion and accelerated testing in the field of metallic-coated sheets.

Vince was a resident of Chesterton, Indiana for 30 years. He was married to Clare Breckenridge on 15 April 1939, and leaves a married son, John, and married daughters, Ann Donahue and Dottie Johnson, and a mother, Dagmar Johansen, a sister, Mrs. Samuel Bond, and five grandchildren. He was a precinct committeeman, served on the Board of Zoning Appeals for many years, and was a Cub Master.

Vince came into ASTM activity when the giants of another era were completing their work. He learned well and soon picked up the reigns of Subcommittee XIV on Sheet Tests. When Committee G-1 was activated, it was Vince who was called upon to coordinate the effort to gain membership. His organizing ability, his enthusiasm, and thoroughness in these tasks made him a giant of sorts in his own right. He left us with several viable committee structures in which we and future members can function effectively. Vince prepared the tabulation forms for the annual sheet inspection of A05.15 and G01.4.2. He prepared all subcommittee and section reports. He photographed all specimens and presented thoroughly documented photographic reports at the annual meetings which will serve as a model of effectiveness. He conducted the 50th Annual Inspection by rededicating the State College rural test site in a ribbon-cutting ceremony. Vince was equally active in atmospheric corrosion affairs in the National Association of Corrosion Engineers where he was the chairman of the newly formed Unit Committee on Atmospheric Corrosion. He became a corrosion specialist in 1971.

It can truly be said of Vincent Paul Pearson—who faithfully served his country, was a successful investigative corrosion engineer, inventor, author, organizer, parent, loving husband, and a dedicated citizen—that he was man for all seasons.

Foreword

This publication contains papers presented at the Golden Anniversary Symposium Commemorating 50 Years' Atmospheric Exposure Testing at the State College Rural Test Site held at Pennsylvania State University, State College, Pa., 18-19 May 1976. The symposium was sponsored by the American Society for Testing and Materials Committees A-5 on Metallic-Coated Iron and Steel Products and G-1 on Corrosion of Metals. D. C. Pearce, American Smelting and Refining Company, and S. K. Coburn, United States Steel Corporation, presided as symposium co-chairmen. Mr. Coburn is editor of this publication.

Related ASTM Publications

Galvanic and Pitting Corrosion—Field and Laboratory Studies, STP 576 (1976),04-576000-27

Stress Corrosion—New Approaches, STP 610 (1976), 04-610000-27

Chloride Corrosion of Steel in Concrete, STP 629 (1977), 04-629000-27

A Note of Appreciation to Reviewers

This publication is made possible by the authors and, also, the unheralded efforts of the reviewers. This body of technical experts whose dedication, sacrifice of time and effort, and collective wisdom in reviewing the papers must be acknowledged. The quality level of ASTM publications is a direct function of their respected opinions. On behalf of ASTM we acknowledge with appreciation their contribution.

ASTM Committee on Publications

Editorial Staff

Contents

Introduction

In the February 1958 issue of the ASTM Bulletin, H. F. Hormann, Chairman of Committee A-5 on Corrosion of Iron and Steel, authored a brief history covering its first 50 years' activity. On 18–19 May 1976, the 50th annual spring inspection at the State College, Pennsylvania, Rural Exposure Test Site, was performed by the members of Subcommittees XIV, XV, and XVI on Sheets, Wire, and Hardware, respectively. To mark the occasion, a Golden Anniversary Symposium on Atmospheric Corrosion was held simultaneously at the Keller Conference Center on the campus of the Pennsylvania State University at University Park, Pennsylvania, in conjunction with the more recently formed Committee G-1 on Corrosion of Metals, under whose jurisdiction all future atmospheric exposure tests for ASTM are being conducted.

To properly appreciate the significance of this event one must note that during the Ninth Annual ASTM meeting held in June 1906, Edgar Marburg, Secretary-Treasurer, after listening to all the heat generated by the papers and the discussion on the corrosion of iron and steel, made the following motion: "In view of the importance of this subject and the lack of knowledge concerning the same, it would seem to be eminently proper for the Society to appoint a standing committee on the general subject of the corrosion of iron and steel." The motion carried and it was announced at the 1907 Annual Meeting that Committee U on the Corrosion of Iron and Steel had been formed. In 1910 the designation was changed to Committee A-5.

One can appreciate that wrought iron, being the oldest form of commercial ferrous material, held a tactical advantage over the comparative newcomer—steel—because of the inconsistent performance of some of the available compositions. Today wrought iron is no longer produced. Differences of opinion concerning the variation in corrosion rates of iron and steel not only caused heated debates during this period, but led to the starting of several lawsuits. Obviously, comparative exposure data were lacking and the effects of differences in the environment were not generally recognized as influencing performance.

Among reasons offered for these inconsistencies in performance were too high manganese, too low phosphorus, protection offered by slag, electrolysis due to sulfurous acid in the air, and failure to carry tests through to destruction. Because of the sulfurous atmospheres, the committee believed that immersion of specimens in 20 percent sulfuric acid would provide performance differences which were sufficient to furnish a basis for concluding that metal manufactured by one process was superior to that manufactured by another. The results, however, indicated that such differences did not furnish a basis for discrimination between products.

The early work of the committee thus was devoted to conducting field tests to fulfill the need for generating comparative performance data for different materials under identical conditions of exposure. The first test was put out in 1908, and dealt with segregation within the ingot, as well as the influence of concentration levels of carbon and manganese. Billets were taken from the top, middle, and bottom of selected ingots, and rods and wire were drawn, galvanized, woven into fence, and exposed around the campus of the old Carnegie Institute of Technology (now Carnegie-Mellon University) in Pittsburgh, Pennsylvania.

In 1910, work commenced on the evaluation of the Preece Test using a solution of copper sulphate as a means for determining the zinc coating weight on sheets and wire. It was not until 1915 that work was initiated to investigate the corrosion rates of iron and steel as influenced by different levels of copper. Between 1916 and 1917 specimens were exposed at the Naval Academy at Annapolis, Maryland, at the military installations at Fort Pitt in Pittsburgh, Pennsylvania, and at Fort Sheridan, Illinois. The tests were terminated in 1923 at Pittsburgh, in 1928 at Fort Sheridan, and in 1954 at Annapolis because of the need for the property in these respective locations.

In 1924, Committee A-5 decided to begin a new series of tests involving the atmospheric exposure of bare and galvanized steel sheets and wire of the same steel with different coating weights, and pole line hardware with a variety of coatings. The sheet tests commenced at State College, Altoona, and Brunot Island in Pittsburgh, Pennsylvania, in the fall of 1925, and at Key West, Florida and Sandy Hook, New Jersey, in the winter of 1926. The first inspection at State College was performed in the spring of 1926. The time to the first appearance of rust was used to evaluate the galvanized steel sheets while the time to perforation was the criterion for judging the resistance of the uncoated steel sheets. The coated hardware specimens were placed in test in 1929, and the coated wire tests were underway by 1936.

Despite the massive increase in population and industrial growth in isolated centers throughout the country since 1926, the self-purifying ability of the atmosphere permitted the State College site to retain its rural aspect. Although all of the specimens at nearby industrial Altoona have deteriorated, the slow deterioration rate of specimens at State College permitted the discrimination necessary to fulfill the purposes of Edgar Marburg's motion in 1906.

As a result of the installation of high-speed, continuous galvanizing lines in the 1950s, a critical need developed for information concerning the relative performance of this new product as it related to the known performance of the earlier product obtained from the galvanizing pot in the hot dip process. Accordingly, Subcommittee XIV on Sheet Tests secured representative specimens from several producers of the continuous galvanized product. Similar specimens, in the same range of coating weights of zinc, were obtained from producers supplying material from the same equipment used to produce the hot-dip galvanized specimens exposed in the initial test of 1926. The new test commenced in 1960, and annual inspection reports have been filed together with the reports of the remaining 1926 test at State College. The results of these two long term investigations can be obtained by an inspection of the reports of Committee A-5 in the yearly *Proceedings* of ASTM.

For many years there had been a growing interest in ASTM for the formation of a committee devoted exclusively to the corrosion of metals. During the existence of ASTM, Committee A-5 increasingly concentrated its efforts towards specifications for coated steel products; in 1967 its title and scope changed to Metallic Coated Iron and Steel to properly reflect this activity. Likewise, Committee B-3 on Corrosion of Nonferrous Metals and Alloys was limited in its scope in dealing with the corrosion of other metals. The earliest discussions towards this end, however, began in 1941. By 1963, recommendations were made by an ad hoc committee headed by K. G. Compton to dissolve Committee B-3 and create a committee whose scope was expanded as follows: "The promotion and stimulation of research, the collection of engineering data, and the development of methods of tests and nomenclature relating to corrosion of metals." This recommendation was accepted by the Board of Directors of the Society on 21 January 1964. Thus, a new entity, entitled Committee G-1 on Corrosion of Metals, came on the scene with its first chairman, F. L. LaQue. At the same time the name of the Advisory Committee on Corrosion was changed to the more precise Advisory Committee on Exposure Test Facilities.

On 9 February 1965, with the writer as chairman, Subcommittee IV of G-1 on Atmospheric Corrosion held its initial meeting. By 1966, Subcommittee IV defined four areas of responsibility: Section 1 on Weather, Section 2 on Metal Coatings on Steel, Section 3 on Ferrous Metals and Alloys, and Section 4 on Nonferrous Metals. It was agreed that no new tests would be initiated by Subcommittees XIV, XV, and XVI of the newly termed Committee A-5, and that Committee A-5 members would hold dual membership in Committees A-5 and G-1 so as to continue existing field testing programs. Accordingly, the completion of the worldwide calibration tests in 44 locations, initiated in Committee A-5 were reported in Committee G-1.

In 1967, Committee G-1 conducted a symposium entitled Metal Corrosion in the Atmosphere. The papers, including the aforementioned calibration test data, were published in STP 435, by the same title, emphasizing the testing aspects of corrosion technology. In 1956, Committee A-5 cooperated with the American Welding Society in the inspection aspects of the elaborate exposure tests they established utilizing thermally sprayed steel panels.

The study was designed to evaluate the protection afforded by sealed and unsealed panels of sprayed zinc and aluminum exposed in various industrial, rural and marine ASTM test sites.

In 1968, another test was begun with galvanized steel sheets to compare the performance of products whose coating thickness was controlled either by exit rolls or by an air knife.

This Golden Anniversary Symposium marks the completion of the hopes of those members who, in 1941, believed there should be a committee devoted to all of the common construction metals. You will note herein that there are several papers devoted to each of the metals: steel, zinc, aluminum, and copper, and that the testing aspect has been duly recognized.

S. K. Coburn

Corrosion engineer, Special Technical Service, Metallurgy, United States Steel Corporation, Pittsburgh, Pa.; symposium chairman and editor.

P. R. Grossman[1]

Investigation of Atmospheric Exposure Factors that Determine Time-of-Wetness of Outdoor Structures*

REFERENCE: Grossman, P. R., "**Investigation of Atmospheric Exposure Factors that Determine Time-of-Wetness of Outdoor Structures,**" *Atmospheric Factors Affecting the Corrosion of Engineering Metals, ASTM STP 646,* S. K. Coburn, Ed., American Society for Testing and Materials, 1978, pp. 5-16.

ABSTRACT: Wetness of outdoor structures is caused partly by condensation of water from the atmosphere, which we recognize as dew. Rain is the source of part of the wetness. The condensation process means that heat must be removed from air at the surface where condensation occurs. This heat exchange process by radiation from the exposed surface to the cold sky is examined in detail. Temperature differences between an insulated black surface, facing skyward, and ambient air conditions were observed to be as high as 8°C (15° F). Effects of wind velocity, orientation, and surface characteristics are given. Time-of-wetness measurements for test panels exposed at Miami, Florida are reported, including the "black box" exposure method used for coated panels. Comparisons of time-of-wetness investigations reported by Guttman and Sereda are given.

KEY WORDS: atmospheric corrosion, environments, test panels, corrosion rates, panel radiation, sky radiation

Outdoor test sites for observing the performance of materials all have a common problem of defining the characteristics of the environment at that particular location. There are many factors involved, including moisture levels, duration of the moisture condition, air pollution, temperatures, and surface characteristics. Organic materials have additional factors inherent in sunlight degradation processes. We now use computers to segregate the most important and pertinent information, so that useful development

---

*Original experimental data were measured in U.S. customary units.

[1] Vice president, Q-Panel Co., Cleveland, Ohio 44135.

work can proceed and materials can be developed to achieve a greater resistance to the deteriorating forces of weather.

Even when the magnitude of the problem is reduced to a study of the deteriorating forces of wetness, as is done in the field of corrosion, there are still many variables involved with many complex interactions. We get around the problem by measuring the degradation process, such as corrosion, at a Site A, such as Penn State, and then expose the same material at a Site B, such as at Kearney, N.J., the result being a relative degradation at the two sites. Large amounts of data are collected, and one can go a long way in explaining just why Site B is more aggressive than Site A. However, there remains a continuing need to better define the factors which contribute to the observed corrosion or deterioration at a given location.

A new measuring tool came on the scene some twelve years ago, and it was called a time-of-wetness meter, a device which measured just how much of the time a test panel is wet. Technical activity was conducted by people working together in ASTM, and results of measurements made and correlation with corrosion of metals in the atmosphere were reported [*1*].[2] The initial work came out of the National Research Council of Canada, and P. J. Sereda was a leader and a prolific writer in this work [*1-4*].

For background information, we should first review just what is a time-of-wetness meter. Fig. 1 shows the principles involved. A zinc plate has a platinum electrode glued to its face, with platinum spaced about 0.1 mm (4/1000 in.) from the zinc with an insulating adhesive. Electrical leads are attached to the two dissimilar metals. When wetness bridges the space between the two metals, we have a battery that generates about 1 V. When the voltage goes over 0.2 V, a running time meter is activated to record wetness time. The platinum zinc interface is 53 cm (21 in.) in length, and the electrical circuitry is such that 1/50 of a μA is the current flow once the wetness time interval has started.

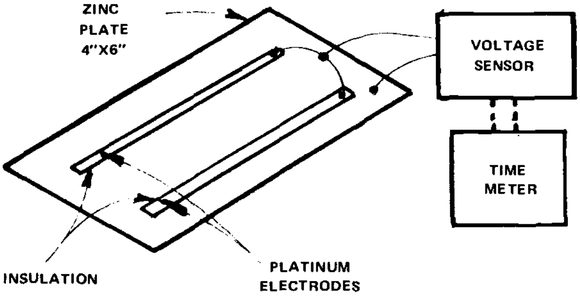

FIG. 1—*The time-of-wetness meter.*

---

[2] The italic numbers in brackets refer to the list of references appended to this paper.

It is important to note that this is a new and different method for measuring wetness. Other wetness detectors are in use which have a wick measuring electrical conductivity changes in response to relative humidity changes in the air. The zinc-platinum battery device tells us that there is an electrolyte present at the interface of the two metals. The electrolyte comes from the transformation of water vapor in the atmosphere to liquid water phase on the surface. Although relative humidity is a very significant parameter in the process of changing the innocuous water vapor content of the air to the aggressive liquid phase water, it is most important to recognize that heat exchange must take place to change water vapor to water liquid. The latent heat of vaporization must be extracted by some cooling force in order to condense water out of the air.

To demonstrate this point, high relative humidity without heat flow can be compared to the same humidity with heat flow in a condensing type of humidity cabinet, as illustrated in Fig. 2. A steel panel, hung inside the chamber and positioned so that no heat transfer occurs, will collect rust very slowly, and sometimes not at all. Another panel, positioned on the walls of the heated test chamber, has humidity, as well as heat flow and condensation progresses; here the corrosion processes of liquid water proceed and rust is quickly apparent.

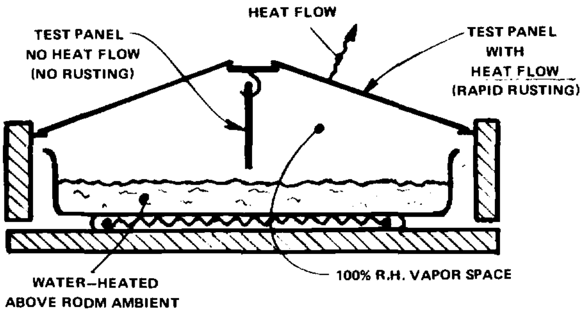

FIG. 2—*Demonstrating humidity with heat flow.*

For more background on the time-of-wetness meter, we should observe some of its characteristics. Guttman [*1*] reported on wetness time of a metal panel at Birchbank, British Columbia, shown in Fig. 3. It can be seen that wetness time there ranges between 10 and 60 percent of the time. There was a period of time of more than four months when wetness was over 50 percent. The groundward side of the panel was always wet for more time than the skyward side.

It was also necessary to review the study of atmospheric conditions observed at the start of the wetness period reported by Sereda [*2*]. Relative humidity was recorded at the initiation of wetness, as shown in Fig. 4.

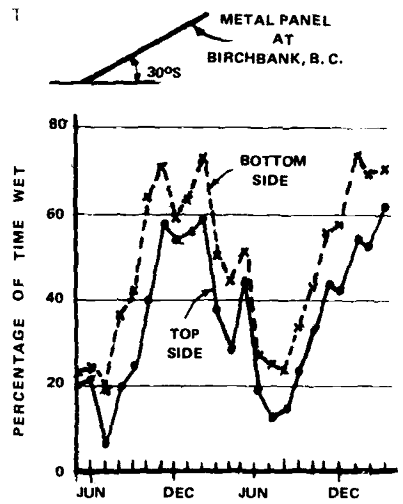

FIG. 3 —*Monthly wetness time.*

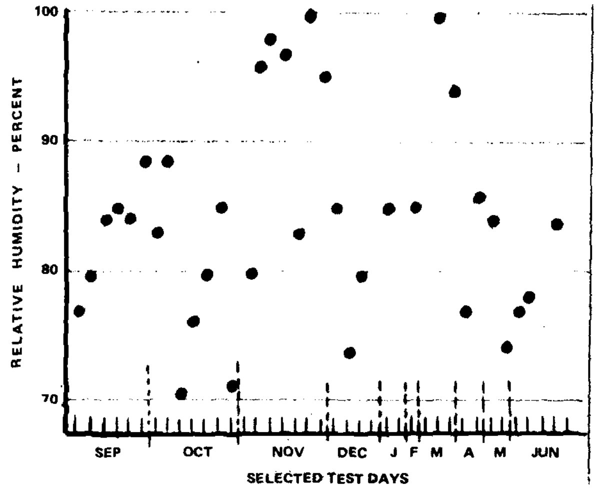

FIG. 4—*Relative humidity at start of wetness.*

Although relative humidity was always over 70 percent when wetness began, it is apparent that relative humidity alone is not a good indicator of the wetness condition.

With this background in hand, we can now proceed with our study of just how and why these conditions are occurring. The cooling force that causes condensation to occur outdoors is the "cold sky," and it is necessary to make some observations on just how this cooling force operates. Surfaces located outdoors at night radiate heat to the cold sky and become colder than ambient air. At the surface there is a film of air that can and often does cool down to dew point, at which time the continuing heat exchange process starts to condense water on the surface. Moisture can be present as invisible droplets, as surface films, as wetness of oxide surfaces, or as wetness of particular matter on the surface. A prolonged period of heat exchange is required to produce the dew that we actually see on the surface.

To demonstrate the cooling force of the cold sky, a test panel was constructed as shown in Fig. 5. The thermometer located under the panel measured the approximate panel temperature. A second thermometer placed just under the insulated box measured the ambient temperature. Temperature differences between the panel and ambient were measured outdoors, away from any radiation barriers such as trees, during the night period.

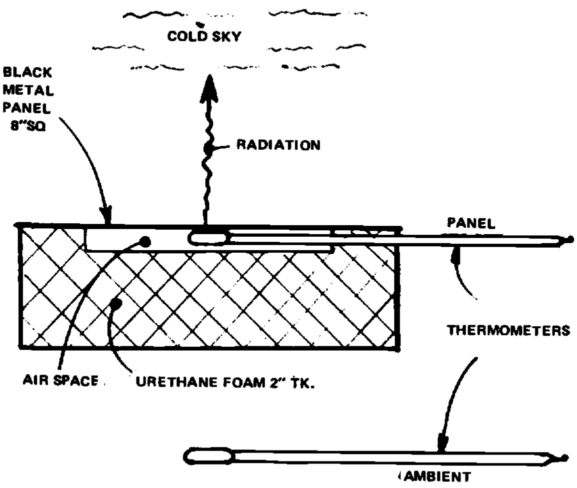

FIG. 5—*Measuring cold sky radiation (1 in. = 25.4 mm).*

Maximum temperature difference observed on a horizontal panel was 8°C (16°F) with a clear, cloudless sky and no wind. Some particular type of temperature gradient between the ground and the sky must have existed, but there was no way to measure this. The presence of wind or a cloud cover reduces the temperature differential. Sometimes a low temperature differential exists, with no apparent reason. Often, when there is no wind, the black panel will range 2 to 6°C (5 to 10°F) below ambient as early as twilight, when there is still sufficient light in the sky to read the thermometers. In a vertical position, the panel will "see" only half of the hemispherical enclosure of cold sky, so it will not be as cold as a flat panel facing upward. Turning the panel face downward eliminates the sky as a heat sink for cooling by radiation, and the panel will measure ambient temperature.

A bare flat panel exposed outdoors undergoes convection heat exchange with the air on the bottom side, and convection heat gain plus radiation heat loss to the cold sky on the top side. The metal panel strikes an average between the heat exchange forces acting on the two sides, so it will be warmer and less capable of taking heat out of the air to promote condensation than an insulated backed panel.

In order to examine the process of dew formation, we must consider the psychrometric properties of the air, as shown in Table 1. For example, if the panel-to-ambient differential is 5.4°C (10°F), whenever the relative humidity is above 70 percent condensation of water vapor will be occurring on the surface. Temperature differences for other relative humidities are shown.

TABLE 1—*Dew formation conditions.*

Relative Humidity (percent) (50°F air)	Temperature Difference to Cause Condensation, °F (°C)
100	0
90	2.7 (1.6)
80	5.9 (3.9)
70	9.5 (5.4)
60	13.5 (7.4)

The effect of the wind can be established from heat transfer considerations, as shown in Table 2. The surface-to-air heat transfer film coefficient is well known [5]. The table shows that if we have a still air condition of 5°C (9°F) ambient-to-panel differential, condensation can occur at 70 percent relative humidity. With an 8-km/h (5-mph) wind, the heat transfer between the panel and the air is increased, and the panel-to-ambient differential drops to 2.5°C (4.5°F); now condensation will not start until the relative humidity exceeds 85 percent.

TABLE 2—*Effect of wind velocity on condensation.*

Wind velocity, mph	0	5	10
Heat transfer film coefficient	1.6	3.2	6.0
Surface-to-air temperature differential, °F (°C)	9.0 (5)	4.5 (2.5)	2.4 (1.3)
Relative humidity where condensation begins	70%	85%	92%

NOTE—10 mph ~ 16 km/h.

The radiant emissivity of the panel was studied. A shiny (low emissivity) panel takes longer to cool down to the dew point of the air. Therefore, time-of-wetness for a shiny panel is less than that for a black panel. However, it should be noted that a shiny panel often collects particulate matter, or has corrosion products, so the emissivity may change with time.

The daily temperature cycle of the panel can be observed. There is a crossover point in the evening before sundown when the panel starts to be cooler than the air. This is the point where wetness potential begins. If relative humidity approaches 100 percent, wetness can actually start at that time. Usually the cooling conditions of the night hours will cause the panel temperature to drop slowly; wetness starts later in the evening, depending on the dew point of the air at the panel surface. The temperature of the wetness period is fairly close to the minimum temperature of the day.

All of the conditions described so far apply to clean surfaces, a condition found rarely outdoors. Frequently there is particulate matter on the surface. The particulates sometimes have desiccant properties which draw water out of the air, causing wetness to occur before the air reaches dew point. Corrosion products on the surface may also have desiccant properties. Clean metal surfaces or surfaces covered with nonhydroscopic corrosion products will be dry at a given relative humidity, whereas metals covered with hydroscopic corrosion products will be wet [*6*].

When we reflect upon all of the factors that determine when wetness begins, we can readily conclude that it is actually very difficult to predict from observation and measurements of the weather just when wetness begins. One should really make a direct measurement of this condition, and that is what the time-of-wetness meter attempts to do. In other words, the time-of-wetness meter is a device that pulls together the complex environmental factors involved and provides a very useful measurement for outdoor exposure testing.

Tests conducted at one of the environmental exposure sites in Miami, Florida illustrate this point. Coatings research has gravitated to Florida because it gives a more rapid response for sunlight and wetness deteriorating forces. Automotive coatings must be tested in Florida as they have improved to the point where it takes just so long to test them that methods are employed to accelerate degradation at the test site. One of these is the black box exposure method, whereby test panels get hotter than ambient conditions during sunlight conditions, as do some parts of an automobile. The degradation forces of sunlight are increased with higher temperature. Black box exposure testing produces the same results in something less than two thirds of the time. Users of this method may not be aware that the black box also changes the time-of-wetness of panels at night. The observed acceleration of degradation processes for coatings could be due to more wetness during night hours, higher temperature during sunlight hours, or some combination of both of these elements.

Wetness time was measured with three different exposure methods. Panel A was a bare zinc plate, with both top and bottom sides exposed to air at 5 deg south direction and elevation. Panel B was the same type of zinc plate backed with plywood 12 mm (½-in.) thick. Panel C was mounted on a black box, 120 cm (4 ft sq.) by 23 cm (9 in.) deep, with several panels forming the top face of the box, and a dead air space behind all of the panels. Methods B and C provide insulation of the bottom side of the panel from ambient air effects, but each has different insulating characteristics.

Time-of-wetness results observed are shown in Table 3. Although comparisons were not made simultaneously, the relative times-of-wetness were 1.0 for Panel A, 2.2 for Panel B, and 1.6 for Panel C. Thus, a very significant variation in the response to a given atmospheric environment can be seen depending on just how the panels are subjected to the wetness deteriorating forces of that particular environment.

TABLE 3—*Time-of-wetness versus exposure method.*

Test Period	Plain Panel A	Plywood Backed Panel B	Black Box Panel C
Dec. 1974	...	44.8	32.1
Jan. 1975	...	30.0	22.2
Feb. 1975	...	35.4	24.6
Mar. 1975	...	31.5	22.0
Dec. 1975	23.1	...	37.2
Jan. 1976	23.5	...	47.8
Feb. 1976	39.2	...	54.0
Mar. 1976	23.7	...	35.8
Relative Time-of-Wetness	1.0	2.2	1.6

Further study and analysis of Guttman and Sereda's findings will reveal new information about the characteristics of different test environments. It will be recalled that there were six different test locations. Panels were mounted in a similar manner with carefully standardized time-of-wetness recorders. Nighttime temperatures were recorded, sulfur dioxide (SO_2) content of the air was measured, and monthly readings of weight loss of steel panels were done. Observations continued for 24 consecutive months. The response of the corrosion process of steel panels to the characteristics of the various test environments was not sufficiently separated out from the other information given. It is now pertinent to do this in line with the present review of time-of-wetness factors.

A summary of the data and the regression analyses reported is shown in Fig. 6 which provides a characterization of the individual test sites. It is important to note that time-of-wetness, not time of exposure, is a variable.

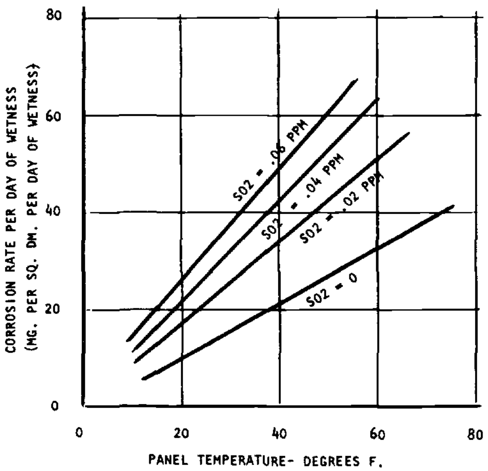

FIG. 6—*Regression analysis results in simplified graphical form* (°C = 5/9 (°F − 32)).

Other variables are temperature during the wetness period and sulphation activity of the air during the wetness period.

The 24 consecutive months of information for each individual site is shown in Fig. 7. A review of each site indicates quite a bit of variation, so other variables must have also been involved. At some of the test sites it is difficult to draw a line through the data points; at others the line is a fairly good representation of the variables involved. It should be remembered that some of the scatter of points on Fig. 7 may be attributed to variations of SO_2 levels at a given location. It was necessary to use all of the data from six locations to come up with the delineation of the SO_2 variable as given on Fig. 6.

Transferring the lines to another plot, (Fig. 8) provides some useful information about the individual test sites. Cleveland and Ottawa are the most corrosive environments, per day of wetness; this can be attributed to the SO_2 content of the air. Although the 24-m (80-ft) lot at Kure Beach has the most metal loss per month, it was well below Cleveland and Ottawa on a per-day-of-wetness basis. The 24-m lot and the 245-m (800-ft) lot at Kure Beach had about the same response at wintertime metal temperatures of 4 °C (40 °F). However, during summer months the 245-m lot had only about half of the weight loss per day of wetness. South Bend had no significant temperature factor.

In the manner shown, we have developed some useful information about the test sites themselves, made possible by the time-of-wetness measurement. Another measurement, sulphation activity of the air, was useful. Today this is a simple measurement to take, as standard sulphation plates are

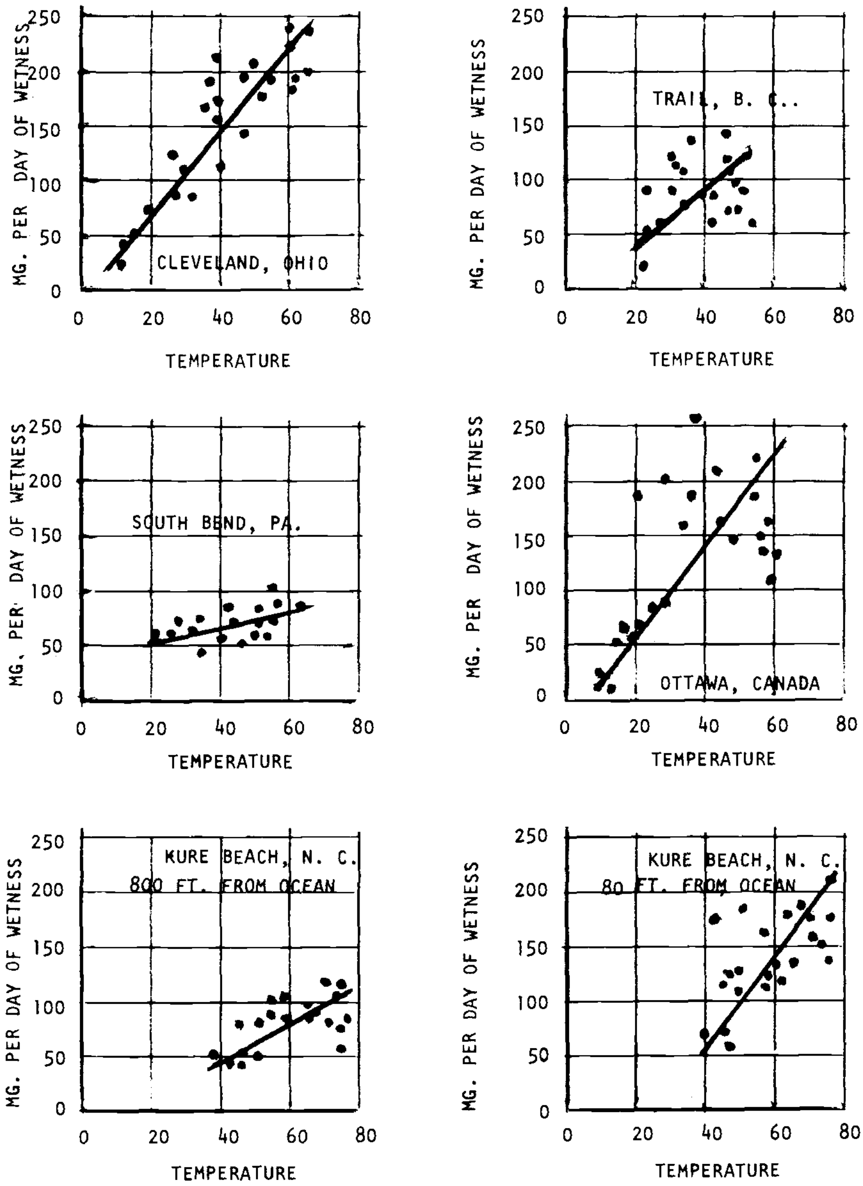

FIG. 7—*Corrosion rates for steel panels.*

commercially available, along with analysis service, and a monthly determination of sulphation activity can be obtained for less than $5.

From the studies presented here, we can now draw some conclusions about exposure testing for the degradation forces of wetness.

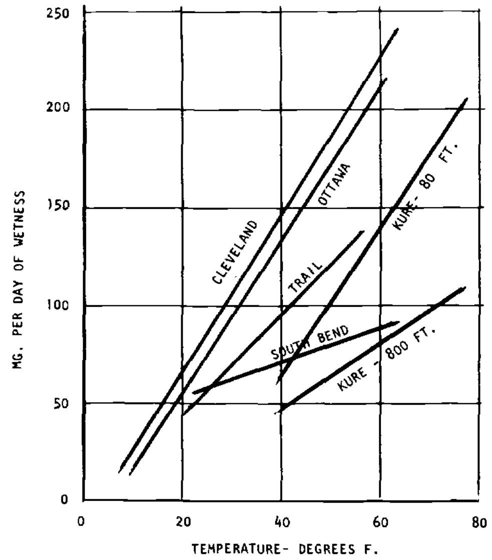

FIG. 8—*Comparison of six test sites.*

1. Time-of-wetness is an important parameter for defining the interaction of a given material with a specific environment.
2. If time-of-wetness is measured, the accelerating action of increased temperature can be established and correlated.
3. If sulphation activity is measured, the accelerating action of higher SO_2 content in the air can be established and correlated.
4. Insulated test panel exposure methods can be used to accelerate the effect of wetness at any given test site.
5. The positioning of test panels with respect to the cold sky is an important test parameter.

At the start of this report it was stated that the search for measuring tools to characterize a test site is an ongoing process. A report on where we stand today is in order. From the information presented herein, we certainly can conclude that time-of-wetness is a useful measurement. It should be standardized using the procedures available in the ASTM. The zinc and platinum detector is in the process of being written up as a standard by the ASTM Subcommittee G1.04. At the same time, the National Research Council of Canada has been busy working on expanding the capabilities of the wetness detector. They are well along in this work, and are presently developing a zinc-gold detector on a small, thin insulating substrate which would be glued to the material being tested. It would be useful for measuring wetness on plastic materials or wetness within a structure, such as a building or an automobile.

References

[*1*] Guttman, H. and Sereda, P. J. in *Metal Corrosion in the Atmosphere, ASTM STP 435*, American Society for Testing and Materials, 1968, pp. 326-359.

[*2*] Sereda, P. J., "Measurement of Surface Moisture—A Progress Report," *ASTM Bulletin*, No. 228, 1958, pp. 53-55.

[*3*] Sereda, P. J., "Measurement of Surface Moisture—Second Progress Report," *ASTM Bulletin*, No. 238, 1959, pp. 61-63.

[*4*] Sereda, P. J., "Measurement of Surface Moisture and Sulfur Dioxide Activity of Corrosion Sites," *ASTM Bulletin*, No. 246, 1960, pp. 47-48.

[*5*] Heating, Ventilation, Air Conditioning Guide 1958, American Society of Heating and Ventilating Engineers, 1958, p. 177.

[*6*] Rozenfeld, I. L., *Atmospheric Corrosion of Metals*, National Association of Corrosion Engineers, English language edition, Houston, Tex., pp. 104-111.

Robert Baboian[1]

Final Report on the ASTM Study: Atmospheric Galvanic Corrosion of Magnesium Coupled to Other Metals

REFERENCE: Baboian, Robert, "**Final Report on the ASTM Study: Atmospheric Galvanic Corrosion of Magnesium Coupled to Other Metals,**" *Atmospheric Factors Affecting the Corrosion of Engineering Metals, ASTM STP 646,* S. K. Coburn, Ed., American Society for Testing and Materials, 1978, pp. 17-29.

ABSTRACT: In 1949 a study was initiated by H. O. Teeple sponsored by Subcommittee VIII on Galvanic and Electrolytic Corrosion of the American Society for Testing and Materials (ASTM) Committee B-3 on Corrosion of Nonferrous Metals and Alloys. This study covered the atmospheric galvanic corrosion of magnesium coupled to a number of dissimilar metals and alloys. Previously, results were reported for two and one half years exposure at State College and Kure Beach. This report, sponsored by Subcommittee VII on Galvanic Corrosion of ASTM Committee G-1 on Corrosion of Metals, presents the final data from this study after an approximate 22-year exposure at these test sites.

KEY WORDS: corrosion, atmospheric corrosion, galvanic corrosion, magnesium, magnesium alloys, marine atmospheres, rural atmospheres

In 1949, H. O. Teeple initiated a study sponsored by Subcommittee VIII on Galvanic and Electrolytic Corrosion of ASTM Committee B-3 on Corrosion of Nonferrous Metals and Alloys. This study covered the atmospheric galvanic corrosion of magnesium coupled to a number of dissimilar metals and alloys.[2] Test sites included New York City, State College, Pennsylvania, Kure Beach, North Carolina, 245-m (800-ft) lot, and Miraflores, Panama Canal Zone.

The disk-type couples used in this study consisted of four disks, each with a central hole and a different outside diameter mounted on and in-

---

[1] Manager, Electrochemical and Corrosion Laboratory, Texas Instruments Inc., Attleboro, Mass. 02703

[2] Teeple, H. O. in *Symposium on Impact Testing, ASTM STP 175,* American Society for Testing and Materials, 1955, pp. 89-113.

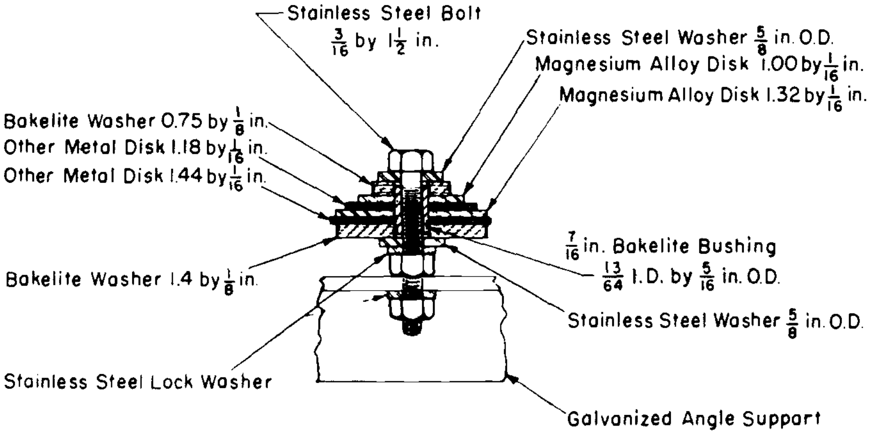

FIG. 1—*ASTM galvanic couple for magnesium alloy tests (1 in. = 2.54 cm).*

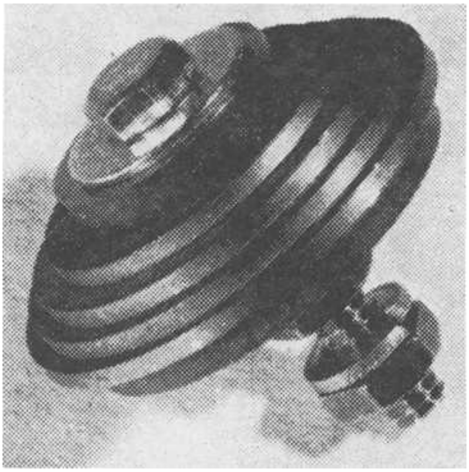

FIG. 2—*Disk-type dissimilar metals galvanic couple assembly.*

sulated from a stainless steel cap bolt. The top and bottom disks were also insulated from the assembly by bakelite washers. The dissimilar metals were the two middle disks. A diagram of the assembly is shown in Fig. 1, and a photograph is shown in Fig. 2.

The comparison material in this study was magnesium in the form of two alloys: AZ31B and M1A. These magnesium alloys were coupled, respectively, with a number of metals and alloys, which are listed in Table 1. The compositions of these materials are shown in the Appendix to this paper.

At each of four locations, the couples were exposed in three sets of four

TABLE 1—*Metals and alloys galvanically coupled with AZ31B and M1A magnesium alloys.*

With AZ31B Mg
AZ31B Mg (control)
24S-T aluminum [a]
75S-T aluminum [a]
52S aluminum [a]
2S aluminum [a]
red brass
carbon steel
Monel
nickel
Type 304 stainless steel
zinc
cadmium-plated steel
zinc-plated steel
With M1A Mg
M1A Mg (control)
52S aluminum [a]
2 S aluminum [a]
red brass
zinc

[a] The aluminum alloy designations in the text are the ones in use during the initiation of this study. The current designations are as follows: 24S-T is 2024; 25S-T is 7075; 52S is 5052; 2S is 1100.

couples each, including control couples of each metal or alloy. The total number of couples exposed was 1440. A total of 480 couples were evaluated after the first retrieval representing approximately 2½ years of exposure except for New York, where exposure time was about 4 years. Results of this retrieval have been reported previously by Teeple.[2]

Subsequently, this study was abandoned and was rediscovered in early 1972. Unfortunately, couples exposed at New York and Canal Zone were not located; however, the second and third retrieval specimens at State College and Kure Beach were found. Several laboratories (see Acknowledgment) participated in the retrieval and evaluation of the couples under the sponsorship of Subcommittee VII on Galvanic Corrosion of ASTM Committee G-1 on Corrosion of Metals. Exposure time for couples included in this report are listed in Table 2. Cleaning procedures were the same as those used in Teeple's study.

Results

Weight data for metals coupled to AZ31B and M1A magnesium at State College and Kure Beach are listed in Tables 3 through 6. Included are

TABLE 2—*Test location and time of exposure.*

Location	Test Period	Days	Years
State College	5/8/50 to 11/21/52	927	2.54
State College	5/8/50 to 4/18/72	8015	21.95
Kure Beach, 245-m (800-ft) lot	11/2/49 to 8/6/52	904	2.48
Kure Beach, 245-m (800-ft) lot	11/2/49 to 6/9/72	8255	22.60

control and coupled weight losses and the net change for both retrieval times.

Weight loss data for the magnesium alloys in the galvanic couples at State College and Kure Beach are listed for both retrieval times in Tables 7 and 8.

Increase in corrosion of the magnesium alloys was calculated from the difference between the coupled and control weight data. These data are listed in Tables 9 and 10 and show the increase in magnesium weight loss when coupled to various metals at State College and Kure Beach.

Discussion

All metals coupled to AZ31B and M1A magnesium exposed at State College for 22 years had a reduction in weight loss compared to the control exposure. The most pronounced effect was exhibited by mild steel and plated mild steel materials. As observed in Tables 3 and 5, zinc had an increase in corrosion when coupled to the magnesium alloys at the end of a 2.54-year exposure. However, significant protection of the zinc was observed after a 22-year exposure in the galvanic couples.

Results of exposure at Kure Beach in Tables 4 and 6 are similar to those obtained at State College. The largest effect was observed with the steels, though cadmium-plated steel had a larger weight loss in the coupled exposure. The net change is positive for zinc at the end of 2.48 years at Kure Beach; however, significant reduction in corrosion in the couple with magnesium is observed after 22.6 years. These results for zinc at both State College and Kure Beach are reproducible indicating that this behavior is real and should be further investigated.

It is interesting to note that the AZ31B and M1A magnesium alloys had similar effects on the behavior of the metals in the galvanic couples.

Weight loss for the magnesium alloys in the galvanic couples was significantly greater after 22 years than after 2.5 years of exposure as expected. The magnesium alloy control specimens had higher weight losses at State College than at Kure Beach. Also, magnesium alloys coupled to aluminum had higher weight losses at State College. This is an interesting result since State College is considered a clean rural site and Kure Beach is considered a corrosive marine environment. The magnesium alloys

TABLE 3—*Weight data for metals coupled to AZ31B magnesium at State College, Pa.*

Metal in Couple	2.54 Years			21.95 Years		
	Control, Weight Loss, g	Coupled, Weight Loss, g	Net Change	Control, Weight Loss, g	Coupled, Weight Loss, g	Net Change
24S-T Al	0.001	0.001	0	0.004	0.002	−0.002
75S-T Al	0.001	0.001	0	0.004	0.001	−0.003
52S Al	0.001	0	−0.001	0.004	0.001	−0.003
2S Al	0.001	0.001	0	0.003	0.002	−0.001
85-15 Br	0.010	0	−0.010	0.057	0.001	−0.056
Mild steel	0.144	0.005	−0.139	0.619	0.007	−0.612
Monel	0.005	0.002	−0.003	0.014	0.001	−0.013
Nickel	0.005	0.003	−0.002	0.024	0.0191	−0.005
304 SS	0.002	0.002	0	0.002	0.0011	−0.001
Zn	0.007	0.009	+0.002	0.104	0.006	−0.098
Cd PL steel	0.064	all specimens lost		0.270	0.019	−0.251
Zn PL steel	0.013	0.014	+0.001	0.231	0.002	−0.229

TABLE 4—*Weight data for metals coupled to AZ31B magnesium at Kure Beach, N.C. 245-m (800-ft) lot.*

	2.48 Years			22.60 Years		
Metal in Couple	Control, Weight Loss, g	Coupled, Weight Loss, g	Net Change	Control, Weight Loss, g	Coupled, Weight Loss, g	Net Change
24S-T Al	0.010	0.002	−0.008	0.013	0.022	+0.009
75S-T Al	0.005	0.001	−0.004	0.010	0.003	−0.007
52S Al	0	0	0	0.009	0.002	−0.007
2S Al	0.003	0.002	−0.001	0.012	0.004	−0.008
85-15 Br	0.012	0.001	−0.011	0.040	0.004	−0.036
Mild steel	0.243	0.006	−0.237	1.106	0.030	−1.076
Monel	0.006	0.002	−0.004	0.018	0.0016	−0.016
Nickel	0.001	0.004	+0.003	0.008	0.0047	−0.003
304 SS	0.005	0.002	−0.003	0.007	0.0011	−0.006
Zn	0.002	0.004	+0.002	0.073	0.012	−0.061
Cd PL steel	0.045	0.029	−0.016	0.092	0.104	+0.012
Zn PL steel	0.013	0.004	−0.009	0.141	0.004	−0.137

TABLE 5—*Weight data for metals coupled to M1A magnesium at State College, Pa.*

Metal in Couple	2.54 Years			21.95 Years		
	Control, Weight Loss, g	Coupled, Weight Loss, g	Net Change	Control, Weight Loss, g	Coupled, Weight Loss, g	Net Change
52S Al	0.001	0.001	0	0.004	0.002	−0.002
2S Al	0.001	0.002	+0.001	0.003	0.003	0
85-15 Br	0.010	0.001	−0.009	0.057	0.001	−0.056
Zn	0.007	0.020	+0.013	0.104	0.007	−0.097

TABLE 6—*Weight data for metals coupled to M1A magnesium at Kure Beach, N. C., 245-m (800-ft) lot.*

Metal in Couple	2.49 Years			22.60 Years		
	Control, Weight Loss, g	Coupled, Weight Loss, g	Net Change	Control, Weight Loss, g	Coupled, Weight Loss, g	Net Change
52S Al	0.001	0.002	+0.001	0.009	0.004	−0.005
2S Al	0.003	0.003	0	0.012	0.005	−0.007
85-15 Br	0.012	0.001	−0.011	0.040	0.004	−0.036
Zn	0.002	0.007	+0.005	0.073	0.018	−0.055

TABLE 7—*Weight loss data for magnesium alloys in galvanic couples at State College, Pa.*

	AZ31B Mg		M1A Mg	
Metal in Couple	2.5 Years	21.95 Years	2.54 Years	21.95 Years
Control	0.034	0.214	0.036	0.197
24S-T Al	0.064	0.351	...	...
75 S-T Al	0.062	0.337	...	...
52S Al	0.059	0.318	0.075	0.336
2S Al	0.060	0.323	0.078	0.349
85-15 Br	0.109	0.558	0.115	0.604
Mild steel	0.137	0.633	...	...
Monel	0.1145	0.580	...	...
Nickel	0.1103	0.568	...	...
304 SS	0.0963	0.532	...	...
Zn	0.063	0.380	0.080	0.453
Cd PL steel	0.121	0.523	...	...
Zn PL steel	0.057	0.392	...	...

TABLE 8—*Weight loss data for magnesium alloys in galvanic couples at Kure Beach, 245-m (800-ft) lot.*

	AZ31B Mg		M1A Mg	
Metal in Couple	2.48 Years	22.60 Years	2.48 Years	22.60 Years
Control	0.024	0.167	0.024	0.137
24S-T Al	0.055	0.330	...	...
75S-T Al	0.047	0.285	...	...
52S Al	0.045	0.266	0.056	0.256
2S Al	0.045	0.304	0.058	0.270
85-15 Br	0.121	0.664	0.1428	0.670
Mild steel	0.170	0.561	...	...
Monel	0.1293	0.791	...	...
Nickel	0.1423	0.895	...	...
304 SS	0.1126	0.683	...	...
Zn	0.054	0.414	0.066	0.390
Cd PL steel	0.092	0.470	...	...
Zn PL steel	0.063	0.444	...	...

coupled to brass, Monel, nickel and Type 304 stainless steel all had higher weight losses at the Kure Beach site. The AZ31B and M1A magnesium alloys behaved similarly in the galvanic couples.

The increase in corrosion of magnesium alloys when coupled to the various metals (Tables 9 and 10) provides valuable information on the galvanic behavior of these systems. When arranged according to increasing magnesium corrosion in the galvanic couple, the metals form a galvanic series. The atmospheric galvanic series derived from the increases in AZ31B magnesium alloy corrosion are listed in Table 11.

TABLE 9—*Increase in corrosion in AZ31B magnesium when coupled to various metals.*

	State College Increase in Corrosion, g		Kure Beach, 245-m (800-ft) Lot Increase in Corrosion, g	
Metal in Couple	2.54 Years	21.95 Years	2.48 Years	22.60 Years
24S-T Al	0.030	0.137	0.031	0.163
75S-T Al	0.028	0.123	0.023	0.118
52S Al	0.025	0.104	0.021	0.099
2S Al	0.026	0.109	0.021	0.137
85-15 Br	0.075	0.344	0.097	0.497
Mild steel	0.103	0.419	0.146	0.394
Monel	0.080	0.366	0.105	0.624
Nickel	0.076	0.354	0.118	0.728
304 SS	0.062	0.318	0.089	0.516
Zn	0.029	0.166	0.030	0.247
Cd PL steel	0.087	0.309	0.068	0.303
Zn PL steel	0.023	0.178	0.039	0.277

TABLE 10—*Increase in corrosion of M1A magnesium when coupled to various metals.*

	State College Increase in Corrosion, g		Kure Beach, 245-m (800-ft) Lot Increase in Corrosion, g	
Metal in Couple	2.54 Years	21.95 Years	2.48 Years	22.60 Years
52A Al	0.039	0.139	0.032	0.119
2S Al	0.042	0.152	0.034	0.133
85-15 Br	0.079	0.407	0.119	0.533
Zn	0.044	0.256	0.042	0.253

There are significant differences between the series for the mild State College site and the series of the Kure Beach site, particularly in the position of steel. Interestingly, the 2.54-year series and 21.95-year series at State College are quite similar (except for the position of the plated steels), whereas, there are differences in the 2.48-year and 22.60-year series at Kure Beach. Thus, short-term exposures at the mild State College site appear adequate in predicting the long-term galvanic behavior of uncoated metals; however, this is not the case at the Kure Beach marine site.

Table 12 shows a comparison of the atmospheric galvanic series derived from the metals arranged according to increasing magnesium corrosion in galvanic couples (Kure Beach) and the seawater galvanic series derived from the metals arranged according to their measured potentials in flowing seawater (Wrightsville Beach, North Carolina). There is a remarkable similarity in the two series even though their derivations, as well as the environments from which they are derived, are quite different.

TABLE 11—*Metals arranged according to increasing magnesium corrosion in galvanic couple.*

Kure Beach, 245-m (800-ft) Lot	
22.60 Years	2.48 Years
Al	Al
Zn	Zn
Zn PL steel	Zn PL steel
Cd PL steel	Cd PL steel
Steel	304 SS
85-15 brass	85-15 brass
304 SS	Monel
Monel	nickel
Nickel	steel
State College	
21.95 Years	2.54 Years
Al	Zn PL steel
Zn	Al
Zn PL steel	Zn
Cd PL steel	304 SS
304 SS	85-15 brass
85-15 brass	nickel
Nickel	Monel
Monel	Cd PL steel
Steel	steel

TABLE 12—*Galvanic series.*

Metals Arranged According to Increasing Mg Corrosion in Atmospheric Galvanic Couple Exposure, Kure Beach, 245-m (800-ft) Lot	Metals Arranged According to Their Potentials in Seawater, Wrightsville Beach, N.C.
Al	Zn
Zn	Al
Zn PL steel	Cd
Cd PL steel	steel
Steel	85-15 brass
85-15 brass	nickel
304 SS	304 SS
Monel	Monel
Nickel	

Acknowledgments

This report is made possible by the original work by H. O. Teeple who initiated the study and conducted the first retrieval.

Persons participating in the second and final retrieval, including evaluation of the 22-year specimens and interpretation of the results, are: W. H. Ailor, Reynolds Metals; R. Baboian, Texas Instruments; E. A. Baker, INCO; S. Coburn, U.S. Steel; A. Gallaccio, Frankford Arsenal; G. S. Haynes, Texas Instruments; W. W. Kirk, INCO; H. H. Lawson, Armco; and J. F. Rynewicz, Lockheed.

APPENDIX

Chemical Analysis of Metals and Alloys Used in Atmospheric Galvanic Exposure Tests with Magnesium Alloys

MAGNESIUM ALLOYS, %

	AZ31B[a]	M1A[b]
Aluminum	2.6	0.003
Copper	0.014	0.015
Manganese	0.78	1.4
Lead	0.004	0.001
Tin	0.001	0.01
Calcium	0.01	0.10
Iron	0.001	0.015
Nickel	0.0005	0.001
Silicon	0.02	0.001
Zinc	0.81	0.01
Finish	commercial	commercial

ALUMINUM ALLOYS,[c] %

	2S-H14	52S-H34	24S-T4	75S-T6
Silicon	0.06	0.11	0.12	0.14
Iron	0.56	0.19	0.19	0.21
Copper	0.14	0.06	4.32	1.50
Manganese	...	0.04	0.65	0.16
Magnesium	...	2.42	1.48	2.58
Zinc	...	...	0.06	5.80
Chromium	...	0.21	...	0.24
Titanium	...	0.01	...	...
Finish	commercial	commercial	commercial	commercial

Chemical Analysis of Metals and Alloys Used in Atmospheric Galvanic Exposure Tests with Magnesium Alloys

Nickel and Monel, %		
	Nickel[c]	Monel[c]
Carbon	0.04	0.12
Manganese	0.13	0.98
Iron	0.12	1.91
Sulfur	0.005	0.005
Silicon	0.03	0.09
Copper	0.15	30.80
Nickel	99.50	66.07
Chromium	...	...
Finish	cold rolled	cold rolled

Type 304 Stainless Steel,[c] %	
Carbon	0.07
Manganese	0.41
Phosphorus	0.015
Sulfur	0.015
Silicon	0.041
Nickel	9.46
Chromium	18.89
Finish	No. 4

85-15 Red Brass ,[c] %	
Iron	0.02
Lead	0.015
Zinc	14.65
Copper	85.31
Finish	cold rolled

Mild Steel, %	
Carbon	0.073
Manganese	0.034
Phosphorus	0.007
Sulfur	0.029
Copper	0.072
Finish	machined

Zinc,[b] %	
Lead	0.10
Cadmium	0.003
Iron	0.01
Zinc	balance
Finish	hot rolled

Chemical Analysis of Metals and Alloys Used in Atmospheric Galvanic Exposure Tests with Magnesium Alloys

ZINC-PLATED STEEL,[d] oz/gal[e]	
Plated at 20 A/ft^2 at 35 °C	
Solution	
Zinc cyanide	9
Sodium Cyanide	13.6
Sodium hydroxide	11.2
Thickness: 0.0005 in.[e]	
Finish: as plated	

CADMIUM-PLATED STEEL,[d] oz/gal[e]	
Plated at 3 A/ft^2 at 35 °C	
Solution	
Cadmium oxide	4.3
Sodium oxide	12.2
Thickness: 0.0005 in.[e]	
Finish: as plated	

---

[a] Analysis of material furnished for State College exposure, but presumed to be typical for other exposures.

[b] Typical analysis.

[c] Actual analyses of alloys used.

[d] Analyses of the plated coatings was not made but both were put on the same mild steel as was exposed bare.

[e] 1 oz/gal = 7.49 g/litre
1 A/ft^2 = 10.76 A/m^2

F. H. Haynie,[1] *J. W. Spence,*[1] *and J. B. Upham*[1]

Effects of Air Pollutants on Weathering Steel and Galvanized Steel: A Chamber Study

---

REFERENCE: Haynie, F. H., Spence, J. W., and Upham, J. B., "**Effects of Air Pollutants on Weathering Steel and Galvanized Steel: A Chamber Study,**" *Atmospheric Factors Affecting the Corrosion of Engineering Metals, ASTM STP 646,* S. K. Coburn, Ed., American Society for Testing and Materials, 1978, pp. 30-47.

ABSTRACT: A statistically designed laboratory study of the effects of gaseous air pollutants on materials was completed. Weathering steel and galvanized steel were among materials exposed in controlled environment chambers. The direct and synergistic effects of relative humidity, sulfur dioxide, nitrogen dioxide, and ozone in a programmed dew/light cycle were studied. For weathering steel, sulfur dioxide, relative humidity, and interaction between the two were the important corrosion rate factors. For galvanized steel, only the direct effects of sulfur dioxide and relative humidity were important. The remainder of the fifteen possible direct and synergistic effects were statistically insignificant.

KEY WORDS: atmospheric corrosion, air pollution, weathering steel, galvanized steel, controlled atmospheres

Field and laboratory investigations have been conducted to assess the detrimental effects of air pollutants on materials [*1*-*5*].[2] The ultimate goal of these studies has been to develop dose-response relationships for various materials. This information is needed to serve as input for cost-benefit studies and as criteria for developing secondary air quality standards.

A statistically designed laboratory study has been completed using controlled environment exposure chambers. The study objective was to assess both direct and synergistic effects of air pollutants and other environmental factors on six different classes of materials. Essentially, the study consisted

[1] Environmental engineer, chemist, and environmental engineer, respectively, Environmental Protection Agency, Environmental Sciences Research Laboratory, Environmental Research Center, Research Triangle Park, N.C. 27711.

[2] The italic numbers in brackets refer to the list of references appended to this paper.

of exposing economically important materials to controlled environments of clean air and polluted air and comparing the resulting effects. Over 20 000 h of exposure time, including 4000 h of clean air exposures, were accumulated. Weathering steel and galvanized steel were among the materials evaluated. This paper presents and discusses the controlled environment exposure results for these economically important materials.

Methodology

Study Design

A two-level factorial arrangement was selected as the experimental design to identify statistically the environmental factors, or combination of factors, or both, that cause significant effects on exposed materials [*6*]. An experiment of this type should include as many environmental factors as possible that are likely to cause an effect. Table 1 shows the four factors at two levels chosen for the study.

TABLE 1—*Environmental factors and levels chosen for the exposure study.*

Environmental Factors	Level Low	 High
Sulfur dioxide, $\mu g/m^3$	79 (0.03 ppm)	1310 (0.50 ppm)
Nitrogen dioxide, $\mu g/m^3$	94 (0.05 ppm)	940 (0.50 ppm)
Ozone, $\mu g/m^3$	157 (0.08 ppm)	980 (0.50 ppm)
Relative humidity, %	50	90

The required number of exposure conditions was 2^4 or 16, and did not include replication. Although temperature was an obvious environmental factor, all exposures were conducted at a constant high temperature of 35 °C so as to reduce by one half the total number of exposure conditions. The rationale for this decision was that according to reaction kinetics, factors that are statistically insignificant at high temperatures are not likely to show significant interactions with temperature. Clean air exposures, which served as controls, were, however, conducted at two temperature levels (35 and 13 °C).

Total time for each exposure condition was 1000 h. Effects measurements were made on all materials after exposure periods of 250, 500, and 1000 h.

Exposure System

The controlled environment exposure system consisted of five chambers, each with independent controls for regulating temperature, relative humidity, and concentrations of sulfur dioxide (SO_2), nitrogen dioxide (NO_2), and ozone (O_3) [7]. Chamber operations were dynamic in that fresh, conditioned air continuously entered each chamber at about 1.5 air changes per min. Incoming air contained specified concentrations of pollutants at a specified constant temperature and relative humidity.

To achieve accelerated "weathering," the chambers operated on a programmed dew/light cycle. Each chamber featured a xenon lamp to simulate sunlight during the light cycle and a chill rack to hold specimens of materials. Coolant flowed through the chill rack during most of the dew cycle and resulted in moisture condensing on the cooled exposed material specimens. The moisture evaporated during the light cycle. The duration of the dew/light cycle was 40 min including 20 min of light (xenon lamp). Temperature and humidity inside the chambers and especially adjacent to the exposed material specimens varied depending on which part of the dew/light cycle was operating.

Material Selection

Both weathering steel and galvanized steel are widely used. Weathering steel was developed for use in unpainted exterior architectural designs. In most environments, the steel develops a small-grained, strongly adherent rust coating that tends to serve as a protection film against subsequent corrosion. The weathering steel exposed in this study was Cor-Ten A, a product of U.S. Steel Corporation. This steel has been used in the design and construction of the Chicago Civic Center, the Seattle Washington Battelle Memorial Institute Building, and the New York Ford Foundation Office.

Table 2 gives the elemental analysis of the Cor-Ten A weathering steel. The measured yield point and ultimate tensile strength were 35 820 and 54 480 N/cm^2, respectively.

Galvanized steel is used extensively for such exterior applications as

TABLE 2—*Elemental analysis of weathering steel.*

Element	Percent
Carbon	0.11
Manganese	0.37
Phosphorus	0.10
Sulfur	0.018
Silicon	0.39
Copper	0.29
Nickel	0.11
Chromium	0.90
Iron	remainder

roofing, guttering, highway railing, and chain link fencing. Commercial grade 18-gage galvanized steel sheet with an approximate 25-μm zinc coating was selected for exposure.

Effects Assessment

Corrosion rates of most metals normally accelerate when metals are exposed to polluted environments. The rate of corrosion, therefore, was selected as the means for assessing the effects produced by the various controlled environment exposure conditions. Corrosion was measured by the weight-loss method. This method consisted of weighing the panel before exposure, and then removing the corrosion products after exposure and reweighing. The difference in weight was a measure of the amount of corrosion that developed during the exposure period.

For both metals, 7.6 by 12.7-cm panels were sheared from sheet stock. The panels were cleaned by scrubbing them in a warm detergent solution and were rinsed first in distilled water, then in acetone. They were then weighed on an analytical balance to within ± 0.1 mg.

Six panels of each metal were exposed to each of the 16 polluted and 4 clean air conditions. The panels were placed randomly on chamber exposure racks. Silicon paste was applied to the back sides of the panels. The paste served as a thermal conductor, held the panels in place, and protected the unexposed back side from corrosion. After nominal exposure periods of 250, 500, and 1000 h, two panels of each metal were removed randomly from a chamber and mechanically cleaned of silicon paste.

The corrosion products on the weathering steel were removed chemically by immersion for 1 h or longer in Clark's solution, in accordance with ASTM Recommended Practice for Preparing, Cleaning, and Evaluation of Corrosion Test Specimens (G 1-72), followed by scrubbing and rinses in distilled water and acetone. The panels were then weighed, the weights corrected for the loss of base metal (0.06 g/[panel h]) experienced by panels while in Clark's solution, and final weight-loss values were calculated. To render the weight-loss values (g/panel) more meaningful, they were converted to equivalent thickness-loss values (μm) by using the factor 13.345 μm/g.

The galvanized panels were processed in a similar manner except that the zinc corrosion products were removed by immersion for about 10 min in a 10 percent aqueous ammonium chloride solution maintained at 72–80°C. The correction factor for zinc lost during chemical cleaning was 0.0009 g/ (panel min). Multiplying the corrected weight-loss values (g/ panel) by 14.98 μm/g converted them to equivalent zinc film thickness-loss values (μm).

Results and Discussion

Weathering Steel

Corrosion of weathering steel is normally a parabolic function of time. The corrosion data collected in this study, however, were essentially linear with time. The relatively short exposure periods (1000 h) probably accounted for the deviation.

Because of the linear relationship, an average corrosion rate for each exposure condition was calculated using the method of least squares through the origin (based on six data sets per exposure condition). Tables 3 and 4 present individual corrosion rates for the polluted air and clean air exposures, respectively. Corrosion rates in polluted air ranged from 84 to 762 μm/year with an average of 383 μm/year. The best estimate of the standard deviation on individual corrosion rates in polluted air was ± 72 μm/year. Clean air corrosion rates ranged from 1 to 86 μm/year. The highest

TABLE 3—*Corrosion rates of weathering steel exposed to designated controlled polluted environmental conditions.*

	Corrosion Rate and Standard Deviation, μm/year			
	High Relative Humidity		Low Relative Humidity	
Exposure Condition	High SO_2	Low SO_2	High So_2	Low SO_2
High NO_2				
High O_3	753	256	414	179
	± 85	± 27	± 151	± 30
Low O_3	762	178	607	162
	± 121	± 44	± 105	± 62
Low NO_2				
High O_3	736	230	479	123
	± 90	± 27	± 78	± 26
Low O_3	656	147	371	84
	± 56	± 13	± 18	± 14

TABLE 4—*Corrosion rates of weathering steel exposed to designated controlled clean air environmental conditions.*

	Corrosion Rate and Standard Deviation, μm/year	
Temperature	High Relative Humidity	Low Relative Humidity
35°C	86	28
	± 31	± 10
13°C	1.03	1.07
	± 0.17	± 0.06

clean air corrosion rate was about the same as the lowest rate in polluted air.

Tables 5 and 6 show analyses of variance of the experimental data for the polluted and clean air exposure conditions, respectively. On the basis of calculated *F*-values, the important factors controlling corrosion were concentration of SO_2, relative humidity, and temperature. The interaction between SO_2 and relative humidity was significant at a lower confidence level.

As shown in previous studies [*9,10*], electrolytic corrosion occurs only when metal panels are wet. During dew/light cycles in the chambers, panel temperatures continually varied, causing changes in relative humidity adjacent to the panels. When temperatures were below the dew point, moisture condensed on the panels. Because of the hydroscopic nature of corrosion products, panels also became moist even at temperatures above the dew point.

Thermocouples attached to panels were used to monitor panel temperatures during the dew/light cycles for each clean air exposure condition. Figure 1 shows the results. Theoretically, the critical factors controlling corrosion are the time-of-panel-wetness and the geometric mean temperature during the time panels are wet. Since the moisture content of the air entering the chambers was essentially constant (set by the input conditions), time-of-panel-wetness per cycle was estimated by using the cycling temperature data to calculate relative humidity values (adjacent to panels) as a function of time. Visual observations, however, detected moisture on panels

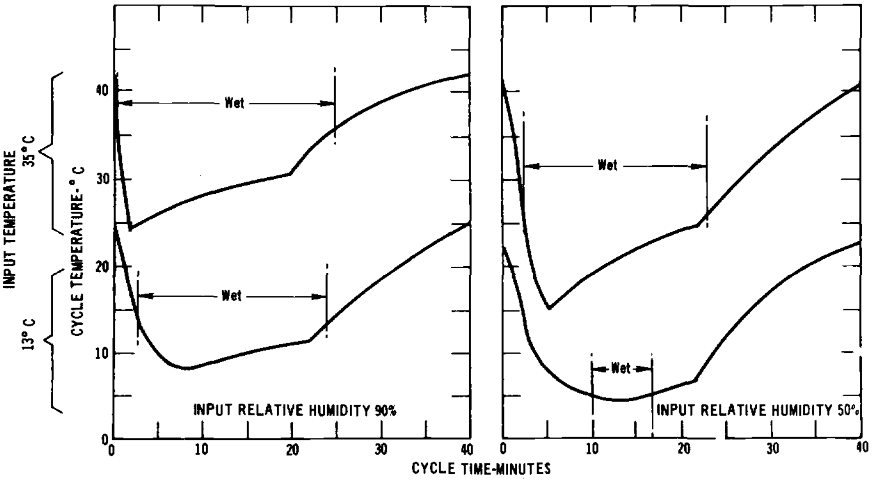

FIG. 1—Temperature-time profiles for exposed metal panels during chamber dew/light cycles.

TABLE 5—*Analysis of variance of weathering steel corrosion data for polluted exposure conditions.*

Factor	Contrast	Sum of Squares	Degrees of Freedom	Mean Square	F	R^2
SO_2	213.7	730726	1	730726	258.11[a]	0.790
RH	12.7	105138	1	105138	37.14[a]	0.114
O_3	12.7	2590	1	2590	0.91	0.003
NO_2	30.4	14810	1	14810	5.23	0.016
SO_2 × RH	48.3	37264	1	37264	13.16[b]	0.040
SO_2 × NO_2	- 14.4	3322	1	3322	1.17	0.004
SO_2 × NO_2	6.5	673	1	673	0.24	0.001
RH × O_3	16.3	4231	1	4231	1.49	0.005
RH × NO_2	- 7.8	975	1	975	0.34	0.001
O_3 × NO_2	- 26.1	10870	1	10870	3.84	0.012
Residual		14155	5	2831		0.003
Total		924754	15	2831		0.003

NOTES—F uses the residual mean square in the denominator.
R^2 is the coefficient of determination excluding the within chamber variability.
[a] 0.99 probability level of significance.
[b] 0.95 probability level of significance.

TABLE 6—*Analysis of variance of weathering steel corrosion data for clean air exposure conditions.*

Factor	Contrast	Sum of Squares	Degrees of Freedom	Mean Square	F	R^2
RH	14.49	839.8404	1	839.8404	3.24	0.085
Temperature	27.75	3080.2550	1	3080.2550	11.89[a]	0.310
RH × T	14.51	842.1604	1	842.1604	3.25	0.085
Error		5181.7875	20	259.0894		0.521
Total		9944.0383				

[a] 0.99 probability level of significance.

at a calculated relative humidity of about 85 percent. This was probably due to the hydroscopic nature of the corrosion products. Thus, panels were considered wet at temperatures corresponding to relative humidities equal to or greater than 85 percent. Table 7 shows the calculated times-of-panel-wetness per dew/light cycle and geometric mean temperatures of panels when wet for each clean air exposure condition.

TABLE 7—*Time-of-panel-wetness per dew/light cycle and geometric mean panel temperature when wet as a function of input temperature and relative humidity.*

	Input Relative Humidity	
Input Temperature	90%	50%
35°C	24.5 min	20.7 min
	302.4 K	293.4 K
13°C	22.0 min	7.0 min
	283.2 K	277.6 K

NOTE—Calculated values are for both weathering steel and galvanized steel.

Because steel corrodes only when wet, the corrosion data were analyzed in terms of the expected times-of-wetness. On the basis of long-term atmospheric corrosion studies, the corrosion-time function should be more nearly parabolic than linear as was observed in the short term chamber exposures.

In the clean air exposures, the reactants (steel, water, and oxygen) were present in excess and the reaction rate should be activation-controlled. Thus, the theoretically expected relationship between corrosion, time, and temperature should be

$$\ln \frac{\text{corr}}{\sqrt{t_w}} = \ln a_0 - \frac{E}{RT}$$

where

corr = thickness-loss, μm,
t_w = time-of-wetness, year,
E = activation energy, cal/(g-mol K),
R = gas constant, 1.9872 cal/g-mol,
T = geometric mean temperature of panels when wet, K, and
a_0 = regression coefficients.

A least squares fit of the clean air experimental data resulted in

$$\ln \frac{\text{corr}}{\sqrt{t_w}} = 55.44 - \frac{31\ 150}{RT}$$

or

$$\text{corr} = \sqrt{t_w}\, e^{\left(55.44 - \frac{31\ 150}{RT}\right)}$$

This empirical function accounted for 92 percent of the variability in the clean air experimental data.

The reaction of steel with moisture and oxygen occurs with or without SO_2 present. Thus, the contribution of moisture and oxygen to the total corrosion may be excluded when analyzing the direct and synergistic effects of SO_2. This amount of corrosion, therefore, was calculated and subtracted from the corresponding sets of data from the polluted air exposures. The resulting data fitted to the relationship

$$\ln\left[\frac{\text{corr}}{\sqrt{t_w}}\right] = \ln a_0 + a_1 \ln SO_2 - \frac{E}{RT}$$

where

corr = thickness-loss, μm,
t_w = time-of-panel-wetness, year,
SO_2 = concentration of SO_2, μg/m^3,
E = activation energy, cal/(g-mol K),
R = gas constant, 1.9872 cal/g-mol,
T = geometric mean panel temperature when wet, K, and
a_0, a_1 = regression constants.

The calculated constant, E/R, was small, positive, and statistically insignificant. This fact strongly suggested that the reaction of SO_2 with steel was diffusion controlled rather than activation controlled. The coefficient for ln SO_2 was not statistically different from 0.5; therefore, corrosion appeared to be proportional to $\sqrt{SO_2}$. Thus, the weathering steel experimental data were reevaluated as a function of the square root of the dose, $\sqrt{t_w\ SO_2}$, and the resulting best fit of the theoretically consistent relationship was

$$\text{corr} = \left[5.64\sqrt{SO_2} + e^{\left(55.44 - \frac{31\,150}{RT}\right)}\right]\sqrt{t_w}$$

This empirical function accounted for 91 percent of the variability in the experimental data from both the clean and polluted air exposure conditions.

Figure 2 shows a plot of predicted versus experimental data. The deviation at the high end of the graph is probably due to the fact that the experimental data were more consistent with a linear-time function than a parabolic-time function.

A better test of an empirical function is to determine how accurately it

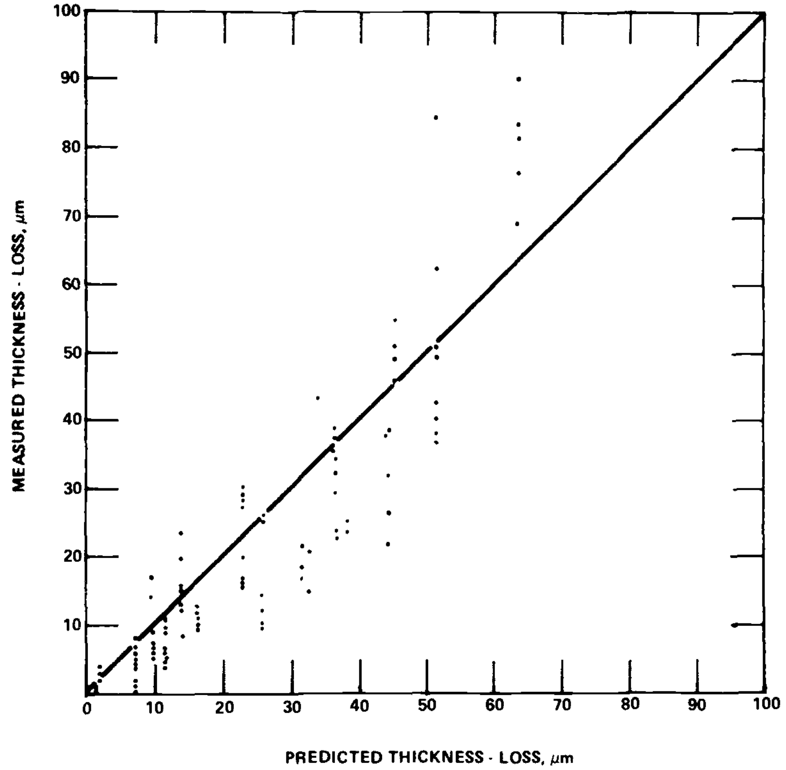

FIG. 2—*Relationship between predicted and laboratory measured thickness-loss for weathering steel.*

predicts actual long-term atmospheric corrosion results. Fortunately, corrosion data for a similar weathering steel are available from a field study conducted in eight cities [5]. Although time-of-panel-wetness and temperature during time-of-wetness were not measured in the field study, average temperature and relative humidity during the total time of exposure were calculated. Thus, if relationships between average relative humidity and time-of-panel-wetness, and between average temperature and geometric mean temperature when panels are wet can be obtained, the empirical function may be expressed in terms suitable for making comparisons with the field data.

Guttman [*10*] has plotted the probable time-of-wetness as a function of relative humidity for both groundward and skyward surfaces of exposed metal panels. Assuming the average probability for the two surfaces represents the fraction of the total time panels are wet, the data fit a relationship

$$f_w = e^{\left(4.04 - \frac{404}{RH}\right)}$$

where

f_w = fractional time-of-panel-wetness and
RH = relative humidity, %.

On the basis of the temperature cycle data in Fig. 1, the geometric mean panel temperature when wet was about 6 K less than the average panel temperature for the total time of exposure. This information together with the field study data, were used to calculate factors (Table 8) that affected the atmospheric corrosion of weathering steel in each city. Thus, these factors may be used in the empirical function to predict the amount of corrosion likely to develop in each city.

TABLE 8—*Factors affecting atmospheric corrosion of weathering steel exposed at urban sites.*

City	Geometric Mean Panel Temperature When Wet, K	Fractional Time-of-Panel-Wetness, f_w	Average Pollutant Concentration g/m^3		Combined Factor[a]
			SO_2	O_x	
Chicago	277.3	0.1136	406	47	38.42
Cincinnati	280.2	0.1628	79	59	20.47
Detroit	277.2	0.1367	118	24	22.77
Los Angeles	285.2	0.0841	39	75	10.68
New Orleans	287.5	0.2992	24	35	16.48
Philadelphia	279.1	0.1248	218	57	29.60
San Francisco	281.3	0.2244	34	37	15.94
Washington	281.0	0.0932	126	50	19.54

[a] $$\left[5.64\sqrt{SO_2} + e^{\left(55.44 - \frac{31\,150}{RT}\right)}\right]\sqrt{f_w}$$

A measure of corrosion predictability is the coefficient of variation, R^2, between predicted and field study values. Values of R^2 were calculated for each city in the field study; results are given in Table 9. With the exception of Los Angeles, predicted corrosion values agreed poorly with actual corrosion measured in cities with relatively high oxidant levels. The Los Angeles data were probably in good agreement because the low time-of-panel-wetness did not allow much corrosion to develop; thus, the magnitude of error was small. Regressions on the field data, however, strongly suggested that oxidants inhibited corrosion. The major oxidant in natural environments is ozone, but the chamber exposures showed that ozone produced neither inhibiting nor accelerating effects. In the field study, some other oxidant,

TABLE 9—*Corrosion predictability as measured by coefficient of variation, R^2, between predicted and field values.*

High Oxidant Cities		Low Oxidant Cities	
City	R^2	City	R^2
Cincinnati	0.544	Chicago	0.976
Los Angeles	0.984	Detroit	0.997
Philadelphia	0.392	New Orleans	0.998
Washington	0.701	San Francisco	0.978
Overall R^2			0.846

or some unmeasured factor that was covariant with oxidant, apparently caused the inhibiting effect. Excluding the data from the high oxidant cities, the average coefficient of variation was 0.986. This was exceptionally good, especially considering the simplifying assumptions that were made.

Galvanized Steel

As was theoretically expected, corrosion of the galvanized steel was essentially linear with time. Thus, an average corrosion rate for each of the 16 polluted air exposure conditions was calculated by the method of least squares through the origin (based on six data sets per exposure condition). Table 10 shows the corrosion rates. They ranged from 3 to 33 μm/year, and the best estimate of the standard deviation on individual rates was ±5 μm/year.

TABLE 10—*Corrosion rates of galvanized steel exposed to designated controlled polluted environmental conditions.*

	Corrosion Rate and Standard Deviation, μm/year			
	High Relative Humidity		Low Relative Humidity	
Exposure Condition	High SO_2	Low SO_2	High SO_2	Low SO_2
High NO_2				
High O_3	33 ±7.1	17 ±5.2	19 ±4.1	6.6 ±0.9
Low O_3	28 ±1.5	12 ±4.3	15 ±2.1	3.8 ±0.6
Low NO_2				
High O_3	29 ±10	20 ±11	17 ±1.3	4.0 ±0.9
Low O_3	25 ±3.1	16 ±6.6	16 ±3.5	3.2 ±2.1

Corrosion rates for galvanized steel exposed to clean air conditions were unexpectedly high and have been presented and discussed as a separate publication [*12*].

An analysis of variance (Table 11) was performed on the calculated polluted air corrosion rates. Both SO_2 and relative humidity produced highly significant positive effects (0.99 probability level) on the corrosion rate of galvanized steel. Excluding within chamber error, these two factors accounted for 94 percent of the variability. Ozone also appeared to be a significant factor at the 0.95 probability level; however, it only accounted for about 3 percent of the variability. Therefore, it was not considered in further analysis of the data.

According to accepted corrosion theory, zinc surfaces corrode only when wet. Therefore, the data in Table 10 may be reevaluated in terms of time-of-panel-wetness and geometric mean panel temperature (Table 8) rather than total time. To convert to corrosion rates during time-of-panel-wetness, the corrosion results in Table 10 were divided by the time-of-wetness expressed as a fraction (0.6125 for high relative humidity and 0.5175 for low relative humidity).

The corrosion of galvanized steel should be consistent with the following theoretical relationship

$$\text{corr} = (a_0\,\text{SO}_2 + e^{b-E/RT})\,t_w$$

where

corr = zinc thickness-loss, μm,
a_0, b = regression coefficients,
SO_2 = SO_2 concentration, $\mu g/m^3$,
t_w = time-of-wetness, year,
E = activation energy, cal/(g-mol K),
R = gas constant, 1.9872 cal/g-mol, and
T = geometric mean temperature of panels when wet, K.

A best fit of the experimental data yielded

$$\text{corr} = (0.0187\,\text{SO}_2 + e^{41.85 - 23\,240/RT})\,t_w$$

This empirical function accounts for 91 percent of the variability in the experimental data from the polluted exposure conditions. A comparison of the actual zinc thickness-loss values with predicted values is shown in Fig. 3.

Previous research has shown that zinc corrodes more rapidly in urban and industrial areas than in rural areas [*13,14*]. Researchers suspect that atmospheric pollutants, especially SO_2, accelerate the corrosion of zinc by preventing the formation of a protective film, which probably consists of

TABLE 11—*Analysis of variance of galvanized steel corrosion data for polluted exposure conditions.*

Factor	Contrast	Sum of Squares	Degrees of Freedom	Mean Square	F	R^2
SO_2	6.2188	618.7781	1	618.7781	189.61[a]	0.484
RH	6.0272	581.2318	1	581.2318	178.10[a]	0.455
O_3	1.5893	40.4146	1	40.4146	12.38[b]	0.032
NO_2	−0.2644	1.1188	1	1.1181	0.34	0.000
SO_2 × RH	0.0565	0.0512	1	0.0512	0.02	0.000
SO_2 × O_3	0.1374	0.3022	1	0.3022	0.09	0.000
SO_2 × NO_2	−0.8088	10.4668	1	10.4668	3.21	0.008
RH × O_3	0.5486	4.8147	1	4.8147	1.48	0.004
RH × NO_2	0.3598	2.0714	1	2.0714	0.63	0.002
O_3 × NO_2	−0.4093	2.6806	1	2.6806	0.82	0.002
Residual		16.3176	5	3.2635		0.013
Total		1278.2478	15			

NOTES—F uses the residual mean square in the denominator.

R^2 is the coefficient of determination excluding the within chamber variability.

[a] 0.99 probability level of significance.

[b] 0.95 probability level of significance.

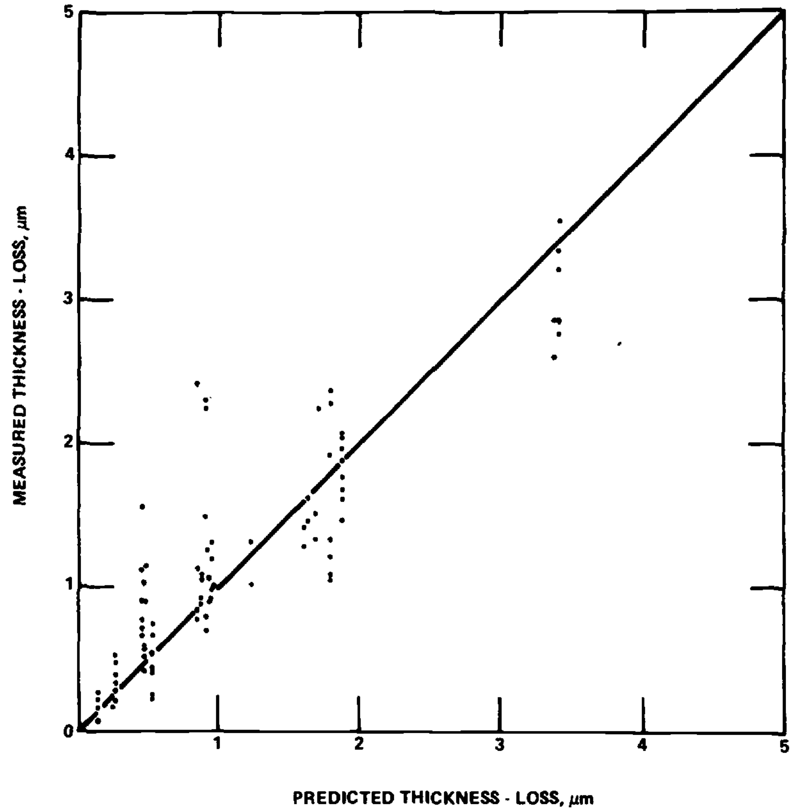

FIG. 3—*Comparison of predicted and actual thickness-loss values for galvanized steel exposed to laboratory controlled polluted conditions.*

an insoluble zinc oxide and carbonate mixture. Several investigators have developed relationships between the amount of zinc corrosion and atmospheric concentration of SO_2 [*4,10*]. The previous research, however, involved field exposures of high purity zinc panels to environmental factors that could not be controlled.

In the chamber study, galvanized steel panels were exposed to controlled levels of gaseous pollutants, temperature, and humidity. No attempt was made to remove oxygen or carbon dioxide from the air circulated through the chambers. These gases along with the pollutants were, therefore, readily available to react with the zinc coating during the time-of-panel-wetness.

Two reactions are believed to occur simultaneously in the presence of the chamber pollutants: (*a*) formation of zinc hydroxide or oxide, and (*b*) formation of zinc sulfate. The analysis of variance of the chamber data, however, indicated that of the three gaseous pollutants, only SO_2 significantly accelerated the corrosion rate. Therefore, the formation of sulfur containing

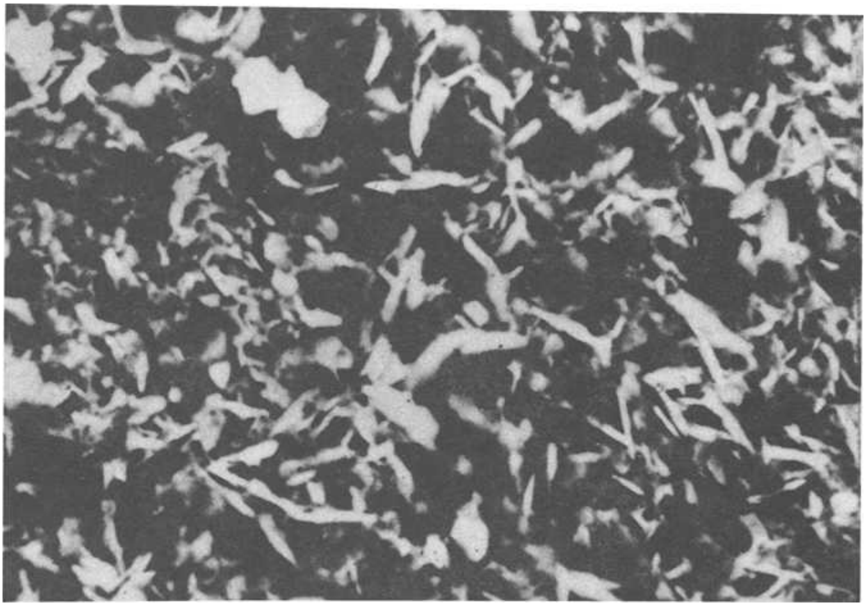

FIG. 4—*Scanning electron photomicrograph of an exposed galvanized steel panel showing uniformly dispersed crystalline material over the zinc surface.*

corrosion products would be expected. Scanning electron photomicrographs of exposed panels (Fig. 4) revealed crystalline material uniformly dispersed over the zinc surface. X-ray diffraction patterns of the corrosion products were complex and indicated one or more unidentifiable hydrated compounds. Microprobe scans, however, revealed sulfur atoms, likely in the form of sulfate, to be distributed uniformly over the zinc surface.

During the dew cycle, the pH of the thin layer of condensate that formed on the galvanized panels was measured and found to remain acidic (pH of 5.6). However, the zinc corrosion products (oxides or hydroxides and sulfates) are known to be soluble in acidic media. Corrosion rates, therefore, should remain constant with time because the acidic dew not only dissolves the corrosion products but distributes them uniformly across the zinc surface (Fig. 4). The process continues during each cycle of dew formation.

The reactant (oxygen) producing the hydroxide or oxide was readily available during exposure; thus, the reaction with the zinc surface should be activation controlled. In comparison, sulfur dioxide levels were considerably lower; therefore, the formation of sulfate should be diffusion controlled. Carbon dioxide was also readily available to react with the zinc coating; however, the protective zinc carbonate film was not likely to form in the presence of an acidic (sulfurous acid) medium.

The best fit of the corrosion data produced an empirical function that accounted for 91 percent of the variability. Unfortunately, the predictability of this relationship cannot be tested because no comparable field data exist for exposed galvanized steel. However, field data for the corrosion of pure zinc panels are available [4]. After making minor transformations in the empirical corrosion function, predicted corrosion values for galvanized steel were consistently lower than corrosion values for pure zinc measured during field exposures. The empirical function accounted for only 29 percent of the variability in the field data.

Summary

Results from a controlled environment chamber study show that concentration of SO_2 is a major factor in accelerating the corrosion rates of weathering steel and galvanized steel. For both metals, empirical relationships expressing corrosion rate as a function of SO_2 concentration, time-of-panel-wetness, and geometric mean temperature accounted for 91 percent of the variability in the experimental data. Using the empirical function for weathering steel, predicted corrosion agreed reasonably well with actual atmosphere corrosion measured in a previous field study. Unfortunately, no field data is available to adequately test the predictability of the empirical function for galvanized steel.

References

[1] Campbell, G. G., Schurr, G. G., Slawikowski, D. E., and Spence, J. W., *Journal of Paint Technology*, Vol. 46, 1974, pp. 59-71.

[2] Beloin, N. J., *Textile Chemist and Colorist*, Vol. 4, 1972, pp. 77-82.

[3] Beloin, N. J., *Textile Chemist and Colorist*, Vol. 5, 1973, pp. 128-133.

[4] Haynie, F. H. and Upham, J. B., *Materials Protection and Performance*, Vol. 9, 1970, pp. 35-40.

[5] Haynie, F. H. and Upham, J. B., *Materials Protection and Performance*, Vol. 10, 1971, pp. 18-21.

[6] Spence, J. W. and Haynie, F. H. in *Corrosion in Natural Environments, ASTM STP 558*, American Society for Testing and Materials, 1974, pp. 279-291.

[7] Spence, J. W., Stump, F. D., Haynie, F. H., and Upham, J. B., *EPA-650/3-75-001*, Environmental Protection Agency, Research Triangle Park, N.C., Jan. 1975.

[8] Guttman, H. and Sereda, P. J. in *Metal Corrosion in the Atmosphere*, ASTM STP *435*, American Society for Testing and Materials, 1968, pp. 326-359.

[9] Guttman, H. in *Metal Corrosion in the Atmosphere, ASTM STP 435*, American Society for Testing and Materials, 1968, pp. 223-239.

[10] Haynie, F. H. and Upham, J. B. in *Corrosion in Natural Environments, ASTM STP 558*, American Society for Testing and Materials, 1974, pp. 33-51.

[11] Spence, J. W. and Haynie, F. H., *Galvanic and Pitting Corrosion, ASTM STP 576*, American Society for Testing and Materials, 1976, pp. 132-146.

[12] Larrabee, C. P. and Ellis, O. B., *Proceedings*, American Society for Testing and Materials, Vol. 59, 1959, p. 183.

[13] Coburn, S. K. in *Metal Corrosion in the Atmosphere, ASTM STP 435*, American Society for Testing and Materials, 1968, p. 360.

D. R. Marx,[1] *W. R. Bitler,*[1] *and H. W. Pickering*[1]

Metallic Barriers for Protection of Contacts in Electronic Circuits from Atmospheric Corrosion

---

REFERENCE: Marx, D. R., Bitler, W. R., and Pickering, H. W., "**Metallic Barriers for Protection of Contacts in Electronic Circuits from Atmospheric Corrosion,**" *Atmospheric Factors Affecting the Corrosion of Engineering Metals, ASTM STP 646,* S. K. Coburn, Ed., American Society for Testing and Materials, 1978, pp. 48-57.

ABSTRACT: The effectiveness of a variety of 1 to 2-μm-thick barriers in preventing the interdiffusion of copper substrates with gold overplates was investigated. These studies were carried out at both elevated (400 and 500°C) and low temperatures (100 and 175°C). In the high temperature range, of the materials studied, only the cobalt and cobalt-5 weight percent phosphorous were found to be effective barriers. Their effectiveness was comparable to that of the nickel-8 weight percent phosphorous barrier reported by Turn.

The low temperature results were anomalous in that the specimens annealed at 100°C show greater penetration than those annealed at 175°C. It is proposed that this temperature effect is related to the concurrent recrystallization of the gold overplate taking place to a larger degree during the higher temperature diffusion anneal. Thus, at the lower temperature the high density of grain boundaries characteristic of as-plated structures is better preserved and leads to a larger overall (grain-boundary) diffusive flux.

KEY WORDS: corrosion, atmospheric corrosion, electronic circuits, circuit protection, nickel, nickel alloys, gold plating, barrier coatings, metal coatings

Miniaturization of electronic components and devices has resulted in atmospheric corrosion problems that are unique because minutely small quantities of contaminants and corrosion products, which cannot be detected by usual methods, can cause a significant degradation of performance or even total failure of a device. A good example of this and a well-recognized problem is the atmospheric corrosion of electrical contacts, as discussed by Frant [*1*][2] and by Antler [*2*]. Oxide or sulfide tarnish films on separable

---

[1] Graduate student, professor, and professor and chairman, respectively, Metallurgy Section, Department of Material Sciences, Pennsylvania State University, University Park, Pa. 16802.

[2] The italic numbers in brackets refer to the list of references appended to this paper.

contacts increase the contact resistance. For low force, low voltage contacts, films as thin as 100–500 Å may have sufficient resistance to cause an effective open circuit [*3*]. Furthermore, small changes in the contact resistance caused by minor changes in the tarnish film introduce circuit noise, which can be a problem in some applications, such as communications.

To prevent tarnish film formation these contacts are coated with a noble metal, most frequently, gold. However, to conserve gold and to reduce costs, the thickness of the coating is reduced to the minimum necessary to provide protection, that is, to prevent failure. One of the possible failure mechanisms is diffusion of the base metal, usually copper or one of its alloys, through the noble coating until it reaches the outer surface, where, in contact with the atmosphere, it tarnishes. This process may occur at an increasingly accelerated rate [*2*], suggesting that diffusive transport of the base metal through the coating becomes more rapid with time, as occurs with an associated local increase in temperature. Other aspects of corrosion in electronic applications can be found in a recent review by Frankenthal [*3*].

In order to minimize gold usage while maintaining a tarnish free contact surface, it is necessary to know the interdiffusion coefficient of the base metal in the noble metal coating. It would also be desirable to have a barrier layer between these metals to retard the diffusion process. Certain underplates are used as barriers which tend to block transport of the substrate metal into the noble-metal overplate. For example, nickel [*3–5*] and nickel alloys [*4–6*] layered between copper and a gold overplate are known to inhibit the diffusion of copper into the gold.

The purpose of the present paper is to evaluate the effectiveness of several metallic barriers in delaying the diffusive transport of copper through gold overplates, particularly at lower temperatures ($\lesssim 250^\circ$C) where grain boundary diffusion may be the primary transport process and for which relatively few data are available. The study was divided into two sections: (*a*) high-temperature studies, done at temperatures well above electronic component operating temperatures but in the temperature range of annealing and joining operations, and (*b*) lower-temperature studies with anneals corresponding to the upper limit of component operating conditions.

Experimental

Bars (7.6 cm long by 1.3 cm in diameter) of OFHC copper were plated with the following barrier metals: platinum, palladium, rhodium, chromium (from CrIII and CrVI baths), nickel and nickel alloys, cobalt and a cobalt alloy, and tin-nickel. A high-purity gold deposit served as the noble-metal overplate.

Prior to depositing the barrier metals, the bars were given the pretreatment shown in Table 1. Immediately following the surface pretreatment specimens were prepared with barriers which were nominally 1 to 2 μm

TABLE 1—*Pretreatment procedure for plating on copper.*

1. Alkaline soak cleaner at 80°C
    - 30g/litre Na_2CO_3
    - 30g/litre $Na_2P_4O_7$
    - 1g/litre Dupanol ME
2. Distilled H_2O rinse
3. Bright-dip at room temperature
    - 45.0% H_2SO_4
    - 22.0% HNO_3
    - 0.09% HCl
    - 32.9% H_2O
4. Distilled H_2O rinse
5. Surface activation for
    - (*a*) Electrodeposition
        - Direct current
        - 45 g/litre KCN
        - 6 V for 20 s
    - (*b*) Electrolessdeposition
        - 0.1 g/litre $PdCl_2$
        - 0.1 ml/litre HCl
        - Room temperature
        - 30 s immersion
6. Distilled H_2O rinse
7. Dilute H_2SO_4 dip (electrodeposition only)
8. Distilled H_2O rinse (electrodeposition only)

thick by electro- and electroless-deposition procedures shown in Table 2. Specimens with platinum, palladium, chromium, and cobalt barriers were given gold strikes and outgassed at 150°C and 10^{-5} torr for 5 h to prevent blistering, in accord with the recommendation of Turn [*4,5*].

Gold was plated subsequently from an Ehrhart bath [*9*] to thicknesses of up to 100 μm after a pretreatment which was essentially the same as that in Table 1 except for omission of the bright dip step. Specimens were prepared by cutting the bars into 0.3 to 0.4-cm-thick cross sections after discarding the top and bottom 1.3 cm of the bar.

For the diffusion anneals at low temperature (100 and 175°C) the specimens were stacked between alumina spacers in Pyrex boats, enclosed in evacuated Pyrex capsules, and placed in box-type muffle furnaces for 550 days. High-temperature (400 and 550°C), short-term (12 to 55 h) anneals were carried out by suspending a Pyrex basket loaded with the specimens and spacers in a vacuum annealing furnace controllable to ±2°C.

After annealing, the specimens were quenched, nickel-plated for edge protection, polished, and examined for the presence of blistering, cracking, porosity, and grain size. Analytical examination was performed on the cross section with a two-crystal ARL electron microprobe. Characteristic X-rays of the copper and the barrier were collected as the specimen was scanned across the copper barrier and gold overplate. Raw data were con-

TABLE 2—*Plating conditions for barriers on copper.*

Barrier	Concentration, g/litre	Temperature, °C	i, mA cm^{-2}	pH	Comment	Source
Palladium (Palladex IV)	10	45 to 65	3.2 to 6.5	9.0 to 9.5	vigorous agitation	Sel-Rex
Platinum (Platanex III)	10	75 to 85	11 to 32	very low	moderate agitation	Sel-Rex
Rhodium (Rhodex)	5	50	11	. . .	moderate agitation	Sel-Rex
Chromium (VI)	250 chromic acid 2.5 sulfate	43 to 49	106 to 124	. . .		Udylite
Chromium (Duramir III)	40	35 to 38	54 to 27	3.1 at 30°C	air agitation	duPont
Cobalt (Udyco CN-1)	90 to 105 $CoCl_2 \cdot 6H_2O$ 60 H_3BO_3 0.25 H_2O (30%)	49 to 54	32 to 38	2.5 to 3.5	air agitation	Udylite
Co$\simeq$5 weight %P	30 $CoCl_2 \cdot 6H_2O$ 10 $NaH_2PO_2 \cdot H_2O$ 35 $Na_3C_6H_5O_7 \cdot 5.5H_2O$ 50 NH_4Cl	>90	. . .	9 to 10	electroless moderate agitation	*Ref 7*
Ni-B (Nibel-Sylex 201)	dimethylamine borane	65	. . .	6.5	electroless	duPont
Ni-8 weight %P	30 nickel chloride 100 sodium citrate 50 ammonium chloride 10 sodium hypophosphite	94	. . .	8.6	electroless	duPont
Nickel (sulfamate)	75 323 nickel sulfamate 0 to 15 nickel chloride 30 to 45 boric acid	27 to 49	22 to 135	3.0 to 4.0	agitation	Sel-Rex
Nickel (Lectro-Nic 10-03S)	75 323 nickel sulfamate 40.5 boric acid 63.4 ml/litre anode activator 1.06 stress reducer	54	43	3.0	moderate agitation	Sel-Rex
Tin-nickel	58.4 $SnCl \cdot 2H_2O$ 300.0 $NiCl \cdot 6H_2O$ 56.2 NH_4HF_2	65	27	2.5 to 2.8	moderate agitation	*Ref 8*

verted to concentration-versus-distance profiles employing Colby's MAGIC IV computer program [*10*].

The false gradient due to the finite size of the probed volume was taken into account to a first approximation by applying the correction used by Turn [*4*]. This correction subtracts the profile of an undiffused standard from that of a diffused specimen. Penetration distances were similarly corrected by subtracting the distance between the barrier midplane or Matano interface (unbarriered specimens) and the 7.5 weight percent copper composition plane in the gold overplate of a standard specimen, from that of a diffused specimen. This particular treatment of the data, though biased in the direction of giving shorter than actual penetrations by 1.5 to 2.0 μm, provided an opportunity for comparison with the earlier results [*4,5*].

Results and Discussion

The high-temperature results are shown in Table 3. The cobalt and cobalt-5 weight percent phosphorus (Co-5 weight percent P) barriers are the most effective of those investigated in this work, and are comparable to the nickel-8 weight percent phosphorus (Ni-8 weight percent P) barrier investigated by Turn [*4,5*]. Chromium and tin-nickel failed to impede copper penetration significantly and are similar to the precious metals in this regard.

Anomalous results were obtained in the low-temperature, long-time studies. Recalling that diffusion is a thermally activated process, it would be expected that specimens annealed at 175°C would show a greater copper penetration than those annealed at 100°C. Table 4 shows that opposite results have been obtained. In addition, Table 4 shows the relative effectiveness of different barriers at 175 and 100°C, that is, significant void formation occurs for certain barriers at 100 but not at 175°C, and that the copper level is actually higher at the gold surface than within the gold overplate for the nickel-barriered specimens. This copper buildup negates the otherwise favorable (low) penetration data for Ni-8 weight percent P and nickel (sulfamate) barriers. The values reported for the barriers are the average of from 3 to 12 scans on 1 to 4 specimens. Reproducibility was ±1 μm for small penetrations ($\lesssim 5$ μm), and ranged upwards to ±4 μm for the largest penetrations due to an increased roughness of the interface and variation from specimen to specimen.

Unbarriered copper/gold couples were examined in hopes of explaining the aforementioned temperature discrepancy. A Boltzmann-Matano graphical diffusion analysis [*11*] of several specimens showed that the apparent volume chemical-diffusion coefficient at 100°C was about an order of magnitude larger than that at 175°C. The measured coefficient at 100°C was above, whereas that at 175°C was essentially on the extrapolation of the high-temperature log D versus $1/T$ plot for gold plated on copper determined by Pinnel and Bennett [*12*], Fig. 1. At 100°C, Pinnel and Bennett also

TABLE 3—*High temperature copper penetration through different 1 and 2-μm-thick barriers and into 20-μm gold overplates, in terms of the distance from the midplane of the barrier to the 7.5 weight percent copper plane in the gold overplate.*

		Diffusion Heat Treatments		
Barrier	Nominal Barrier Thickness, μm	400°C, 24 h	400°C, 53 h	550°C, 12 h
None[a]	...	7	13	18
Platinum[a]	1	9	16	18
	2	7	16	17
Palladium[a]	1	7	14	16
	2	6	10	18
Rhodium[a]	1	6	14	14
	2	5	18	17
Ni-8 weight %P[a]	1	1	1	8
	2	ND	ND	ND
Ni (sulfamate)[a]	1	1	6	10
	2	5	11	12
Chromium[a] (CrVI bath)	1	ND	1	10
	2	ND	ND	ND
Chromium (CrIII bath)	1	ND	1(3)[b]	5(15)[b]
	2	ND	ND(2)[b]	5(12)[b]
Cobalt	1	2	1	10
	2	ND	ND	ND
Co≃5 weight %P	1	2	1	10
	2	ND	ND	1
Tin-nickel	1	5	8	[c]
	2	5	7	[c]

[a] Data of Turn [*4,5*] presented for comparison.

[b] Penetration values within the parentheses are through the cracked regions of the CrIII specimens.

[c] The tin-nickel has completely gone into solution.

NOTE—ND = nonmeasurable copper level in the gold (implies less than 1 μm penetration).

experienced higher-than-extrapolated values, though theirs were lower than the values in the present work; the scatter in their values was significant and is indicated by the crosshatched area in Fig. 1. Though not shown in Fig. 1, in a recent paper Hall, Morabito, and Panousis [*13*] found the chemical diffusion coefficient at 100°C to be even lower and to lie on the extrapolation.

Figure 2 shows in cross section the microstructures of the gold overplate for specimens annealed at 100 and 175°C. In the as-plated condition (not shown), the typical fine-grained columnar structure was observed. Some recrystallization of the as-plated columnar structure is evident. The specimen annealed at 100°C shows only partial recrystallization of the gold; that at 175°C shows a more complete recrystallization and a greater amount of grain growth.

A rational explanation of the low temperature results can be formulated on the basis of the variation in grain size of the gold overplate. At 175°C

TABLE 4—*Low temperature copper penetration through different 1-μm-thick barriers and into 20-μm-thick gold overplates, in terms of the distance from the midplane of the barrier to the 7.5 weight percent copper plane in the gold overplate.*

Temperature, °C	Barrier	Penetration, μm	Comments
175	none	5	...
175	rhodium	ND	...
175	platinum	ND	...
175	palladium	ND	...
175	chromium (VI)	3	...
175	Ni-B	ND	...
175	Ni-8 weight %P	ND	...
175	nickel (sulfamate)	ND	...
175	nickel (10-03S)	ND	...
100	none	15	significant void formation
100	rhodium	>20	significant void formation
100	platinum	>20	significant void formation
100	palladium	6	significant void formation
100	chromium (VI)	9	significant void formation
100	Ni-B	>20	copper build-up on surface
100	Ni-8 weight %P	3	copper build-up on surface
100	nickel (sulfamate)	1	copper build-up on surface
100	nickel (10-03S)	10	copper build-up on surface

NOTE—ND = nonmeasurable copper level in the gold (implies less than 1 μm penetration).

recrystallization and grain growth is relatively rapid, whereas grain boundary diffusion is significant only for a relatively short (initial) period during existence of the favorably oriented, fine columnar structure. Thus, only a small penetration is observed. At 100°C, on the other hand, recrystallization is much slower and is not complete even at the end of the diffusion anneal; thus, the numerous, favorably oriented grain boundaries of the columnar or fine recrystallized structures or both contribute appreciably to the overall transport process and yield a greater penetration than expected solely on the basis of volume-diffusion transport. For this reason, in the case of specimens at 100 and 175°C, an actual reversal in the usual temperature dependence is observed.

The diffusivity variation reported by Pinnel and Bennett [*12*] in the low-temperature region is consistent with this proposed grain-size model, but cannot be used as a check of it since grain sizes are not reported in their paper. Such an effect is different than the one proposed by Pinnel and Bennett [*12*] in which the recrystallization process itself is considered to enhance the penetration of copper through gold.

The extent of the variation in penetration rate at any given temperature ($\lesssim$250°C) corresponds to a variation in the effective D, ranging upward from the volume diffusion value (obtained by extrapolation of high-temperature diffusivity data to the temperature in question). This could easily amount to a manyfold change in penetration rate, for example, at 100°C,

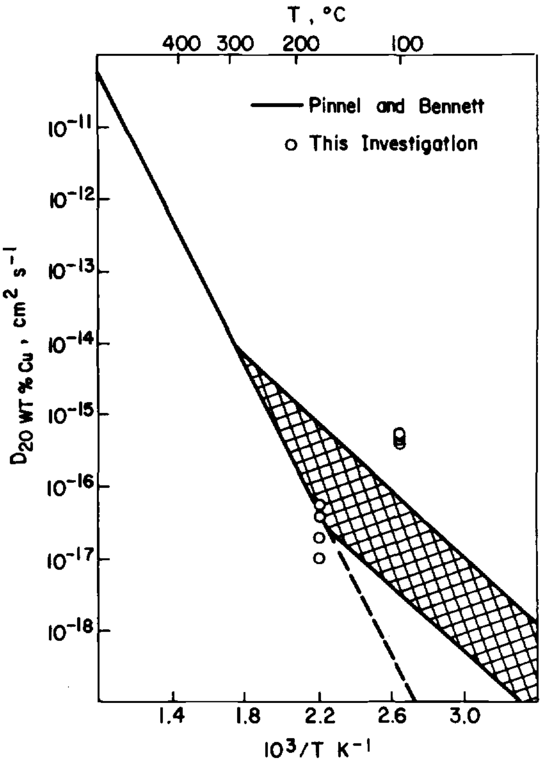

FIG. 1—*Comparison of measured diffusivities at 100 and 175°C in this investigation with those reported by Pinnel and Bennett* [10].

by conversion to a large-grained equiaxed structure, the interdiffusivity could, in principle, be reduced from the measured value of about 5×10^{-16} cm^2 s^{-1} to a limiting (volume diffusion) value of about 10^{-19} cm^2 s^{-1}. This corresponds to a hundredfold decrease in the penetration rate.

For those applications which do not preclude a soft, coarse-grained structure, a potential technological advance may be achieved by inserting into the processing sequence an annealing step designed to produce a large grain size in the overplate. A suitable time-at-temperature anneal would be that which develops a large grain size accompanied by a small or negligible penetration of the substrate metal(s) into the overplate. Other consequences of the anneal would also have to be considered [*14*]. Since the recrystallization grain size is known to be a function of time and temperature of the anneal, as well as the total strain and other factors, there will be an optimum time-at-temperature treatment to accomplish the aforementioned. Use of a barrier underplate would further restrict substrate penetration

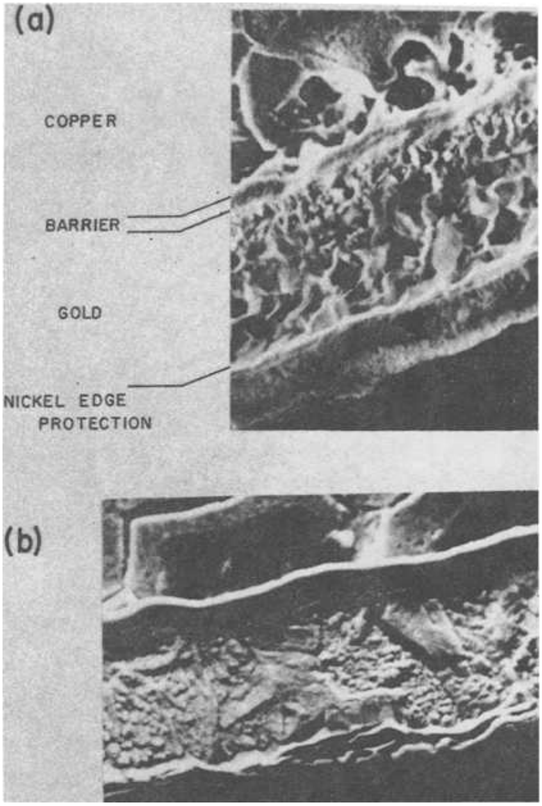

FIG. 2—*Cross-sectional micrographs of diffusion couples annealed 550 days at* (a) *100°C showing a fine-grained partially recrystallized structure, and* (b) *175°C showing a large-grained fully recrystallized structure; orientation of phases is same as in* (a).

into the overplate during the anneal as well as during subsequent service at operating temperatures.

Conclusions

The results show that for the 400 to 550°C range cobalt and Co-5 weight percent P barriers are essentially comparable to the Ni-8 weight percent P barrier which was shown previously to be effective [*4,5*] for delaying the diffusive transport of copper through gold overplates. At the lower temperatures it was found that transport of copper through the gold overplate is strongly dependent on the grain size of the gold. The larger the recrystallized grain structure is, the closer the observed interdiffusivity is to the lower limiting value given by volume diffusion. At the low temperatures for which the grain boundary diffusivity is large compared to the volume diffusivity, average penetration of the substrate metal into the overplate can be, in principle, greatly reduced by converting the as-plated, favorably oriented columnar structure of the overplate to a recrystallized large-grained structure.

Acknowledgments

The authors gratefully acknowledge the assistance of J. Turn, Jr. who initiated the low temperature runs, E. L. Owen for input on the initial planning of the project, R. P. Frankenthal, Bell Laboratories, for his helpful comments, the authors of Ref *13* for providing a preprint of their paper prior to publication, and the assistance of Sel-Rex Company, The Udylite Corporation, and E. I. duPont de Nemours Company, Inc. in preparing some of the specimens. This work was partially supported by the American Electroplaters' Society, Project No. 29.

References

[*1*] Frant, M. S., *Plating,* Vol. 48, 1961, p. 1305.
[*2*] Antler, M., *Plating,* Vol. 57, 1970, p. 615.
[*3*] Frankenthal, R. P. in *Properties of Electrodeposits: Their Measurement and Significance,* R. Sard, H. Leidheiser, Jr., and F. Ogburn, Eds. The Electrochemical Society, Inc., Princeton, N.J., 1975, p. 142.
[*4*] Turn, J. C., Jr., Masters thesis, The Pennsylvania State University, University Park, 1973.
[*5*] Turn, J. C., Jr. and Owen, E. L., *Plating,* Vol. 61, 1974, p. 1015.
[*6*] Marx, D. R., Masters thesis, The Pennsylvania State University, University Park, 1976.
[*7*] Brenner, A. and Riddell, G., *Proceedings,* American Electroplaters' Society, Vol. 34, 1947, p. 156.
[*8*] Langdon, P. H. in *Metal Finishing Guidebook,* Vol. 34, Metals and Plastics Publications, Inc., Westwood, N.J., 1966, p. 314.
[*9*] Ehrhardt, R. A., *Proceedings,* American Electroplaters' Society, Vol. 47, 1960, p. 78.
[*10*] Colby, J. W., *Advanced X-Ray Analysis,* Vol. 11, 1968, p. 287.
[*11*] Lundy, T. S., *Techniques of Metals Research IV* (9A), Interscience Publishers, New York, 1971.
[*12*] Pinnel, M. R. and Bennett, J. E., *Metal Transactions,* Vol. 3, 1972, p. 1989.
[*13*] Hall, P. M., Morabito, J. M., and Panousis, N. T., *Thin Solid Films,* in press.
[*14*] Raub, Ch. J., Khan, H. R., and Lendvay, J., *Gold Bulletin*, Vol. 9,(4), 1976, p. 123.

M. A. Pelensky,[1] *J. J. Jaworski,*[1] *and A. Gallaccio*[1]

Corrosion Investigations at Panama Canal Zone

REFERENCE: Pelensky, M. A., Jaworski, J. J. and Gallaccio, A., "**Corrosion Investigations at Panama Canal Zone,**" *Atmospheric Factors Affecting the Corrosion of Engineering Metals, ASTM STP 646,* S. K. Coburn, Ed., American Society for Testing and Materials, 1978, pp. 58-73.

ABSTRACT: This paper reports on the progress of investigations being conducted at Panama Canal Zone, relative to corrosion of dissimilar metal couples exposed in the atmosphere, in the soil, and in seawater. Machined specimens of aluminum, brass, magnesium, Monel, steel, stainless steel, and titanium alloys are included in this study.

Exposure of dissimilar and similar (control) metal couples was initiated over 2 years ago for a planned maximum 5-year exposure. Couple replicates (four of each metal) are removed from exposure periodically and returned to the laboratory for visual examination and weight loss determinations to evaluate the corrosion effects of each of the environments on the various couples. A total of seven removals from each environmental exposure is planned during the course of the corrosion investigations. To date, five removals of atmospheric specimens, five removals of seawater immersion specimens, and four removals of soil burial specimens, have been completed over a 2-year period and evaluated by this laboratory. Results of findings to date are presented in this paper.

KEY WORDS: corrosion, galvanic corrosion, pitting, crevice, alloys, atmospheric exposure, soil burial, seawater

Military materiel is deployed and used worldwide under varied and sometimes severe environmental conditions. In the design and fabrication of military equipment, dissimilar as well as similar metal combinations are often employed because of structural, electrical, or other design criteria. Consequently, galvanic corrosion problems may be encountered, particularly in tropical or marine environments.

To aid the designer in the selection of metal combinations for use in

---

[1] Chemical engineer, chemist, and supervisory chemist, respectively, Materials and Manufacturing Technology Division, U.S. Armament Research and Development Command, Philadelphia, Pa. 19137.

military equipment, there is a continuing need for specific data concerning corrosion tendencies of metal combinations exposed to the more severe environments (including tropical or marine atmospheres). The intent of this study is to investigate these tendencies.

An initial report[2] includes specimen details, cleaning procedures and early preliminary results. This report includes results of exposures to date. However, since the study is still in progress (roughly 60 percent completed), only interim results are presented. Approximately two additional years of exposure are planned, and a final report of findings will be prepared after completion of the study.

Experimental

Materials

The alloys included in this study are 6061-T6 and 7075-T6 aluminum, 360 brass, AZ31 magnesium, 400 Monel, 4340 steel, Type 316 stainless steel, and titanium 6Al-4V.

Atmospheric specimens are flat, rectangular plates 0.55 by 2.54 by 3.81 cm (0.215 by 1.0 by 1.5 in.). The plates are coupled using a stainless steel machine screw insulated from the faces of the specimen.

Specimens for soil burial and seawater immersion are 2.54 cm in diameter by 1.27 cm long (1.0 by 0.5 in.) coupled using a steel screw but separated by a plexiglass rod, with a lengthwise drilled hole to accommodate the fastening screw.

Specimen details have been described and illustrated previously.[2]

Procedure

Prior to exposure, specimens were individually cleaned, and specimen weights were determined to the nearest milligram.

ASTM exposure test racks fabricated from Monel are employed for the atmospheric exposures at the Fort Sherman, Panama Canal Zone, open field site. This exposure was initiated in April 1973 and seven exposure periods are planned at 2, 4, 8, 15, 24, 36, and 48 months.

Soil burial couples are installed at the water table, buried at a depth of 1.2 m (4 ft) below the soil surface, in an area adjacent to the open field site. This exposure was initiated in October 1973 and seven exposure periods are planned at 2, 6, 12, 24, 36, 48, and 60 months.

The seawater couples are completely immersed approximately 1.4 m

---

[2] Pelensky, M. A., Jaworski, J. J., and Gallaccio, A. in *Galvanic and Pitting Corrosion—Field and Laboratory Studies, ASTM STP 576,* American Society for Testing and Materials, 1976, pp. 94–113.

(4.5 ft) below the water surface at low tide and approximately 1.7 m (5.5 ft) below the surface at high tide in Manzanillo Bay at the Coco Solo Naval Station, Panama Canal Zone. The seawater exposure was initiated in October 1973, and seven exposure periods are planned at 2, 4, 7, 12, 18, 28, and 42 months.

Details of procedure, including cleaning prior to and after exposures, exposure site descriptions, and specimen rack mounting, have been described previously.[2]

Discussion of Results

Total (general, galvanic, crevice) corrosion rates, in mm/year, are shown in the tables and figures. The corrosion rates shown are of the alloy indicated, when coupled with the various dissimilar metals. For comparison purposes, the similar metal average corrosion rate is also indicated. Table 1 presents atmospheric corrosion rates at 5 exposure periods (2, 4, 8, 15, and 24 months). It may be noted from Table 1 and Fig. 1 that the total corrosion rate after the 2-month exposure of AZ31 magnesium is greatest when coupled with steel (0.096 mm/year) and Monel (0.092 mm/year) and least when coupled with the aluminum alloys (0.047 mm/year). No correction has been made at this time for corrosion encountered with similar

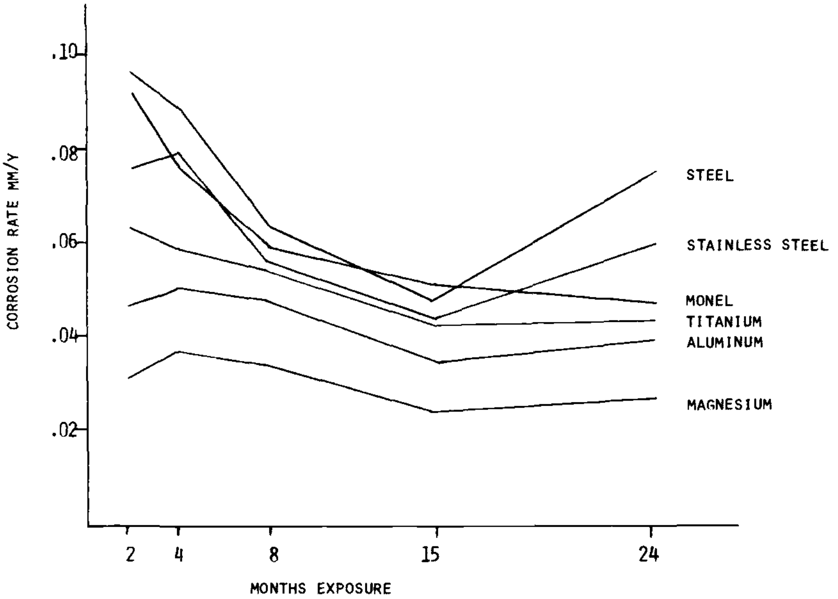

FIG. 1—*Magnesium couples in atmospheric exposure.*

TABLE 1—*Atmospheric exposure corrosion rates, mm/year.*

Alloy	Exposure Time, months	Magnesium	Stainless Steel	Steel	6061 Aluminum	7075 Aluminum	Brass	Monel	Titanium
AZ31 magnesium	2	0.031	0.076	0.096	0.047	0.047	0.074	0.092	0.063
	4	0.037	0.079	0.089	0.050	0.040	0.066	0.077	0.059
	8	0.034	0.057	0.064	0.048	0.048	0.064	0.059	0.055
	15	0.025	0.045	0.049	0.036	0.037	0.048	0.052	0.044
	24	0.028	0.061	0.076	0.040	0.039	0.051	0.049	0.045
4340 steel	2	0.033	0.071	0.069	0.069	0.061	0.068	0.074	0.072
	4	0.018	0.050	0.055	0.055	0.050	0.050	0.050	0.057
	8	0.014	0.036	0.037	0.038	0.036	0.036	0.036	0.037
	15	0.013	0.047	0.046	0.030	0.031	0.038	0.044	0.049
	24	0.011	0.049	0.048	0.026	0.025	0.037	0.049	0.047
6061-T6 aluminum	2	0.002	0.006	0.005	0.002	0.002	0.006	0.005	0.005
	4	0.001	0.002	0.006	0.002	0	0.004	0.002	0.002
	8	0.001	0.001	0.004	0.001	0.001	0.002	0.001	0.002
	15	0	0.002	0.006	0.001	0.001	0.003	0.003	0.003
	24	0	0.003	0.007	0.001	0.001	0.007	0.003	0.003
7075-T6 aluminum	2	0.003	0.007	0.009	0.005	0.003	0.010	0.007	0.007
	4	0.002	0.005	0.005	0.002	0.003	0.004	0.003	0.004
	8	0.001	0.003	0.004	0.001	0.001	0.003	0.003	0.003
	15	0	0.003	0.016	0.002	0.001	0.005	0.003	0.003
	24	0	0.003	0.012	0.002	0.001	0.010	0.003	0.004
360 brass	2	0.003	0.009	0.006	0.005	0.005	0.007	0.008	0.008
	4	0.001	0.004	0.003	0.002	0.002	0.003	0.004	0.003
	8	0.001	0.002	0.002	0.001	0.001	0.001	0.002	0.002
	15	0.001	0.002	0.002	0.001	0.001	0.001	0.001	0.001
	24	0	0.002	0.002	0.001	0.001	0.001	0.001	0.001

NOTE—Essentially zero corrosion rate for Type 316 stainless steel, 400 Monel, and titanium 6Al-4V specimens.

metal coupling. However, after a 2-month exposure, the corrosion rate for magnesium coupled with magnesium is 0.031 mm/year.

The data indicate the trend of the magnesium total atmospheric corrosion rates. The initial relatively high corrosion rate decreased with time because of the limited protection afforded by the corrosion accumulation on the specimen surface. A leveling off of corrosion rate is indicated after a 15-month exposure, except where coupled with steel and stainless steel where the magnesium corrosion rate increases again.

The corrosion rates of magnesium-magnesium couples (Table 2) roughly parallel those of magnesium coupled with dissimilar alloys except during the early months where the rate of the top-positioned specimen is still increasing (beyond the 2-month exposure). An appreciable difference in rates between the top and bottom specimens is indicated.

TABLE 2—*Corrosion rates for atmospheric exposure of upper and lower similar specimens, mm/year.*

Exposure Time, months	AZ31 Magnesium		4340 Steel	
	Top	Bottom	Top	Bottom
2	0.034	0.029	0.063	0.077
4	0.046	0.028	0.055	0.054
8	0.041	0.027	0.032	0.043
15	0.031	0.020	0.035	0.047
24	0.033	0.024	0.038	0.058

NOTE—6061-T6 and 7075-T6 aluminum alloys, 360 brass, and 400 Monel showed no apparent significant difference between upper and lower specimens. Essentially zero corrosion rate resulted for Type 316 stainless steel and titanium 6Al-4V specimens.

The data for the 4340 steel in atmospheric exposure (Table 1 and Fig. 2) indicate a high initial corrosion rate decreasing with exposure time, and a tendency toward leveling off after the 8-month exposure. The greatest rates occur in coupling with stainless steel and Monel, and the least, as expected, in coupling with magnesium, which affords sacrificial protection to the steel. Note, however, that the similar coupling of steel with steel (Table 2) indicates a corrosion rate of the bottom steel specimen to be even greater than when steel is coupled with dissimilar metals. (The similar couples of magnesium show greater attack on the top specimen.)

Very little corrosion of the aluminum and brass alloys and essentially zero corrosion rate is indicated for Type 316 stainless steel, Monel, and titanium 6Al-4V specimens. No significant difference was apparent between the top and bottom similar couple specimens of 6061-T6 aluminum, 7075-T6 aluminum, and 360 brass.

Table 3 presents results of 2, 6, 12, and 25-month soil burial exposures.

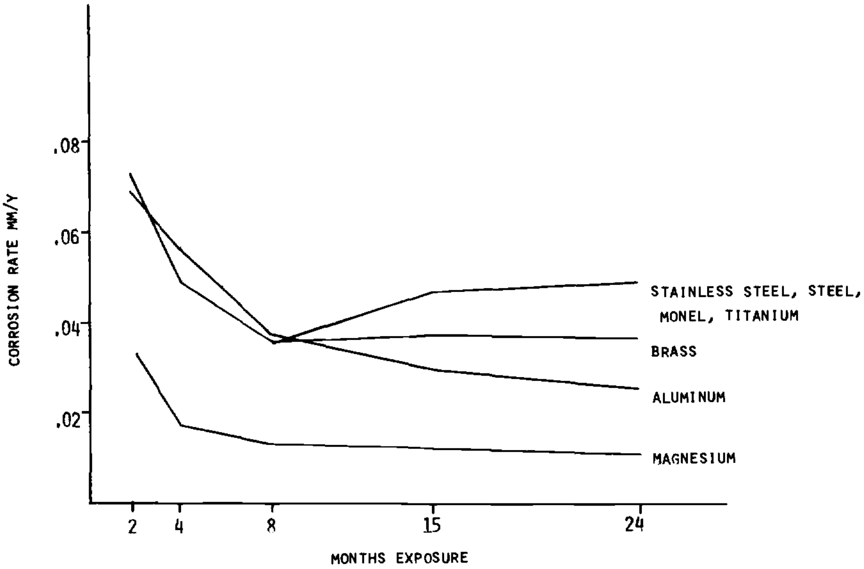

FIG. 2—*Steel couples in atmospheric exposure.*

Coupling of AZ31 magnesium with steel, stainless steel, and Monel resulted in the greatest magnesium attack (Fig. 3).

The 4340 steel shows a tendency toward slightly increased attack when

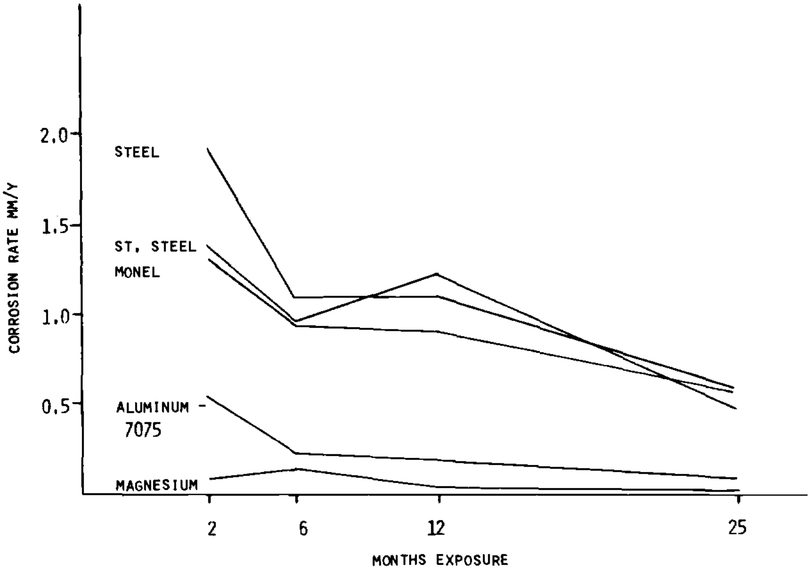

FIG. 3—*Magnesium couples in soil burial exposure.*

TABLE 3—*Soil burial exposure corrosion rates, mm/year.*

Alloy	Exposure, months	Magnesium	Stainless Steel	Steel	6061 Aluminum	7075 Aluminum	Brass	Monel	Titanium
AZ31 magnesium	2	0.093	1.398	1.920	0.264	0.551	0.967	1.322	1.021
	6	0.137	0.953	1.099	0.164	0.233	0.932	0.936	0.745
	12	0.045	1.225	1.108	0.093	0.208	0.848	0.912	0.562
	25	0.029	0.490	0.580	0.056	0.109	0.561	0.603	0.497
4340 steel	2	0.005	0.069	0.060	0.048	0.048	0.057	0.061	0.057
	6	0.001	0.104	0.085	0.087	0.100	0.113	0.119	0.091
	12	0.001	0.082	0.081	0.068	0.080	0.090	0.083	0.074
	25	0.001	0.055	0.058	0.040	0.057	0.069	0.062	0.062
6061-T6 aluminum	2	0.067	0.003	0.003	0.003	0.003	0.004	0.007	0.004
	6	0.017	0.008	0.001	0.005	0.009	0.011	0.013	0.008
	12	0.009	0.008	0.006	0.002	0.001	0.010	0.011	0.006
	25	0.003	0.006	0.003	0.001	0.005	0.007	0.008	0.005
7075-T6 aluminum	2	0.044	0.006	0.003	0.003	0.013	0.003	0.004	0.003
	6	0.019	0.017	0.001	0.006	0.011	0.020	0.020	0.018
	12	0.021	0.016	0.001	0.009	0.007	0.019	0.012	0.016
	25	0.006	0.011	0.002	0.001	0.005	0.015	0.016	0.013
360 brass	2	0.004	0.016	0.006	0.006	0.005	0.005	0.005	0.005
	6	0.001	0.015	0.001	0.001	0.001	0.007	0.014	0.011
	12	0	0.012	0	0.001	0	0.005	0.009	0.011
	25	0.001	0.007	0	0	0.001	0.004	0.008	0.007
400 Monel	2	0	0.003	0.001	0.001	0.001	0.001	0.001	0
	6	0.001	0.009	0	0.001	0.001	0.004	0.005	0.009
	12	0	0.010	0	0.001	0	0.002	0.004	0.008
	25	0	0.007	0	0	0	0.002	0.004	0.005

NOTE—Essentially zero corrosion rate for Type 316 stainless steel and titanium 6Al-4V specimens.

coupled with brass and Monel and somewhat less when coupled with 6061-T6 aluminum; appreciable sacrificial protection is indicated when coupled with magnesium (Fig. 4).

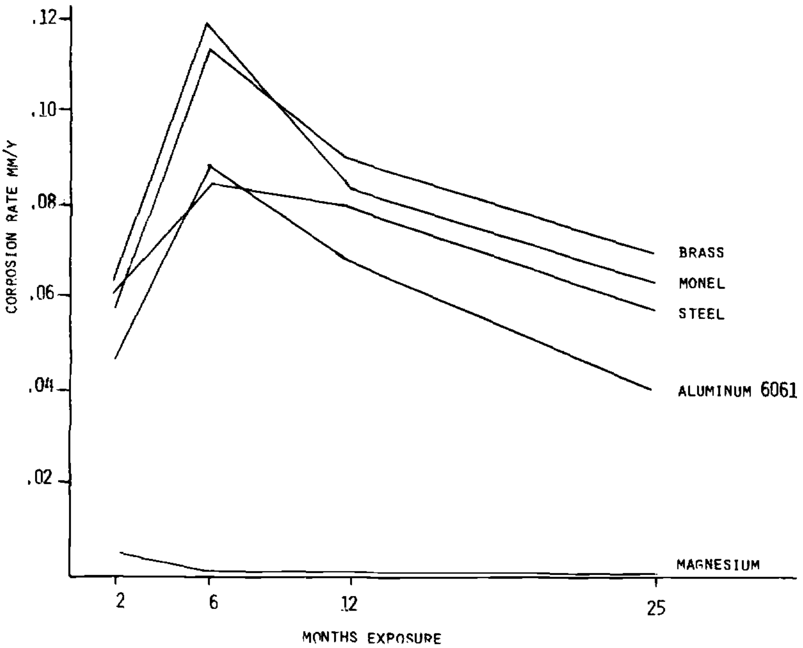

FIG. 4—*Steel couples in soil burial exposure.*

Significant corrosion rates of 6061-T6 and 7075-T6 aluminum alloys are indicated at the early exposure period (2 months) when coupled with magnesium, but little or no corrosion of the aluminum beyond the initial attack is indicated (see Table 3). Relatively low corrosion rates of aluminum coupled with the other alloys are indicated.

Corrosion rates of the other alloys (Type 316 stainless steel, 360 brass, 400 Monel, and titanium 6Al-4V) when exposed in the soil are considered slight or negligible.

Seawater immersion results are presented in Table 4. Extensive corrosion and complete early dissolution of magnesium occurs as expected when coupled with stainless steel, steel, brass, Monel, and titanium. Heavy corrosion is also evident in similar magnesium-magnesium coupling.

The Type 316 stainless steel evidences essentially no corrosion when coupled with magnesium, steel, aluminum, and brass alloys. However, in stainless-stainless coupling and in dissimilar coupling with Monel and titanium, crevice pitting attack occurs. It should be noted, however, in

TABLE 4—*Seawater immersion corrosion rates, mm/year.*

Alloy	Exposure, months	Magnesium	Stainless Steel	Steel	6061 Aluminum	7075 Aluminum	Brass	Monel	Titanium
AZ31 magnesium	2	1.581	SM	SM	2.336	5.640	12.122	[b]	10.369
	4	1.293	. . .	. . .	2.149	4.732	7.660	[b]	9.893
	7	1.021	. . .	. . .	1.724	6.165	[b]	6.281	[b]
	12	0.811	. . .	. . .	[b]	[b]	[b]	[b]	[b]
	18	SM[a]	. . .	. . .	1.628	. . .	. . .	[b]	
316 stainless steel	2	0	0.097[c]	0	0	0	0	0.105[c]	0.088[c]
	4	0	0.034[a]	0	0	0	0	0.033[c]	0.017[c]
	7	0	0.036[c]	0	0	0	0	0.061[c]	0.028[c]
	12	0	0.013[c]	0	0	0	0	0.028[c]	0.015[c]
	18	0.003	0.551[c]	0	0	0	0	. . .	0.482
4340 steel	2	0.024	1.143	0.635	0.018	0.020	1.257	1.238	1.015
	4	0.093	0.831	0.468	0.004	0.006	0.802	0.813	0.813
	7	SM	0.770	0.612	0.012	0.014	0.921	0.922	0.725
	12	SM	0.436	0.289	0.005	0.004	0.542	0.453	0.328
	18	SM	0.596	0.338	0.005	0.004	0.504	0.535	0.589
6061-T6 aluminum	2	0.449	0.378	0.252	0.043	0.073	0.437	0.385	0.304
	4	0.782	0.275	0.176	0.021	0.024	0.233	0.256	0.196

	7	0.864	0.302	0.189	0.017	0.017	0.288	0.288	0.294
	12	0.698	0.171	0.107	0.007	0.010	0.186	0.200	0.153
	18	0.645	0.139	0.081	0.006	0.031	0.118	0.148	0.153
7075-T6 aluminum	2	5.143	0.465	0.340	0.013	0.040	0.411	0.490	0.613
	4	4.145	0.303	0.187	0.009	0.029	0.301	0.298	0.306
	7	3.563	0.297	0.253	0.016	0.023	0.275	0.229	0.261
	12	2.097	0.212	0.135	0.002	0.014	0.189	0.193	0.173
	18	1.445	0.086	0.113	0.002	0.049	0.142	0.172	0.164
360 brass	2	0.009	0.339	0.006	0.007	0.005	0.124	0.293	0.179
	4	0.004	0.184	0.003	0.005	0.002	0.106	0.190	0.124
	7	0.004	0.159	0.008	0.022	0.008	0.190	0.223	0.133
	12	0.002	0.130	0.002	0.001	0.002	0.139	0.160	0.146
	18	0.001	0.110	0.001	0.001	0.001	0.115	0.146	0.111
400 Monel	2	0.001	0.011	0.001	0.001	0	0.002	0.034	0.010
	4	0.001	0.015	0.001	0.001	0	0.002	0.006	0.007
	7	0.001	0.009	0.002	0.001	0.001	0.002	0.008	0.010
	12	0.001	0.006	0.001	0	0.001	0.002	0.007	0.010
	18	0.001	0.015	0.001	0	0	0.001	0.027	0.025

NOTE—Essentially, zero corrosion rate for the titanium 6Al-4V specimens.

[a] SM = Specimens missing.

[b] Total dissolution of magnesium presumed.

[c] Stainless steel attack-crevice pitting.

several instances of coupling with Monel, that stainless is not attacked, while Monel is preferentially attacked.

Increased attack on 4340 steel in seawater occurs in coupling with stainless steel, brass, Monel, and titanium alloys. Protection is afforded by coupling with the magnesium and aluminum alloys.

The most severe attack on the 6061 and 7075 aluminum alloys occurs when these are coupled with magnesium, and this is attributable to cathodic attack by generated alkali. All other couplings resulted in galvanic attack on the aluminum (Fig. 5).

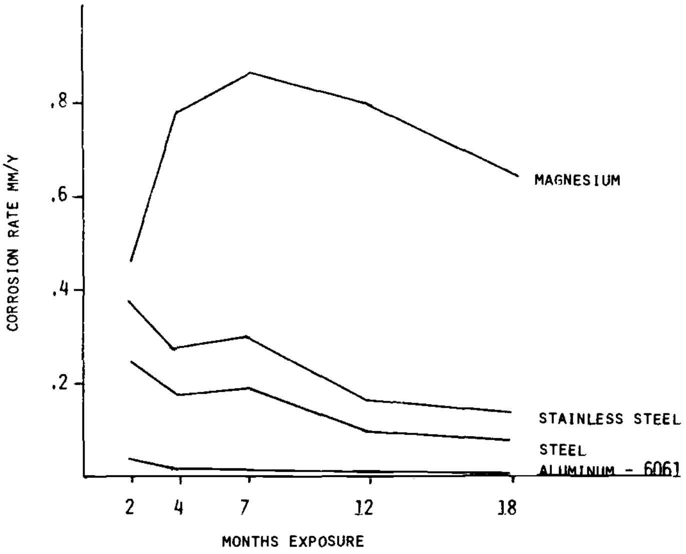

FIG. 5—*6061 aluminum couples in seawater exposure.*

The 360 brass is protected when coupled with magnesium, steel, and aluminum; attack is accelerated when coupled with the other alloys.

The 400 Monel is protected when coupled with magnesium, steel, aluminum, and brass alloys; however, pitting of the Monel occurs when coupled with titanium and also in similar Monel-Monel coupling, as well as in some instances of coupling with stainless steel.

No corrosion of titanium was observed in this environment. Corrosion rates of similar metal couples are presented in Tables 5, 6, and 7, and compared in Figs. 6, 7, and 8. The seawater environment, of course, is the most severe. The atmospheric exposure and soil burial are of about the same order with the soil environment the more corrosive of the two, particularly toward the magnesium specimens during earlier exposure periods.

In atmospheric exposure the rate of attack on steel is greatest and is

TABLE 5—*Atmospheric exposure corrosion rates of similar metal couples, mm/year.*

Time, Months	Magnesium	Steel	6061 Aluminum	7075 Aluminum	Brass	Monel
2	0.031	0.069	0.002	0.003	0.007	0.001
4	0.037	0.055	0.002	0.003	0.003	0
8	0.034	0.037	0.001	0.001	0.001	0
15	0.025	0.046	0	0.001	0.001	0
24	0.028	0.048	0.001	0.001	0.001	0

NOTE—No corrosion of stainless steel and titanium alloys.

TABLE 6—*Soil burial corrosion rates of similar metal couples, mm/year.*

Time, Months	Magnesium	Steel	6061 Aluminum	7075 Aluminum	Brass	Monel
2	0.093	0.060	0.003	0.013	0.005	0.001
6	0.137	0.085	0.005	0.011	0.007	0.005
12	0.045	0.081	0.002	0.007	0.005	0.004
25	0.029	0.058	0.001	0.005	0.004	0.004

NOTE—No corrosion of stainless and titanium alloys.

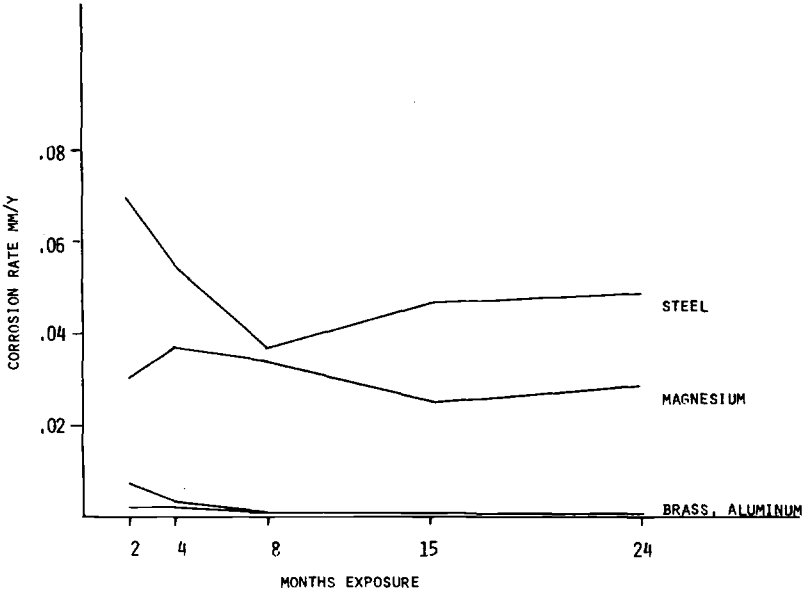

FIG. 6—*Similar metal couples in atmospheric exposure.*

TABLE 7—*Seawater corrosion rates of similar metal couples, mm/year.*

Time, Months	Magnesium	Steel	6061 Aluminum	7075 Aluminum	Brass	Monel	Stainless Steel
2	1.581	0.635	0.043	0.040	0.124	0.034	0.097
4	1.293	0.468	0.021	0.029	0.106	0.006	0.034
7	1.021	0.612	0.017	0.023	0.190	0.008	0.036
12	0.811	0.289	0.007	0.014	0.139	0.007	0.013
18	SM	0.338	0.006	0.049	0.115	0.027	0.031

NOTE—No corrosion of titanium.
SM = Specimens missing.

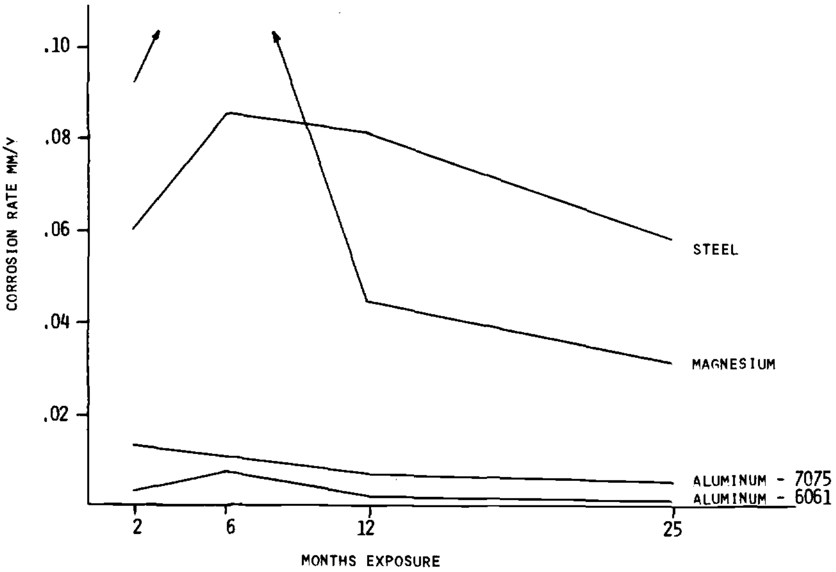

FIG. 7—*Similar metal couples in soil burial exposure.*

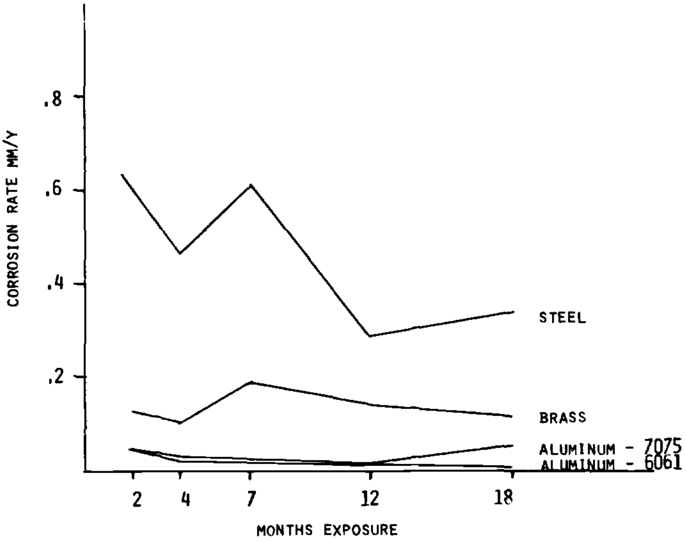

FIG. 8—*Similar metal couples in seawater exposure.*

appreciably greater than that of magnesium. The attack on other alloys is slight or negligible (see Table 5 and Fig. 6).

In soil burial, the rate of magnesium attack is greater than that of steel during the earlier exposure periods, but this tendency is reversed after a 12-month exposure. Attack on other alloys in soil is slight or negligible (see Table 6 and Fig. 7).

The greatest rate of attack in seawater, as expected, is on the magnesium alloys, with decreasing rates for steel, brass, stainless steel, aluminum, and Monel. No attack on titanium has occurred (see Table 7 and Fig. 8).

Conclusions

Certain trends are indicated in each of the environmental exposures.

The seawater environment, of course, is the most aggressive, while the soil and atmospheric exposure are of about the same order with the soil being the more aggressive.

In atmospheric exposure, the rate of attack is greatest on similar couples of steel, and this rate is significantly greater than that for similar couples of magnesium. This trend is also observed in soil after the 12-month exposure; however, the rate of magnesium attack is greater at lesser exposure periods.

In galvanic exposures in the atmosphere, relatively high magnesium corrosion rates are generally indicated initially, with a subsequent drop and leveling off after 15 months, except where coupled with steel and stainless steel, in which instances the corrosion rate increases after 15 months.

Relatively high corrosion rates of steel in galvanic coupling are also indicated initially in atmospheric exposure, with a subsequent drop of corrosion rate and tendency to level off after the 8-month exposure period. However, where steel is coupled with steel, an increase in corrosion rate is indicated after the 8-month exposure.

Galvanic couples of magnesium in soil indicate a pattern of early high corrosion rate, with a subsequent drop and tendency toward leveling off.

Corrosion rates of galvanic couples of steel in soil reveal an early increase between 2 and 6 months' exposure, followed by a drop. Leveling off of corrosion rates is not indicated to date.

Galvanic couples of aluminum alloys in soil show a leveling off in corrosion rates after 6 months' exposure. Coupling with magnesium results in a relatively high initial corrosion rate, while coupling with the other alloys shows a low initial corrosion rate.

In the case of seawater immersion, only the aluminum alloys indicate a leveling off of corrosion rates with exposure periods to date. Severe attack on aluminum alloys occurs when they are coupled with magnesium.

No corrosion of titanium occurred in any of the three environments.

Little or no corrosion of stainless steel and Monel occurred in the atmospheric and soil environments. However, crevice pitting attack on stainless occurs where coupled with Monel and titanium, and also where coupled with itself in seawater. Pitting of Monel is also indicated where coupled with titanium, and in some instances where coupled with stainless steel and other Monel specimens.

G. German[1]

Behavior of Zinc-Coated Steel in Highway Environments*

REFERENCE: German, G., "**Behavior of Zinc-Coated Steel in Highway Environments,**" *Atmospheric Factors Affecting the Corrosion of Engineering Metals, ASTM STP 646,* S. K. Coburn, Ed., American Society for Testing and Materials, 1978, pp. 74-82.

ABSTRACT: Results of 3 to 7-year exposure periods of galvanized steel specimens in Ontario and Quebec highway environments are reported. Continuous hot-dip, batch hot-dip, and electrogalvanized materials were used. Results indicated that a coating life of five years per mil of coating can be expected in urban environments, and 10 to 20 percent longer protection in rural environments. The method of zinc application appeared to have no significant influence.

KEY WORDS: galvanized steels, atmospheric corrosion, corrosion, highway corrosion, zinc

In the mid-1960s, the Department of Highways of the Province of Quebec specified electrogalvanized posts in their highway building programs. Early rusting of the steel was evident. Discussions with the Department led to involvement of the Noranda Research Centre and this study.

A series of steel coupons were galvanized using the three different methods—continuous hot-dip galvanizing, batch hot-dip galvanizing and electrogalvanizing. In addition, a set of primed and painted steel coupons and a set of galvanized and painted steel coupons were exposed along various highways in Quebec and Ontario to assess the corrosion behavior of the various zinc coatings. Laboratory examination of test coupons for the different types of galvanizing were carried out after 3 and 5-year exposure periods.

The remaining coupons were removed from all the sites after 7 years of exposure. These were examined at the Noranda Research Centre by means of visual inspection, determination of the weights of corrosion products, and metallographic examination.

---

*Original experimental data were measured in U.S. customary units.

[1] Manager, Zinc Sales, Noranda Sales Corp. Ltd., Toronto, Ont.

Description of Specimens and Test Locations

Unpainted Galvanized Steel Specimens

Zinc coatings on steel coupons were obtained following three galvanizing methods, each resulting in a different mean thickness of the coating: (*a*) continuous hot-dip galvanized—mean coating thickness, 0.0046 cm; (*b*) batch hot-dip galvanized—mean coating thickness, 0.0089 cm; and (*c*) electrogalvanized—mean coating thickness, 0.0025 cm. Coating thicknesses were determined by metallographic analyses.

The edges of the test coupons were protected with a polyurethane coating prior to installation at the test sites. Series of seven test coupons per type of galvanizing were installed on racks at various locations along major highways in Ontario and Quebec. The exposure sites, the orientation of the specimens, and the remaining number of specimens which were removed after 7 years are listed in Tables 1 and 2 for the Ontario and the Quebec locations, respectively. All the exposure sites in Ontario, as well as two sites (KA and KD) in Quebec, can be considered as being in urban atmosphere corresponding to severe corrosive environments. Sites KB and KC in Quebec are in rural atmosphere, and the corrosivity of the environment can therefore be considered as less severe.

TABLE 1—*Test locations and nature of coupons exposed in Ontario.*

			Number of Coupons Removed		
Site	Location	Orientation[a]	CG[b]	HDG[b]	EG[b]
OA	Highway 401, near Keele St.	north	4	4	4
		south	3	4	3
OB	Highway 401, west of Avenue Road	north	5	5	5
		south	...[c]	...[c]	...[c]
OC	Highway 401, near CFTO-TV Station	north	...[c]	...[c]	...[c]
		south	...[c]	...[c]	...[c]
OD	Formerly QEW,[d], between Etobikoke Creek and Highway 2, near lamp post 78; moved (1968) west on QEW, west of the Mississauga Rd. cut-off, between cut-off and Mississauga Rd. sign on eastbound lane	north	5	5	4
		south	5	5	5

[a] Orientation shows the direction in which the coupons were facing.

[b] CG = continuous hot-dip galvanization.
HDG = batch hot-dip galvanization.
EG = electrolytic galvanization.

[c] The specimen racks at these locations were missing.

[d] QEW = Queen Elizabeth Way, between Toronto, Ontario, and Niagara Falls, Ontario.

TABLE 2—*Test locations and nature of coupons exposed in Quebec.*

Site	Location	Orientation[a]	Number of Coupons Removed		
			CG[b]	HDG[b]	EG[b]
KA	Metropolitan Blvd. facing National Firm Board	north	. . .[c]	. . .[c]	. . .[c]
		south	5	5	5
KB	Eastern Townships Autoroute, 48.2 miles	north	5	5	5
		south	5	5	5
KC	Eastern Townships Autoroute, 65.6 miles	north	5	5	5
		south	5	5	5
KD	Laurentian Autoroute, east entrance to Metropolitan Boulevard	north	6	6	5
		south	5	5	5

[a] Orientation shows the direction towards which the coupons were facing.
[b] CG = continuous hot-dip galvanization.
HDG = batch hot-dip galvanization.
EG = electrolytic galvanization.
[c] The specimen rack at this location was missing.
[d] 1 km = 0.62 miles.

Painted Steel Specimens

Three sets of painted steel coupons differing by the nature of their undercoat were exposed at one location in Ontario (Highway 401). The nature of the coatings on the steel coupons was as follows: (*a*) steel coupons galvanized at the Research Centre and painted by the Ontario Department of Highways with a dry thickness of 25 μm yellow guard-rail paint; (*b*) coupons cut from a primed section of Weststeel sheet steel painted by the Ontario Department of Highways with a dry thickness of 25 μm, yellow guard-rail paint; and (*c*) steel coupons furnished by Noranda Research Centre and prepared by the Ontario Department of Highways by washing and spray-painting with a dry thickness of 38-μm, prime coat plus a dry thickness of 25-μm yellow guard-rail paint. All edges of the coupons were protected after painting with a polyethylene coating.

The location and the number of remaining steel coupons which were removed after 7 years are described in Table 3.

Examination Procedures of the Test Coupons

The coupons were first subjected to a mild cleaning procedure to remove sand and other loosely adherent materials. This consisted of washing in running distilled water, dipping in a neutral detergent solution (Oakite NST), rinsing in alcohol, and drying in a stream of air. No brushes or abrasive materials were used. A visual examination of the coupons was carried out with special attention being given to the occurrence and extent

TABLE 3—*Test location and nature of painted coupons exposed in Ontario.*

			Number of Coupons Removed		
Site	Location	Orientation	Noranda PP[a]	Weststeel PP[a]	GP[a]
OA	Highway 401, facing DHO Building, west-bound centre lane	north	4	4	4
	East-bound centre lane	south	3	3	3

[a] Noranda PP—Steel coupons furnished by Noranda Research Centre and painted with a 38-μm dry thickness of prime coat plus 25-μm dry thickness of yellow guard rail paint.

Weststeel PP—Steel coupons cut from a primed section of Weststeel sheet steel and painted with a 25-μm dry thickness yellow guard rail paint.

GP—Steel coupons galvanized at the Research Centre and painted with a 25-μm dry thickness of yellow guard rail paint.

of rust staining. It was assumed that materials remaining on the zinc coating after the mild cleaning procedure were zinc corrosion products; measurements of their weights would therefore provide an indication of the extent of corrosion as a function of test site location. Results were thus indicative on a semiquantitative basis of the corrosiveness of the test sites. The method of Stroud [*1*][2] was used to effect quantitative removal of corrosion products without attacking the underlying zinc. In this method the specimens were immersed at room temperature in a solution containing 10 weight percent chromic anhydride and 2 weight percent silver chromate, and saturated with an excess of strontium chromate. The solution was vigorously stirred and a 5 to 15-min immersion of the specimens followed by weight determination, was made periodically until the specimen weight loss between two consecutive determinations was not greater than 10 mg. One coupon of galvanized type for each site was used for the determination of the weight of corrosion products.

Microscopic examinations of the cross section of one specimen from each set of coupons were also carried out to examine the continuity of the coatings and their adhesion to the steel surface.

Results of Specimen Examination

Visual Examination

Unpainted Galvanized Steel Coupons—All specimens were examined following the mild cleaning procedure described previously. The test coupons of Site KA (facing south) were covered with an irregular layer of white paint which was not removed during the preliminary mild cleaning step.

---

[2] The italic numbers in brackets refer to the list of references appended to this paper.

The upper right corners of the five continuous hot-dip galvanized and of the three batch hot-dip galvanized steel coupons of Site KC (facing south) were found to be mechanically damaged over a relatively small surface area. The presence of rust at these areas was noted for some of the specimens.

(*a*) *Continuous hot-dip galvanized steel coupons*—All continuous hot-dip galvanized specimens from both the Ontario and the Quebec sites were in good condition. The coupons had a dull appearance due to dust or corrosion product accumulation. The grain structure of the zinc coating was apparent in most cases. No rust staining was observed on the specimens except for the coupons of Site KC (facing north and south) on which very few tiny spots of rust were observed randomly distributed on the surface of the specimens. The damaged upper right corners of the five coupons of Site KC (facing south) were rusted.

(*b*) *Batch hot-dip galvanized steel coupons*—All batch hot-dip galvanized specimens from both Ontario and Quebec sites were in a good condition. The coupons had a dull appearance due to dust or corrosion products accumulation. No rust staining was observed on the specimens except for the coupons of Site KC (facing north and south) on which tiny spots of rust were observed randomly distributed on the surface of the specimens. The damaged upper right corners of three coupons of Site KC (facing south) did not show any sign of rust.

(*c*) *Electrogalvanized steel coupons*—The electrogalvanized steel coupons were generally corroded to various degrees. The results of visual examination of these specimens are presented in Table 4. The coupons of Sites KB and KC (rural atmospheres) were generally less rusted than those of other sites (urban atmospheres). No marked differences were observed between the appearances of coupons exposed in urban atmospheres in Ontario and in Quebec. With regard to the effect of orientation of the coupons, it was observed that the coupons facing south tended to be more corroded than those facing north. However, the difference between specimens facing north and south as regards extent of rust staining for each site was relatively small.

Painted Coupons—No mild cleaning procedure was used prior to visual examination of the primed and painted and the galvanized and painted steel coupons; this avoided possible distortion of the results by paint removal.

The galvanized and painted steel coupons had a very good appearance. With the exception of one sample, no traces of rust were observed, even at spots where the paint coating had flaked off. One coupon (facing north) was rusted over a width of 0.50 to 0.65 cm along the edges. All the primed and painted steel coupons had a very poor appearance. The paint had flaked off over large surface areas and the surface of the metal was rusted completely. Propagation of rust underneath the remaining paint coating could be observed by lifting the loosely adherent paint flakes. Differences between specimens facing north and south as regards extent of corrosion could not be detected.

TABLE 4—*Results of visual examination of electrogalvanized steel coupons exposed for seven years at different sites in Ontario and Quebec.*

Site	Orientation	Number of Coupons	Occurrence and Extent of Rust Staining
OA	north	2	75% rusted
		1	30% rusted
		1	very small rust spots randomly distributed
OA	south	3	50 to 75% rusted
OB	north	2	80% rusted
		2	25% rusted
		1	5% rusted + small rust spots randomly distributed
OD	north	2	100% rusted
		2	60% rusted
OD	south	2	100% rusted
		2	50% rusted
		1	15% rusted + small rust spots randomly distributed
KA	south	5	rusted under white paint coating
KB	north	1	10% rusted
		2	5% rusted
		2	no rust
KB	south	2	60% rusted
		2	20% rusted
		1	1 to 2% rusted
KC	north	5	few tiny rust spots
KC	south	2	50% rusted
		2	15 to 25% rusted
		1	few tiny rust spots
KD	north	3	100% rusted
		2	80 to 90% rusted
KD	south	4	100% rusted
		1	50% rusted

Determination of the Weight of Corrosion Products

Weight measurements of corrosion products were carried out on one specimen from each set of unpainted galvanized steel coupons. The results of these measurements are presented in Table 5. The values obtained for the electrogalvanized steel coupons were very low compared with those obtained for the two other galvanized types. Because the electrogalvanized specimens were heavily corroded and a large proportion of the protective zinc layer had disappeared, the formation of zinc corrosion products during the last 1 to 2 years of exposure was proportionally smaller. Consequently, the weights of zinc corrosion products obtained for the electrogalvanized steel coupons cannot be attributed to low corrosion rates. As reported previously, the steel coupons removed from Site KA (facing south) were covered with an irregular layer of white paint which dissolved during the gravimetric determination of the weight of zinc corrosion products. As a consequence, the weight loss values obtained were very large and not representative of

TABLE 5—*Weight-loss data for removal of zinc corrosion products from galvanized coupons.*

		Weight Loss, mg/dm^2		
Site[a]	Orientation	CG[b]	HDG[b]	EG[b]
OA	north	1541	1770	1230
OA	south	1258	1443	1041
OB	north	1242	1934	1258
OD	north	2266	2410	1303
OD	south	1791	2098	873
KA[c]	south	3307	6270	7369
KB	north	1148	1049	807
KB	south	1852	1959	959
KC	north	1230	951	836
KC	south	1385	1357	1180
KD	north	1230	1643	246
KD	south	1668	1869	1033

[a] See Tables 1 and 2 for the description of site locations.

[b] CG = continuous hot-dip galvanization.
HDG = batch hot-dip galvanization.
EG = electrolytic galvanization.

[c] Results are erroneous because the coupons were covered with a layer of a white paint coating.

the amount of corrosion products remaining on the surface of the coupons. The results obtained for Site KA were therefore discarded during analysis of the data.

A statistical analysis of the data obtained from the determination of weights of zinc corrosion products was carried out to investigate the influence of the type of galvanizing, the location, and the orientation of the test coupons, as well as the influence of the type of environment on the amount of corrosion products remaining on the specimens. Mean values of weight loss data and standard deviation for each set of data were calculated for various types of test conditions. The results are summarized in Table 6. Although some systematic variations could be observed (for example, average weight loss data were greater for coupons facing south than for those facing north, and were greater for coupons exposed in urban atmosphere than for those exposed in rural atmosphere), the differences obtained were very small and negligible when compared with the standard deviations calculated for each set of data, and are therefore marginally significant.

Discussion

The results of the examination of galvanized steel coupons after a 7-year exposure have shown that zinc coatings are capable of providing excellent corrosion protection for steel in a very severe environment.

Tests carried out by various organizations on a worldwide basis have

TABLE 6—*Averaged values (±one standard deviation) of weight loss data obtained for the removal of corrosion products from galvanized steel coupons.*

Type of Galvanization	Average Weight Loss Values (± One Standard Deviation), mg/dm²						
	All Coupons Tested	Coupons Facing North	Coupons Facing South	Urban Atmosphere[a]	Rural Atmosphere[b]	Ontario Coupons	Quebec Coupons
Continuous hot-dip	1510 (±351)	1443 (±425)	1591 (±259)	1571 (±380)	1404 (±315)	1620 (±426)	1419 (±281)
Batch hot-dip	1680 (±446)	1616 (±551)	1745 (±327)	1881 (±314)	1329 (±454)	1931 (±361)	1471 (±421)
Electrolytic	979 (±299)	947 (±407)	1061 (±158)	998 (±365)	946 (±170)	1141 (±180)	844 (±323)

[a] Coupons exposed at sites OA, OB, OD, and KD.
[b] Coupons exposed at sites KB and KC.

shown that the duration of protection of steel afforded by zinc coatings is directly related to the thickness of the zinc coating, while the method of applying zinc to the steel substrate exerts only a secondary effect [*2-7*]. Comparison of results of examination of test coupons exposed for 5 years in an urban atmosphere, and those described herein for a 7-year exposure, indicate that the protective zinc coating obtained by electrogalvanizing (mean coating thickness, 25 μm) were close to failure after a 5-year exposure. Accepting the linear relationship between the duration of protection and the zinc coating thickness, a total duration of protection of about 9 years for the continuous hot-dip galvanized steel coupons (mean coating thickness, 45 μm) and about 17 years for the batch hot-dip galvanized coupons (mean coating thickness, 88 μm) would be expected. The duration of protection for a given thickness of coating would be somewhat longer for steel exposed in a rural atmosphere. The observations carried out on the batch hot-dip and continuous hot-dip galvanized steel coupons after a total exposure period of 7 years are in agreement with the foregoing assumption.

The excellent condition of the painted galvanized steel coupons exposed in Ontario for 7 years, compared with the very severe corrosion observed on the ungalvanized, primed and painted coupons, shows that the steel has received virtually perfect protection. The excellent adhesion and appearance of the paint illustrates the high value of zinc in combination with paint as a protective coating.

Conclusion

Zinc has been shown to be a most valuable material for protecting steel during 7-year exposure tests on major Ontario and Quebec highways. The results obtained suggest that the duration of protection increases by increasing the thickness of the zinc coating. A zinc coating life of about 5 years per mil of coating would be expected for highways exposed in an urban environment. In a rural environment, the duration of protection would be somewhat longer (most likely 10 to 20 percent). The method of zinc application appeared to have no significant influence.

References

[*1*] Stroud, E. G., *Journal of Applied Chemistry,* Vol. 1, 1951, p. 93.

[*2*] Slunder, C. J. and Boyd, W. K., *Zinc: Its Corrosion Resistance,* Zinc Institute Inc., New York, 1971.

[*3*] Roblin, J. M., *Metal Producing Progress,* Feb. 1966, p. 115.

[*4*] Hudson, J. C. and Stanners, J. F., *Journal of the Iron and Steel Institute,* Vol. 175, 1953, pp. 381-390.

[*5*] Schikorr, G., *Werkstoffe und Korrosion,* Vol. 15, 1964, pp. 537-543.

[*6*] Rajagopalan, K. S. and Ramaseshan, G., *Journal of Science and Industrial Research* (India), Vol. 18B, 1959, pp. 87-89.

[*7*] Daesen, J. R., *Proceedings,* Second International Congress on Metallic Corrosion, National Association of Corrosion Engineers, Houston, Tex., 1965, pp. 686-705.

R. A. Legault[1] *and V. P. Pearson*[1]

Kinetics of the Atmospheric Corrosion of Galvanized Steel*

REFERENCE: Legault, R. A. and Pearson, V. P., "**Kinetics of the Atmospheric Corrosion of Galvanized Steel,**" *Atmospheric Factors Affecting the Corrosion of Engineering Metals, ASTM STP 646,* S. K. Coburn, Ed., American Society for Testing and Materials, 1978, pp. 83–96.

ABSTRACT: Atmospheric corrosion behavior was evaluated separately on skyward and groundward surfaces of galvanized steel test panels exposed in both industrial and marine environments. The behavior in every case can be accurately described by the same general kinetic relationship, $\Delta W = Kt^N$, where the empirically determined coefficients, K and N, can be used to separate the tendency for a corrosion product to form from the effect of that corrosion product on the subsequent reaction. The specific kinetic equations which apply in each case can be used to reliably predict long-term atmospheric corrosion behavior.

KEY WORDS: atmospheric corrosion, galvanized steel, marine atmospheres, industrial atmospheres, kinetics

This work represents an attempt to provide a definitive study of the atmospheric corrosion behavior of galvanized steel in both an industrial and a marine environment. This behavior was evaluated separately on both skyward and groundward surfaces of test panels exposed at East Chicago, Indiana and at Kure Beach, North Carolina. Differences in atmospheric corrosion behavior between the top and bottom surfaces become important in attempting to assess the relative contributions to the corrosion process of experimental parameters which would tend to show different effects for these two surfaces. Examples of such parameters might be the relative amounts of solid versus gaseous contaminants, the amount of rainfall, or the persistence of condensed moisture on panel surfaces.

We have demonstrated previously [*1–3*] that the atmospheric corrosion behavior of galvanized steel at both of these sites can be described accurately

---

* Original experimental data were measured in U.S. customary units.

[1] Senior research engineers, Inland Steel Corporation, East Chicago, Ind. 46312.

[2] The italic numbers in brackets refer to the list of references appended to this paper.

by the same general kinetic relationship, $\Delta W = Kt^N$, where ΔW is the weight-loss in grams per square meter of exposed surface, t is the exposure time expressed in years, and K and N are empirically determined constants.

Equations of this form can be used to reliably predict long-term behavior and to assess the influence of alloying additions or variations in the atmospheric environment. The idea of characterizing atmospheric corrosion behavior with the two empirically determined constants K and N is an important contribution to the understanding of that behavior. The value obtained for K provides a criterion for gaging short-term corrosion susceptibility. It provides a measure of the inherent reactivity of a metal surface as reflected in the tendency for that surface to produce a corrosion product oxide in a 1-year atmospheric exposure. The value of N, on the other hand, provides a criterion for gaging long-term atmospheric corrosion susceptibility. It provides a measure of the resistance to transport processes within the corrosion product once it has formed.

Values of K and N were determined empirically and separately for both skyward and groundward exposures of galvanized steel at both East Chicago and Kure Beach. The four resulting kinetic equations were then used to calculate predicted weight-loss values for 10-year exposures.

Experimental Procedure

The test material used was a normal production class G-90 galvanized steel with a nominal coating weight of 168 g/m^2. The zinc coating also contained 0.33 percent iron, 0.09 percent lead, 0.15 percent antimony, and 0.24 percent aluminum.

The ASTM Recommended Practice for Preparing, Cleaning, and Evaluating Corrosion Test Specimens (G 1-72) was used in preparing, exposing and later in cleaning the corrosion test specimens. The test materials were cut into 10.2 by 15.2-cm (4 by 6 in.) panels, and identification numbers were stamped on that side of the panel which was to be exposed. Each test panel to be exposed was weighed, and the resulting values were recorded to four decimal places. Using a double-stick tape, 6 mm (¼ in.) wide and 0.79 mm (30 mils) thick, two test panels were made into one sandwich-like test specimen for exposure. A sketch of such a test specimen is shown in Fig. 1. This was the technique used to obtain independent atmospheric corrosion data on the skyward and groundward surfaces of the materials under study.

Thirty sandwich-type test specimens of galvanized steel were placed at each exposure site, that is, the industrial site located within the Inland Steel Research complex in East Chicago, Indiana and the marine test site which is the 245-m (800-ft) lot at Kure Beach. The removal schedule called for five specimens at each site to be removed at the conclusion of exposure periods of 6 months, 1 year, 2 years, 3 years, 4 years, and 5 years. Fivefold

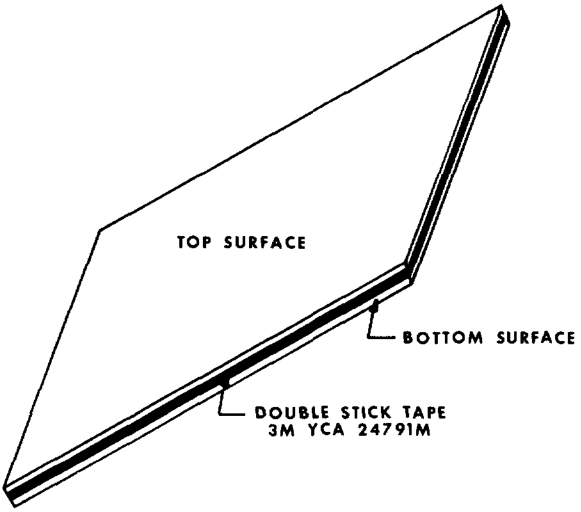

FIG. 1—*Schematic diagram of sandwich-type test panel.*

replication allowed for the occasional accidental loss of a few test specimens without jeopardizing the obvious benefits to be derived from a generous replication. As indicated earlier, corrosion product removal was accomplished using ASTM Recommended Practice G 1-72.

Test Results

Data obtained in East Chicago exposures of 1, 2, 3, and 4 years are shown for skyward panels in Table 1. Mean values identified as X are

TABLE 1—*Top side weight-loss measurements obtained in exposures of galvanized steel at East Chicago, g/m²*

0.9966 Years	1.9986 Years	2.9979 Years	4.0027 Years
25.0907	54.3793	82.8283	115.2104
25.6913	51.9251	80.1352	114.3579
24.7484	52.0736	79.9285	111.4517
26.1434	50.7626	80.1933	111.3161
25.5944	51.1049	77.2354	106.5756
$\bar{X}$ = 25.4536	$\bar{X}$ = 52.0491	$\bar{X}$ = 80.0641	$\bar{X}$ = 111.7823
LL = 24.7793	LL = 50.2950	LL = 77.6070	LL = 107.5822
UL = 26.1280	UL = 53.8033	UL = 82.5213	UL = 115.9826

NOTE—$\bar{X}$ represents the mean value, LL represents the lower 95 percent confidence limit, and UL represents the upper 95 percent confidence limit. The density of the coating was taken as 7.11 g/cm³ and the exposed area as 0.0155 m² (24 in.²) The actual exposure times were measured in hours.

shown for each exposure time along with the 95 percent confidence limits. Similar data obtained in exposures of 1, 2, 3, 4, and 5 years are shown for the comparable groundward panels in Table 2. Weight-losses were clearly more severe on skyward surfaces than on groundward surfaces. The data shown in the Tables 1 and 2 were fitted to the logarithmic form of the general kinetic expression referred to earlier, and the results of this curve fitting are shown in Table 3. The quality of fit obtained in each case is amply testified to by the R^2 and F values listed. Although the difference between

TABLE 2—*Bottom side weight-loss measurements obtained in exposures of galvanized steel at East Chicago, g/m².*

0.9966 Years	1.9986 Years	2.9979 Years	4.0027 Years	4.9993 Years
23.3921	40.0224	50.3945	71.5908	86.4256
22.6688	37.6845	49.3224	67.0053	78.5852
22.2748	39.1117	50.7303	68.4068	77.6939
23.1273	38.8857	50.0457	66.8826	87.2910
21.8357	37.8911	47.9209	66.5533	77.3968
$\bar{X}$ = 22.6598	$\bar{X}$ = 38.7191	$\bar{X}$ = 49.6828	$\bar{X}$ = 68.0878	$\bar{X}$ = 81.4785
LL = 21.8793	LL = 37.5358	LL = 48.2995	LL = 65.5031	LL = 75.3481
UL = 23.4003	UL = 39.9023	UL = 51.0660	UL = 70.6724	UL = 87.6089

NOTE—$\bar{X}$ represents the mean value, LL represents the lower 95 percent confidence limit, and UL represents the upper 95 percent confidence limit. The density of the coating was taken as 7.11 g/cm³ and the exposed area as 0.0155 m² (24 in.²). The actual exposure times were measured in hours.

TABLE 3—*Curve fitting of the data obtained on galvanized steel at East Chicago.*

	Top Side	Bottom Side
Exposure times, years	1, 2, 3, 4	1, 2, 3, 4, 5
Observations	20	25
ln K	3.2314	3.1072
SE ln K	0.0114	0.0190
N	1.0592	0.7872
SE N	0.0120	0.0170
K	25.315	22.358
R^2	0.998	0.989
F	7833	2137
10-year prediction	290.09 g/m²	136.96 g/m²

T = Test difference in ln K	12.1
Degrees of freedom	7
% confidence that ln K-values differ	>99.9
T = Test for difference in N	28.1
Degrees of freedom	7
% confidence that N-values differ	>99.9

NOTE—To indicate a significant difference at the 99.9 percent confidence level with 7 degrees of freedom, the calculated T-value should exceed 5.407.

In *K*-values is not large, the confidence level indicated for that difference leaves little doubt that it is real. The difference in *N*-values along with the confidence level indicated for that difference show clearly that although the tendency to form a corrosion product oxide may not be much larger on the skyward than on the groundward surface as indicated by the relative *K*-values, corrosion product once formed does offer considerably less resistance to a continuation of the corrosion process than does its counterpart on the groundward surface. This can be seen readily in Fig. 2 which shows the comparison of the weight-loss versus time curves calculated for each surface from the equations derived in the curve fitting.

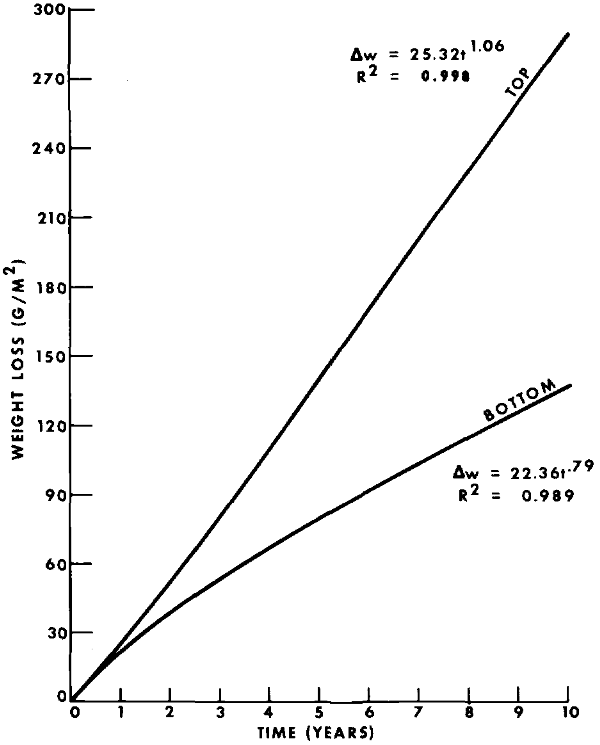

FIG. 2—*Predictive equations for East Chicago exposure of galvanized steel.*

Data obtained in Kure Beach exposures of 1, 2, 4, and 5 years are shown for skyward panels in Table 4. Again, mean values are shown for each exposure time along with the 95 percent confidence limits. Similar data obtained for the same exposures are shown for the comparable groundward panels in Table 5. As in the industrial environment, weight-losses are larger from skyward surfaces than from groundward surfaces. The data

TABLE 4—*Top side weight-loss measurements obtained in exposures of galvanized steel at Kure Beach, g/m^2.*

1.0760 Years	2.0753 Years	4.0849 Years	5.0815 Years
23.9605	36.2313	57.8991	68.4133
21.9261	36.9934	56.9884	55.8001
21.7000	34.1647	56.8657	64.2993
19.9563	34.3713	57.2274	61.6966
20.4923	36.1926	56.3878	62.1228
$\bar{X}$ = 21.6070	$\bar{X}$ = 35.5907	$\bar{X}$ = 57.0737	$\bar{X}$ = 62.4664
LL = 19.6829	LL = 34.0381	LL = 56.3867	LL = 56.7838
UL = 23.5312	UL = 37.1432	UL = 57.7607	UL = 68.1490

NOTE—$\bar{X}$ represents the mean value, LL represents the lower 95 percent confidence limit, and UL represents the upper 95 percent confidence limit. The density of the coating was taken as 7.11 g/cm^3 and the exposed area as 0.0155 m^2 (24 in.^{2}). The actual exposure times were measured in hours.

TABLE 5—*Bottom side weight-loss measurements obtained in exposures of galvanized steel at Kure Beach, g/m^2.*

1.0760 Years	2.0753 Years	4.0849 Years	5.0815 Years
11.8704	23.7150	35.8374	37.9170
12.4775	22.5784	32.3111	36.7092
11.5023	17.9542	30.6449	32.7761
10.6175	17.4957	29.7665	28.6944
	16.4042	30.2251	28.1842
$\bar{X}$ = 11.6170	$\bar{X}$ = 19.6295	$\bar{X}$ = 31.7570	$\bar{X}$ = 32.8562
LL = 10.3805	LL = 15.5536	LL = 28.6856	LL = 27.3199
UL = 12.8534	UL = 23.7054	UL = 34.8283	UL = 38.3925

NOTE—$\bar{X}$ represents the mean value, LL represents the lower 95 percent confidence limit, and UL represents the upper 95 percent confidence limit. The density of the coating was taken as 7.11 g/cm^3 and the exposed area as 0.0155 m^2 (24 in.^{2}). The actual exposure times were measured in hours.

shown in Tables 4 and 5 were also fitted to the general kinetic expression, and the results of this curve fitting are shown in Table 6. Again, a good fit is indicated in each case by the R^2 and F values listed. As at the other site, the confidence level indicated for the difference in ln K- values leaves little doubt that the tendency to form a corrosion product is greater on the skyward surface than on the groundward surface. On the other hand, there is no evidence that the N-values are really different. Thus, unlike what occurs at the other site, the corrosion products formed which represent the two surfaces do not appear to differ in the effect they have on the subsequent corrosion processes. This can be seen in Fig. 3 which shows a comparison of the weight-loss versus time curves calculated from the equations derived in the curve fitting.

TABLE 6—*Curve fitting of the data obtained on galvanized steel at Kure Beach.*

	Top Side	Bottom Side
Exposure times, years	1, 2, 4, 5	1, 2, 4, 5
Observations	20	19
ln K	3.0390	2.4338
SE ln K	0.0246	0.0567
N	0.6943	0.6853
SE N	0.0217	0.0487
K	20.884	11.402
R^2	0.983	0.921
F	1027	198
10-year prediction	103.30	55.24

Test for difference in ln K	19.6
Degrees of freedom	4
% confidence that ln K-values differ	$>$99.9
T = Test for difference in N	0.338
Degrees of freedom	4
% confidence that N-values differ	$<$30

NOTE—To indicate a significant difference at the 99.9 percent confidence level with 4 degrees of freedom, the calculated T-value should exceed 8.609.

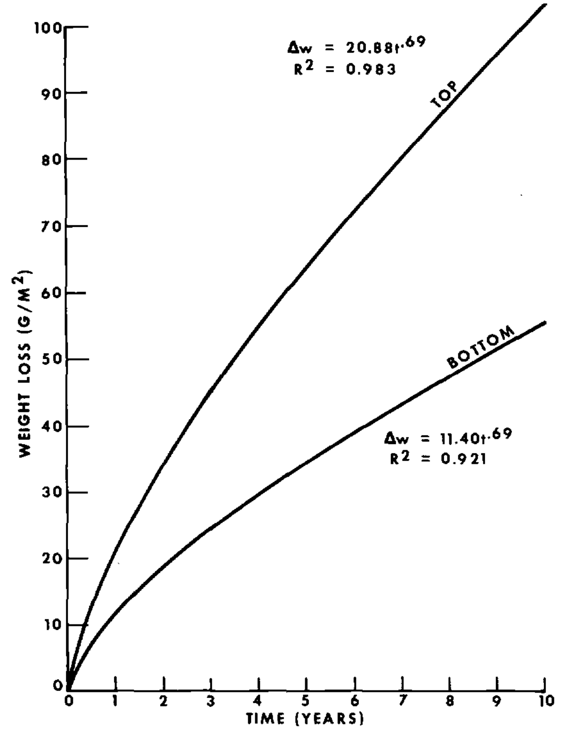

FIG. 3—*Predictive equations for Kure Beach exposure of galvanized steel at 245-m (800-ft) lot.*

Data comparing the corrosion behavior of galvanized steel at these two sites are shown in Table 7. The East Chicago site appears to be more aggressive toward galvanized steel than the Kure Beach location. It is interesting to note from the lower portion of this table that the difference between sites is at a minimum for short-term data obtained on the skyward surface. Table 8 summarizes the difference in regression equation constants for these two sites. The significance of the difference in *K*-values is beyond question for both top and bottom sides. As to *N*-values, the significance of the difference noted for skyward surface is overwhelming, while that for the groundward surface is somewhat less impressive. Figure 4 shows a comparison of the weight-loss versus time curves for the two sites; here the differences from one surface to the other are very apparent at both sites.

TABLE 7—*Comparison of East Chicago versus Kure Beach corrosion behavior of galvanized steel, g/m*^{2}.

Years		Skyward Side		Groundward Side	
		East Chicago	Kure Beach	East Chicago	Kure Beach
1	$\bar{X}$	25.4536	21.6070	22.6598	11.6170
1	LL	24.7793	19.6829	21.8793	10.3805
1	UL	26.1280	23.5312	23.4003	12.8534
2	$\bar{X}$	52.0491	35.5907	38.7191	19.6295
2	LL	50.2950	34.0381	37.5358	15.5536
2	UL	53.0833	37.1432	39.9023	23.7054
4	$\bar{X}$	111.7823	57.0737	68.0878	31.7570
4	LL	107.5822	56.3867	65.5031	28.6856
4	UL	115.9826	57.7607	70.6724	34.8283
5	$\bar{X}$	...	...	81.4785	32.8562
5	LL	...	...	75.3481	27.3199
5	UL	...	...	87.6089	38.3925

	$\bar{X}_{EC}/\bar{X}_{KB}$	
	Skyward	Groundward
1 year	1.18	1.95
2 years	1.46	1.97
4 years	1.96	2.14
5 years	...	2.48

NOTE—The confidence limits shown are for 95 percent. EC = East Chicago. KB = Kure Beach.

Discussion

The data shown demonstrate that for galvanized steel exposures at East Chicago, the tendency to form an oxide is somewhat greater on skyward than on groundward surfaces. The data have also shown that once formed,

TABLE 8—*Differences in the regression equations obtained at East Chicago and Kure Beach for galvanized steel.*

	Top Side		Bottom Side	
	East Chicago	Kure Beach	East Chicago	Kure Beach
ln K	3.2314	3.0390	3.1072	2.4338
N	1.0592	0.6943	0.7872	0.6853
10-year prediction	290.1 g/m^2	103.3 g/m^2	137.0 g/m^2	55.2 g/m^2
T = Test for difference in ln K			14.2	22.8
Degrees of freedom			4	4
% confidence that ln K-values differ			>99.9	>99.9
T = Test for difference in N			29.4	3.99
Degrees of freedom			5	4
% confidence that N-values differ			>99.9	~98

NOTE—To indicate a significant difference at the 99.9 percent confidence level with 4 degrees of freedom, the calculated T-value should exceed 8.609. With 5 degrees of freedom, it should exceed 6.868.

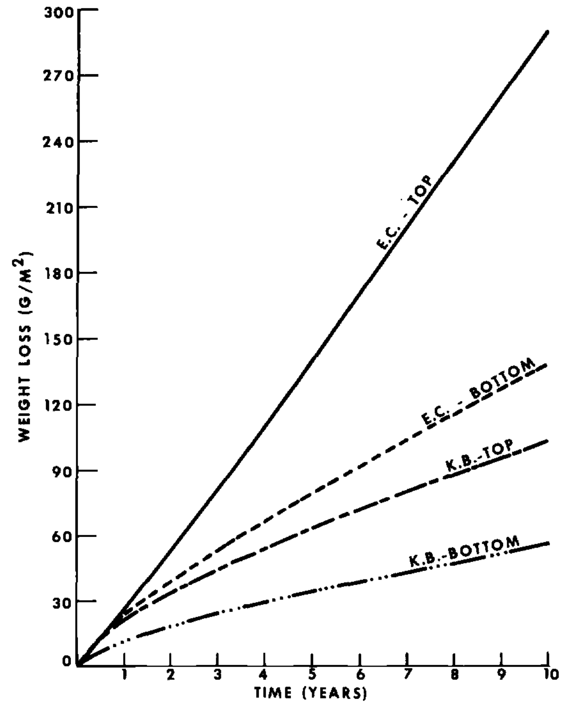

FIG. 4—*Comparison of predictive equations for galvanized steel at Kure Beach and East Chicago.*

the corrosion product on the skyward surface offers less resistance to a continuation of the corrosion process than does its counterpart on the groundward surface.

It appears to be generally accepted that the atmospheric corrosion of zinc coatings on steel is very nearly linear with time of exposure [*4*]. The data shown here indicate that this is indeed the case for skyward surfaces exposed at East Chicago. It is, however, clearly not the case for the comparable groundward surfaces. This discrepancy in behavior between skyward and groundward surfaces has been reported previously for both rolled zinc and galvanized steel by Guttman [*5*] and others. However, this observation has been largely ignored because the behavior does approach linearity when the reactions on both surfaces are taken together.

The mechanism of the atmospheric corrosion of zinc has been considered in detail by Anderson [*6*]. The data we obtained on galvanized steel are not inconsistent with the phenomenological model advanced by Anderson. Contact of a zinc surface with condensed moisture in the form of rain, mist, or dew will result in the formation of zinc hydroxide and the release of hydrogen. The zinc hydroxide then reacts with carbon dioxide from the atmosphere to form an insoluble basic zinc carbonate. Condensation in an industrial area tends to be acidic—pH values as low as 3 have been observed. Such a low-pH water in contact with the zinc will result in a rapid dissolution of the metal, but as the reaction proceeds the pH of the water increases until a basic salt, usually the carbonate, precipitates. Once this precipitated film forms, it will inhibit corrosion until it is dissolved by an additional supply of acid moisture.

Skyward surfaces are subjected to fresh acid moisture more frequently and to a greater extent than are the groundward surfaces for two reasons: (*a*) whatever rain falls will pick up acid contaminants from the atmosphere and will not affect groundward surfaces; and (*b*) any solid contaminants in the atmosphere which would either be acidic of themselves or have acidic gaseous contaminants absorbed would tend to fall out on the skyward surfaces but not on the groundward surfaces. Thus, the large discrepancy in behavior between the two surfaces that we have noted is not inconsistent with the model described by Anderson.

The data we have shown demonstrate that for galvanized steel exposures at Kure Beach, the tendency to corrode is much greater on skyward surfaces than on groundward surfaces. The data also show that the corrosion product on the skyward surface, once formed, offers essentially the same resistance to a continuation of the corrosion process as does its counterpart on the groundward surface. Corrosion rates on both surfaces clearly decrease with lengthening time of exposure.

In marine exposures as in other atmospheric environments, contact of the zinc surface with condensed moisture in the form of rain, mist, or dew will result in the formation of zinc hydroxide which then reacts with carbon dioxide from the atmosphere to form an insoluble basic zinc carbonate. Such a corrosion product film would tend to inhibit a continuation of the corrosion process and provide decreasing corrosion rates with increasing exposure times. Nonindustrial marine environments such as that at the 245-m (800-ft) lot at Kure Beach do not provide the acid-condensed moisture which is characteristic of industrial environments. There is thus no mechanism for destroying the protective basic carbonate film once it has formed. Accordingly, one would expect *N*-values to be somewhat less than unity. One would also expect no difference in the *N*-value between surfaces since while the rate of initial formation might be different, once they are formed the films on both surfaces would be expected to be the same stable corrosion product.

Weight-losses on skyward surfaces are clearly indicated to be greater than on the groundward surfaces for short-term exposures. In a 1-year exposure, for instance, the weight-loss on the topside is almost double that on the bottomside. Since the *N*-values are very nearly equal, that ratio can be expected to persist with lengthening exposure times.

Rainfall in the Kure Beach area is said to average approximately 152 cm (60 in.) per year. This average of better than 2.54 cm (1 in.) a week could wash considerable amounts of nonadherent zinc hydroxide from the topside surfaces. This would accomplish two ends: (*a*) it would promote the corrosion of zinc by removing a corrosion product; and (*b*) it would slow down the formation of the basic carbonate which functions as a protective film. Accordingly, the observation that topside surfaces corrode at approximately twice the rate of bottomside surfaces does not appear unreasonable.

The relative atmospheric corrosion behavior of galvanized steel can be summarized by comparing the kinetic equation coefficients obtained at these two exposure sites. Figure 5 shows a three-dimensional diagram of the relative values of *K* where the surface depicted summarizes the relative tendencies for galvanized steel to corrode in short-term atmospheric exposures at these two sites. This figure shows clearly that for a 1-year exposure, weight-losses are greater at East Chicago than at Kure Beach with this effect of site more pronounced on groundward surfaces than on skyward surfaces. Similarly it shows that weight-losses are greater on skyward surfaces than on groundward surfaces with this effect much more pronounced at Kure Beach than at East Chicago. It will be recalled that the East Chicago environment provides a mechanism for destroying the protective basic carbonate film which forms on zinc. The Kure Beach environment, while it does not provide a mechanism for destruction of the film once it has formed, does provide a mechanism which interferes with its formation on the skyward surface. Thus, *K*-values at Kure Beach are much lower on the groundward surfaces than on the skyward. Although the film formed at East Chicago can be destroyed on both surfaces, the more pronounced effect noted for skyward surfaces is attributable to the additional influence

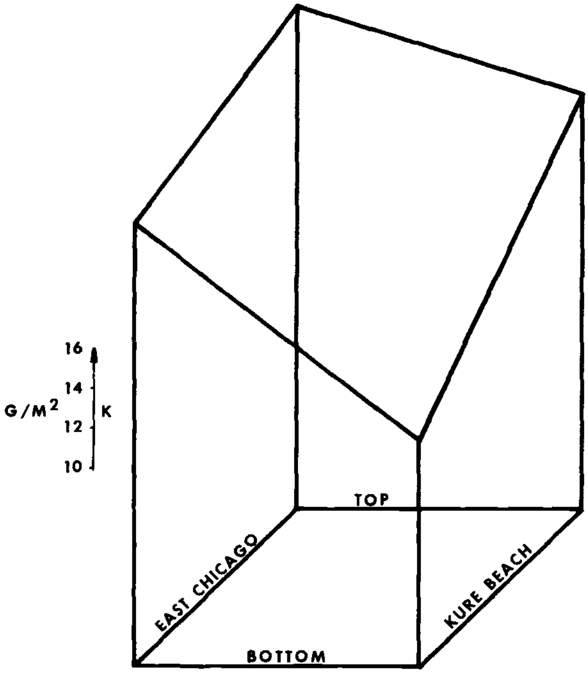

FIG. 5—*Comparison of galvanized steel K-values for East Chicago and Kure Beach.*

of solid pollutants which come to rest on the top surfaces. It is interesting to note that the effect of providing a mechanism for interfering with the formation of a protective film on topside surfaces at Kure Beach approaches in magnitude the effect of providing a mechanism for destruction of the film at East Chicago. Figure 6 shows a three-dimensional diagram of the relative values of N where the surface depicted summarizes the relative protective characteristics of the corrosion product films formed at these two sites. It is apparent that N-values are essentially identical for the two surfaces exposed at Kure Beach. This follows from the observation that no effective mechanism is provided at Kure Beach for the destruction of the carbonate film once it has formed. On the other hand, at East Chicago there is not only a mechanism for destruction of the film once it is formed, but the tendency to do this is greater for skyward surfaces than for groundward surfaces. Accordingly, N-values are larger on skyward surfaces.

Summary

For the atmospheric corrosion behavior of galvanized steel in both an industrial and a marine environment, the tendency for a corrosion product to form has been separated from the effect of that corrosion product on the

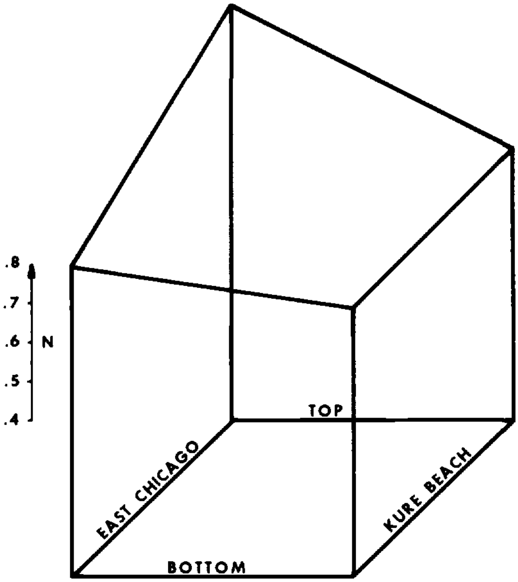

FIG. 6—*Comparison of galvanized steel* N-*values for East Chicago and Kure Beach.*

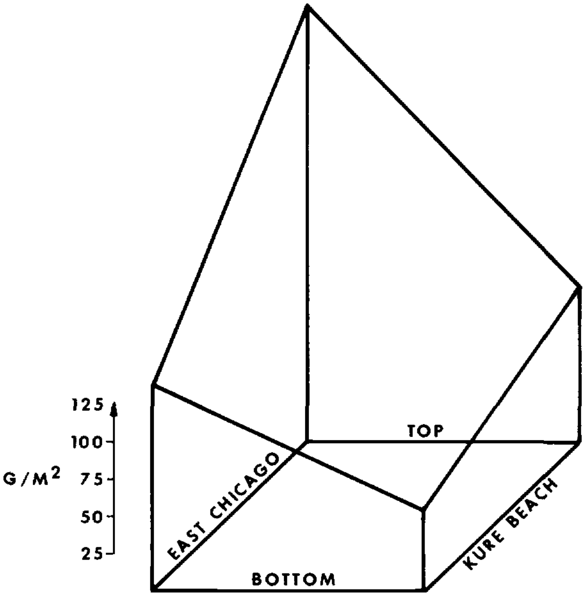

FIG. 7—*Ten-year predicted weight-losses for galvanized steel.*

subsequent reaction. The results shown are consistent with reasonable phenomenological models for the processes which take place. The kinetic equations developed here allow reliable long-term predictions. Weight-losses to be expected in a 10-year exposure, for instance, provide a concise summary of the atmospheric corrosion behavior of galvanized steel at these two sites. These are shown in Fig. 7. The diagram in this summarizing figure shows the following weight-losses predicted for 10-year exposures:

East Chicago: skyward 290 g/m^2–groundward 137 g/m^2
Kure Beach: skyward 103 g/m^2–groundward 55 g/m^2

The 10-year exposure level was selected because this represents a rather long exposure for galvanized steel in these environments and because this length of exposure provides an indication of the practical effect of the variation in N-values.

References

[1] Legault, R. A. and Preban, A. G., *Corrosion*, Vol. 31, 1975, p. 117.
[2] Legault, R. A., *Proceedings*, Meeting of the National Association of Corrosion Engineers, Toronto, Ont., 1975.
[3] Legault, R. A. and Pearson, V. P., *Proceedings*, Offshore Technological Conference, Houston, Tex., 1975.
[4] *Proceedings*, American Society for Testing and Materials, Vol. 44, 1944, p. 44.
[5] Guttman, H. in *Metal Corrosion in the Atmosphere, ASTM STP 435*, American Society for Testing and Materials, 1968, p. 230.
[6] Anderson, F. A. in *Atmospheric Corrosion of Nonferrous Metals, ASTM STP 175*, American Society for Testing and Materials, 1956, p. 132.

F. N. Longo[1] *and G. J. Durmann*[2]

Corrosion Prevention with Thermal-Sprayed Zinc and Aluminum Coatings*

REFERENCE: Longo, F. N. and Durmann, G. J., "**Corrosion Prevention with Thermal-Sprayed Zinc and Aluminum Coatings,**" *Atmospheric Factors Affecting the Corrosion of Engineering Metals, ASTM STP 646,* S. K. Coburn, Ed., American Society for Testing and Materials, 1978, pp. 97-114.

ABSTRACT: This paper presents the results of 19 years' testing, undertaken by the American Welding Society, to evaluate flame-sprayed zinc and aluminum coatings, sealed and unsealed, applied to low-carbon steel.

Panels were exposed to seawater at mean tide and below low tide levels at two different locations. Panels were also exposed to atmospheric conditions at six different locations including rural, industrial, salt air, and salt spray environments.

The results indicate that low-carbon steel can be protected from the corrosive effects of these environments for 19 years or more by the application of flame-sprayed zinc or aluminum coatings.

KEY WORDS: corrosion, atmospheric corrosion, marine atmospheres, industrial atmospheres, rural atmospheres, flame spraying, zinc coatings, aluminum coatings, carbon steels

This paper reports the results of a 19-year study of the corrosion protection afforded by wire flame-sprayed aluminum and zinc coatings applied to low-carbon steel. The program was initiated in July 1950 by the Committee on Metallizing (now the Committee on Thermal Spraying) of the American Welding Society (AWS). The first panels were exposed in January 1953. This report is a partial presentation of the results of an inspection made of the metallized coated steel panels exposed for 19 years. See *AWS 19-Year Report*[3] for full details.

*Original experimental data were measured in U.S. customary units.

[1] Manager, Materials Engineering Department, METCO, Inc., Westbury, N.Y. 11590.

[2] President, Coating Systems and Technology, Inc., North Babylon, N.Y.

[3] "Corrosion Tests of Metallized Coated Steel, 19-Year Report," AWS C2.14-74, American Welding Society, 1974.

Originally, exposure periods of 1, 3, 6, and 12 years were scheduled. At the end of each of these periods, a complete set of panels, consisting of three identical panels of each type was to be removed from the exposure racks for laboratory examination. At the same time, the panels of each type remaining on site were to be inspected and their condition recorded. However, early inspections indicated that nearly all coatings would last for more than 12 years at all exposure sites. Accordingly, the panels scheduled for removal at 6 years were left on exposure for 12 years, and the 12-year set was left exposed for 19 years. Results of the 6-year and 12-year inspections are reported in AWS publications C2.8-62[4] and C2.11-67,[5] respectively.

The initial program details discussed here, with minor deletions, were taken directly from the AWS 12-year report (C2.11-67[5]).

Test Sites

Test sites were selected to provide a wide variety of environmental conditions. These exposure sites and the exposure dates for the panels in this program are listed in Appendix I. All sites are recognized ASTM test areas. No mild, rural exposures were included; some degree of atmospheric contamination, either saline or industrial, exists at all sites. Seawater tests include full- and half-tide immersion in quiet seawater, and full immersion in flowing seawater (approximately 3 knots). Test panels for atmospheric exposure are mounted on racks at a 30 deg angle. Panels for seawater immersion are mounted in a vertical position.

Test Panels

Test panels were made of low-carbon steel sheet (0.08 percent carbon, 0.30 percent manganese, 0.008 percent phosphorus, 0.03 percent sulfur, 0.003 percent silicon, 0.30 percent copper). The steel panels for atmospheric and seawater exposure were 102 by 152 by 3.2 mm (4 by 6 by 1/8 in.) and 102 by 305 by 3.2 mm (4 by 12 by 1/8 in.), respectively.

The aluminum and zinc wire flame-sprayed coating thickness for atmospheric exposure tests were 0.08, 0.15, 0.23, 0.34, and 0.41 mm (0.003, 0.006, 0.009, 0.012, and 0.015 in.). A coating thickness of 0.49 mm (0.018 in.) was added in the seawater exposure tests.

Panel Preparation

The as-supplied panels were hot-rolled steel which had been pickled to

---

[4] "Corrosion Tests of Metallized Coated Steel, 6-Year Report," AWS C2.8-62, American Welding Society, 1962.

[5] "Corrosion Tests of Metallized Coated Steel, 12-Year Report," AWS C2.11-67, American Welding Society, 1967.

remove mill scale. Surfaces were inspected and panels showing gross defects were rejected.

The panels were then thoroughly blast cleaned using a forced-feed blast generator and a minimum pressure of 90 psi (620 kN/m^2) at the generator with the types and mesh sizes of abrasives shown in Appendix II.

The flame-spraying operation was done on a special automatic machine on which 36 panels were flame-sprayed at a time. The speed of rotation and traverse of both panels and the speed of the wire flame-spray gun across the surface were controlled automatically in order to obtain uniformity of coating thickness.

Three types of wire were used: (*a*) 3.2-mm (1/8-in.)-diameter aluminum, 99.0 percent minimum purity; (*b*) 3.2-mm (1/8-in.)-diameter zinc, 99.9 percent minimum purity; and (*c*) 3.2-mm (1/8-in.)-diameter steel, SAE 1010 grade: 0.08 to 0.12 percent carbon, maximum 0.04 percent phosphorus, and maximum 0.05 percent sulfur.

The steel wire was used for a flash-bonding coat on some specimens, and was applied automatically to a thickness of 0.03 mm (0.001 in.). This bonding is not considered as part of the coating thickness.

Sealing treatments, where used, were applied by spraying. Appendix III shows the composition of the sealing materials. These formulations were thinned sufficiently to ensure good penetration and were applied sparingly, the purpose being to fill the surface and subsurface pores of the sprayed metal, rather than to overcoat. By actual measurements the sealers used added little or nothing to the coating thickness.

The types of aluminum- and zinc-coated panels are listed in Appendixes IV and V; Types 14 to 28 inclusive, were included in order to determine the effect of preparation of the steel on the life of the coating. All of these panels had a coating thickness of 0.23 mm (0.009 in.) and are located at only two of the test sites: Kure Beach, North Carolina, 24-m (80-ft) lot, for atmospheric exposure, and Wrightsville Beach, North Carolina (mean tide) for seawater exposure.

Conclusions

1. Aluminum coatings 0.08 to 0.15 mm (0.003 to 0.006 in.) both sealed and unsealed give complete base metal protection from corrosion in seawater and in severe marine and industrial atmospheres.
2. Unsealed zinc coatings require 0.34 mm (0.012 in.) for complete protection in seawater for 19 years. In severe marine and industrial atmospheres 0.23 mm (0.009 in.) of unsealed zinc or 0.08 to 0.15 mm (0.003 to 0.006 in.) of sealed zinc are needed for 19 years' protection.
3. The application of one coat of wash primer plus one or two coats of aluminum vinyl enhances the appearance and extends the life of aluminum and zinc coatings.

4. Thin coats of aluminum perform better than thick coats of aluminum because they have less tendency to develop pits and blisters.
5. The corrosion protection afforded by zinc and aluminum coatings is not affected by the method of steel preparation. Specifically, a steel flash is not essential as a bond coat.
6. The use of flame-sprayed aluminum and zinc coatings is a means to extend the life of iron and steel structures and thereby help to conserve these natural resources.

Results

The following results are divided into three separate sections: Seawater Exposure—Total Immersion and Mean Tide, Marine Atmosphere, and Industrial Atmosphere. It should be kept in mind that these results pertain primarily to the overall general condition of the test panels at each of the above three types of exposure sites.

Seawater Exposure—Total Immersion and Mean Tide

Wrightsville Beach, North Carolina—Mean Tide

Aluminum coated panels—Unsealed aluminum-coated panels at this site show a few blisters which originate at the coating's steel interface. The heavier the coating the larger the blisters, in some cases 8 mm (5/16 in.) diameter. In those cases where a blister has broken open, the exposed steel is relatively free of corrosion. A layer of iron oxide is present, but no measurable loss of steel is evident. While the aluminum surrounding these broken blisters probably contributed to the protection of the steel there is no significant evidence of corrosion of the aluminum. See Fig. 1 for the typical aluminum structure. Scraping the aluminum surface presents a bright, metallic luster.

All vinyl-sealed panels are in excellent condition including those which were coated with only 0.08 mm (0.003 in.) of aluminum (see Fig. 2). A few small blisters are present on some of the sealed panels but considerably smaller than on the unsealed aluminum panels. Breaking open these blisters reveals typical voluminous aluminum corrosion products and a thin layer of rust on the steel. No measurable loss of steel is evident. This is also true where the coatings were damaged mechanically at the edges by the ceramic mounting insulators. Areas as large as 3 by 13 mm (1/8 by 1/2 in.) of exposed steel show no significant loss of steel. No progressive corrosion of the aluminum surrounding these areas is evident.

There is no noticeable difference in coating performance as a function of the variations in surface preparation methods tested (see Appendix II).

Zinc-coated panels—All unsealed zinc-coated panels of less than 0.34 mm (0.012 in.) in coating thickness have failed. The 0.34, 0.41, and 0.49-mm

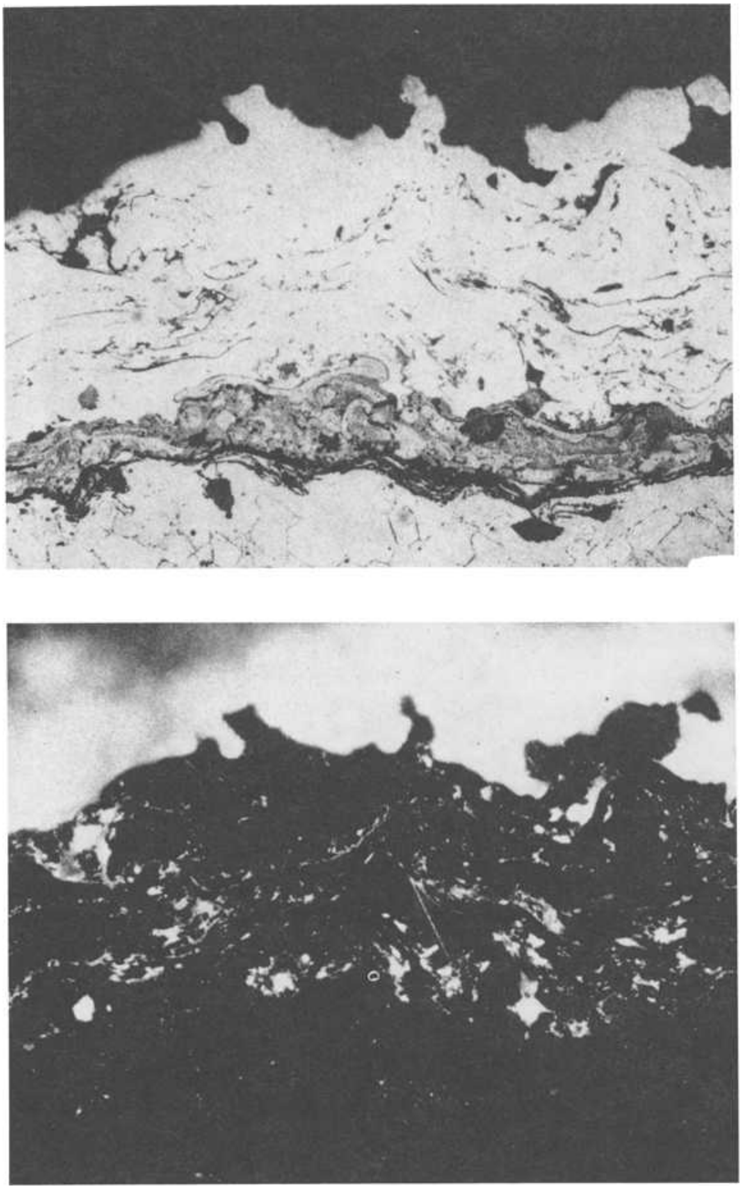

FIG. 1—(top) *Flame-sprayed aluminum coating, 0.15 mm (0.006 in.) thick, no sealer, over a flash coat of carbon steel, exposed for 19 years at Wrightsville Beach, N.C., in seawater at mean tide level (nital etch. ×250).* (bottom) *Same specimen under polarized light, showing the amount of coating which has converted to aluminum corrosion product* (white area) *and remaining aluminum* (black area).

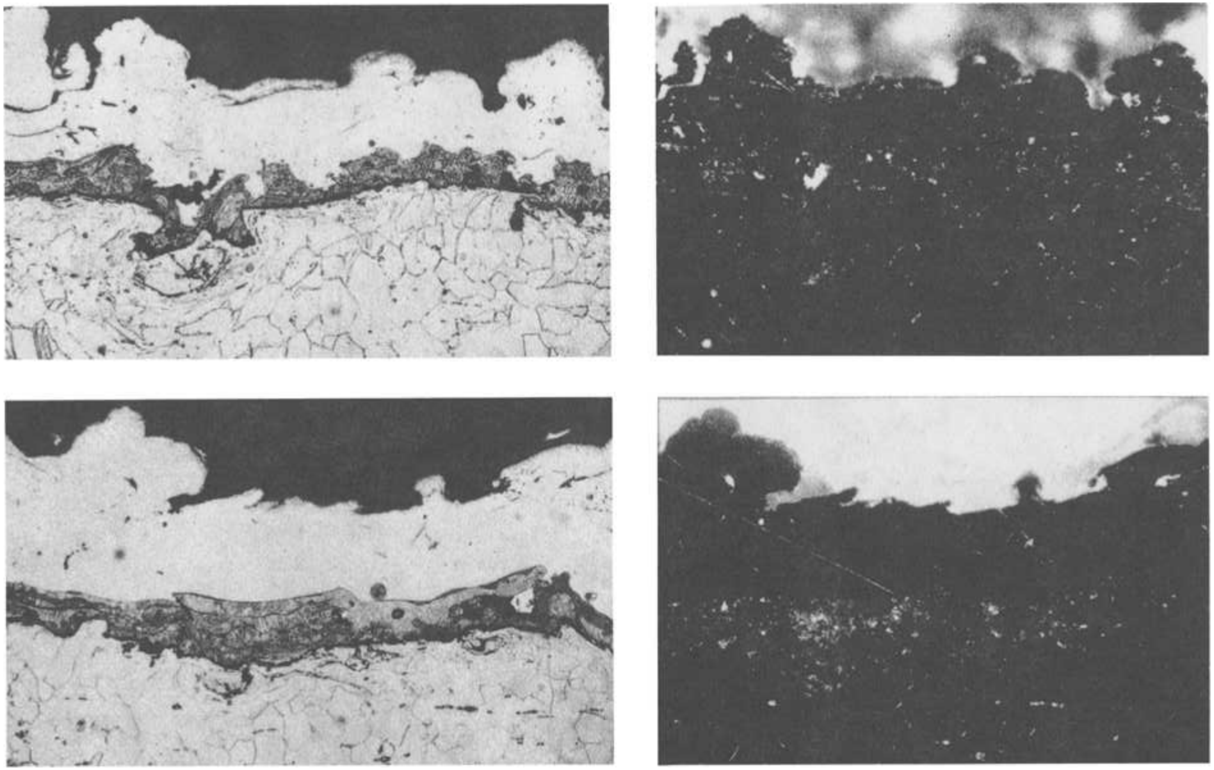

FIG. 2—(top left) *Flame-sprayed aluminum coating, 0.08 mm (0.003 in.) thick, with one coat of primer and two coats of vinyl, exposed for 19 years below low tide at Wrightsville Beach, N.C. (nital etch, ×250)* (top right) *Same specimen under polarized light, illustrates the relatively small amount of aluminum corrosion.* (bottom left) *Reserve panel with same coating, never exposed.* (bottom right) *Reserve panel with same coating, never exposed, under polarized light.*

(0.012, 0.015, and 0.018 in.) thick unsealed zinc coatings show little or no rust, but the coatings have been converted almost completely to corrosion product (see Fig. 3).

Chlorinated rubber sealers on zinc did not perform satisfactorily. The steel is deeply pitted where coatings have failed, and the appearance indicates that the residual zinc corrosion product has become cathodic to the exposed steel. There is no evidence to show that there is any difference in coating performance as a result of the surface preparation methods tested.

Wrightsville Beach, North Carolina—Total Immersion

Aluminum-coated panels—Unsealed aluminum coatings at this site appear to blister slightly more than those at the mean tide level. The steel is still being protected, even where the blisters have broken open, as in the case of the aluminum-coated panels exposed at the mean tide level.

The vinyl-sealed panels are in excellent condition, showing a few small, unbroken blisters. The coatings on these panels are in a condition similar to the aluminum-sealed panels exposed at the mean tide level.

Zinc-coated panels—The performance of zinc coatings in this exposure is very similar to those exposed at the mean tide level.

Zinc coatings less than 0.34 mm (0.012 in.) thick, sealed and unsealed, have failed. Zinc coatings of 0.34, 0.41, and 0.49 mm (0.012, 0.015, and 0.018 in.), sealed and unsealed, have protected the base metal, but it appears that the zinc has been converted to corrosion products (see Fig. 3). This tightly adherent mixture of white rust and foulants appears to be providing the corrosion protection to the base metal. All panels which have failed are very deeply pitted.

Freeport, Texas—Seawater Exposure—Panels at this site were lost in a hurricane. The only documented test information available at this site can be obtained by reference to the *AWS Twelve-Year Report*.[5]

Marine Atmosphere

Kure Beach, North Carolina—24-m (80-ft) Lot—At this site the specimens face the surf in a southeasterly direction at an average distance of 24 m (80 ft) from the normal mean tide level, exposing them to ocean spray, salt air, and the weather.

Aluminum-coated panels—All unsealed panels have a dull, gray-brown, blotchy appearance, with evidence of blistering of the aluminum in thicknesses greater than 0.08 mm (0.003 in.). Unsealed panels with 0.15-mm (0.006-in.)-thick coatings have approximately 6 to 20 blisters, 3.2 mm (1/8 in.) in diameter, per 2.54 cm^2 ($in.^2$). Unsealed aluminum panels with 0.23-mm (0.009 in.)-thick coatings have over 20 blisters, 3.2 mm (1/8 in.) in diameter, per 2.54 cm^2 ($in.^2$). Blisters do not appear to be as prevalent on the groundward surfaces.

One coat of aluminum vinyl sealer on 0.08 mm (0.003 in.) of aluminum

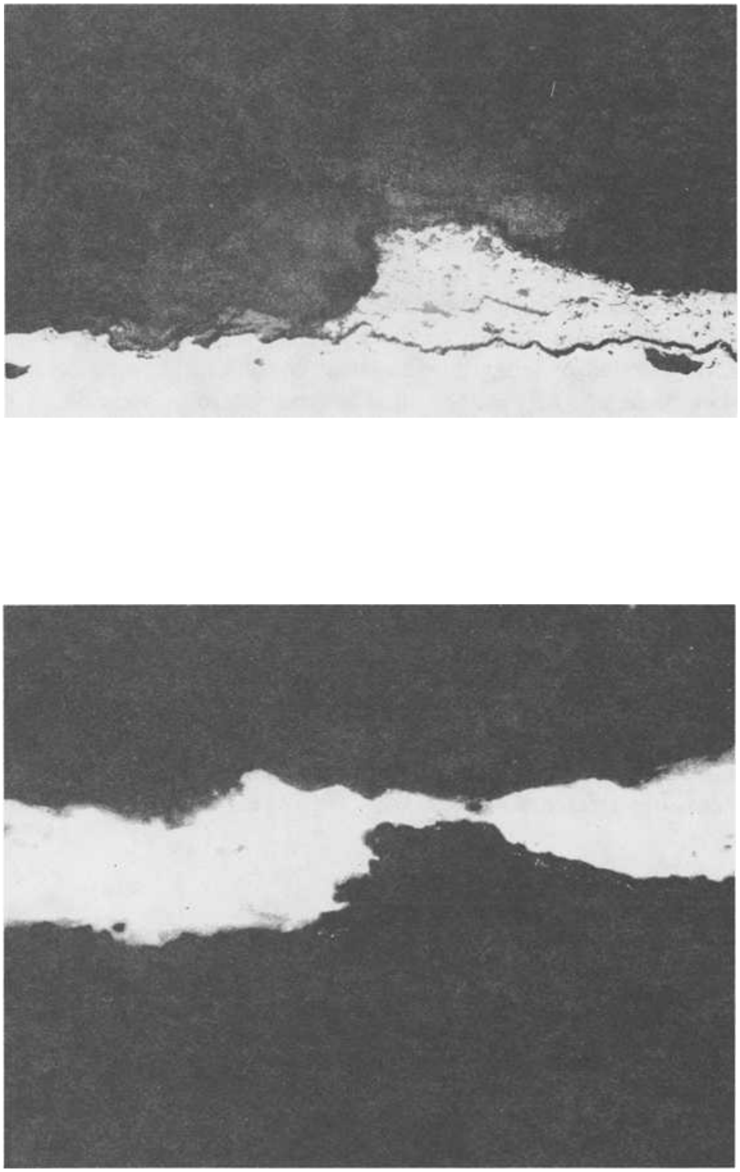

FIG. 3—(top) *Flame-sprayed zinc coating, 0.34 mm (0.012 in.) thick, no sealer, exposed for 19 years at Wrightsville Beach, N.C. in seawater at mean tide level (nital etch, ×60).* (bottom) *Same area under polarized light, illustrating zinc corrosion product* (white area) *and remaining zinc* (black area).

appears slightly duller than two coats. Aluminum vinyl-sealed panels seem to be in excellent condition (see Fig. 4). There is evidence of a few blisters in coatings thicker than 0.08 mm (0.003 in.) sealed with one and two coats of aluminum vinyl. The groundward side of these panels have a slightly blotchy appearance but no evidence of any blisters of metal.

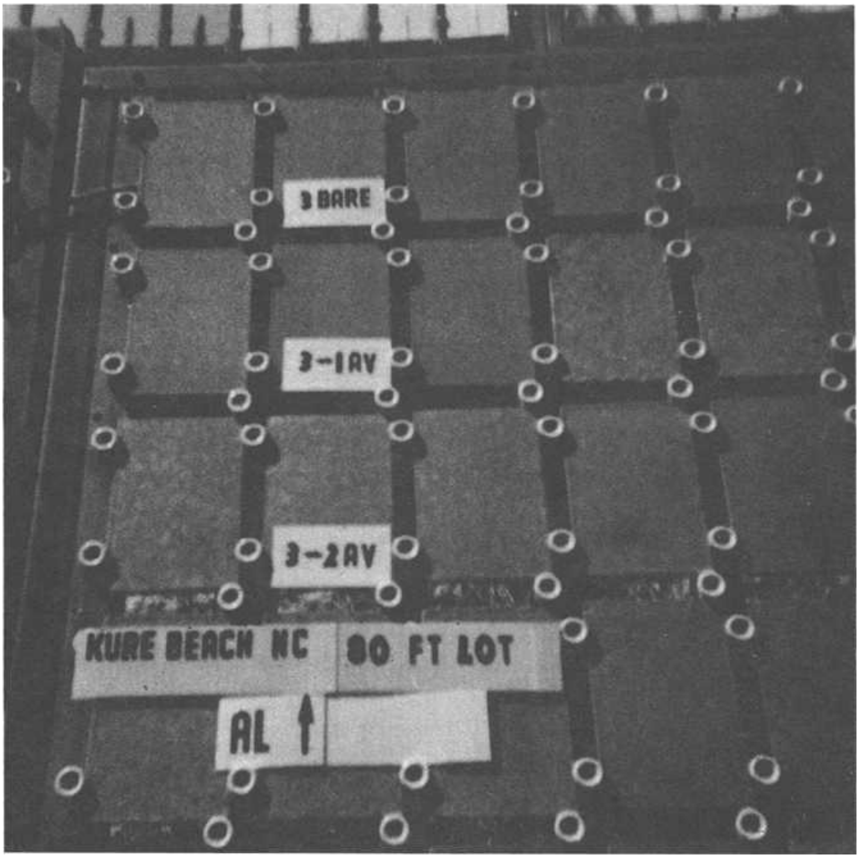

FIG. 4—*Test panels at Kure Beach, N.C., 24-m (80-ft) lot, normal mean tide level, facing the surf. Three panels at top left are coated with 0.08 mm (0.003 in.) aluminum, no sealer. Three panels at center left are coated with 0.08 (0.003 in.) aluminum, followed by wash prime and one coat of aluminum vinyl. Three panels at lower left have same aluminum coating plus two coats of aluminum vinyl.*

No difference in general appearances or tendency to blister could be observed as a function of surface preparation method.

Zinc-coated panels—Unsealed zinc coatings 0.08 mm (0.003 in.) exhibited heavy rusting of the base metal (see Fig. 5).

Aluminum vinyl sealer has deteriorated completely on the 0.08-mm (0.003-

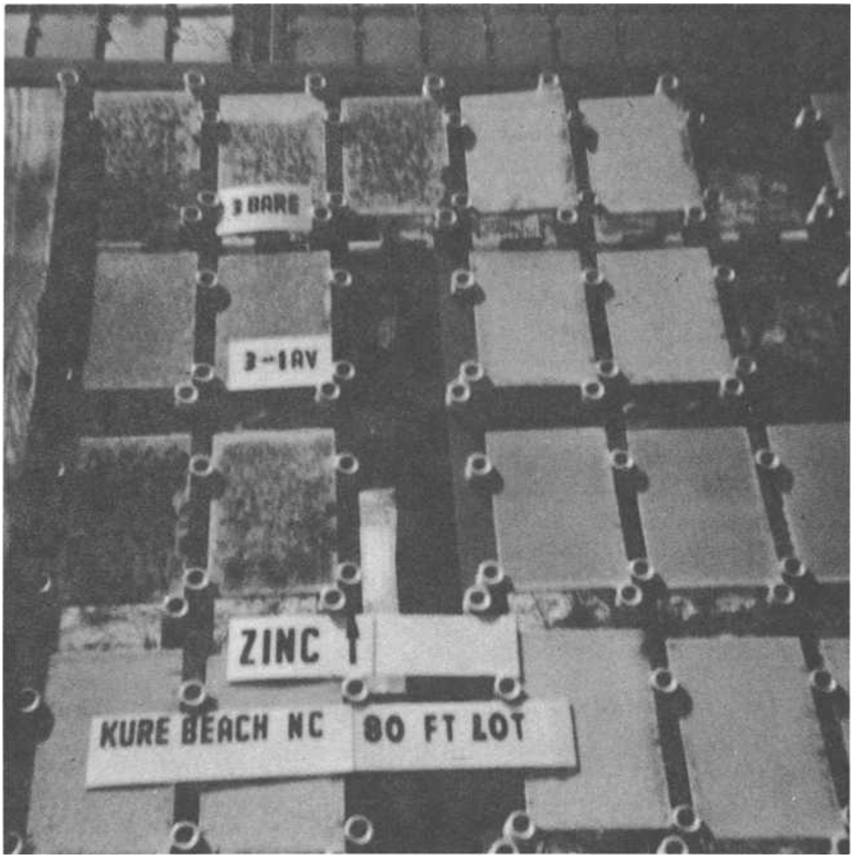

FIG. 5—*Test panels at Kure Beach, N.C., 24-m (80-ft) lot, normal mean tide, facing the surf, exposed for 19 years. Three panels at top left are coated with 0.08 mm (0.003 in.) zinc, no sealer. Two panels at center left are coated with 0.08 mm (0.003 in.) zinc.*

in.) zinc with rust at the edges of the base and encroaching on the faces. Both skyward and groundward surfaces are covered with white rust. Unsealed 0.15-mm (0.006-in.) zinc panels are rusting at the edges of the base metal and flat surfaces are covered with small nodes of heavy white rust.

Zinc coatings sealed with chlorinated rubber are similar in appearance to unsealed zinc.

Unsealed coatings of zinc 0.23 mm (0.009 in.) or greater are covered with many small nodes of white rust; there is no evidence that the base material is rusting.

The aluminum vinyl is gone from the skyward surface of most of the panels to which it was applied. Heavy white rust is evident. The groundward surfaces have very little aluminum vinyl remaining.

The fact that the aluminum vinyl sealer has deteriorated completely on the zinc panels in this severe marine atmosphere appears to justify the decision not to use the vinyl sealer on the seawater test panels. Early laboratory tests with vinyl-sealed zinc-coated panels exposed in the seawaters off Long. Island, New York indicated failure of the vinyl as a sealer for zinc. This may be a function of the chloride ion, since vinyl-sealed zinc has performed very well in the industrial atmospheres where there are fewer chlorides available.

No difference in the condition of panels as a function of surface preparation method is apparent.

Kure Beach, North Carolina—245-m (800-ft) Lot

Aluminum coated-panels—All panels are in excellent condition at this site (see Fig. 5). Unsealed panels with 0.08-mm (0.003-in.) thick coatings are light gray in color on the skyward surface with a slightly darker gray stain and some light rust staining on the groundward surface. No rust staining is evident on the heavier unsealed aluminum coatings.

All aluminum vinyl-sealed panels are in excellent condition. Those with one coat of sealer have a dark mottled appearance over 95 percent of the skyward surface, while those with two coats have the mottled appearance on 20 to 25 percent of the area. The groundward surfaces have retained their original appearance.

Zinc-coated panels—The unsealed 0.08-mm (0.003-in.) zinc panels are dark blue in color with horizontal stripes of white rust that appear to conform to the spray pattern (see Fig. 5). This condition is apparent on both surfaces with the groundward surface having a slightly darker blue color.

About 10 to 20 percent of the skyward surface of zinc panels with one coat of aluminum vinyl sealer 0.08 mm (0.003 in.) thick appears mottled, with a few pinpoint blisters of the aluminum vinyl. Groundward surfaces are in very good condition with the exception of one panel that has approximately 5 percent deterioration of the sealer. The chlorinated rubber sealer has long since disappeared leaving those panels very similar to the unsealed panels, though with slightly less horizontal striping. Panels with coating thickness greater than 0.08 mm (0.003 in.) appear to have absorbed the aluminum vinyl sealer better than those with 0.08-mm (0.003-in.) coatings. The groundward surfaces are in very good condition. There is no evidence of rusting of the base metal on any of the panels in the 245-m (800-ft) lot.

Brazos River, Texas—This test site cannot be considered a very severe marine atmosphere. All panels are in very good condition with no evidence of the base metal corroding. All panels have a light tan discoloration which appears to be the color of the dust in the area.

Aluminum-coated panels—The groundward surfaces of unsealed aluminum, 0.15 to 0.41 mm (0.006 to 0.015 in.) thick show some evidence of blisters which is not apparent on the skyward surfaces. The unsealed panels with 0.08-mm (0.003-in.)-thick coatings had no evidence of blistering on either side. The aluminum vinyl sealer has developed a blotchy appearance on most of the panels. Vinyl-sealed 0.08-mm (0.003-in.) aluminum coating is in excellent condition with groundward surfaces having an as-new appearance. Panels with one coat of aluminum vinyl 0.23 to 0.34 mm (0.009 to 0.012 in.) thick have developed a blotchy appearance on the groundward surface. Those with two coats of vinyl sealer are in excellent condition.

Zinc-coated panels—Zinc-coated panels at this site are in good condition. A tan discoloration on all panels is evident, particularly at the edges. There is no evidence of the base metal rusting. Unsealed zinc panels have taken on a light blue color.

The aluminum vinyl sealer shows some deterioration—as much as 25 percent of the skyward surface on some of the panels—with zinc corrosion products evident. The groundward side of the panels sealed with aluminum vinyl is in good condition.

Panels sealed with chlorinated rubber are similar in appearance to the unsealed panels except that a horizontal striping effect is more pronounced. There is no evidence of any chlorinated rubber remaining.

Point Reyes, California

Aluminum-coated panels—Unsealed aluminum coatings, 0.08 mm (0.003 in.) thick, have developed a black discoloration over 25 to 75 percent of the skyward surfaces, with no evidence of nodes or blisters. The groundward surfaces have a slight rust stain. Thicker coatings of unsealed aluminum have some discoloration, but it is lighter, and covers less area.

All panels sealed with one coat of aluminum vinyl have a mottled appearance, while those with two coats are in excellent condition.

There is no rusting of the base on any of the panels.

Zinc-coated panels—Unsealed zinc panels have a blue color on the skyward surface with the familiar horizontal stripes more evident on the 0.08-mm (0.003-in.) coatings than on the heavier coatings. The groundward surfaces on all unsealed panels are a dark blue color.

The panels with coatings 0.08 mm (0.003 in.) thick sealed with one coat of aluminum vinyl exhibit blistering of the sealer on 5 to 10 percent of the skyward surfaces. The remaining area is bright and in excellent condition. It is apparent that the aluminum vinyl sealer is deteriorating to a greater extent on the heavier coatings of zinc than on thinner coatings. This deterioration is accompanied by corrosion of the zinc. Since heaver coatings absorb more, two coats of vinyl sealer would be in order.

Panels sealed with chlorinated rubber have a tan discoloration—a combination of zinc corrosion product and deteriorated sealer—on both surfaces.

Industrial Atmosphere

New York City Area (Kearny, New Jersey)

Aluminum-coated panels—Unsealed 0.08-mm (0.003-in.) aluminum coatings show many nodes of corrosion on the skyward surface that are black in color due to retained contamination. The groundward surface is gray to black in color with some indication of nodular corrosion. No rusting of the base is evident.

Unsealed 0.15, 0.23, and 0.34-mm (0.006, 0.009, and 0.012-in.) aluminum coatings show heavy blistering of aluminum on the skyward surface. The groundward surfaces exhibit nodular type corrosion.

Aluminum vinyl-sealed coatings show evidence of a few scattered nodes of corrosion product on the skyward surface of the panels with 0.08-mm (0.003-in.) coatings. Heavier coatings show indications of a few scattered blisters. Groundward surfaces are all in excellent condition.

All coating thicknesses sealed with two coats of aluminum vinyl are in excellent condition on both surfaces.

Zinc-coated panels—Unsealed 0.08-mm (0.003-in.) zinc coatings failed completely on the skyward surface and approximately 75 percent of the groundward surface. The 0.08-mm (0.003-in.) zinc coatings sealed with chlorinated rubber also failed completely on the skyward surface and failed on about 10 percent of the groundward surface. Zinc coatings 0.08 mm (0.003 in.) thick sealed with aluminum vinyl are in excellent condition and appear brighter and cleaner than aluminum coatings with the equivalent amount of sealer. It is interesting to note that the vinyl is in better condition on the 0.08-mm (0.003-in.) coatings than on the heavier zinc coatings where it has deteriorated 10 to 30 percent in some cases. This is probably because 0.08-mm (0.003-in.) coatings are smoother and do not absorb as much sealer as the heavier coatings.

Unsealed 0.15-mm (0.006-in.) zinc coatings exhibit some rusting on the skyward surface and less on the groundward surface. Unsealed 0.23 and 0.34-mm (0.009 and 0.012-in.) coatings are blue in color with some deposit staining. No rusting of base metal is evident.

- *Columbus, Ohio*

Aluminum-coated panels—All unsealed sprayed aluminum panels have a black nodular type of corrosion product with the size of the nodule increasing with the thickness of coating. There is no evidence of the base metal corroding. Panels sealed with one coat of aluminum vinyl are beginning to show some indications of these black nodes forming. Panels with two coats of aluminum vinyl sealer are in excellent condition.

Zinc-coated panels—Panels with unsealed 0.08-mm (0.003-in.) zinc coating lost approximately 90 percent of the zinc on the skyward surfaces and the base metal is rusting. Edges are also rusting. The groundward side of the panels is covered with white rust stained with red rust. All zinc-coated panels sealed with aluminum vinyl are in good condition. One panel in each of the 0.15 and 0.23-mm (0.006 and 0.009-in.) coating groups, sealed with aluminum vinyl, is exhibiting a 5 to 10 percent deterioration of the sealer with some white rust evident. Panels with unsealed 0.15-mm (0.006-

in.) coatings show some red rust at the edges of the identifying notches. Some black nodes are evident which are probably white rust with deposit stain.

East Chicago, Indiana—This is a very heavy industrial environment with all panels having a dark brown discoloration.

Aluminum-coated panels—All unsealed aluminum panels with coatings of 0.15 mm (0.006 in.) or more have evidence of blistering of the aluminum on the skyward surfaces. Unsealed aluminum coatings 0.08 mm (0.003 in.) thick have a more nodular type of corrosion on the skyward surface with less evidence of aluminum corrosion on the groundward surface. Aluminum vinyl-sealed panels have a very heavy deposit stain on both surfaces. Two coats of aluminum vinyl appear slightly better than one coat. No corrosion is evident on the sprayed aluminum.

Zinc-coated panels—Sprayed zinc-coated panels sealed with aluminum vinyl are in very good condition with some deposit staining on the vinyl sealer.

APPENDIX I

Test Site Data

	Number of Panels		
Test Site and Environment	Aluminum	Zinc	Date Exposed
Atmospheric exposure			
Brazos River, Tex. (salt air)	156	156	March 1954
Columbus, Ohio (urban)	120	120	Nov. 1953
East Chicago, Ind. (industrial)	120	120	Nov. 1953
Kure Beach, N.C.			
24-m (80-ft) lot (severe marine)	336	336	Jan. 1953
240-m (800-ft) lot (salt air)	156	156	Jan. 1953
New York City Area (industrial)	120	120	Nov. 1953
Point Reyes, California (salt air)	156	156	Dec. 1953
102 by 152-mm (4 by 6 in.) panels reserved	156	156	
Seawater exposure			
Freeport, Tex.	156	156	Oct. 1953
Wrightsville Beach, N.C.			
below low tide	156	156	Oct. 1953
mean tide	336	336	Oct. 1953
102 by 305-mm (4 by 12 in.) panels reserved	156	156	
Totals	2124	2124	

APPENDIX II

Types of Abrasive Used for Blast Cleaning Specimens in this Test Program[a]

Types of Abrasive	Mesh Distribution	Description
	TYLER SCREEN SIEVE ANALYSIS	
Coarse silica sand	+ 14 mesh 5% – 14 + 20 mesh 48% ± 10% – 20 + 28 mesh 40% ± 10% – 28 + 35 mesh 10% ± 10% – 35 mesh 5%	washed angular silica sand, dry and free of feldspar, clay, or or other friable constituents
	U.S. STANDARD SCREEN ANALYSIS	
Fine silica sand	+ 20 mesh 5% – 20 + 30 mesh 67% ± 10% – 30 + 40 mesh 24% ± 10% – 40 mesh 10%	washed angular silica sand, dry and free of feldspar, clay, or other friable constituents
Chilled iron grit	Conforms to SAE specification for G-25 angular chilled iron grit	angular chilled iron grit

[a] It should be noted that the precise mesh distribution shown would probably not be obtainable in all areas, and they should not be used for specification purposes.

APPENDIX III

Composition and Description of Seal Coats

Seal Coat	Composition	Description
Wash primer[a]	resin component: pigment insoluble type, inert, zinc chromate, 8.2% nonvolatile vehicle: polyvinyl butyral, 9.5% volatile vehicle: butyl and isopropyl alcohol, 82.3% acid component: phosphoric acid, 16.0% ethyl (or isopropyl alcohol) plus water, balance	air drying, two-part, acid-zinc chromate wash coat primer
Aluminum vinyl	pigment: nonleafing aluminum flake, 10% nonvolatile vehicle: vinyl copolymer and plasticizer, 20% volatile vehicle: toluene and ketones, 70%	vinyl copolymer aluminum flakes, air drying type of coating material

Seal Coat	Composition	Description
Clear vinyl	pigment: none nonvolatile vehicle: vinyl chloride-acetate resin, 16% plasticizer, 1.4% volatile vehicle: ketones, 37.6% aromatic hydrocarbons, (toluene, benzol, xylol), 45%	clear, vinyl copolymer, air drying coating material
Chlorinated rubber	solids: chlorinated rubber plus two types of chlorinated paraffins plus a stabilizer, 34% solvents: aromatic petroleum solvents, 66%	clear, air-drying, chlorinated rubber type coating material

[a] Mix four parts of the resin component with one part of the acid component to obtain final primer composition.

APPENDIX IV

Panel Types for Atmospheric Exposure

		Aluminum Flame-Sprayed Panels		Zinc Flame-Sprayed Panels	
Coating Thickness mm (in.)	Panel Type	Surface Preparation[a]	Seal Coat[b]	Surface Preparation[a]	Seal Coat[b]
0.08 (0.003)	1	1		1	
	2	1	WP+AV-1	1	WP+AV-1
	3	1	WP+AV-2	1	CR-2
0.15 (0.006)	4	1		1	
	5	1	WP+AV-1	1	WP+AV-1
	6	1	WP+AV-2	1	CR-2
0.34 (0.012)	10	2		2	
	11	2	WP+AV-1	2	WP+AV-1
	12	2	WP+AV-2	2	CR-2
0.23 (0.009)	7	1		1	
	8	1	WP+AV-1	1	WP+AV-1
	9	1	WP+AV-2	1	CR-2
	13	2		2	
	14	2		2	

		Aluminum Flame-Sprayed Panels		Zinc Flame-Sprayed Panels	
Coating Thickness mm (in.)	Panel Type	Surface Preparation[a]	Seal Coat[b]	Surface Preparation[a]	Seal Coat[b]
	15	2	WP+AV-1	2	WP+AV-1
	16	2	WP+AV-2	2	CR-2
	17	4		4	
	18	4	WP+AV-1	4	WP+AV-1
	19	4	WP+AV-2	4	CR-2
	20	6		6	
	21	6	WP+AV-1	6	WP+AV-1
	22	6	WP+AV-2	6	CR-2
	23	3		3	
	24	3	WP+AV-1	3	WP+AV-1
	25	3	WP+AV-2	3	CR-2
	26	5		5	
	27	5	WP+AV-1	5	WP+AV-1
	28	5	WP+AV-2	5	CR-2

[a] Types of surface preparation
1 = coarse silica sand
2 = coarse silica sand and steel flash
3 = fine silica sand
4 = fine silica sand and steel flash
5 = chilled iron grit
6 = chilled iron grit and steel flash

[b] Types of seal coat
WP = wash primer
AV = aluminum vinyl
CR = chlorinated rubber
-1 = one coat of specified seal coat
-2 = two coats of specified seal coat

APPENDIX V

Panel Types for Seawater Exposure

		Aluminum Flame-Sprayed Panels		Zinc Flame-Sprayed Panels	
Coating Thickness, mm (in.)	Panel Type	Surface Preparation[a]	Seal Coat[b]	Surface Preparation[a]	Seal Coat[b]
0.08 (0.003)	1	2	WP+CV-1	2	CR-1
	2	2	WP+CV-2	2	CR-2
0.15 (0.006)	3	2		2	

		Aluminum Flame-Sprayed Panels		Zinc Flame-Sprayed Panels	
Coating Thickness, mm (in.)	Panel Type	Surface Preparation[a]	Seal Coat[b]	Surface Preparation[a]	Seal Coat[b]
	4	2	WP+CV-1	2	CR-1
	5	2	WP+CV-2	2	CR-2
0.41 (0.015)	12	2		2	
0.49 (0.018	13	2		2	
0.34 (0.012)	9	2		2	
	10	2	WP+CV-1	2	CR-1
	11	2	WP+CV-2	2	CR-2
0.23 (0.009)	6	2		2	
	7	2	WP+CV-1	2	CR-1
	8	2	WP+CV-2	2	CR-2
	14	1		1	
	15	1	WP+CV-1	1	CR-1
	16	1	WP+CV-2	1	CR-2
	17	3		3	
	18	3	WP+CV-1	3	CR-1
	19	3	WP+CV-2	3	CR-2
	20	5		5	
	21	5	WP+CV-1	5	CR-1
	22	5	WP+CV-2	5	CR-2
	23	4		4	
	24	4	WP+CV-1	4	CR-1
	25	4	WP+CV-2	4	CR-2
	26	6		6	
	27	6	WP+CV-1	6	CR-1
	28	6	WP+CV-2	6	CR-2

[a] Types of surface preparation
- 1 = coarse silica sand
- 2 = coarse silica sand and steel flash
- 3 = fine silica sand
- 4 = fine silica sand and steel flash
- 5 = chilled iron grit
- 6 = chilled iron grit and steel flash

[b] Types of seal coat
- WP = wash primer
- CV = clear vinyl
- CR = chlorinated rubber
  - -1 = one coat of specified seal coat
  - -2 = two coats of specified seal coat

J. H. Payer[1] *and W. H. Safranek*[1]

Atmospheric Corrosion of Electroplated Zinc Alloy Die Castings

---

REFERENCE: Payer, J. H. and Safranek, W. H., "**Atmospheric Corrosion of Electroplated Zinc Alloy Die Castings,**" *Atmospheric Factors Affecting the Corrosion of Engineering Metals, ASTM STP 646*, S. K. Coburn, Ed., American Society for Testing and Materials, 1978, pp. 115–128.

ABSTRACT: The effect of electroplating variables on atmospheric corrosion of copper, nickel, and chromium electroplates on zinc alloy die castings was investigated at mobile and stationary test sites. More than 3000 electroplated die castings were exposed on Detroit, Michigan, trucks; Youngstown, Ohio, trucks; New York City tugboats; Detroit, Michigan, roof tops; and Kure Beach, North Carolina, 245-m (800-ft) lot, for periods of up to 10 years. Exposure to mobile test sites provided a valuable supplement to the more conventional stationary test site. The application of microdiscontinuous chromium proved to be the most influential factor for improved corrosion resistance.

KEY WORDS: atmospheric corrosion, corrosion, electroplating, copper plating, nickel plating, chromium plating, zinc alloys, marine atmospheres, industrial atmospheres

Electroplating is used extensively on zinc alloy die castings for decorative purposes. More than 5×10^8 kg of zinc alloy die castings are electroplated yearly with copper, nickel, and chromium in the United States and Europe. The objective of this study was to determine the effects of electroplating variables on atmospheric corrosion of plated zinc die castings. Information from the study undertaken by Battelle-Columbus Laboratories for The International Lead Zinc Research Organization, Incorporated, provides guidance in the selection of corrosion-resistant plating systems. The approach was to expose plated zinc alloy die cast panels to both mobile and stationary corrosion test sites. Initiated in 1959, the study comprised seven successive exposure programs. More than 3000 electroplated die castings were evaluated. Comprehensive and detailed reports of the individual exposure programs were made previously [*1*–*5*].[2]

---

[1] Principal research metallurgist and research leader, respectively, Corrosion and Electrochemical Technology Section, Battelle-Columbus Laboratories, Columbus, Ohio 43201.

[2] The italic numbers in brackets refer to the list of references appended to this paper.

Experimental Procedure

Electroplating Procedures

An electroplated system comprised of layers of copper, nickel, and chromium was applied to SAE 903 zinc alloy die castings. Details of the plating procedures have been reported previously [*1,6–9*]. Plating variables investigated included surface finish prior to electroplating, copper layer, nickel layer, and chromium layer. Both thickness and composition were varied.

The effect of surface finish was investigated by exposing panels which were either polished and buffed using procedures described in ASTM Practice for Preparation of Zinc-Alloy Die Castings for Electroplating (B 252-69), or vibratory finished. Copper layer variables investigated were (*a*) copper plated from a copper sulfate solution versus a cyanide solution, and (*b*) thickness of the copper layer.

Two nickel electroplates were evaluated: bright nickel, containing about 0.1 percent sulfur, and duplex nickel, consisting of a semibright layer of nickel containing less than 0.005 percent sulfur and a bright layer containing 0.1 percent sulfur. For duplex nickel, the ratio of semibright to bright nickel thickness was approximately 3:1. Other nickel electroplate variables investigated include the effect of duplex nickel layer thickness and the effect of satin finish on duplex nickel. Satin finish duplex nickel was achieved by mechanical polishing of the duplex nickel prior to application of conventional chromium electroplate.

Four chromium electroplates were evaluated on nickel-plated die castings: (*a*) conventional chromium 0.25 μm thick, (*b*) crack-free chromium 0.75 to 1.25 μm thick, (*c*) microporous chromium 0.25 μm thick, and (*d*) microcracked chromium 0.5 to 3.75 μm thick. The latter two are examples of microdiscontinuous chromium: 10000 pores/cm^2 for microporous chromium and 240 to 1500 cracks/cm for microcracked chromium.

Conventional chromium thickness is usually limited to 0.25 μm because resistance to corrosion provided by thicker deposits is only slightly improved and is not commensurate with increased cost. Corrosion through the relatively few larger cracks is the inevitable consequence of thickening conventional chromium. To develop one effective microcrack pattern, thickness has to be increased to about 0.75 μm, although some recent reports indicate that a thickness of 0.5 μm may be effective. In any case, data from the program described in this paper, show that corrosion resistance can be further improved by increasing the thickness of microcracked chromium to >0.75 μm.

Exposure Procedures

Mobile exposure was carried out on trucks in Detroit, Michigan, and

Youngstown, Ohio, and on tugboats in New York Harbor. The trucks traveled in-plant and on public highways within approximately 62 km (100 miles) of their base location. Stationary exposure was carried out at the 245-m (800-ft) lot in Kure Beach, North Carolina, and on rooftops in Detroit, Michigan. For these exposures a ranking of the aggressiveness of the environments based on Detroit as 1.0 would yield Kure Beach, 2 to 3, Youngstown, 4, and New York Harbor, 5. New York Harbor tugboats provided the most aggressive atmospheric exposure. In a typical exposure program, 100 to 120 castings were exposed at each of the exposure sites. Specimens were inspected at approximately 6-month intervals after they were cleaned with a wet sponge. In some cases, cleaning with soap and a synthetic fiber brush was required for panels exposed on trucks. Corrosion performance ratings were assigned by a procedure similar to that detailed in ASTM Committee B-8 report [*10*]. In this procedure, specific corrosion defects are weighted as shown in Table 1. Exposed areas occupied by each defect are measured as percentages of total area and the sum of the weighted areas converted to a rating number using the following logarithmic expression

TABLE 1—*Weight factors for corrosion defects.*

Substrate		Coating	
craters	4.0	large pits (>1.5 mm)	1.0
blisters	2.0	irregular pits (crow's feet)	0.5
pinpoints	1.0	small pits	0.3
flaking	1.0	cracks	0.1
stain	0.3	dark stain	0.1
		light stain	0.1

$$R = 3\,(2 - \log_{10} \text{weighted area})$$

This rating system results in a scale of 0 to 10 with 10 representing excellent corrosion resistance and 0 to 3 poor corrosion resistance.

Results of Atmospheric Corrosion Exposure

Prefinish and Copper-Plating Variables

No significant effect of mechanical polish and buff finish versus vibratory finish was observed on die cstings given two different electroplates: (*a*) copper (10 μm), duplex nickel (30 μm), and conventional chromium (0.25 μm), and (*b*) copper (10 μm), duplex nickel (30 μm), and microcracked chromium (0.75 μm).

A direct comparison of bright copper deposited from a cyanide solution and bright, leveling copper deposited from a copper sulfate solution was made. No effect was observed for electroplate comprised of copper (10 μm), duplex nickel (30 μm), and conventional chromium (0.25 μm). Decreasing copper thickness to 1.25 or 2.0 μm from 10 μm decreased the corrosion resistance for an electroplate comprised of copper, bright nickel (20 μm), and crack-free chromium (1.3 μm), while decreasing copper thickness from 10 to 5 μm had no significant effect on corrosion resistance for an electroplate of copper, duplex nickel (30 μm), and conventional chromium (0.25 μm). Thus, it appears that once a minimum copper thickness which prevents corrosion is achieved, further increase in thickness provides no further corrosion resistance.

Nickel-Plating Variables

Three effects of nickel plating were investigated: the effect of duplex nickel versus bright nickel, the effect of duplex nickel thickness, and the effect of mechanical polishing of nickel prior to chromium plating. Nickel variables were studied under several different kinds of chromium plate.

Duplex nickel was superior to bright nickel in all cases. Results of a 3-year exposure on New York tugboats, Youngstown trucks, Detroit trucks, and the 245-m (800-ft) lot at Kure Beach for duplex nickel versus bright nickel under a crack-free chromium layer are shown in Fig. 1. Duplex nickel provided greater corrosion resistance at all four locations. Corrosion was more severe at the three mobile sites than at the stationary sites and most severe for New York tugboats. It is likely that the vibrational abuse accompanying mobile exposure contributed to the introduction of flaws in the crack-free chromium coating and subsequently increased corrosion.

The advantage of duplex nickel was more apparent under conventional chromium than under microporous chromium. Under 0.25 μm of conventional chromium duplex nickel supplied approximately twice as much corrosion protection as a single layer of bright nickel at nickel layer thicknesses of 35 and 25 μm; while under 0.75 μm of microcracked chromium duplex nickel was only slightly better than bright nickel. For the latter specimens, relatively little corrosion occurred on the die casting plated with microcracked chromium, and the corrosion which did occur was limited to nickel pitting and staining with no substrate corrosion.

Corrosion resistance was found to increase with increasing nickel layer thickness under conventional chromium, microcracked chromium, and microporous chromium. Figure 2 shows the effect of 10, 20, and 30 μm of duplex nickel under 0.25 μm of conventional chromium exposed to Detroit rooftops, Detroit trucks, and Kure Beach. The effect of changing duplex nickel layer thickness under microcracked chromium for New York tugboats, Youngstown trucks, Detroit trucks and Kure Beach is shown in

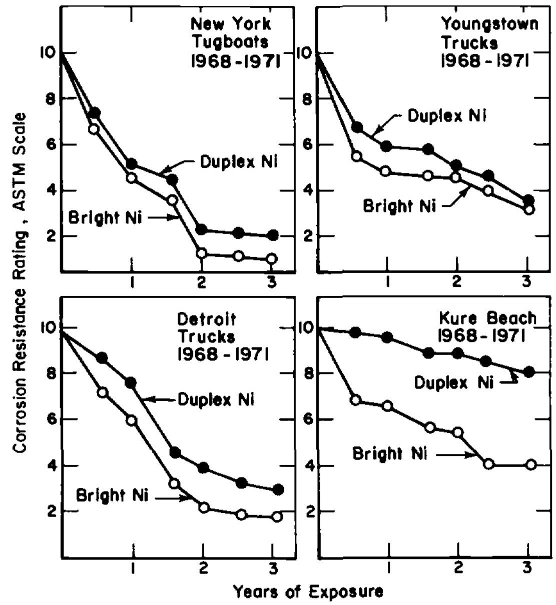

FIG. 1—*Effect of duplex nickel versus bright nickel for 1.0-μm crack-free Cr, 35-μm Ni, and 12-μm Cu.*

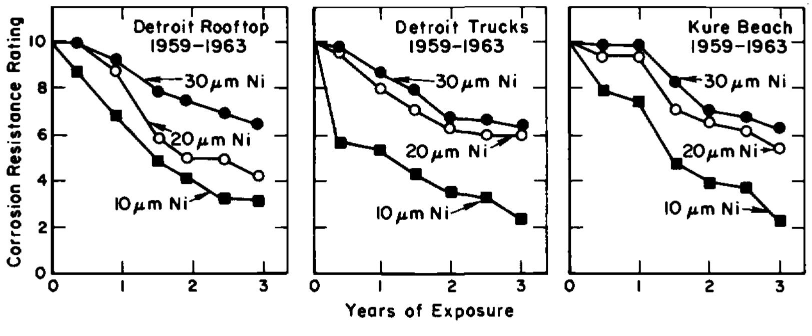

FIG. 2—*Effect of duplex nickel layer thickness for 0.25-μm conventional Cr, duplex Ni, and 10-μm Cu.*

Fig. 3. A thicker duplex nickel provides more protection at all sites. Again, the increased severity of mobile exposure compared to stationary exposure at Kure Beach is observed. Corrosion at the three mobile sites is more severe after the 3-year exposure than after the 10-year exposure at the stationary site. Similar results for the effect of nickel thickness under microporous chromium are shown in Fig. 4. Increasing duplex nickel thickness from 16 to 30 μm greatly enhanced corrosion resistance for exposure on

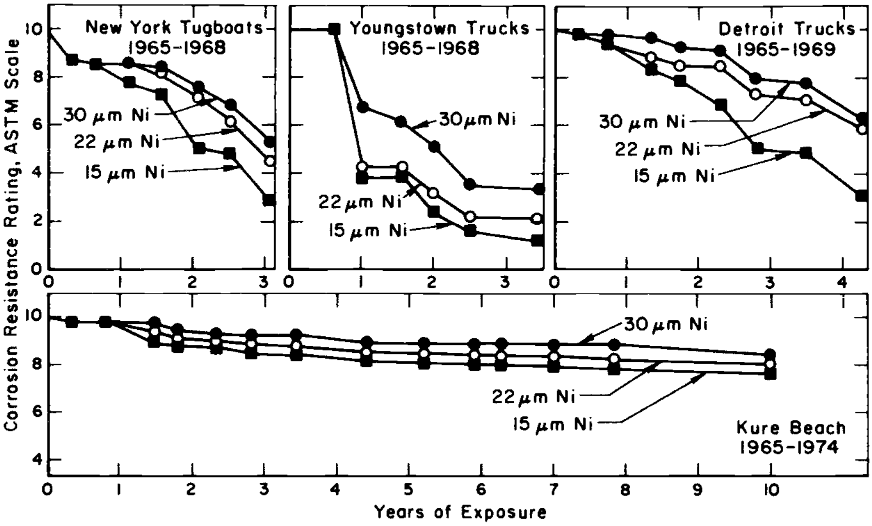

FIG. 3—*Effect of duplex nickel layer thickness for 0.75-μm microcracked Cr, duplex Ni, and 10-μm Cu.*

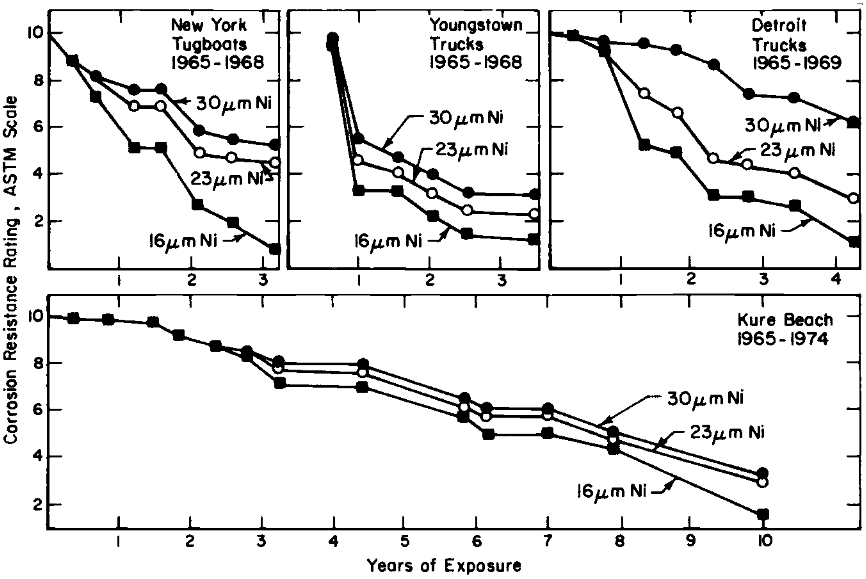

FIG. 4—*Effect of duplex nickel layer thickness for 0.25-μm microporous Cr, duplex Ni, and 10-μm Cu.*

New York tugboats, Youngstown trucks, Detroit trucks, and Kure Beach. Once again, more damage was observed at the mobile corrosion site than at the stationary site.

The effect of mechanical polishing to develop a satin finish prior to plating with 0.25 μm of conventional chromium on duplex nickel at two thicknesses is shown in Fig. 5. Satin finish specimens were superior to unpolished duplex nickel specimens on New York tugboats, Youngstown trucks, Detroit trucks, and the 245-m (800-ft) lot at Kure Beach. Mechanical polishing prior to conventional chromium plating provided more protection with 25 μm of nickel than did 35 μm of nickel without mechanical polishing. Enhanced corrosion protection provided by the satin-finished nickel in this latter case is attributed to the large number of pores which develop in the conventional chromium plate over the micrograph satin finish.

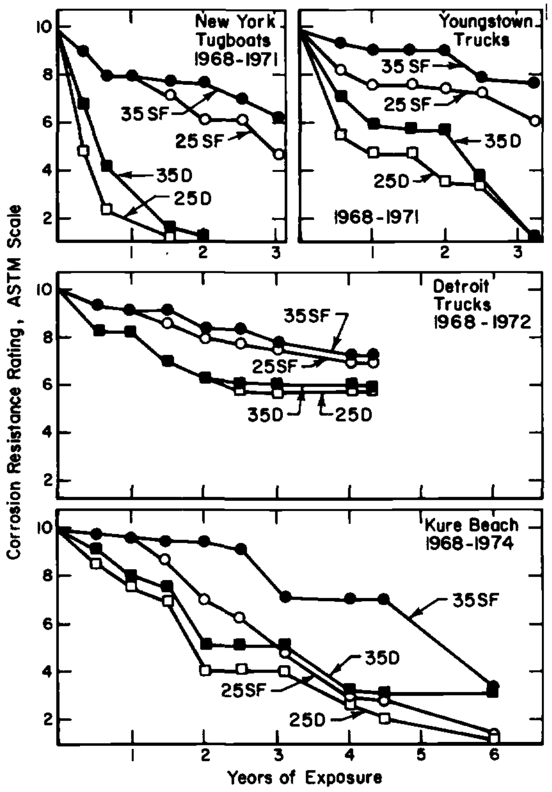

FIG. 5—*Effect of mechanical polishing (SF) versus standard treatment (D) prior to chromium plating for 0.25-μm conventional Cr, 25 or 35-μm duplex Ni, and 10-μm Cu.*

A series of specimens compared the corrosion resistance of semibright nickel mechanically polished to a bright finish versus duplex nickel without mechanical polishing at the same thicknesses under different chromium plates. For conventional chromium plate, equal protection was afforded by the two systems at a nickel thickness of 25 μm, while at 35-μm nickel thickness, mixed results were observed; mechanically polished, semibright nickel was better in industrial environments and duplex nickel was better in marine environments. Under microcrack chromium, the duplex nickel was superior at all locations. Under crack-free chromium, mechanically polishing semibright nickel was catastrophic and led to very rapid plating failure and substrate corrosion. This last series of observations indicates the danger of considering only one plating variable and emphasizes the importance of considering the entire, composite plate system.

Chromium Plate Variables

A major portion of the program was devoted to a comparison of microdiscontinuous chromium versus conventional chromium. Results for 0.75-μm microcracked chromium, 1.25-μm microcracked chromium, and 0.25-μm conventional chromium over 20 μm of bright nickel are shown in Fig. 6. The definite superiority of microcracked chromium over conventional chromium for exposure on New York tugboats, Detroit trucks, Detroit rooftops, and the 245-m (800-ft) lot at Kure Beach is clearly shown. Re-

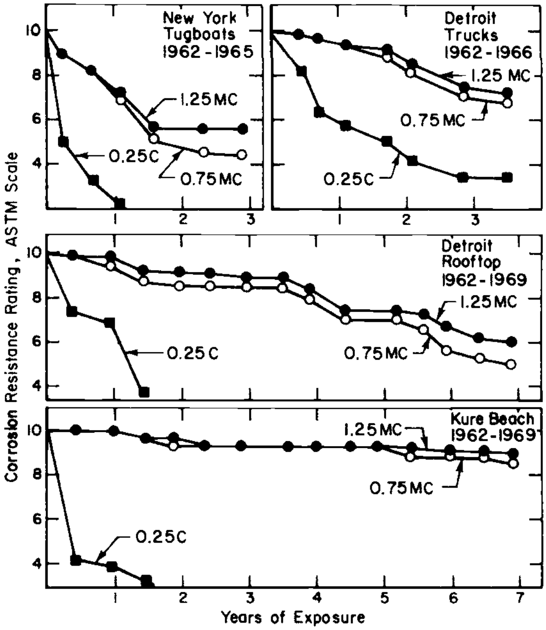

FIG. 6—*Effect of 0.75 or 1.25-μm microcracked chromium versus 0.25-μm conventional chromium for Cr, 20-μm bright Ni, and 10-μm Cu.*

sults of other exposure programs confirmed the superiority of microcracked chromium. Severe corrosion at Kure Beach and on Detroit trucks was observed on panels with 0.25 μm of conventional chromium over 30 μm of duplex nickel after approximately 1½ years of exposure, while 1.25 μm of microcracked chromium over 30 μm of duplex nickel provided 6 years of service prior to severe corrosion. A 1.375-μm layer of microcracked chromium over 20 μm of bright nickel resisted substrate corrosion for over 10 years at Kure Beach, while conventional chromium blistered after 2 to 3 years. Moreover, 3.75 μm of microcracked chromium over 20 μm of bright nickel exhibited only superficial pitting after a 15-year exposure at Kure Beach.

Varying the crack density from 240 to 950 per centimeter did not affect the corrosion performance of microcracked chromium. Increasing the crack density to 1500 cracks/cm, resulted in a slight increase in nickel staining. Decreasing the crack density to 100 cracks/cm, increased nickel pitting; however, corrosion resistance provided by this low crack density still remained greater than that provided by conventional chromium.

Atmospheric corrosion results on New York tugboats, Youngstown trucks, Detroit trucks, and the 245-m (800-ft) lot at Kure Beach for 0.75 μm of microcracked or 0.25 μm of microporous chromium as compared to 0.25 μm of conventional chromium over 30 μm of duplex nickel are presented in Fig. 7. Both microdiscontinuous forms of chromium are clearly superior to

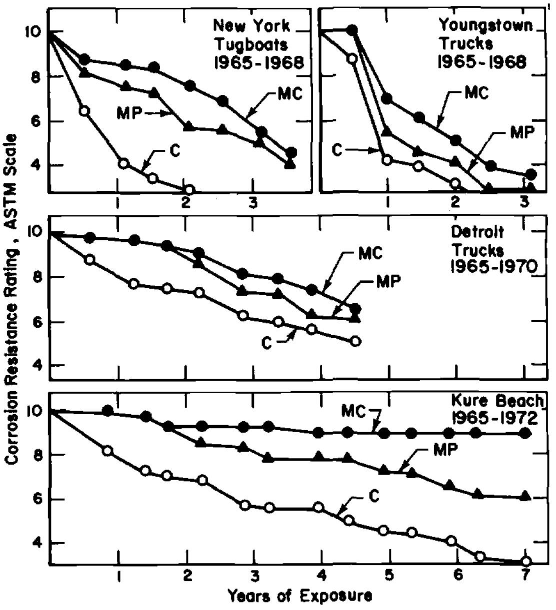

FIG. 7—*Effect of 0.75-μm microcracked (MC) chromium or 0.25-μm microporous (MP) chromium versus 0.25-μm conventional (C) chromium for Cr, 30-μm duplex Ni, 10-μm Cu.*

conventional chromium plate at all exposures. Microcracked chromium performed better than microporous chromium. The major point here is the benefit derived from microdiscontinuous chromium as compared to conventional chromium. Microdiscontinuous panels evaluated in this program were prepared under ideal laboratory conditions and in practice other factors must be considered in choosing the form of microdiscontinuous chromium to be used, for example, consistency of products and ease of bath control.

The benefit of microdiscontinuous chromium translates to either greatly improved corrosion resistance at identical nickel thicknesses or equivalent corrosion resistance for lower nickel thicknesses. These trends are supported by the data in Fig. 8, which presents results for microcracked chromium

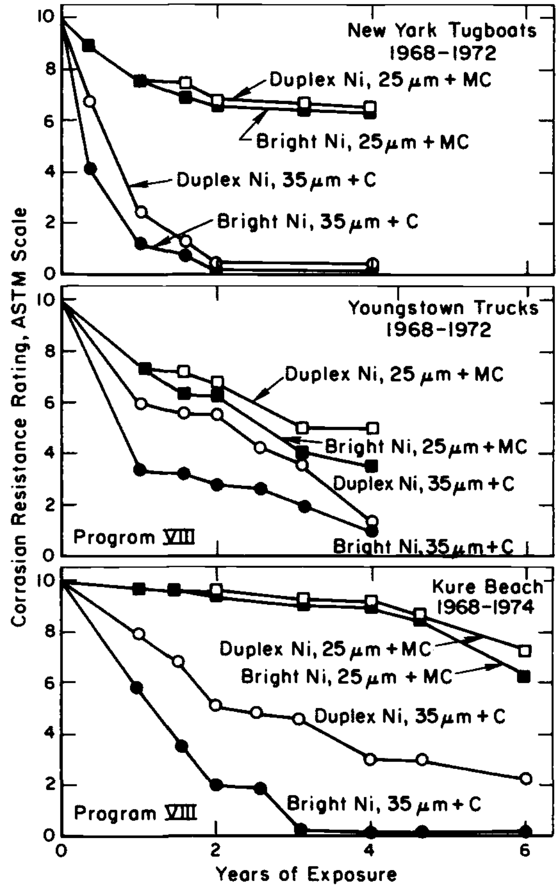

FIG. 8—*Effect of 1.0-μm microcracked (MC) chromium with 25-μm duplex or bright nickel versus 0.25-μm conventional (C) chromium with 35-μm duplex or bright nickel for Cr, Ni, and 12-μm Cu.*

and conventional chromium over 25-μm and 35-μm nickel plates. The superiority of microcracked chromium is more apparent for the two marine exposures, New York tugboats and Kure Beach, than for the industrial exposure (Youngstown trucks). Microcracked chromium provided more corrosion protection than conventional chromium over both 25 and 35 μm of bright or duplex nickel. Moreover, the microcracked chromium provided more corrosion protection over 25 μm of nickel than did conventional chromium over 35 μm of nickel. The beneficial effects of duplex as opposed to bright nickel is also shown by these results with the advantage of duplex nickel becoming more evident in the case of conventional chromium plate.

Morphology of Corrosion

A photomicrograph of a panel after a 3-year exposure on a New York tugboat is shown in Fig. 9. The plating system comprised 0.25-μm conventional chromium, 35-μm duplex nickel, and 12-μm copper. Large pits and blisters greater than 2 mm in diameter with penetration into the zinc die casting substrate were observed over the entire surface. Specimens with 0.25-μm microporous chromium and 1-μm microcracked chromium over 25-μm duplex nickel and 12-μm copper after identical exposures exhibited only surface staining with no penetration to zinc substrate. Metallographic cross sections through the microdiscontinuous chromium-plated specimens

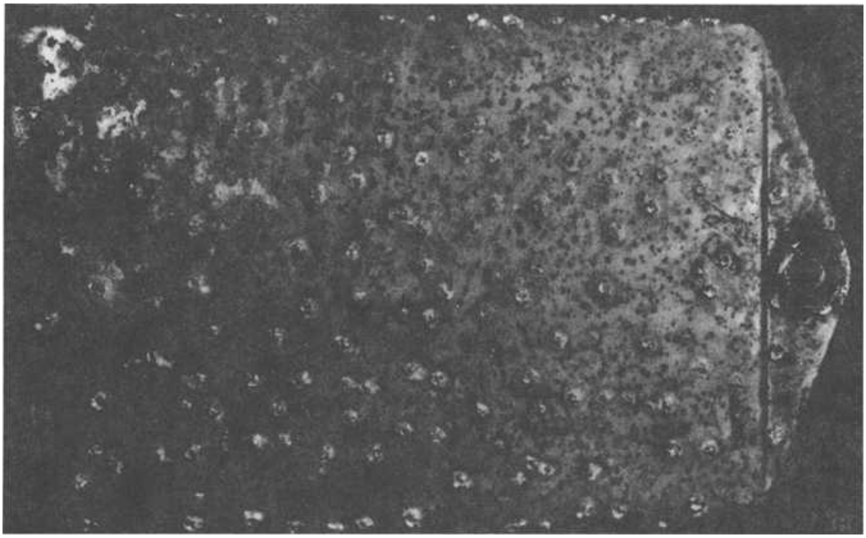

FIG. 9—*Severe pitting corrosion after 3 years of of exposure on a New York tugboat for a zinc die casting plated with 0.25-µm conventional Cr, 35-µm duplex Ni, and 12-µm Cu. (panel 10 by 15 cm).*

found many shallow pits in the duplex nickel layer but no penetration through the nickel.

Significant differences were noted in the morphology of corrosion pits in duplex nickel under different kinds of chromium. For example, pits under conventional chromium grew laterally to a diameter of greater than 1 mm during a 6-year exposure at Kure Beach, whereas pits under microporous chromium were generally limited to a diameter of approximately 0.1 mm after the same period of exposure. The smaller, 0.1-mm pits reduced the reflectivity of the bright surface because of their large number (greater than 10 000/cm^2), but they did not destroy the mirrorlike appearance of the surface to the same degree as the fewer but larger 1-mm pits on the panels plated with conventional chromium. Corrosion under microcracked chromium proceeded in a channel-like fashion. Similar behavior was observed for all atmospheric exposures. A photomicrograph of a cross section through a plating system comprised of 0.75-μm microcracked chromium, 25-μm duplex nickel, and 10-μm copper on a zinc alloy die casting is shown in Fig. 10. The panel had been exposed on Detroit trucks for 2 years. Corrosion of the nickel layer initiated at cracks in the chromium plate and proceeded laterally along the outer (high sulfur) portion of the duplex nickel layer with little or no penetration deeper into the plating system.

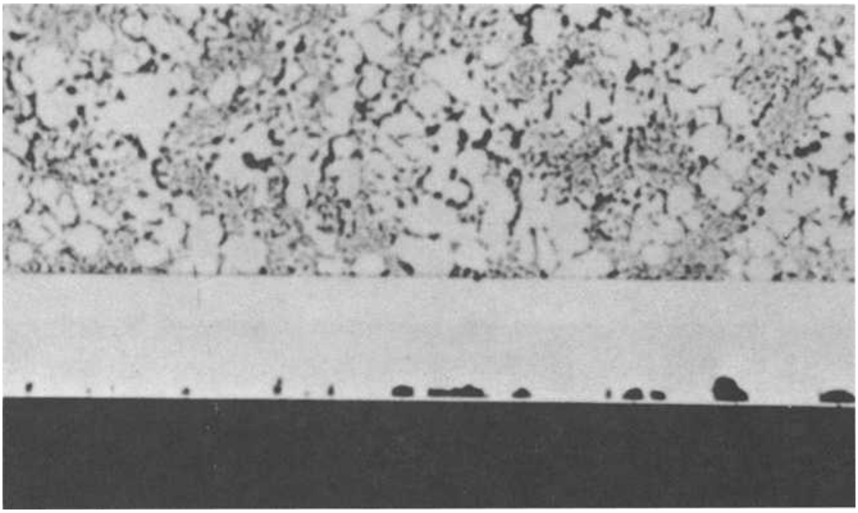

FIG. 10—*Photomicrograph of cross section through 0.75-μm microcracked chromium. 25-μm duplex nickel, and 10-μm copper after 2 years of exposure on a Detroit truck* (×500).

These results for plating systems on zinc alloy die castings correlate well with previously reported results for the beneficial effects of microdiscontinuous chromium [*11–14*] and duplex nickel [*16–18*] for increasing corrosion resistance. Enhanced atmospheric corrosion resistance is the result of (*a*) corrosion occurring at a far greater number of sites in the microdiscontinuous chromium plating but at much less intensity at any given site, and (*b*) preferential attack of the high sulfur outer nickel layer of the duplex nickel plate. Preferential attack of the outer nickel layer of the semibright and bright nickel layers is attributed to a favorable galvanic action due to sulfur content. Further decrease in corrosion rate is realized because of high ohmic resistance and the onset of concentration polarization in the tightly restricted pits under a very small flaw in the outer chromium plate.

Thus, the combined effect of microdiscontinuous chromium over duplex nickel is that firstly, the duplex nickel promotes lateral growth of pits instead of deep penetration, and secondly, the microdiscontinuous chromium promotes many corrosion sites. Shallow pits for microporous chromium and shallow channels for microcracked chromium are observed in nickel layer, whereas, conventional chromium results in only a few sites of corrosion initiation and deep penetration into the underlying zinc substrate.

Conclusions

The application of microdiscontinuous chromium was the most influential factor for improved corrosion resistance, with the benefit of greatly increased corrosion protection at a given nickel thickness. Even with a 30 to 40 percent reduction in nickel thickness relative to that specified for severe environments, the corrosion protection supplied by microcracked chromium was better than that obtained with conventional chromium over the thicker duplex nickel. Duplex nickel provided better corrosion protection than single layer nickel at the same thickness. The combination of microdiscontinuous chromium and duplex nickel provided the best corrosion protection for all exposures. The corrosion resistance was not significantly affected at copper thicknesses of 12, 10, or 5 μm, but was degraded at thicknesses below these levels. Atmospheric corrosion resistance was found to be insensitive to surface finish prior to the plating or to the solution used for copper plating.

Results of this study indicate the advantage of combined mobile and stationary exposure. The primary advantage of mobile exposure is that the vibrational abuse imposed upon the specimen can more readily simulate service conditions. Major disadvantages of mobile exposures are (*a*) a less clearly defined environment, and (*b*) decreased accessibility to panels for inspection and removal. By combining mobile and stationary exposure these disadvantages can be minimized.

Acknowledgments

The support of the International Lead Zinc Organization, Incorporated is greatly appreciated. The authors also acknowledge the cooperation of

Chrysler Corporation, Ford Motor Company, Industrial Platers, Incorporated, International Nickel, Lancaster Plating Company, McAlister Brothers, and the Youngstown Sheet and Tube Company in providing for exposure of electroplated die castings at selected sites. The contributions of H. R. Miller to the program are also acknowledged.

References

[1] Safranek, W. H. and Payer, J. H., *Plating and Surface Finishing*, Vol. 63, 1976, p. 40.
[2] Safranek, W. H. and Brooman, E. W., *Finishing and Electroplating Die Cast and Wrought Zinc*, International Lead Zinc Research Organization, Inc. and Zinc Institute New York, 1973.
[3] Safranek, W. H., Miller, H. R., and Cook, A. R., Society of Automotive Engineers, Reprint No. 710197, Jan. 1971; *Die Casting Engineering*, Vol. 12, No. 3, 1968, p. 17.
[4] Safranek, W. H., Cook, A. R., and Radtke, S. R., *Die Casting Engineering*, Vol. 12, No. 3, 1968, p. 17.
[5] Safranek, W. H. and Faust, C. L., *Transactions of the Institute of Metal Finishing*, Vol. 40, 1963, p. 217.
[6] Safranek, W. H. and Miller, H. R., *Plating and Surface Finishing*, Vol. 55, 1968, p. 233.
[7] Brown, H. and Tomaszewski, T. W., U. S. Patents Nos. 3,152,971-3, 13 Oct. 1964.
[8] DuRose, A. H., U.S. Patent No. 2,635,076, 14 April 1953.
[9] Safranek, W. H. and Miller, H. R., *Plating and Surface Finishing*, Vol. 51, 1964, p. 543.
[10] *Proceedings*, American Society for Testing and Materials, Vol. 53, 1953, p. 53.
[11] Seyb, E. J., *Proceedings*, American Electroplaters' Society, Vol. 50, 1963, p. 175.
[12] Brown, H. and Silman, H., *Transactions of the Institute of Metal Finishing*, Vol. 42, 1964, p. 50.
[13] Beacom, S. E., Hardesty, D. W., and Doty, W. R., *Transactions of the Institute of Metal Finishing*, Vol. 42, 1964, p. 77.
[14] Carter, V. E., *Transactions of the Institute of Metal Finishing*, Vol. 48, 1970, pp. 16, 19.
[15] Ward, J. J. B., Christie, I. R. A., and Carter, V. E., *Transactions of the Institute of Metal Finishing*, Vol. 49, 1971, p. 97.
[16] DuRose, A. H., *Proceedings*, American Electroplaters' Society, Vol. 47, 1960, p. 83.
[17] Safranek, W. H., Miller, H. R., and Hardy, R. W., *Proceedings*, American Electroplaters' Society, Vol. 48, 1961, p. 156.
[18] Flint, G. N. and Melbourn, S. H., *Transactions of the Institute of Metal Finishing*, Vol. 38, 1961, p. 35.

W. H. Ailor[1]

ASTM Atmospheric Corrosion Testing: 1906 to 1976*

REFERENCE: Ailor, W. H., "**ASTM Atmospheric Corrosion Testing: 1906 to 1976,**" *Atmospheric Factors Affecting the Corrosion of Engineering Metals, ASTM STP 646,* S. K. Coburn, Ed., American Society for Testing and Materials, 1978, pp. 129–151.

ABSTRACT: In the early fall of 1976 ASTM Committee G-1 on Corrosion of Metals exposed more than 40 ferrous and nonferrous sheet materials at five test locations. These exposures are a part of the third 20-year atmospheric test program generated by ASTM corrosion groups since 1932. Metals include new alloys, tempers, and coatings developed since the initiation of the last program.

Exposures have triplicate exposed panels for removal periods of 2, 5, 10, and 20 years at test sites at Kure Beach, North Carolina, 24-m (80-ft) lot; Newark-Kearny, New Jersey; Point Reyes, California; State College, Pennsylvania; and Panama Canal Zone.

Ten metal suppliers are participating in this new long-term test program. Among the metals exposed are aluminum, copper, lead, magnesium, nickel, stainless steel, titanium, and zinc alloys. Aluminized and galvanized coated steels are also being tested.

Evaluation of these materials includes weight loss (corrosion rates), pitting depth, and changes in mechanical properties.

One task group is monitoring weather conditions at the sites and another group is calibrating the site corrosivities through periodical short-term (1 and 2 year) exposures of steel and zinc panels during the course of the 20-year tests.

KEY WORDS: metal corrosion, atmospheric corrosion, atmospheric corrosion tests, galvanized steel

The Society's work on atmospheric exposure tests dates back approximately 70 years to the formation of the committees now designated as Committee D-1 on Paint and Related Coatings and Materials and Committee A-5 on Metallic-Coated Iron and Steel Products [*1*][2]. In 1906 Committee D-1 initiated tests on a painted railroad bridge at Havre de Grace, Maryland and soon thereafter Committee A-5 began exposure tests at Pittsburgh of twelve specimens of galvanized wire having different coating weights.

*Original experimental data measured in U.S. customary units.

[1] Research engineer, Reynolds Metal Company, Richmond, Va. 23261.

[2] The italic numbers in brackets refer to the list of references appended to this paper.

Early tests included painted steel fence panels at Atlantic City in 1910 (Committees A-5 and D-1) [*1*], and, from 1916 to 1917, exposures of uncoated copper-bearing and noncopper-bearing steel sheet by Committee A-5 at Fort Sheridan, Illinois, Pittsburgh, Pennsylvania, and Annapolis, Maryland. A 1946 report gives results of the sheet steel tests.

Committee A-5 on Corrosion of Iron and Steel

In 1920 Committee A-5 made plans for long-term atmospheric tests in three separate phases [*1*].

Uncoated and Coated Galvanized Corrugated Sheets

Uncoated and galvanized corrugated sheets were exposed in 1926 at five test locations (Altoona, Pennsylvania; Brunot Island, Pittsburgh,; Sandy Hook, New Jersey; State College, Pennsylvania; and Key West, Florida). Published reports included a report on failures of all galvanized sheets after 7 years at Altoona (1934) and failure of all sheets at Pittsburgh after 8½ years (1935). Initial failures were noted at State College in 1938. Data from these tests were reported in 1946, 1948, 1950, and 1952 by Committee A-5.

Loss of panels caused the discontinuation of the sheet tests at Sandy Hook in 1951 and the Brunot Island site was disestablished in 1951. The Key West location was relocated twice (in 1949 and 1952).

Metallic Coated Hardware, Structural Shapes, Tubular Goods, etc.

In 1928 Committee A-5 commenced studies at the five aforementioned locations for a number of coatings [*1*]: hot-dipped zinc, electrodeposited zinc, sherardized (zinc) applied in gas heated drum, sherardized (zinc) applied in electrically heated drum, electrodeposited cadmium, hot-dipped aluminum, hot-dipped lead (Amaloy), and parkerized.

The 2,4, and 6-year inspection results were reported in 1931, 1933, and 1935. A 1938 report noted changes since the 1935 report. The 1944 Committee A-5 report gave the test progress to date. Site changes included Altoona (discontinued in 1942 due to specimen loss), Pittsburgh (discontinued in 1939 due to specimen loss), Key West (relocated in 1949 and 1952), and Sandy Hook (discontinued in 1952).

Wire and Wire Products

Exposures were started in 1936 at eleven test sites (Table 1) [*1*]. Test materials included uncoated wire and fencing (noncopper- and copper-bearing), zinc-coated wire and fencing, corrosion resisting steel wire and

TABLE 1—*Test sites used for ASTM long-term exposures, 1906 to 1976.*

Atmosphere	1906[a] Program	1908[b] Program	1915[c] Program	1926[d] Program	1928[e] Program	1931[f] Program	1936[g] Program	1957[h] Program	1976[i] Program
Industrial	Pittsburgh, Pa.	...	Pittsburgh, Pa.	Pittsburgh, Pa.	Pittsburgh, Pa.	Pittsburgh, Pa.	Pittsburgh, Pa.	...	...
Industrial	...	...	...	Altoona, Pa.	Altoona, Pa.	Altoona, Pa.	...	...	...
Rural	...	...	Fort Sheridan, Ill.	State College, Pa.	State College, Pa.	State College, Pa.	State College, Pa.	State College, Pa.	State College, Pa.
Industrial	...	...	...	...	...	New York, N. Y.	...	Newark, N. J.	Newark-Kearny, N. J.
Marine	...	Atlantic City, N. J.	Annapolis, Md.	Sandy Hook, N. J.	Sandy Hook, N. J.	Sandy Hook, N. J.	...	Kure Beach, 24-m (80-ft) lot	Kure Beach 24-m (80-ft) lot
Industrial	...	...	...	...	...	Rochester, N. Y.	...	...	...
Marine	...	...	...	Key West, Fla.	Key West, Fla.	Key West, Fla.	...	...	...
Desert	...	...	...	...	...	Phoenix, Ariz.	...	...	...
Marine	...	...	...	...	..	La Jolla, Calif.	...	Point Reyes, Calif.	Point Reyes, Calif.
Tropical	...	...	...	...	...	...	...	...	Panama Canal Zone

[a] ASTM Committee D-1 on Painted Steel at Havre de Grace, Pa. and ASTM Committee A-5 on Galvanized Wire at Pittsburgh, Pa.

[b] ASTM Committee D-1 on Painted Fence Panels.

[c] ASTM Committee A-5 on Copper-Bearing and Noncopper-Bearing Uncoated Steel Sheets.

[d] ASTM Committee A-5 on Uncoated and Galvanized Corrugated Sheet.

[e] ASTM Committee A-5 on Metallic-Coated Hardware, Structural Shapes, etc.

[f] ASTM Committee B-3 on 24 Nonferrous Metals and Alloys.

[g] ASTM Committee A-5 on Wire and Wire Products. Other rural exposure sites for this program were Lafayette, Ind.; Ames, Iowa; Manhattan, Kans.; Ithaca, N. Y.; Santa Cruz, Calif.; College Station, Tex.; and Davis, Calif.

[h] ASTM Committee B-3 on 77 Nonferrous Metals and Alloys.

[i] ASTM Committee G-1 on 40 Ferrous and Nonferrous Metals and Alloys.

fencing, lead-coated wire and fencing, and copper-coated wire and fencing.

The 1951 Committee A-5 report summarized the 14-year data, and 20-year results can be found in *ASTM STP 290, Twenty-Year Atmospheric Corrosion Investigation of Zinc-Coated and Uncoated Wire and Wire Products* [*2*].

Committee A-5, the American Electroplaters Society, and the National Bureau of Standards jointly exposed electrodeposited coatings in 1932 at six locations [*1*]. Reports were issued in 1933, 1934, and 1936. A new committee, B-8 on Electrodeposited Metallic Coatings, assumed responsibility for this program in 1941.

In 1958 Committee A-5 exposed approximately 750 flat, bent, and round specimens at Newark, and at the 24 and 245-m (80 and 800-ft) lot at Kure Beach [*3*]. Materials included carbon steel, four low-alloy steels, and two nodular irons in the bare condition which were coated with hot-dipped, sprayed, and electrodeposited zinc, and hot-dipped and sprayed aluminum. Pitting depth and time to coating failure is recorded. The 20-year removals are now due.

Committee A-7 on Malleable Iron Castings

In 1958 Committee A-7 on Malleable Iron Castings initiated an atmospheric test program for a series of 1620 malleable iron plates for exposure periods of 1, 3, 7, and 12 years [*2*]. Test sites were at Point Reyes, East Chicago, Newark, Kure Beach, and State College. This program included 600 standard malleable, 600 pearlitic malleable, 240 nodular iron, and 180 steel specimens, each having both as-cast and machined surfaces. Wrought plates were of structural carbon copper-bearing and low-alloy steels. Evaluation was based on loss in weight determinations.

Committee A-10 on Iron-Chromium, Iron-Chromium-Nickel, and Related Alloys

Over 4000 stainless steel panels and coiled wire springs were exposed by Committee A-10 during 1958 at sites at Newark; State College; Columbus, Ohio; Freeport, Texas; and the 24 and 245-m (80 and 800-ft) lots at Kure Beach [*2*]. Changes in appearances and in tensile and fatigue strength were evaluated for 3, 7, and 15-year test periods.

Committee B-3 on Corrosion of Nonferrous Metals and Alloys

In 1931 Committee B-3 on Corrosion of Nonferrous Metals and Alloys started 20 to 25-year exposure tests on 24 nonferrous metals and alloys at nine test sites [*1*]. These sites included State College; Pittsburgh; Altoona; New York City; Sandy Hook; Rochester, New York; Key West, Florida; Phoenix, Arizona; and LaJolla, California. The 10-year evaluations were reported in ASTM Symposium on Atmospheric Exposure Tests on Nonferrous Metals (1946) and the final 20-year results are in *ASTM STP 175* [*3*]. The LaJolla site was disestablished in 1950.

Committee B-3 initiated galvanic couple tests in 1931 at the same sites listed in the foregoing section [*1*]. After the final report on these results was released in 1939, a new series was started in 1941. These 1941 couples included stainless steels (Types 304 and 316) joined to eight nonferrous metals and mild steel. The four test sites were New York City, State College, Altoona, and Kure Beach. Five-year results were reported in 1948 and the 15-year data in 1960. Other galvanic couple tests included disk-type specimens (two types of magnesium joined to other metals) exposed at New York, Kure Beach, State College, and Miraflores, Canal Zone in 1950. Spool and plate-type specimens have also been exposed.

In 1952 the exposure of wire-wound bolt specimens for couples of magnesium and other metals was started [*4*]. Exposures were for periods of four months and one year.

A subcommittee on weather of Committee B-3 was organized in 1942 to study those environmental factors which influence atmospheric corrosion. This group also attempted to correlate these factors with the performance of materials. In 1948, exposures of mild steel and rolled zinc sheet specimens were made in an effort to evaluate relative corrosivities at eight locations. These sites included Sandy Hook; State College; Pittsburgh (Brunot Island); Kure Beach; New York City; Vandergrift, Pennsylvania; Kearny, New Jersey; and Middletown, Ohio. By 1952 panels were also exposed at Point Reyes. Removals were scheduled for 1, 2, 4, and 8-year intervals [*1*]. In 1952 iron and zinc calibration panels were exposed at State College, New York City, Point Reyes, Kure Beach, and Pittsburgh [*4*]. The weather subcommittee also developed a technique for relating surface moisture to corrosion and Sereda reported this work in the February 1958 *ASTM Bulletin* [*5*].

In 1958 Committee B-3 initiated a program for exposure of 77 alloys of nonferrous metals at sites at State College, Newark, Point Reyes, and Kure Beach 24-m (80-ft) lot [*3*]. Removal periods were 2, 7, and 20 years for all metals, plus a 1-year removal for aluminum and its alloys. Evaluations included weight loss, changes in tensile properties, and pitting depths. Three reports have been issued [*6–8*]. During the same year Committee B-3 prepared specimens of two magnesium alloys bolted to other metals for exposure at State College, Newark, and the 24 and 245-m (80 and 800-ft) lots at Kure Beach for 15 years [*6–8*].

Committee B-6 on Die Cast Metals and Alloys

Starting in 1928 Committee B-2 on Nonferrous Metals exposed 35 000 test specimens of 22 different zinc- and aluminum-based die casting alloys [*1*]. Outdoor sites used included State College, Key West, Sandy Hook, Rochester, Altoona, and New York City. Indoor locations were at Coco Solo, Panama Canal Zone; Hanover, New Mexico; New Kensington, Pennsylvania; and Cambridge, Massachusetts. When Committee B-6 on Die Cast Metals and Alloys was organized in 1930, this group took over these tests. A 1960 B-6 report covered the 20-year results. Ten-year data for a series of magnesium and zinc-base alloys exposed in 1939 were reported in 1950.

Committee B-7 on Light Metals and Alloys, Cast and Wrought

Exposures of anodized aluminum panels (Philadelphia; Chicago; New Kensington; Miami; Point Judith, Rhode Island; Oakland, California; and New York City) were started in 1941 [*1*]. Between 1951 and 1954 an extensive exposure program for both aluminum and magnesium wrought and cast specimens was initiated at State College, Freeport, Point Reyes, New York City, and Kure Beach 24-m (80-ft) lot. This work was done by Committee B-7 on Light Metals and Alloys, Cast and Wrought. Results for 1, 3, 5, and 10 years have been reported [*9*].

Committee B-8 on Electrodeposited Metallic Coatings

Committee B-8 started a series of outdoor exposures [*1*] of lead coatings (1944 and 1950) at sites in New York City, State College, Kure Beach, and Tela, Honduras, and of copper-nickel-chromium coatings (1946 and 1950) at sites in New York City, Pittsburgh, State College, and Kure Beach.

Data from these tests have been reported in the Committee B-8 reports for 1946, 1947, 1949, and 1951.

In 1957 a series of 780 chromated cadmium-plated panels representing 14 test films were placed on exposure by Committee B-8 at test sites at Rock Island, Illinois, the New York City area (Bell Telephone Laboratories), and the 245-m (800-ft) lot at Kure Beach [*3*].

Committee C-19 on Structural Sandwich Constructions

In 1955 Committee C-19, now disestablished, exposed a series of sandwich panels having facings of aluminum (some anodized), fiberglass, plate glass, kraft paper, stainless steel, and porcelain-enameled steel with cores of aluminum, kraft paper, and balsa at State College and the 24-m (80-ft) lot at Kure Beach [*10*]. A second series was exposed in 1956 and a third series in 1959 [*10*].

Committee D-1 on Paint, Varnishes, Lacquer, and Related Products

Committee D-1 tested paints on steel as early as 1906 [*1*] and wooden panels by 1909. In 1949 painted wooden panels were exposed at Kure

Beach, State College, Chicago, New York City, Columbus, and Miami and Ormond Beach, Florida. These tests were for a 10-year exposure.

Committee D-14 on Screen Wire Cloth, now disestablished, started atmospheric exposure tests in 1925 on seven nonferrous screen cloth alloys [*1*]. The test materials included 90 percent copper—10 percent zinc; 80 percent copper—20 percent zinc; 75 percent copper—20 percent nickel—5 percent zinc; 70 percent nickel—30 percent copper; 100 percent copper; 98 percent copper—2 percent tin; and 95 percent copper—5 percent aluminum.

Exposures were at Pittsburgh; Portsmouth, Virginia; Balboa Heights, Canal Zone; and at the National Bureau of Standards, Washington, D.C. A final report on the results was published in 1935.

Committee G-1 on Corrosion of Metals

Upon its establishment in 1964 Committee G-1 on Corrosion of Metals became the ASTM committee responsible for all future corrosion tests of the society. One of its subcommittees, G01.98 on Exposure Testing Facilities, now coordinates work for all ASTM test sites [*11*]. All ASTM committees having an interest in atmospheric corrosion testing are represented on this group.

Committee G-1 now has jurisdiction over the ASTM B-3/1957 Test Program (formerly under the disestablished Committee B-3) and will evaluate the 20-year removals in 1978. Committee G-1 has a new 20-year exposure test program that was exposed in the fall of 1976 at five sites—State College, Kure Beach, Newark-Kearny, Point Reyes, and Panama Canal Zone (Table 1).

American Welding Society

A program was started in 1953 to generate atmospheric exposure data on metallized (sprayed) coatings [*10*]. Twenty-eight varieties each of aluminum and zinc coatings on steel were exposed. Half of these specimens have additional organic coatings in both single and double coatings. Exposure periods were for 1, 3, 12, and 18 years at Kure Beach, Newark, Columbus, East Chicago, Freeport, Point Reyes, and three seawater exposures.

ASTM Test Sites

The foregoing narrative refers to the atmospheric test locations used for the many exposure programs sponsored by ASTM committees since 1906. Some of the more extensive programs and test sites are listed in Table 1.

A comprehensive, illustrated review of the environmental test locations appeared in the Report of the Advisory Committee on Corrosion for 1953

[*4*]. Since that time a number of site changes have been made, and the current status is shown in Table 2.

TABLE 2—*ASTM atmospheric test sites operational in 1976.*

GENERAL USE SITES	
State College, Pa.	rural atmosphere
Columbus, Ohio	urban or moderate industrial atmosphere
Newark-Kearny, N.J.	severe industrial atmosphere
Whiting, Ind.	severe industrial atmosphere
Pittsburgh, Pa.	severe industrial atmosphere
New York (Port Authority Building), N.Y.	severe industrial atmosphere
Point Reyes, Calif.	west coast marine atmosphere
Kure Beach, 24-m (80-ft) lot	east coast marine atmosphere
Kure Beach, 245-m (800-ft) lot	east coast marine atmosphere
Freeport, Tex.	gulf coast marine atmosphere
ASTM WIRE TEST SITES	
Ames, Iowa	rural atmosphere
Ithaca, N.Y.	rural atmosphere
Lafayette, Ind.	rural atmosphere
Manhattan, Kans.	rural atmosphere
Santa Cruz, Calif.	rural atmosphere

The open-field tropical site in the Panama Canal Zone is one of five test locations for the ASTM G01.04 1976 Test Program.

In summary, ASTM committees have used more than 60 atmospheric test sites, 6 fresh and seawater immersion test sites, and 7 indoor test locations [*3*]. More than 40 technical reports have been published describing the results of these studies [*3*]. The 10 general-use atmospheric test sites and the 5 test locations used for wire testing are shown in Fig. 1.

ASTM G01.04 1976 Test Program

In 1931 Committee B-3 on Corrosion of Nonferrous Metals and Alloys exposed more than 9000 panels at nine different sites [*12*]. The 24 metals included alloys of zinc, nickel, copper, lead, tin, and aluminum. The 10-year results were published in 1946, in *ASTM STP 67* [*13*]; the 20-year results in 1955 in *ASTM STP 175* [*3*].

To supplement the 1931 program with data for newer alloys developed since that time, Committee B-3 initiated a new series of atmospheric corrosion tests in 1956 [*12*]. This program contained 77 alloys of 9 basis metals including aluminum, copper, lead, magnesium, molybdenum, nickel, tantalum, and zinc. Sites used were Kure Beach 24 m (80-ft) lot, Newark, Point Reyes, and State College. The results of 1, 2, and 7-year

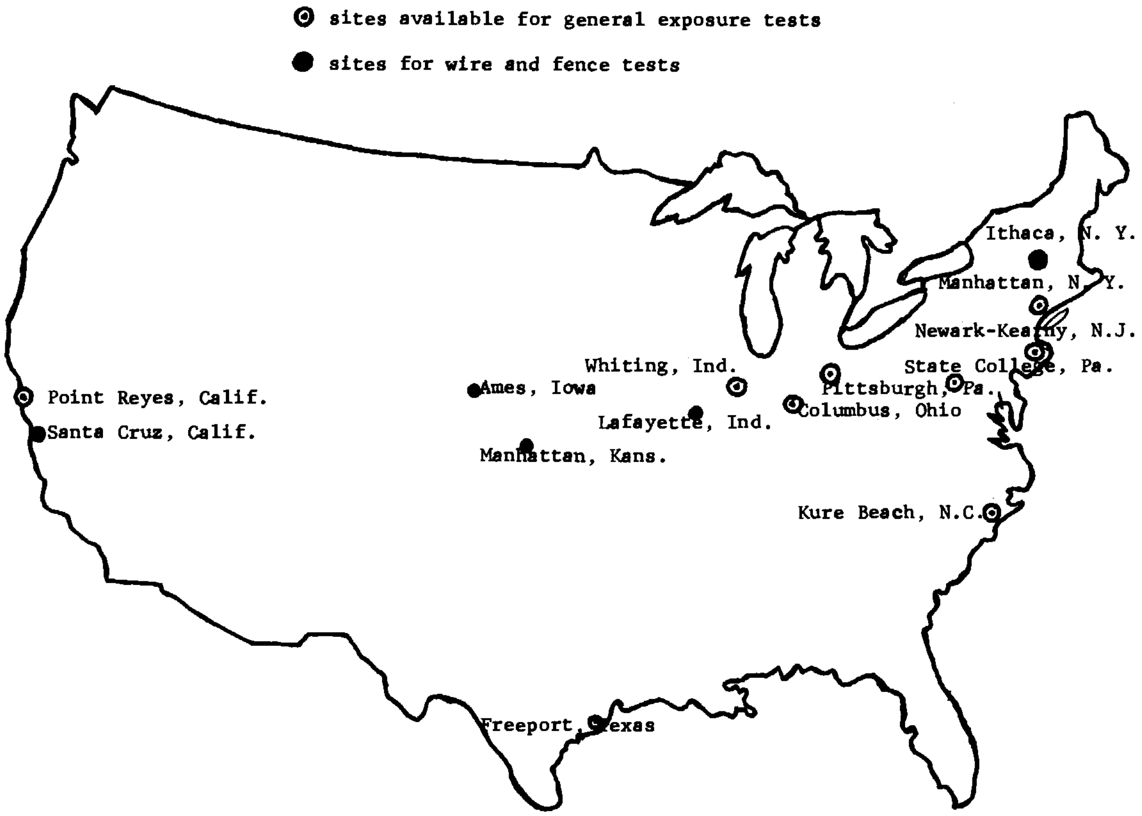

FIG. 1—*Location of test sites maintained by the subcommittee on exposure test facilities (G01.98).*

evaluations have been published [*6–8*]. The 20-year removals are scheduled for 1978.

As an ongoing supplement to the earlier B-3 programs, Committee G-1 on corrosion of Metals developed a new 20-year test program in 1976. This program, designated as ASTM G01.04 1976 Test Program, is discussed here.

Materials

The 1976 program contains 41 alloys of 8 basis metals. The number of alloys in each category is as follows: aluminum (1), copper (18), Lead (2), magnesium (1), nickel (6), stainless steel (4), titanium (2), zinc (3), and metallic coatings on steel (4).

Test Program

Atmospheric Exposure
  Test Site Locations
    Site A: Kure Beach, 24-m lot (80-ft) (east coast marine)
    Site B: Newark-Kearny (industrial)
    Site C: Point Reyes (west coast marine)
    Site D: State College (rural)
    Site E: Panama Canal Zone (tropical)
  Test Periods
    Initial tests (zero point)
    Atmospheric exposure for 2, 5, 10, and 20 years (triplicate panels)
    Storage for 2, 5, 10, and 20 years (duplicate panels)
    Reserve panels in storage (20 panels)
  Test Panels
    20.3 by 10.16 by 0.127 cm (8 by 4 by 0.05 in.)
    (see Fig. 1), with some variations in thickness to be exposed at 30 deg from the horizontal. All panels of each alloy are from a single heat with the 20.3-cm (8-in.) dimension parallel to the direction of rolling.
  Identification

Panels were marked with 0.65-cm (¼-in.) metal stencils. Identification was made as shown in Tables 3 and 4 and Figs. 2 and 3. Panels were randomized within a given test series prior to stencilling. Table 4 shows the number arbitrarily assigned to each alloy in the program with its commercial designation. The six 5-year specimens (2 specimens from each of 3 panels) of any alloy at Kure Beach may be identified by numbers from 25 to 30, by the location, A, and alloy designation as shown in Table 3. Marking was in accordance with Fig. 2: alloy identification at top, followed by test site in center, and then specimen number.

TABLE 3—*Code for identification of atmospheric exposure location.*

Location of Test Site	Code	2 Years	5 Years	10 Years	20 Years
Kure Beach, 24-m (80-ft) lot	A	1 to 6	31 to 36	61 to 66	91 to 96
Newark-Kearny, N.J.	B	7 to 12	37 to 42	67 to 72	97 to 102
Point Reyes, Calif.	C	13 to 18	43 to 48	73 to 78	103 to 108
State College, Pa.	D	19 to 24	49 to 54	79 to 84	109 to 114
Panama Canal Zone	E	25 to 30	55 to 60	85 to 90	115 to 120

A variation in the identification procedure was made for the metal-coated steel products. These panels were coded by use of the template shown in Fig. 3, using drilled holes at the appropriate locations.

Laboratory Tests

Chemical analyses were made on all 41 alloys (see Table 4).

Thickness measurements were made to the nearest 0.025 mm (0.001 in.) on the specific locations shown in Fig. 2.

Length and width measurements were made to the nearest 0.25 mm (0.01 in.).

Weighing of the aluminum and magnesium alloys was to the nearest 0.001 g. All other alloys were weighed to the nearest 0.01 g.

Initial tension tests were made on six specimens, three each from two panels (see Table 5). Tension tests were not made for the metallic-coated steel alloys.

Coating thicknesses were measured at five locations on metallic-coated steel panels using a suitable instrument (Permascope).

Evaluation of Corrosion Damage

Weighing—all panels will be cleaned and weighed to the nearest 0.01 g, except the aluminum and magnesium panels which will be weighed to the nearest 0.001 g.

Tension tests will be made on two specimens cut from each of three exposed panels after cleaning and weighing. Tension specimens will not be cut from metallic-coated steel panels.

Pit depth determinations will be made on the center section of each panel after removal of tension specimens.

Storage of Panels

The storage panels were wrapped in moisture-proof paper, then dipped in wax in order to maintain similar conditions of humidity and temperature. Each alloy was divided into four lots and identified by marking the inner wrapping so that identification could be made without the necessity of breaking the transparent wax seal. A set of 20 reserve panels was packaged separately for each alloy. All storage panels (control and reserve) are stored at ASTM headquarters.

TABLE 4—*Chemical analyses of specimen alloys.*

ALUMINUM ALLOYS

Alloy	Commercial Designation	Aluminum, %	Copper, %	Iron, %	Silicon, %	Manganese, %	Magnesium, %	Zinc, %	Titanium, %
50	1199-F	balance	0.0053	0.0056	0.0025	0.0005	0.0003	0.0014	0.0035

COPPER ALLOYS

Alloy	Commercial Designation	Copper, %	Zinc, %	Tin, %	Phosphorus, %	Lead, %	Iron, %	Silver, %	Manganese, %	Aluminum, %	Silicon, %	Cobalt, %	Nickel, %
14	110	99.90	...	...	...	...	...	...	...	...	...	...	...
15	194 (HSM copper)	balance	0.13		0.035	<0.01	2.4	...	...	...	...	0.98	...
16	195 (Strescon)	balance	0.18	0.56	0.108	<0.01	1.75	...	...	...	...	...	...
17	220 (commercial bronze)	90.1	balance	...	...	<0.01	<0.01	...	...	...	...	...	...
18	230 (red brass)	84.7	balance	...	...	<0.008	<0.008	...	...	...	...	...	...
19	260 (cartridge brass)	68.6	balance	...	...	<0.015	<0.02	...	...	...	...	...	...
20	510 (phosphor bronze)	balance	0.064	4.7	0.13	0.014	0.004	...	...	...	...	...	...
21	511 (phosphor bronze)	balance	<0.1	3.95	0.065	0.008	0.008	...	...	...	...	...	...
22	638 (Coronze)	balance	0.31	...	...	<0.01	0.054	...	0.10	2.6	1.7	0.42	...
23	664 (Coronze)	balance	11.1	<0.02	<0.05	<0.01	1.6	<0.05	...	<0.05	<0.02	0.52	<0.02
24	688 (Alcoloy)	balance	22.6	...	...	<0.01	0.016	...	...	3.3	...	0.30	...
25	725 (Alcoloy)	balance	0.15	2.1	...	<0.01	0.045	...	0.12	...	...	...	9.3

COPPER ALLOYS (cont.)

Alloy	Designation	Copper, %	Zinc, %	Tin, %	Cobalt, %	Lead, %	Iron, %	Nickel, %	Chromium, %	Aluminum, %	Silicon, %	Beryllium, %
44	CA 170	balance	0.02	0.04	0.21	<0.005	0.06	0.03	0.005	0.03	0.07	1.70
45	CA 172 X HMS	balance	<0.02	0.02	0.20	<0.005	0.06	0.05	<0.005	0.04	0.08	1.93
46	CA 172 1/2 HT	balance	<0.02	0.06	0.20	<0.005	0.08	0.025	<0.005	0.03	0.08	1.82
47	CA 175 AT	balance	<0.01	0.013	2.68	<0.005	0.05	0.01	<0.005	0.02	0.06	0.54
48	CA 175 HT	balance	<0.01	0.013	2.68	<0.005	0.05	0.01	<0.005	0.02	0.06	0.54
49	CA 172 AT	balance	<0.02	0.015	0.24	<0.005	0.06	0.01	<0.005	0.03	0.06	1.83
51	aluminum bronze	balance	...	...	...	...	...	1.9	...	7.8	...	...

LEAD ALLOYS

Alloy	Commercial Designation	Lead, %	Silver, ppm	Bismuth, ppm	Tin, %	Antimony, ppm	Other, ppm
26	Pb-0.065Ca	balance	<10	<5	...	<5	<5
27	Pb-0.065-1.3Sn	balance	<10	<5	1.24	<5	<5

MAGNESIUM ALLOYS

Alloy	Commercial Designation	Magnesium, %	Aluminum, %	Calcium, %	Copper %	Iron, %	Manganese, %	Nickel, %	Silicon, %	Zinc, %	Others, %
28	AZ31B-H24	balance	3.0	0.04	0.05	0.005	0.20	0.005	0.10	1.0	0.30

NICKEL ALLOYS

Alloy	Commercial Designation	Nickel, %	Chromium, %	Carbon, %	Manganese, %	Iron, %	Sulfur %	Silicon, %	Copper, %	Aluminum, %	Titanium, %	Molybdenum, %	Columbium + Tantalum, %
29	Nickel 200	99.59	...	0.08	0.26	0.03	0.003	0.03	0.01	...	...	...	...
30	Monel Alloy 400	66.91	...	0.12	1.05	1.18	0.010	0.11	30.62	...	...	...	...
31	Inconel Alloy 600	74.55	16.42	0.03	0.34	8.27	0.003	0.17	0.22	...	...	...	...
32	Inconel Alloy 625	62.34	21.25	0.03	0.10	2.99	0.004	0.20	0.15	0.13	0.34	9.07	3.53
33	Inconel Alloy 800	31.24	19.84	0.05	0.89	46.29	0.004	0.36	0.57	0.29	0.47	...	...
34	Inconel Alloy 825	43.66	22.80	0.02	0.48	27.17	0.007	0.21	1.81	0.09	0.74	3.01	...

STAINLESS STEEL ALLOYS

Alloy	Commercial Designation	Chromium, %	Nickel, %	Molybdenum, %	Carbon %	Manganese, %	Silicon, %	Phosphorus, %	Sulfur, %	Titanium, %
35	409	11.54	nil	nil	0.038	0.17	0.61	0.019	0.020	0.38
36	430	16.33	nil	nil	0.045	0.40	0.40	0.023	0.002	nil
37	304	18.72	9.00	nil	0.066	1.50	0.47	0.023	0.014	nil
38	316	17.60	12.02	2.11	0.042	1.55	0.53	0.027	0.015	nil

Alloy	Commercial Designation	Titanium, %	Carbon, %	Nitrogen, %	Iron, %	Aluminum, %	Vanadium, %	Nickel, %	Manganese, %	Copper, %	Molybdenum, %	Zirconium, %	Oxygen, %	Hydrogen, %	Tin, %
39	Ti-50A	balance	0.022	0.011	0.09	...	...	...	0.001	...	...	...	0.127	0.003	...
40	Ti-Code 12	balance	0.022	...	0.15	0.041	0.001	0.94	0.003	0.001	0.315	0.001	0.12	0.015	0.034

TABLE 4—*Chemical analyses of specimen allowys—Continued.*

ZINC ALLOYS

Alloy	Commercial Designation	Zinc, %	Aluminum, %	Calcium, %	Magnesium, %	Copper, %
41	Zn-22AlHl Rolled Sheet	balance	22.2	0.025	0.040	0.89
43	Zn-7Al-3Cu Gravity Cast Plates	balance	7.9	. . .	0.032	3.0

METALLIC-COATED STEELS

		Coating Analysis					Average Coating Thickness, Skyward Side	
Alloy	Commercial Designation	Zinc, %	Aluminum, %	Silicon, %	Lead, %	Iron, %	Oz/ft^{2b}	Mils
10	Aluminized Steel Type 2[a] (pure Al coating)						0.74	
11	Galvalume (50Zn-50Al)	43.4	55.0	1.6	. . .	. . .	0.31	0.97
12	Galvanized Steel, G60 class	98.8	0.28	. . .	0.08	0.46	0.34	. . .
13	Galvanized steel, G60 class	98.9	0.25	. . .	0.08	0.29	0.51	. . .

[a] Base metal analysis: C, 0.046%; Mn, 0.29%; P, 0.005%; S, 0.022%; Si, <0.05%; Cu, 0.058%.

[b] $\frac{g}{m^2} = 305.4 \times \frac{oz}{ft^2}$

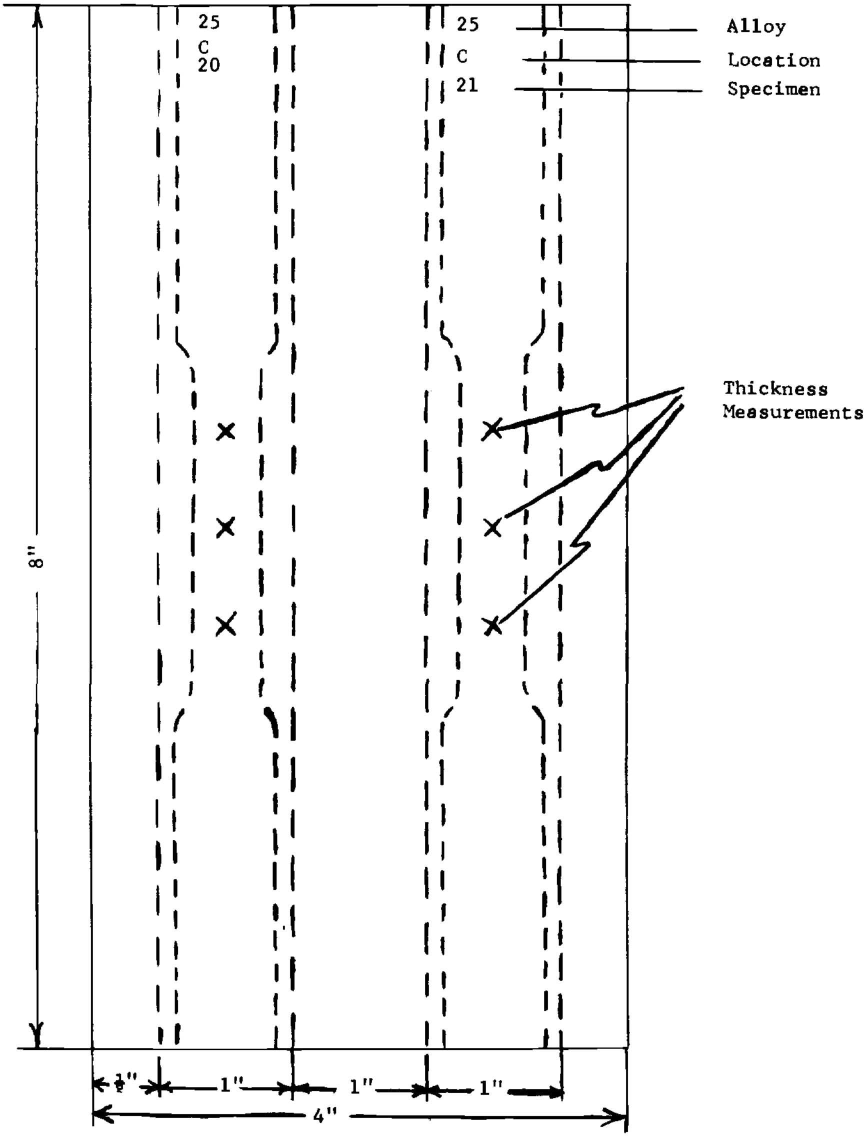

FIG. 2—*Plan for cutting tension specimens from 20.3 by 10.16 by 0.127-cm (8 by 4 by 0.050-in.) test panels.*

Acquisition of Materials

With the approval of the main committee for the organizing of a comprehensive 20-year atmospheric test program, a task group approached various producers for panels of alloys desired in the program. The com-

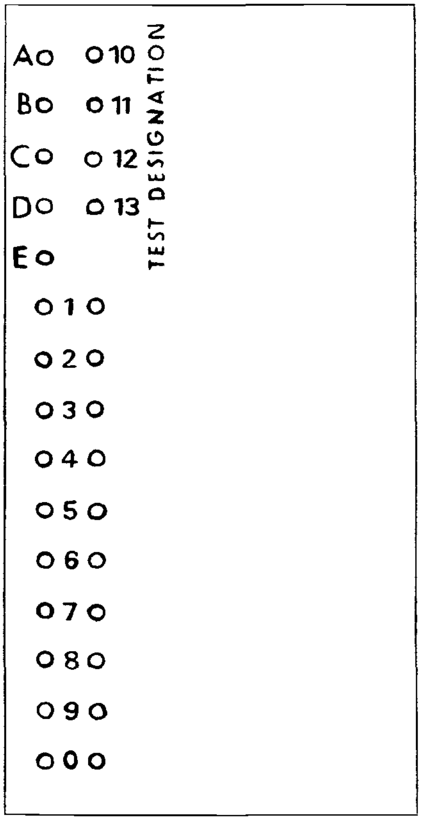

FIG. 3—*Plan for coding coated steel panels by means of drilled holes.*

panies which furnished not only material and laboratory services but manpower and equipment necessary to perform the preliminary tests as well are: Armco Steel Corporation, Bethlehem Steel Company, Brush-Wellman, Incorporated, Conalco, Frankford Arsenal, Inland Steel Company, International Nickel Company, Olin Corporation, St. Joe Minerals, and Titanium Metals Corporation.

Exposure of Specimens

Each alloy was exposed in triplicate for each exposure period at all five sites. The total number of all panels exposed was 2460. The exposures were made in the period September to December 1976 (Table 3*a*).

TABLE 5—*Initial tension test data.*

Alloy	Average Thickness, mm	Width, mm	Area, mm^2	Load, *N*	Tensile Strength, *M Pa*	Elongation, 50 mm, %
11	...	...	...	...	...	...
12	...	...	...	...	...	...
13	...	...	...	...	...	...
14	1.1	12.6	14.5	4 797	331	8.9
15	1.1	12.7	14.5	6 835	471	5.8
16	1.1	12.8	14.6	9 749	668	4.5
17	1.1	12.7	14.5	5 682	392	7.0
18	1.1	12.7	14.5	6 950	479	7.4
19	1.1	12.7	14.5	8 007	554	10.4
20	1.2	12.6	14.8	8 630	581	8.3
21	1.1	12.7	14.5	8 703	599	5.6
22	1.2	12.7	15.1	12 911	855	5.1
23	1.2	12.7	14.7	8 515	580	5.4
24	1.2	12.7	14.7	11 792	804	3.0
25	1.1	12.7	14.4	8 125	563	4.8
26	1.4	12.5	17.4	642	368	25.0
27	1.1	12.5	13.8	1 051	76	9.4
28	1.6	...	...	...	269	6.0
29	1.1	12.7	14.5	6 960	479	35.8
30	1.3	12.7	16.3	8 775	537	40.4
31	1.3	12.7	16.8	11 173	665	40.0
32	1.3	12.7	16.1	13 851	858	54.0
33	1.2	12.7	15.7	9 346	594	39.0
34	1.3	12.7	16.4	12 887	783	32.0
35	1.4	...	...	...	471	32.0
36	1.2	...	...	...	518	28.0
37	1.5	...	...	...	655	54.0
38	1.3	...	...	...	612	52.0
39	1.6	13.2	...	2 176	69	37.6
40	1.3	13.1	...	2 124	81	28.9
41	1.6	12.6	19.7	6 662	338	17.2
43	6.3	12.4	78.8	23 000	291	1.0
44	0.8	12.7	10.2	13 350	1314	5.1
45	0.8	12.7	10.2	12 456	1226	4.8
46	0.8	12.7	10.2	13 299	1309	5.1
47	0.8	12.7	10.2	7 589	747	12.1
48	0.8	12.6	10.1	8 014	795	17.1
49	0.8	12.6	10.1	12 872	1277	8.3
50	1.0	12.6	12.3	1 672	136	4.0

APPENDIX

ASTM Committee G01.04 1976 Test Program

Details of Exposure and Storage

1. Test Site Locations
   A. Kure Beach, 24-m (80-ft) lot (east coast marine)
   B. New York area (Newark) (industrial)

TABLE 3a—*Sites and dates of exposed alloys.*

Site	Alloy	Date
Kure Beach,		
24-m (80-ft) lot (A)	11-34, 39-41, 43-51	7 Oct. 1976
	10, 35-38	10 Nov. 1976
Newark-Kearny, N.J. (B)	14-34, 39-41, 43-51, 10-13, 35-38	4 Oct. 1976
Point Reyes, Calif. (C)	11-34, 41, 43-49, 51	16,22 Sept. 1976
	10, 35-38	4 Dec. 1976
State College, Pa. (D)	10, 11-34, 35-38, 39-41, 43-51	7-8 Dec. 1976
Panama Canal Zone (E)	11-34, 39-41, 41-43, 10, 35-38	7 Oct. 1976

   C. Point Reyes (west coast marine)
   D. State College (rural)
   E. Panama Canal Zone (tropical)

2. Test Periods
   A. Initial tests (zero point)
   B. 2, 5, 10, and 20 years exposed (triplicate panels)
   C. 2, 5, 10, and 20 years storage (duplicate panels)
3. Type of Tests to be Made by the Supplier
   A. Chemical analysis
   B. Thickness measurements at specific positions—to nearest 0.025 mm (0.001 in.) before exposure (see Figs. 2 and 3)
   C. Length and width measurements to nearest 0.25 mm (0.01 in.) before exposure
   D. Initial weight of panel to nearest 0.001 g
   E. Weight change of panel after exposure and cleaning, to nearest 0.001 g
   F. Initial tension tests—6 specimens from 2 panels
   G. Tension tests after exposure—2 specimens per panel after cleaning and weighing (see Figs. 2 and 3)
   H. Pit depth after exposure—center section of each panel after removal of tension specimens (see Figs. 2 and 3)
   I. Test results to be recorded on special test record sheets provided
4. Test Panels (see Figs 2 and 3)
   A. 20.3 by 10.16 by 0.27-cm (8 by 4 by 0.05-in.) panels to be exposed at 30 deg to the horizontal
   B. All panels of each alloy from one heat—20.3-cm (8-in.) dimension parallel to direction of rolling
   C. Triplicate panels for each period providing triplicate specimens for weight change and pit depth and sextuplicate specimens for tension tests
   D. Total panels per alloy, 90

Initial tests	2
5 sites, 4 periods, 3 panels	60
4 storage periods, 2 panels	8
Reserve	20
	90

5. Marking
   A. Exposed panels to be stencilled with 0.65-cm (¼-in.) stencils within 3.81 cm (1½ in.) of top as per identification codes attached (metallic coated steel panels to have coding punched)

B. Panels for storage and reserve stencilled as above but with alloy code only.
C. All panels in a series are to be randomized

6. Packing and shipping
   A. Twelve exposure panels, weighed, measured, and stencilled, for each location packaged as a unit in waterproof paper and held until 1 March 1976, when directions for shipping directly to the test sites will be distributed
   B. Storage specimens packaged in 4 lots of 2 panels each and 1 lot of 20 panels. Each lot wrapped in moisture proof paper and dipped in microcrystalline wax. Identification of each lot evident without breaking wax seal-probably dark china-marking crayon on paper under wax coating. This suggests use of light-colored wax if possible. Each lot should be identified as "Alloy (No.) of ASTM G-1 Test Program," the 5 lots packed in 1 carton and sent to ASTM Headquarters, 1916 Race Street, Philadelphia, Pa. 19103 Attention: ASTM G-1 Test Program—Alloy (No.).
   C. Notify the chairman of the task group of all shipments to ASTM headquarters.

NOTES—Tension tests shall be made in accordance with ASTM Method E 8. Procedures for cleaning and pit depth determinations will be resolved before the end of the first exposure period.

Master Code for Identification of Alloys

Alloy Test Designation	Commercial Designation	Supplier	In Charge
	METALLIC COATINGS		
10	Aluminized steel, Type 2 (pure Al)	Armco	V. P. Pearson
11	Galvalume (50Zn-50Al)	Bethlehem Steel Co.	V. P. Pearson
12	Galvanized steel, G60 class	Inland Steel Co.	V. P. Pearson
13	Galvanized steel, G90 class	Inland Steel Co.	V. P. Pearson
	COPPER ALLOYS		
14	110	Olin Corp.	A. W. Brock
15	194 (HSM copper)	Olin Corp.	A. W. Brock
16	195 (Strescon)	Olin Corp.	A. W. Brock
17	220 (commercial bronze)	Olin Corp.	A. W. Brock
18	230 (red brass)	Olin Corp.	A. W. Brock
19	260 (cartridge brass)	Olin Corp.	A. W. Brock
20	510 (phosphor bronze)	Olin Corp.	A. W. Brock
21	511 (phosphor bronze)	Olin Corp.	A. W. Brock
22	638 (Coronze)	Olin Corp.	A. W. Brock
23	664 (Cobron)	Olin Corp.	A. W. Brock
24	688 (Alcoloy)	Olin Corp.	A. W. Brock
24	725	Olin Corp.	A. W. Brock
44	CA 170	Brush Wellman, Inc.	R. M. Paine
45	CA 172 XHMS	Brush Wellman, Inc.	R. M. Paine
46	CA 172 ½HT	Brush Wellman, Inc.	R. M. Paine
47	CA 175 AT	Brush Wellman, Inc.	R. M. Paine
48	CA 175 HT	Brush Wellman, Inc.	R. M. Paine
49	CA 172 AT	Brush Wellman, Inc.	R. M. Paine

		LEAD ALLOYS	
26	Pb-0.065Ca	St. Joe Minerals	R. F. Dvorak
27	Pb-0.065Ca-1.3Sn	St. Joe Minerals	R. F. Dvorak
		MAGNESIUM ALLOYS	
28	AZ31B	Frankford Arsenal	F. Pearlstein
		NICKEL ALLOYS	
29	Nickel 200	Huntington Alloys Div. INCO	J. C. Hosier
30	Monel alloy 400	Huntington Alloys Div. INCO	J. C. Hosier
31	Inconel alloy 600	Huntington Alloys Div. INCO	J. C. Hosier
32	Inconel alloy 625	Huntington Alloys Div. INCO	J. C. Hosier
33	Inconel alloy 800	Huntington Alloys Div. INCO	J. C. Hosier
34	Inconel alloy 825	Huntington Alloys Div. INCO	J. C. Hosier
		STAINLESS STEELS	
35	409	Armco	H. H. Lawson
36	430	Armco	H. H. Lawson
37	304	Armco	H. H. Lawson
38	316	Armco	H. H. Lawson
		TITANIUM ALLOYS	
39	Ti-50A	Titanium Metals Corporation	H. L. Covington
40	Ti-38A	Titanium Metals Corporation	H. L. Covington
		ZINC ALLOYS	
41	Zn-22Al H1 rolled sheet	St. Joe Minerals	R. F. Dvorak
42	Zn-22Al H3 rolled sheet	St. Joe Minerals	R. F. Dvorak
43	Zn-7Al-3Cu gravity-cast plates	St. Joe Minerals	R. F. Dvorak
		ALUMINUM ALLOYS	
50	1199	Conalco	W. C. Setzer

Task Group

Chairman	W. H. Ailor Reynolds Metals Co. 4th and Canal Sts. Richmond, Va. 23261 (804) 649-1411 X7222

Chairmen for Test Metals

Titanium	L. C. Covington Titanium Metals Corp. P. O. Box 2128 Henderson, Nev. 89015 (702) 564-2544
Copper	A. Castillo Olin Corp. 91 Shelton Ave. New Haven, Conn. 06504 (203) 777-7911 R. M. Paine Brush Wellman, Inc. 17876 St. Clair Ave. Cleveland, Ohio 44110 (216) 486-4200
Lead and Zinc	R. F. Dvorak St. Joe Minerals Corp. Zinc Smelting Division, Box A Monaco, Pa. 15061 (412) 774-1020
Low Alloy Steels	J. B. Horton Homer Research Labs Bethlehem Steel Co. Bethlehem, Pa. 18016 (215) 694-6455
Stainless Steel	H. H. Lawson Research and Technology, Armco Steel Corp. Middletown, Ohio 45042 (513) 425-2738
Magnesium	F. Pearlstein Frankford Arsenal Commander SARSA PDC 64-2 Philadelphia, Pa. 19137 (215) 831-6401
Metallic Coats	V. P. Pearson (deceased) Inland Steel Research Labs 3001 East Columbus Dr. East Chicago, Ind. 46312 (312) 375-6200
Aluminum	W. C. Setzer Conalco P. O. Box 14448 St. Louis, Mo. 63178 (314) 878-6905

Nickel:
J. C. Hosier
Huntington Alloys
Huntington, W. Va. 25720
(304) 696-2102

Ad Hoc Members

Weather
P. R. Grossman
Q-Panel Co.
15610 Industrial Pkwy.
Cleveland, Ohio 44135

Statistics
F. H. Haynie
National Environmental Research Center
Research Triangle Park, N.C. 27711
(919) 549-8411

Sites
F. Pearlstein
Frankford Arsenal
Bridge and Tacony Sts.
Philadelphia, Pa. 19137
(215) 831-6401

Site Calibration
S. K. Coburn
U.S. Steel Corp.
600 Grant St.
Pittsburgh, Pa. 15230
(412) 433-2216

H. N. Alderson
Pacific Gas and Electric Co.
Dept. of Engineering Research
3400 Crow Canyon Rd.
San Ramon, Calif. 94583
(415) 820-2000

References

[1] *Proceedings*, American Society for Testing and Materials, Vol. 52, 1952, pp. 212-238.
[2] *Twenty-Year Atmospheric Corrosion Investigation of Zinc-Coated and Uncoated Wire and Wire Products, ASTM STP 290,* American Society for Testing and Materials, 1959.
[3] *Atmospheric Corrosion of Nonferrous Metals, ASTM STP 175,* American Society for Testing and Materials, 1956.
[4] *Proceedings,* American Society for Testing and Materials, Vol. 53, 1953, pp. 272-290.
[5] Sereda, P. J., *ASTM Bulletin,* Feb. 1958, pp. 53-55.
[6] *Proceedings,* American Society for Testing and Materials, Vol. 61, 1961, pp. 202-228.
[7] *Proceedings,* American Society for Testing and Materials, Vol. 62, 1962, pp. 212-231.
[8] *Proceedings,* American Society for Testing and Materials, Vol. 66, 1966, pp. 552-574.
[9] *Proceedings,* American Society for Testing and Materials, Vol. 66, 1966, pp. 160-200.
[10] *Proceedings,* American Society for Testing and Materials, Vol. 59, 1959, pp. 333-338.
[11] *Proceedings,* American Society for Testing and Materials, Vol. 74, 1974, pp. 492-535.
[12] *Proceedings,* American Society for Testing and Materials, Vol. 59, 1959, pp. 176-182.
[13] *Symposium on Atmospheric Exposure Tests on Nonferrous Metals, ASTM STP 67,* American Society for Testing and Materials, 1946.

L. D. Fitzgerald[1]

Protection of Copper Metals from Atmospheric Corrosion*

REFERENCE: Fitzgerald, L. D., "**Protection of Copper Metals from Atmospheric Corrosion,**" *Atmospheric Factors Affecting the Corrosion of Engineering Metals, ASTM STP 646,* S. K. Coburn, Ed., American Society for Testing and Materials, 1978, pp. 152-159.

ABSTRACT: The development of a synthetic patina process for copper metals is described. The chemistry of the process essentially parallels the natural atmospheric corrosion of copper. Various stages of the patination system are illustrated via scanning electron microscopy (SEM) photographs.

The development of organic resin-based coating systems are described, including passivation systems, solvent selection and resin screening techniques. An accelerated weathering test program for evaluation of clear coatings is detailed. Field evaluation at various test sites are correlated with coating properties. They illustrate the effect of atmospheric contaminants, sea spray contanimation, and high ultraviolet intensity exposure effects as they pertain to coating life.

Field tests of the inorganic patina and of both an organic lacquer and a shop-applied film coating system are described indicating the potential durability of the system.

KEY WORDS: corrosion, atmospheric corrosion, copper metals, patina coatings, accelerated tests, synthetic finishes

Atmospheric corrosion of copper metals seems a strange concept. For centuries copper and its alloys have withstood the elements with impunity [*1,2*].[2] Specimens of patinated metal from 300-year-old roofs in Europe have shown less than a hundred micrometers of copper loss. Thus, the subject of atmospheric corrosion really covers aesthetic effects rather than a concern for structural integrity. This review covers the area of highly durable architectural finishes and, as such, deals only with inorganic and clear systems. There are, as far as atmospheric corrosion is concerned, no other types of finishes in use.

*Original experimental data were measured in U.S. customary units.

[1] Consultant, International Copper Research Association, Inc., N.Y., N.Y. 10022.

[2] The italic numbers in brackets refer to the list of references appended to this paper.

Since copper metals are the only colored metals besides gold, they have always been used in grand and monumental buildings such as cathedrals, government buildings, and universities. In addition to their natural colors, copper metals form oxides and sulfides which create warm brown or brown-black colors. Carrying the nondestructive corrosion of copper and its alloys to the ultimate step, patinas are developed. The patinas signal the termination of corrosion of the copper metal surface and provide a permanent protective coating for the metal. Patinas range in color from green through gray-black and are attained ordinarily by allowing the metals to stand in place for periods of 5 to 15 years. In some arid areas such as Mexico City, Mexico and Denver, Colorado, patination never occurs and the metal turns only a gray-black. Along seacoast areas patination is usually quite rapid and is oftimes completed within 5 years.

Inorganic Finishes

Many experimental techniques have been used to accelerate patination [2]. Vinegar, sprayed or painted on the surface, will accelerate patination by a year or two. Other chemical treatments have been developed by various artists and architects including the famous Frank Lloyd Wright. There are also innumerable proprietary treatments used by metal maintenance companies and roofing firms around the world. All such techniques have the drawbacks that they are difficult to apply with uniformity and that such patinas tend to deteriorate with age since they are artificial rather than natural or synthetic.

In 1966 The International Copper Research Association (INCRA) initiated research in the Department of Mineral Engineering at the University of Utah, with the objective of finding methods for preparing inorganic coatings. The initial study objective was to identify various combinations of reagents which would produce colored, adherent coatings on copper. Since basic sulfates, carbonates, and chlorides have been observed as natural patinas, this seemed a reasonable base for our efforts. It was found that a number of reagents would react to produce colored coatings in a temperature range of 100 to 125°C, provided moderate oxygen pressure was maintained and the pH was adjusted. Thus, at 30 psi oxygen and an initial pH of 5.4, attractive black coatings of cupric-oxide were produced. Green layers of basic sulfate were formed at pH 3 in solutions containing sulfate. Atacamite, a basic chloride which is also green, was produced in solutions at pH 2.0 containing chloride in place of sulfate.

With this initial work completed, the direction shifted toward the development of a synthetic patination process. It was recognized that all patination systems begin via oxidation of the copper surface. In nature this is a major factor in the time of onset of patination. We proposed the use of oxidizing agents which would be strong enough to provide the base oxide in a short time without dissolving the base metals. Chlorates, permanganates, dichromates, peroxides, and persulfates were examined. Of these, the most suitable appeared to be potassium chlorate. This formed a cuprite (Cu_2O) surface at pH 5. Eventually, it was found that the addition of copper sulfate to the oxidizing solution changed the cuprite into a green layer which was shown by X-ray diffraction to be brochantite ($CuSO_4 \cdot 3Cu(OH)_2$), the material of most natural green patinas found on copper. This research was followed by an extensive, fundamental study of the mechanism of brochantite formation [*4*].

Upon completion of this research, pilot studies for the production of brochantite-coated copper sheet were initiated at Revere Copper and Brass Research Laboratories in Rome, New York. At this stage, the process required some 20 days of immersion in order to develop a satisfactory green coating. In addition, the coatings were sometimes loosely adherent and powdery and the color development tended to be spotty when applied on 0.37-m^2 (2-ft^2) sheets. Subsequent changes in the concentration of patination chemicals provided a bath which would satisfactorily coat full-size copper sheets in about 4 days of immersion. This was verified in a full-scale production trial in which several thousand pounds of copper sheet were patinated in order to provide materials for field evaluation.

The patination mechanism begins with the oxidation of copper to cuprous-oxide. This is followed by a partial dissolution of the cuprous-oxide as indicated by weight-losses of the specimens during the initial stages of treatment (Fig. 1). Immediately after this initial weight loss the specimen begins to gain weight and change color. It proceeds through purple and light green to a heavy green color. The purple substance was identified as cuprous-oxide; the green material was shown to be brochantite by X-ray diffraction. The green layer appears subsequent to the formation of the cuprite and, as shown by scanning electron microscopy (SEM) seems to grow at the expense of the cuprite (Figs. 2 and 3).

The pH of the solution increases during treatment as does chloride content of the bath. This appears to be a limiting factor and brochantite formation slows appreciably as chloride develops. After a bath had been recycled through 5 batches it was necessary to remove the chloride and reconstitute the patinating solution by precipitating the copper, filtering, and reformulating a new bath.

Although the patination was carried out successfully in a stainless steel tank with stainless steel racks, it would be more desirable to utilize a nonmetallic container since all surfaces which are in contact with the patinating solution rapidly become coated with a thick, green incrustation.

The final product was manufactured on 2.3-m^2 (3 by 8-ft) sheets. It had a dark green surface made up of microcrystallites of brochantite sticking out from an underlay of cuprous-oxide. The surface was somewhat darker than a natural patina due to the particular crystal structure. Brushing or

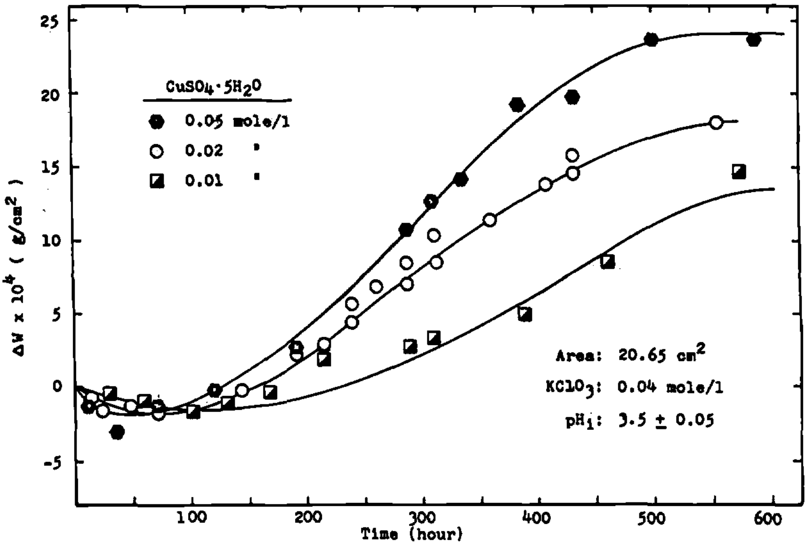

FIG. 1—*Weight change of copper specimens immersed in corroding solution in the patination process at room temperature (28°C).*

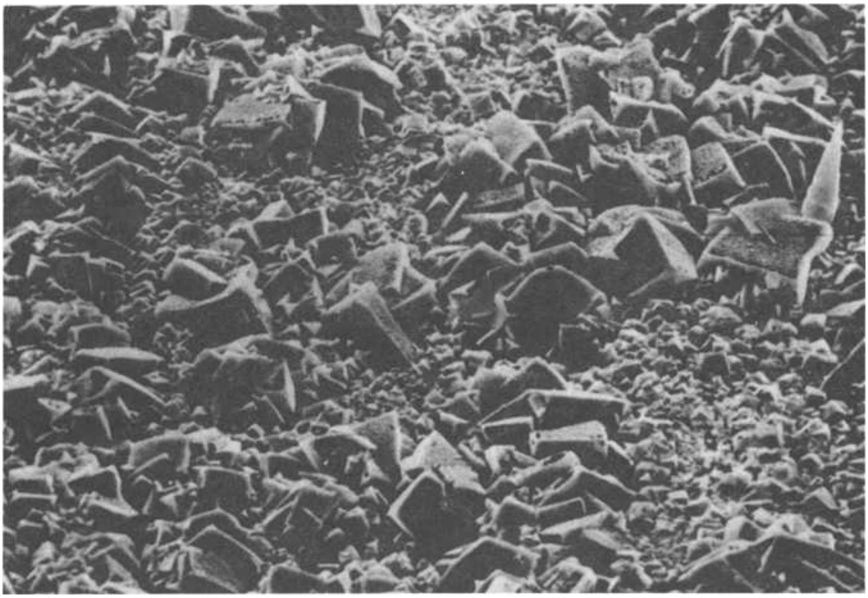

FIG. 2—*Scanning electron microscopy (×1000) shows formation of cubic cuprous-oxide crystals during initial stages of patination.*

FIG. 3—*Scanning electron microscopy (×1000) shows brochantite forming at the expense of cuprous-oxide in latter stages of patination.*

abrading the surface broke off the tips of the crystals, changing the appearance to a much lighter green—almost the exact color of a natural patina. Test installations were made in Canada and in South Carolina. These demonstrated that the patina was extremely adherent, even under conditons of violent mechanical forming (180-deg two-thickness bends hammered tight). The patina sheets varied somewhat in color when installed, but after six months to a year of weathering the color leveled to a uniform tone. The scratches and dents began to heal, and were coated over with fresh oxide and brochantite.

Exposure tests in the eastern United States and Canada have shown that the brochantite structure on the surface spreads and fills in when exposed to the weather to form a uniform patina with the same compositon as a natural patina. These results evoke a high degree of confidence in the durability of the so-called Incra-Patine material in environments where natural patination occurs. Because of the limited markets for copper roofing at current prices this process has never been commercialized though it is patented [*5*]. The use of a synthetic patina in geographies where natural patination does not occur is not recommended. In these areas the brochantite surface can be dehydrated or degraded over a period of time, and there is no natural renovation to preserve the finish. (This is evidenced by patination, or rather, oxidation effects in Mexico City.) It could, however, be considered in areas where patination does occur, though it may require 50 to 100 years due to the lack of pollutants in the atmosphere.

These inorganic coatings are extraordinarily durable and can be considered permanent finishes for copper metals provided they are not exposed in industrial atmospheres where the pH of either the atmospheric contaminants or the settling particulate matter will be so low as to degrade the basic copper salts. These unusual situations have been evidenced in "acid rains" (pH 1.5 to 3) and in soot particles on copper roofing (pH 0.5 to 2).

Organic Coatings

In order to preserve the natural golden colors of copper and its alloys it is necessary to keep the surfaces free from oxide and sulfide. The obvious way to do this is by frequent polishing. With today's high cost of labor, however, this is oftimes impractical.

The alternative to constant polishing is to apply clear coatings. INCRA research has perfected two basic types of such coatings. One is a maintenance lacquer which can be sprayed on the polished metal and removed when worn or damaged. This type of coating provides 3 to 5 years of protection. The second type of coating is designed for long-term protection—from 15 to 25 years— and must be applied in-shop.

INCRA's basic research on finishing copper metals was initiated in the early 1960s. Fundamental work in Britain [*6*] showed that the prime mode of failure for coating systems was due to pinholes and defects in the coating followed by the development of corrosion on the copper metal surface which rapidly spread underneath the existing coating. As a result, underfilm corrosion caused a pinhole to be the initation point for a large, unsightly splotch. A screening program for inhibitors was undertaken. The discovery of benzotriazole as a corrosion inhibitor for copper metals was utilized to provide a surface which corroded only at the bottom of a pinhole and allowed essentially no spread of underfilm corrosion.

In the meantime, another screening program was underway at Chase Brass Laboratories in Waterbury, Connecticut. This study evaluated cleaning techniques and extensively screened the available commercial clear lacquers. Salt spray testing was used as a standard procedure. This research was one of the first extensive uses of a dew point Weather-ometer. These tests on clear coatings soon sorted out the most durable systems. Of the air-dry lacquer resins, the acrylic system proved most durable. High molecular weight acrylics seemed better than partially cross-linked modified acrylics. By the time specimens were ready for exposure testing at various sites in the country, the British research was combined with the Chase work to provide a lacquer system [*7*] designated as Incralac.[3] This is a

---

[3] Incralac is a certification mark of The International Copper Research Association. It is available in commercial quantities from Stanchem Inc., East Berlin, Conn.

Rohm and Haas B-44 acrylic formulated with 1½ percent benzotriazole based on resin solids. In addition, the system is dissolved in toluene and xylene solvents.

Early in the British study, it was found that when retained solvent in a lacquer is held in intimate contact with copper metal, it can cause tarnishing. Oxygenated solvents, such as ketones and aldehydes, were particularly bad. These groups, catalyzed by the copper surface and ultraviolet light, tended to form peroxides. These peroxides would eventually break down, discoloring the metal surface under the intact coating.

While the air-dry coating was being developed, baked finishes and chemically cross-linked systems were also being examined. An ideal subsurface corrosion primer was a transparent, green-tinted chromate containing material from Pennwalt Chemical called Hinac II-P. Specimens of brass with micron thicknesses of Hinac II-P as a primer and a 15 percent melamine-modified, baked acrylic, 25-μm (1-mil) surface coats have withstood over 10 years of exposure testing with no deterioration. Unfortunately, the Hinac primer must be baked on and is thus an extremely brittle base material. Specimens with 3-mm (1/8-in.) mandrel bends or tight post fabricating bends showed rapid deterioration at the formed areas in exposure testing.

Two component polyurethanes have also been evaluated. These materials, while very hard and durable, must be approached with caution. Several such materials passed 18 and 24-month exposures and then failed catastrophically by cross-linking and embrittling. Some aliphatic-based urethanes, however, appear to be satisfactory for extended periods of time and may well be suitable for long-term protection of architectural copper metals.

Subsequent to our work on baked and air-dry lacquer systems, we initiated a project to provide a semipermanent coating for architectural copper metals. The basic criteria for this system were that it be extremely durable and relatively cheap to apply under controlled conditions. This program evolved a duPont Tedlar Fluorocarbon laminate, adhesively applied over a chromate passivation treatment on a coil coating line at 175 to 205°C (350 to 400°F). This system is postformable and has passed the most stringent accelerated testing program we could devise. For instance, the 25-μm (1-mil) Tedlar system designated Incracoat,[4] has satisfactorily stood up under some 7000 h of dew point Weather-ometer testing, over 4000 h of salt spray tests and over 2 years on the Emmaqua test facility in Phoenix, Arizona.

Exterior Exposure Testing

In order to obtain a broad range evaluation of the performance of the various coating systems, test sites were established at Cambridge, Mass-

[4] Incracoat is a certification mark of International Copper Research Association. This material is available on several copper alloys from American Nickeloid Co., Peru, Ill.

achusetts; New York City; Cleveland, Ohio; Salt Lake City, Utah; Berkeley and South San Francisco, California; Dallas, Texas; New Orleans, Louisiana; Kure Beach, North Carolina; and Hialeah and South Miami, Florida. Over 10 years of data on the air-dry and baked lacquer systems and 6 to 8 years of data on the Tedlar laminate system were gathered. The test sites in South San Francisco and Kure Beach seem to provide the worst environments. As a result, there is some specking and deterioration on many of the specimens at these sites. Most of the other sites show little or no deterioration for the Tedlar-coated systems.

The 25-μm (1-mil) acrylic lacquer benzotriazole maintenance coating system is visually satisfactory after 5 years at all sites. Specimens show appreciable deterioration at the San Francisco and Kure Beach sites after some 6 years.

The baked acrylic finishes are still holding up after 10 years at all sites, provided the specimen panels are not defected.

Conclusion

These test data effectively demonstrate that a passivated metal surface coated with an ultraviolet, insensitive clear film will provide an extraordinarily long life system. The Incracoat system up to this time has been used exclusively in architectural metals for roofs and fascias. It has been installed successfully with all the necessary postforming and without damage to the surface, and has a demonstrated life with no signs of deterioration of over 8 years.

References

[1] Vernon, W. J. H. and Whitby, L., *Journal of the Institute of Metals*, Vol. 42, No. 2, 1929 to 1930, pp. 181-182.

[2] Mattsson, E. and Holm, R. in *Metal Corrosion in the Atmosphere, ASTM STP 435*, American Society for Testing and Materials, 1968, pp. 187-210.

[3] Vernon, W. J. H., *Journal of the Institute of Metals*, Vol. 49, 1932, pp. 153-167.

[4] Yoon, Seung Ryul, "A Study of the Properties and Methods of Preparation of Synthetic Inorganic Coatings on Copper," Ph.D. thesis, University of Utah, Salt Lake City, July 1971.

[5] Hanson, C. K. and Whitman, C. I., 24 Feb. 1970, U.S. Patent No. 3,497,401.

[6] Cotton, J. B. and Scholes, I. R., *British Corrosion Journal*, Vol. 2(1), 1967, pp. 1-5.

[7] Spindel, S., *American Paint Journal*, 19 Oct. 1970.

R. D. Smith[1]

An Accelerated Atmospheric Corrosion Test (AACT)*

REFERENCE: Smith, R. D., "**An Accelerated Atmospheric Corrosion Test (AACT),**" *Atmospheric Factors Affecting the Corrosion of Engineering Metals, ASTM STP 646,* S. K. Coburn, Ed., American Society for Testing and Materials, 1978, pp. 160–164.

ABSTRACT: A laboratory test method for accelerated atmospheric corrosion testing has been developed. Copper alloys were the main subject of testing, and the principal atmospheric simulation was urban-industrial. The test method has been very useful in ranking experimental copper alloys relative to commercial alloys and is believed to be adaptable to other alloy systems and environments. Representative reproducible oxide films can be generated for film study work and kinetics of film formation can be followed easily.

KEY WORDS: corrosion, atmospheric corrosion laboratory tests, environmental test chambers, copper, copper alloys, atmospheric corrosion, corrosion, corrosion tests

In the course of an alloy development program at Ledgemont Laboratory of Kennecott Copper Corporation it became necessary to devise an accelerated atmospheric corrosion test (AACT) in order to rank atmospheric corrosion resistance of candidate experimental alloys relative to existing commercial copper base materials.

A survey of the literature revealed that existing accelerated atmospheric tests were not well suited for ranking alloys relative to their performance in outdoor atmospheric exposure. Either the environment was entirely nonrepresentative as in the salt spray test and its various modifications (including the copper chloride, acetic acid, salt spray test (CASS) and the Corrodcote test), or else the corrosion product films formed were of an entirely different character than those observed on real-time exposure panels. Under most ambient condition exposures, both indoors and out,

---

*Original experimental data were measured in U.S. customary units.

[1] Project leader, Alloy Development, Ledgemont Laboratory, Kennecott Copper Corporation, Lexington, Mass. 02173.

the initial film that forms on copper and copper alloys is cuprous oxide (Cu_2O). This film is normally quite adherent, thin, and relatively protective. As time progresses the films transform through natural processes to basic sulfates, oxychlorides, or carbonates depending on the environmental contamination present. What was desired was a method of providing the same assortment of ionic and dissolved species to test specimens as would be encountered in real exposure, while at the same time accelerating the overall process of film growth and stabilization in order to rank more quickly experimental alloys against existing commercial alloys having known performance.

Published results have shown that urban industrial air is one of the most severe staining environments commonly encountered. The single most important contributor to staining of copper base alloys in such environments is sulfur dioxide (SO_2) in conjunction with relative humidity high enough to produce surface wetness. Acidity of rain is also important in the formation of oxide films and the most commonly encountered pH range in industrial areas is from 4 to 5. These factors were taken into account in the design of the apparatus and test. Acceleration relative to real-time exposure is provided by means of (*a*) increasing the frequency of wet/dry cycles (and time of wetness) to 100 cycles per day, (*b*) slightly elevating the temperature (35°C) and (*c*) controlling pH at 4.75 ± 0.25. The "rain" is an 0.05 percent sodium bisulfite ($NaHSO_3$) solution. This sodium bisulfite solution, being slightly unstable, liberates SO_2 which contributes to staining. An acceleration factor of about 100 is achieved, each wet/dry cycle being equivalent to about one day outdoor exposure in New York City. This factor is based on comparative appearance of specimens exposed for several years in New York City and specimens exposed for short times in the "rain box." One obvious difference, however, is the lack of atmospheric fallout such as dust, fly ash, salts, guano, soot, etc., which are indeed present in New York City. The absence of fallout is principally important relative to localized corrosion effects. The AACT is useful for screening purposes and is a reproducible means of generating uniform films for additional study.

Aside from the fallout factor, films generated in the rain box in 1050 cycles are visually the same as those resulting from three years exposure in New York City. Evaluation methods may include weight gain or loss data, measurement of reflectivity versus time, or electrochemical evaluation of the films produced in the AACT. The films formed under the controlled conditions of the AACT apparatus are believed to be quite representative of naturally formed films. Composition and structure studies of the films have been done using X-ray diffraction, scanning electron microscopy (SEM) and film analysis by Auger, and electron spectroscopy for chemical analysis (ESCA) techniques. Films formed at ambient temperature were found to be essentially Cu_2O, but the oxide also contains additional cations from the alloy and other anions from the environment. These dopants play an important role in determining both the mechanical integrity of the film and the resistance of the film to both ionic and electronic flow. Figure 1 shows a typical ESCA concentration scan on an alloy corrosion specimen exposed to 1050 cycles of artificial rain and drying in our rain box. Oxygen, aluminum, and carbon contents decrease from the oxide surface to the base metal, while copper and nickel increase accordingly. The oxide is seen to be significantly enriched in aluminum content, relatively rich in nickel—although still less than in the base alloy—and fairly high in carbon content at the surface. An interesting observation is that although sulfur oxides are important promoters of corrosion film formation, very little, if any, sulfur appears in the bulk film itself in the form of sulfates, sulfites, or sulfides. Apparently if they are formed at all they are sufficiently soluble to leach out during the rain part of the cycle. Chlorine, probably in the form of oxychlorides, has been found in the film and evidence of carbonates also exists, originating from dissolved carbon dioxide (CO_2) in the rain.

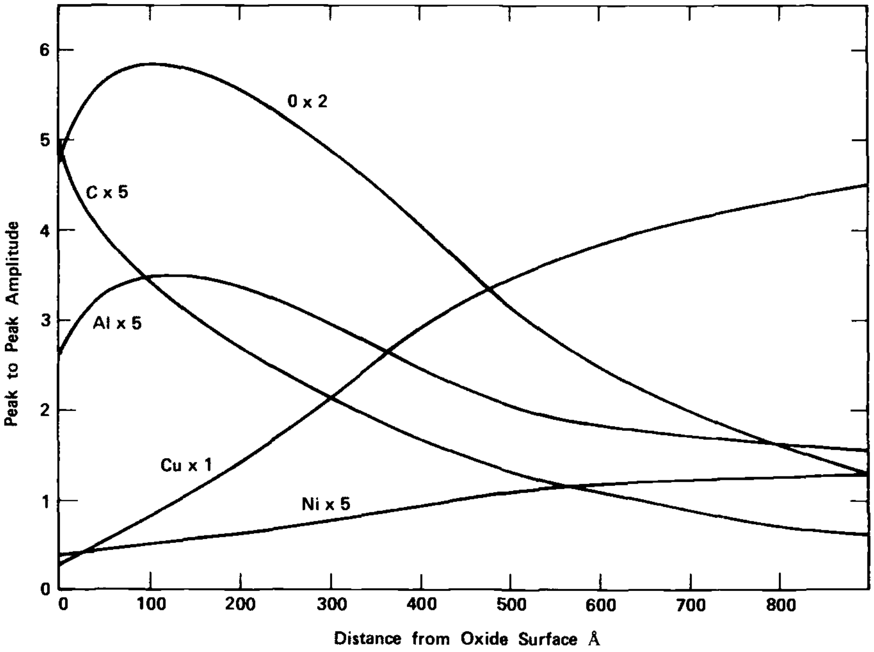

FIG. 1—*Concentration profile by ESCA filmed alloy, Cu + 7Al + 5Ni.*

Procedure

The test procedure is as follows. Figure 2 shows the general configuration of the test setup including the test chamber, a 75-litre (20-gal) solution

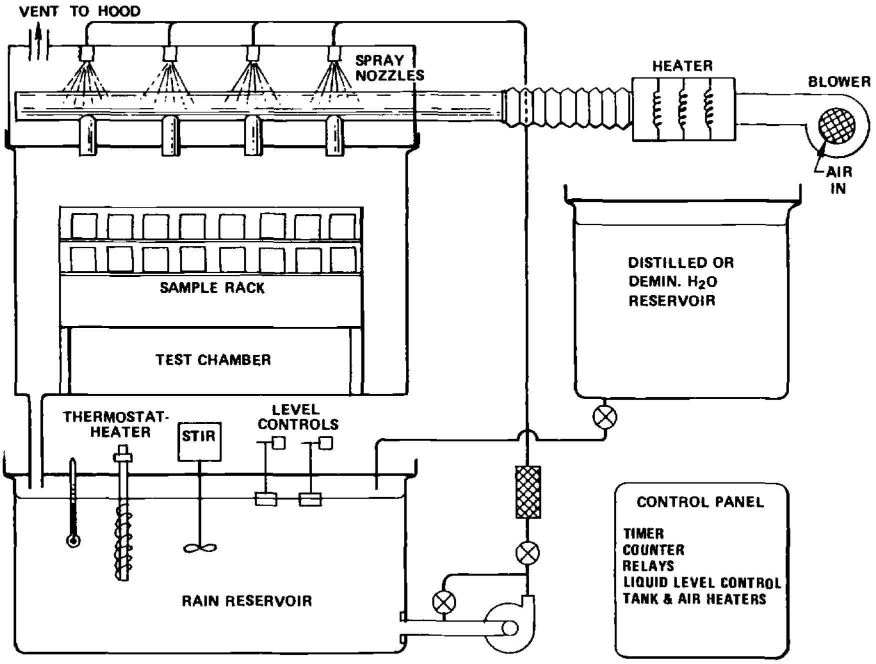

FIG. 2—*Accelerated atmospheric corrosion test apparatus.*

reservoir, circulating pump, warm air system, and control console. A fresh solution of 0.05 percent $NaHSO_3$ is mixed and the system started up and operated for 24 h to reach equilibrium temperature, pH, and dissolved gas (air and CO_2) levels before introduction of specimens. An adjustment of pH is made with $NaHSO_3$ or sodium hydroxide (NaOH) to about 4.75. A simple technique for specimen preparation is abrasion through several grit sizes of silicon carbide abrasive paper ending with 400 grit, followed by cleaning in an ultrasonic cleaning bath with a mild detergent in distilled water, distilled water rinsing, alcohol rinsing, and air drying. The specimens are placed on a rack in the box inclined at about 30 deg to horizontal and the cycle counter set to zero. Cycling rate is 4 cycles/h with 4 min of rain and 11 min of warm (50°C) air during each cycle. Ambient laboratory air is drawn over heating coils producing air dry enough to completely dry the specimens. A daily adjustment to pH is made since pH tends to drift up as the solution decomposes. A stock solution of $NaHSO_3$ is used to bring pH into range. This pH control could be easily automated with appropriate equipment. Liquid level controls are also incorporated in the solution reservoir to add distilled or demineralized makeup water to compensate for evaporation loss.

A plexiglas lid on the rain box allows visual monitoring of the specimens during the test period. As oxide films build up the copper alloys under study can be seen to go through the same sequence of color changes that occur on longer term, outdoor exposure.

Results Section

An example of the results of a typical run in the AACT apparatus is as follows. A group of commercial copper alloys along with a new developmental alloy were prepared and exposed as noted in the procedure section. After 1050 cycles (~ 11 days in the rain box) the specimens were removed and evaluated visually and by the linear polarization electrochemical technique. Results are presented in Table 1. The ranking of the commercial alloys is in excellent agreement with real-time performance in an urban industrial setting. The newly developed alloy CA615 is seen to be significantly better than existing alloys. Perhaps most importantly, the AACT apparatus allows the generation of representative oxide films in a reproducible manner, not subject to the whims of nature. Evaluation of these films by linear polarization allows a quantitative measure of performance rather than simply a qualitative visual comparison. The AACT apparatus is also well-suited to kinetic studies and will be used for this purpose in the future. It is believed that by suitable adjustment in rain composition, other environments could be simulated with equal success. Limited testing of aluminum alloys and stainless steel indicated that the apparatus and method is probably suitable for these systems also.

TABLE 1—*Results of 1050 cycles in AACT apparatus.*

Alloy	Composition (%)	Visual Appearance	Polarization Resistance[a]
CA260	70Cu, 30Zn	dark green	7 K Ω
CA614	91CU, 7Al, 2Fe	dull gray	50 K Ω
CA655	97Cu, 3Si	dull brown	16 K Ω
CA110	100Cu	brown/black	6 K Ω
CA615	90Cu, 8Al, 2Ni	hazy gold	115 K Ω

[a] Polarization resistance is measured in an electrochemical cell using the technique of Stern and Geary also known as the linear polarization method. A good description of the method is given by F. Mansfeld in *Advances in Corrosion Science and Technology*, Plenum Press, New York, Vol. VI, 1967, p. 163.

In summary, we have found the AACT chamber to be a very useful tool for ranking experimental alloys along with commercial alloys relative to their behavior in polluted industrial atmospheres. Secondarily the AACT provides a means for generating quickly and reproducibly films which we believe are quite representative in structure and composition to those produced outdoors in urban industrial environments. These films are then amenable to further study by a wide variety of evaluation techniques.

J. C. Zoccola,[1] *H. E. Townsend,*[1] *A. R. Borzillo,*[1] *and J. B. Horton*[1]

Atmospheric Corrosion Behavior of Aluminum-Zinc Alloy-Coated Steel*

REFERENCE: Zoccola, J. C., Townsend, H. E., Borzillo, A. R., and Horton, J. B., "**Atmospheric Corrosion Behavior of Aluminum-Zinc Alloy-Coated Steel,**" *Atmospheric Factors Affecting the Corrosion of Engineering Metals, ASTM STP 646,* S. K. Coburn, Ed., American Society for Testing and Materials, 1978, pp. 165-184.

ABSTRACT: The influence of the aluminum content of hot-dip aluminum-zinc alloy coatings on their corrosion behavior was studied by means of salt-spray and atmospheric corrosion tests. The objective was to develop an improved aluminum-zinc alloy coating on steel that would be more durable than galvanized coatings and that would be more protective to cut edges and areas of mechanical damage than hot-dip aluminum coatings. The optimum alloy was found to be 55 weight percent aluminum-zinc. This new alloy coating is two to four times as corrosion-resistant as a galvanized coating of similar thickness. Furthermore, for the galvanic protection of cut edges of sheet in some environments, this coating proved to be superior to aluminum coatings.

KEY WORDS: coatings, hot-dip coating, zinc-containing alloys, aluminum-containing alloys, atmospheric corrosion, salt-spray tests, zinc-aluminum alloys

A brief look at the status of the two major metallic coatings for sheet steel—with their important advantages as well as certain shortcomings—will be useful in showing why there was a need to develop an aluminum-zinc alloy coating.

Zinc has been used as a coating for steel products for the past 135 years. Galvanized coatings today occupy a major place among the most successful coatings for steel. Some 4.5 Gkg (5 million tons) of sheet and strip are galvanized for corrosion protection each year. Galvanized coatings have a good initial appearance, a fair-to-good resistance to corrosion in the atmo-

---

*Original experimental data were measured in U.S. customary units.

[1] Corrosion mechanisms engineer, corrosion mechanisms supervisor, hot-dip coatings supervisor, and corrosion prevention and coatings manager, respectively, Homer Research Laboratories, Bethlehem Steel Corp., Bethlehem, Pa. 18016.

sphere, fresh water and soil, and provide excellent galvanic protection to cut edges, thus preventing rust staining. Galvanized steel has, of course, a better, more acceptable corroded appearance than ordinary uncoated steel. Galvanized coatings also tend to suppress pitting of the steel base until the coating has been mostly consumed by corrosion. The chief drawbacks of zinc coatings are inadequate resistance to high temperatures and limited life in severely corrosive environments. As an example of the latter, data have been published [*1*][2] that indicate steel coated with 0.3 kg (1 oz) of zinc per m^2 (ft^2) of sheet would last less than 6 years before the onset of rust in the marine environment of Sandy Hook, New Jersey, and less than 3 years in the industrial environments of Brunot Island and Altoona, Pennsylvania.

Aluminum has been used commercially as a coating for steel sheet and strip for over 30 years and on other products for shorter times. Because of the formation of a more protective oxide film on aluminum, the corrosion and oxidation rates of this metal are generally less than those of zinc. Thus, aluminum appears to solve the major drawbacks of zinc coatings, namely, the need for greater atmospheric and high-temperature durability.

However, aluminum coatings also have drawbacks. For example, aluminum coatings do not galvanically protect steel in industrial and rural atmospheres. Thus, early rust-staining occurs at cut edges and at forming and other mechanical damage to the coating. Although early rust-staining at coating defects and cut edges of sheet has little consequence structurally, it can be aesthetically objectionable and may eventually develop into rust growths, or "pox." It is also recognized that aluminum coatings must be thicker (25.4 to 50.8 μm [1 to 2 mils] is required for hot-dip aluminum coatings as compared to about 25.4 μm [1 mil] for G90 galvanized coatings) than zinc coatings in order to have acceptable corrosion resistance in the atmosphere. Furthermore, temperatures above the melting point 660°C (1220°F) of pure aluminum cause recrystallization and appreciable softening of cold-worked steel during hot-dip coating. Thus, the maximum strength which can be attained by ordinary steel sheet is limited by hot-dip application of pure aluminum coatings. Nevertheless, some 0.27 to 0.45 Gkg (300 000 to 500 000 tons) of aluminum-coated sheet are produced for high temperature and atmospheric applications in this country each year. Thus, there is little question that aluminum coatings are a successful coating for steel products.

As valuable as the contributions of galvanized and aluminum coatings are, their respective shortcomings underlined the need for some type of coating for sheet steel and other products that would combine the best properties of both of these traditional coatings. To meet this need, in 1958 Bethlehem Steel began a research program to develop through alloying either a more durable zinc coating or a more galvanic aluminum coating. There had been many previous studies [*2–5*] of the effects of alloying zinc

---

[2] The italic number in brackets refer to the list of references appended to this paper.

or aluminum with small additions of second elements, but these efforts met with little technical or commercial success. Although Bethlehem researchers also tried many approaches, early in their program they found that combining large amounts of aluminum and zinc to form an aluminum-zinc alloy coating showed the most promise for producing a superior coating. Consequently, our program began a systematic investigation of a broad range of aluminum-zinc alloys as coatings for steel. Although many investigators had studied various combinations of zinc and aluminum in search of better die-casting alloys, there had been very little effort to develop these alloys as coatings for steel. Wehr and Mahlie [*6*] studied the addition of 5 to 20 weight percent aluminum to zinc to improve corrosion and heat properties but encountered severe production difficulties and apparently marginal improvements in performance. Bablik [*7*] showed that the aluminum-zinc alloy system could cause severe alloy growth activity on steel, a discouraging effect. Stanners [*8*] and Hoar et al [*9,10*] used metallizing to apply a full range of aluminum-zinc coatings on grit-blasted steel, and these coatings exhibited good corrosion performance.

Prior to Bethlehem Steel's research and development program that led to the development of the 55 weight percent aluminum-zinc hot-dip coating, however, aluminum-zinc coatings were not being applied by a continuous hot-dip method, the result being that there had simply been no opportunity to learn more about the potentialities of the aluminum-zinc coatings in terms of corrosion resistance and their properties. Our paper outlines briefly the hot-dip coating practice we developed and describes the corrosion resistance of the aluminum-zinc alloy system in the form of hot-dip coatings on steel sheet, the main emphasis being on corrosion behavior of the commercially produced 55 weight percent aluminum-zinc hot-dip-coated sheet currently being marketed in the United States under the name of Galvalume.

Corrosion Test Procedures

Preparation of Aluminum-Zinc Alloy-Coated Sheet Specimens

Aluminum-zinc alloy coating baths were made up containing 0, 1.0, 4.0, 7.4, 12.2, 16.6, 21.0, 24.9, 35.1, 44.6, 53.9, and 69.6 weight percent aluminum, about 3 weight percent silicon with respect to the aluminum content, and a balance of special high-grade zinc.

The preparation and coating of 15.2-cm (6-in.)-wide, 0.043-cm (0.017-in.)-thick, cold-rolled strip on a continuous pilot line is presented in Table 1.

Salt Spray Test

The salt spray test is that described in ASTM Specification for Salt Spray (Fog) Testing (B 117-73). Our coated panels were exposed to a salt fog of

TABLE 1—*Procedure for preparation and coating of aluminum-zinc-coated specimens.*

1. Alkaline cleaning.
2. Water-rinse and drying.
3. Heating to about 649°C (1200°F) in a Selas-type annealing furnace, followed by cooling in a furnace containing hydrogen to protect the strip from oxidation.
4. Coating of strip, the temperature of the bath of each alloy being maintained above the liquidus of the alloy. Coating thicknesses were controlled at about 1 mil[a] on each side of the strip by using rollers on both sides of the strip upon leaving the bath.
5. Air cooling to freeze the coating followed by water quenching of the coated strip.
6. Shearing into 4 by 6-in.[b] panels for corrosion testing in salt spray and in the atmosphere.

[a] 1 mil = 25.4 μm.
[b] 1 in. = 2.54 cm.

5 percent sodium chloride solution at 35°C (95°F). To prevent galvanic effects from exposed areas of bare steel, cut edges of the panels were covered with electroplaters' tape.

Atmospheric Tests

Sheet specimens 10.2 by 15.2 cm (4 by 6 in.) were weighed and exposed 30 deg from the horizontal at the International Nickel Company's Corrosion Station at Kure Beach, North Carolina, 24 and 245 m (80 and 800 ft) from the ocean surf, at Bethlehem, Pennsylvania (Homer Research Laboratories and the Coke Works of the Bethlehem Steel Corporation) and at Saylorsburg, Pennsylvania, representing four typical environments: severe marine, marine, industrial, and rural, respectively. The specimens faced south, except at the 24-m lot, where they faced east. To prevent staining, the panels were placed on stainless steel or Monel racks, and to prevent galvanic corrosion, the specimens were insulated from each other and from the racks by ceramic insulators. Testing was completed at the Bethelehem Coke Works after a 5-year exposure, and tests at the other sites are still in progress.

After a particular exposure period, the specimens were removed from the racks, cleaned in 20 percent chromic acid at 82°C (180°F), rinsed in running tap water, dried, and weighed. Cleaning continued until constant weights were obtained. Specimens were removed from test subsequent to cleaning. Weight losses (W) were determined, and the thickness loss (T) was calculated from the formula

$$T = \frac{W}{AD}$$

where A is the area and D the density of the coating. Thickness losses thus calculated and reported on Figs. 2 and 7 through 10 represent an average value of both skyward and groundward surfaces. Calculations employed the density of the alloy coating in the case of coatings containing up to 22 weight percent aluminum. For calculating thickness losses of aluminum-zinc coatings in the range 22 to 70 weight percent aluminum. The density of a 22 weight percent aluminum alloy was used as an approximation to the density of the zinc-rich portion that was observed to corrode preferentially.

For the corrosion-time curves of the 53.9 weight percent aluminum-zinc coating (referred to henceforth under the collective term "55 weight percent aluminum-zinc coating"), the actual composition of the corroded phase was determined from the weights and analyses of the coatings before and after exposure. The density of this composition was used in calculating the average thickness loss of the 55 weight percent aluminum-zinc coating.

Results and Discussion

The results of the salt-spray and atmospheric tests of the 0 to 70 weight percent aluminum-zinc coatings as well as the 55 weight percent aluminum-zinc coating are summarized in the following section. These results show the effect of aluminum content on the corrosion behavior of aluminum-zinc coatings. Finally, we present data on the microstructure and atmospheric corrosion resistance of the 55 weight percent aluminum-zinc alloy-coated sheet steel.

Effect of Aluminum Content of Coatings

Figure 1 shows the effect of aluminum content on the salt-spray life of aluminum-zinc alloy coatings. Galvanized coatings lasted about 300 h per 25.4 μm (mil) to first rust in salt spray. In contrast, aluminum additions increased the life linearly up to about 5500 h for the 55 weight percent aluminum-zinc coating (the optimum composition), after which performance dropped off with a further increase of aluminum.

Figure 2 shows the effect of aluminum content on atmospheric corrosion resistance after a 5-year exposure. Starting at the zinc end, corrosion resistance increases with aluminum additions up to 4 to 7 weight percent aluminum (eutectic composition at 5 weight percent aluminum), beyond which corrosion resistance decreases, that is, corrosion losses increase with aluminum content to about 21 weight percent aluminum (the eutectoid composition being 22 weight percent aluminum). Generally, the corrosion rate of the eutectoid composition is as high as the corrosion rate of zinc and in milder environments may be even higher. Beyond 21 weight percent aluminum the corrosion decreased to 70 weight percent aluminum more or less linearly. All coatings provided galvanic protection of cut edges, except the 70 weight percent aluminum-zinc coating, which tended to behave like aluminum coatings in this respect.

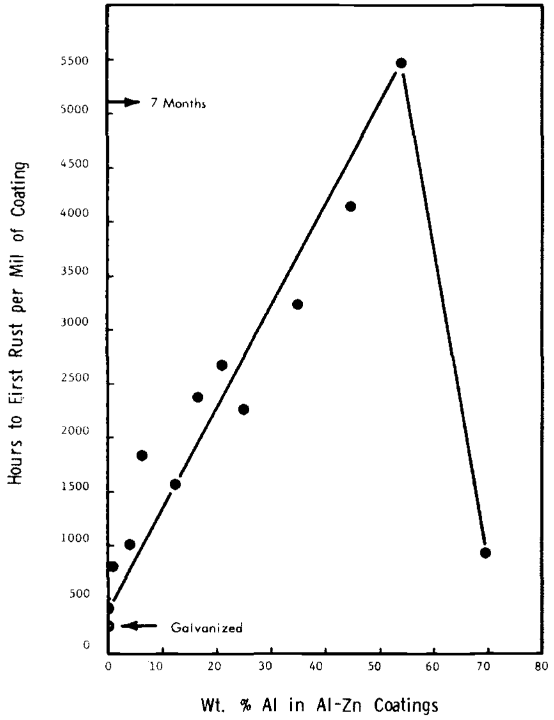

FIG. 1—*Effect of aluminum content on corrosion behavior of aluminum-zinc alloy coatings in salt spray (panels with protected edges). (1 mil = 25.4 μm)*

On the basis of the atmospheric and salt-spray corrosion tests as well as observations of the condition of cut edges, the 55 weight percent aluminum-zinc alloy coating proved to have the best combination of corrosion resistance with galvanic protection and, therefore, was selected for commercial development as our Galvalume sheet coating.

Microstructure of 55 Weight Percent Aluminum-Zinc Coatings

The equilibrium phase diagram for the binary aluminum-zinc system [*11*], Fig. 3, predicts that alpha phase containing about 82 weight percent aluminum is the first solid to form as a 55 weight percent aluminum-zinc alloy is cooled below the liquidus temperature. With nonequilibrium cooling, alpha-phase dendrites grow and reject zinc-rich liquid until the temperature of the rejected liquid is finally sufficiently below its solidus to complete the freezing process. The resulting structure consists of about 80 percent by volume of cored alpha-phase dendrites, with zinc-rich interdendritic alloy filling in the interstices.

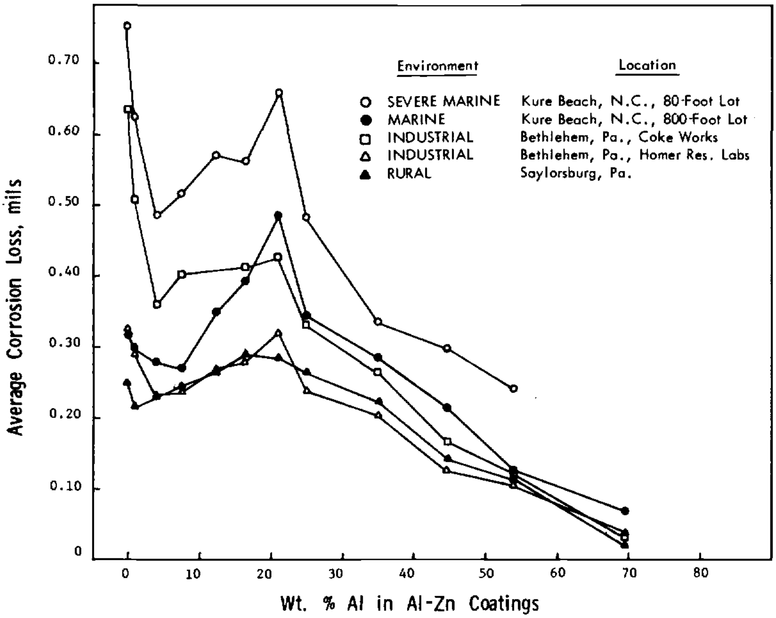

FIG. 2—*Effect of aluminum content on corrosion performance of aluminum-zinc alloy coatings after 5-year exposures in various atmospheres. (1 mil = 25.4 μm; 1 ft ~ 0.305 m)*

The cored dendritic structure of a 55 weight percent aluminum-zinc coating is most apparent when the center of an individual spangle is viewed at high magnification normal to the sheet surface (see Fig. 4). X-ray diffraction analyses indicate that the (111) plane of the light-etching aluminum-rich alpha phase is oriented parallel to the sheet surface, and the sixfold symmetry of the face-centered-cubic (111) plane is evident in Fig. 4. Dark-etching zinc-rich alloy with an average composition of about 22 weight percent aluminum fills the spaces between the secondary branches of the alpha-phase dendrites.

A cross section of steel coated with 55 weight percent aluminum-zinc, Fig. 5, again shows the alpha-phase dendrites and a network of interdendritic zinc-rich alloy. Scattered particles of silicon are also present in the overlay. The coating is bonded to the steel substrate with a thin intermetallic layer comprised of about 48 weight percent aluminum, 24 weight percent iron, 14 weight percent zinc, and 11 weight percent silicon. X-ray diffraction of the intermetallic layer gives lines which are similar to the intermetallic compound $Al_{13}Fe_4$.[3] Based on the chemical analysis we believe that zinc atoms are substituted for about one-third of the iron atoms in the

---

[3] Card file no. 2-1213, *Inorganic Index to the Powder Diffraction File*, Joint Committee on Powder Diffraction Standards, Swarthmore, Pa., 1974, p. 282.

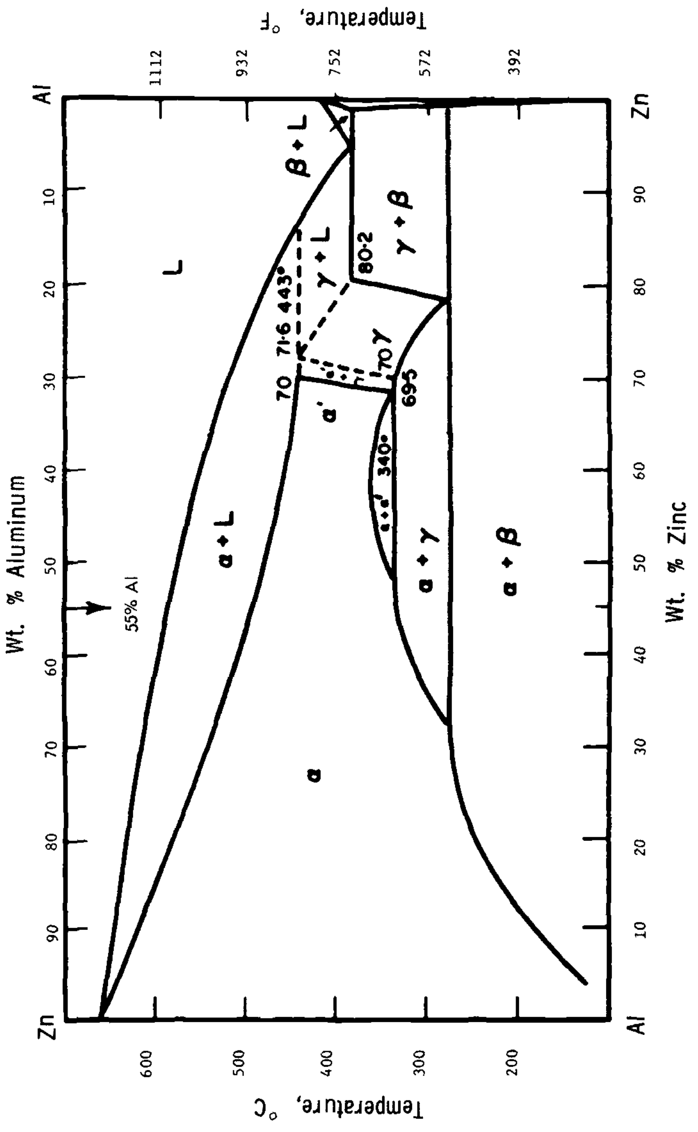

FIG. 3—Phase diagram of aluminum-zinc system.

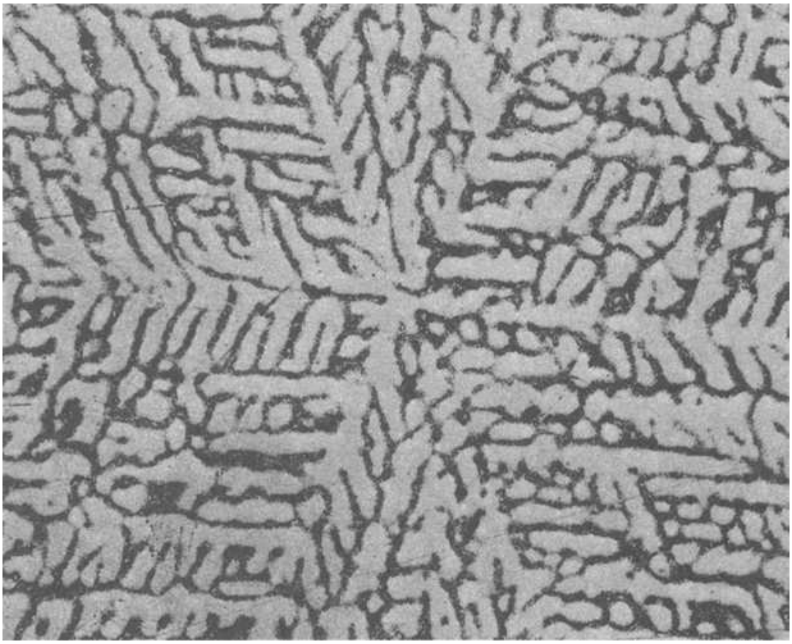

FIG. 4—*Dendritic structure of 55 weight percent aluminum-zinc coating viewed normal to sheet surface at approximate midthickness of coating* (×200, *amyl-nital etch*).

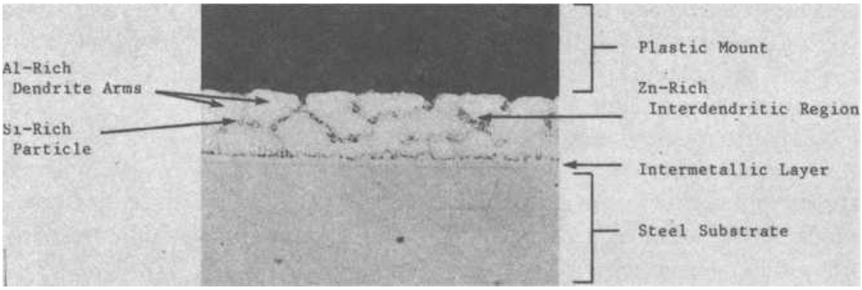

FIG. 5—*Random cross section of a 55 weight percent aluminum-zinc coating* (×500, *amyl-nital etch*).

$Al_{13}Fe_4$ lattice. Electron probe and ion microprobe analyses indicate that most of the silicon associated with the intermetallic layer is concentrated at the overlay/intermetallic layer interface.

Atmospheric Corrosion Resistance of 55 Weight Percent Aluminum-Zinc Alloy-Coated Sheet

After an 11-year exposure in the four environments the 55 weight percent aluminum-zinc alloy-coated, galvanized, and aluminum-coated panels 0.43 to 0.64 cm (0.017 to 0.025 in.) thick had typically the appearance seen in Fig. 6. Before describing the condition of the surfaces in detail, we should note that the small, localized discolorations at the vertical edges of some specimens were points which contacted ceramic insulators.

Severe Marine Atmosphere, 24-m (80-ft) lot—The galvanized coating, which had started to rust after a 4-year exposure, is now heavily rusted. In contrast, panels with 55 weight percent aluminum-zinc and 50.8-μm (2-mil) aluminum coatings are still in good condition, although some corrosion products are starting to creep inward on the faces of panels from cut edges.

Visual inspection of the cut edges show that the 55 weight percent aluminum-zinc panels have slight rust on the cut edges, whereas the galvanized specimens and the 50.8-μm (2-mil) aluminum-coated specimens have considerably more rust.

Marine Atmosphere, 245-m (800-ft) lot—All three types of coatings are still in good condition. Although not visible in the photograph, the cut edges of the aluminum-coated sheets have considerable rust.

Industrial Atmosphere—Most of the galvanized coating has been corroded away and more than ¾ of the steel surface is rusted. The aluminum-zinc and aluminum-coated panels exhibit superficial light-brown oxide stain due to particulate fallout from nearby steelmaking operations, but are otherwise in good condition.

Rural Atmosphere—All three materials are in good condition, but there is some rust staining apparent along the edges of the 50.8-μm (2-mil) aluminum-coated panels.

Observations of cut edges throughout the test period showed that in all but the severe marine atmosphere the galvanized coating provides the best galvanic protection against rust staining from cut edges, followed by the 55 weight percent aluminum-zinc coating, with the aluminum coating providing little or no galvanic protection.

Figures 7 to 10 are the corrosion-time curves for these same three materials after 9 years' exposure. In order to facilitate a comparison of the corrosion resistance of a 55 weight percent aluminum-zinc coating with that of a conventional galvanized coating, we calculated the ratio of the average corrosion rates for the two coatings as shown in Table 2. For each material, the average corrosion rate was determined by dividing the total corrosion loss by the longest exposure time shown in Fig. 7 to 10.

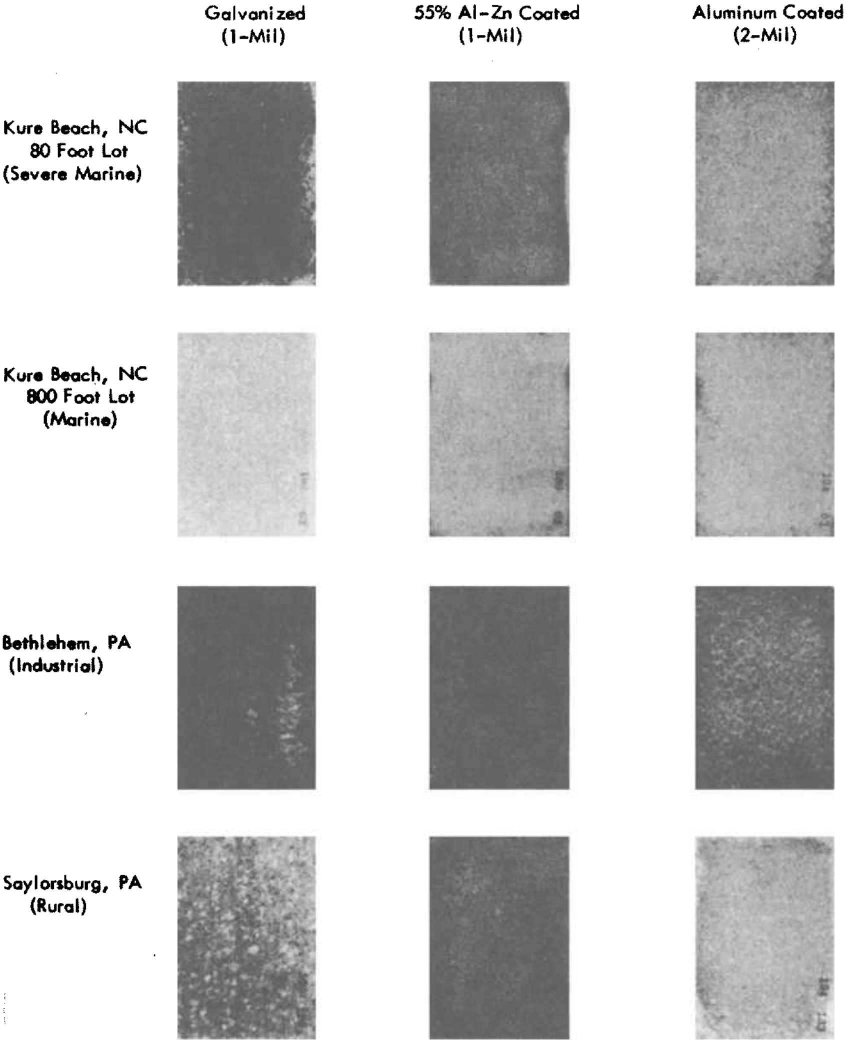

FIG. 6—*Appearance of galvanized, aluminum-coated, and aluminum-zinc-coated steels after an 11-year exposure in the atmosphere (skyward surface). (1 mil = 25.4 μm; 1 ft ~ 0.305 m)*

TABLE 2—*Ratios of average corrosion rates of 55 weight percent aluminum-zinc coating and conventional galvanized coating.*

Site	Ratio of Average Corrosion Rates Galvanized: 55 w/o Al-Zn
Kure Beach, N.C., 24-m (80-ft) lot	3.5:1
Kure Beach, N.C., 245-m (800-ft) lot	2.2:1
Saylorsburg, Pa.	2.9:1
Bethlehem, Pa.	5.3:1

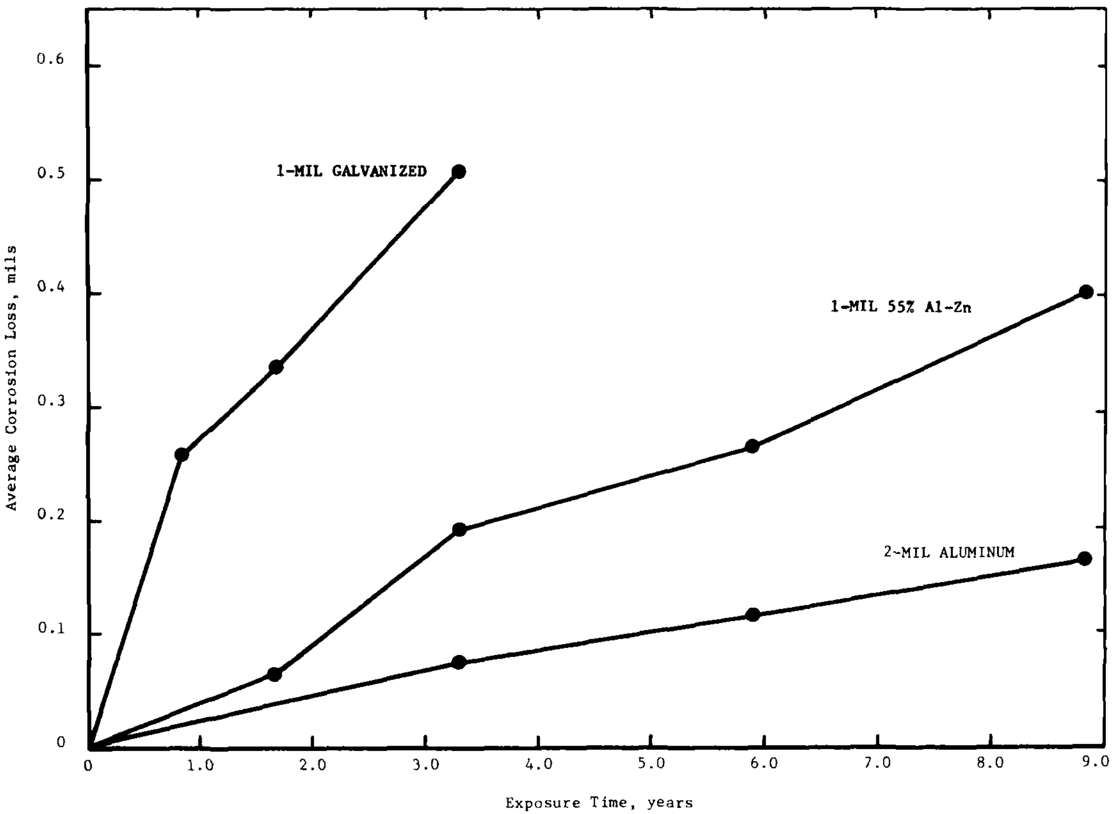

FIG. 7—*Corrosion performance of galvanized, aluminum-coated, and aluminum-zinc-coated steels in severe marine atmosphere (Kure Beach, 24-m [80-ft] lot). (1 mil = 25.4 μm)*

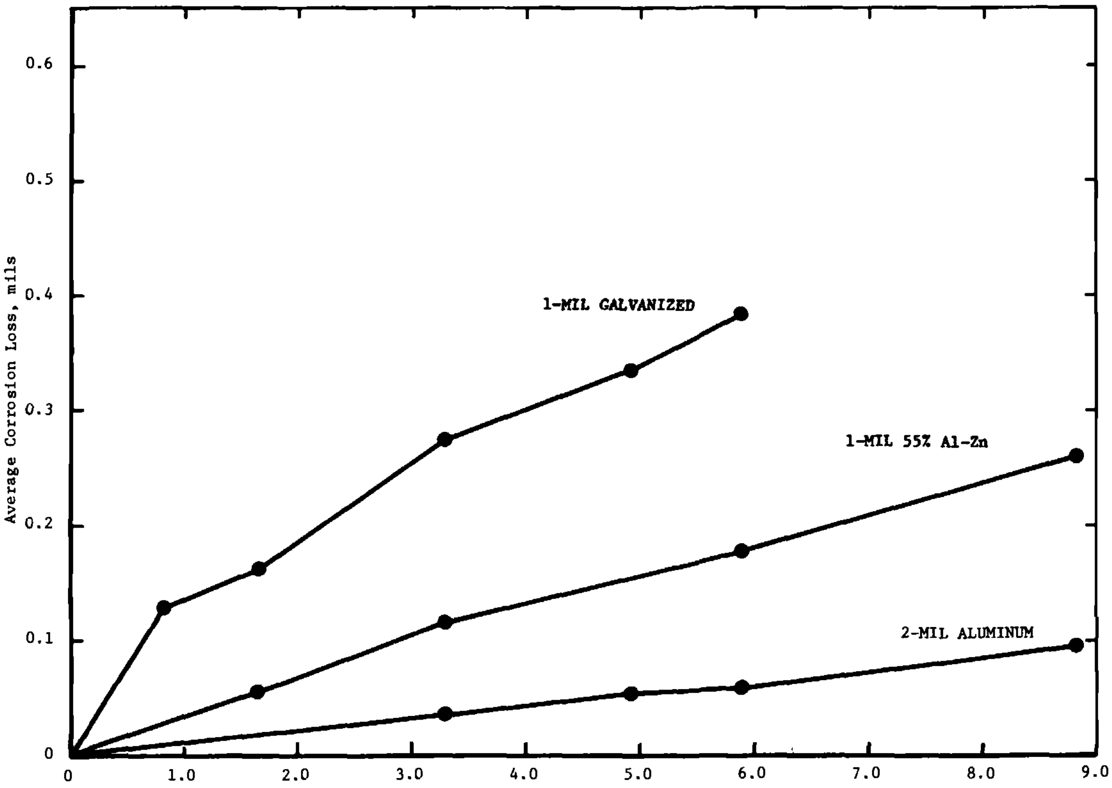

FIG. 8—*Corrosion performance of galvanized, aluminum-coated, and aluminum-zinc-coated steels in marine atmosphere (Kure Beach, 245-m [800-ft] lot). (1 mil = 25.4 μm)*

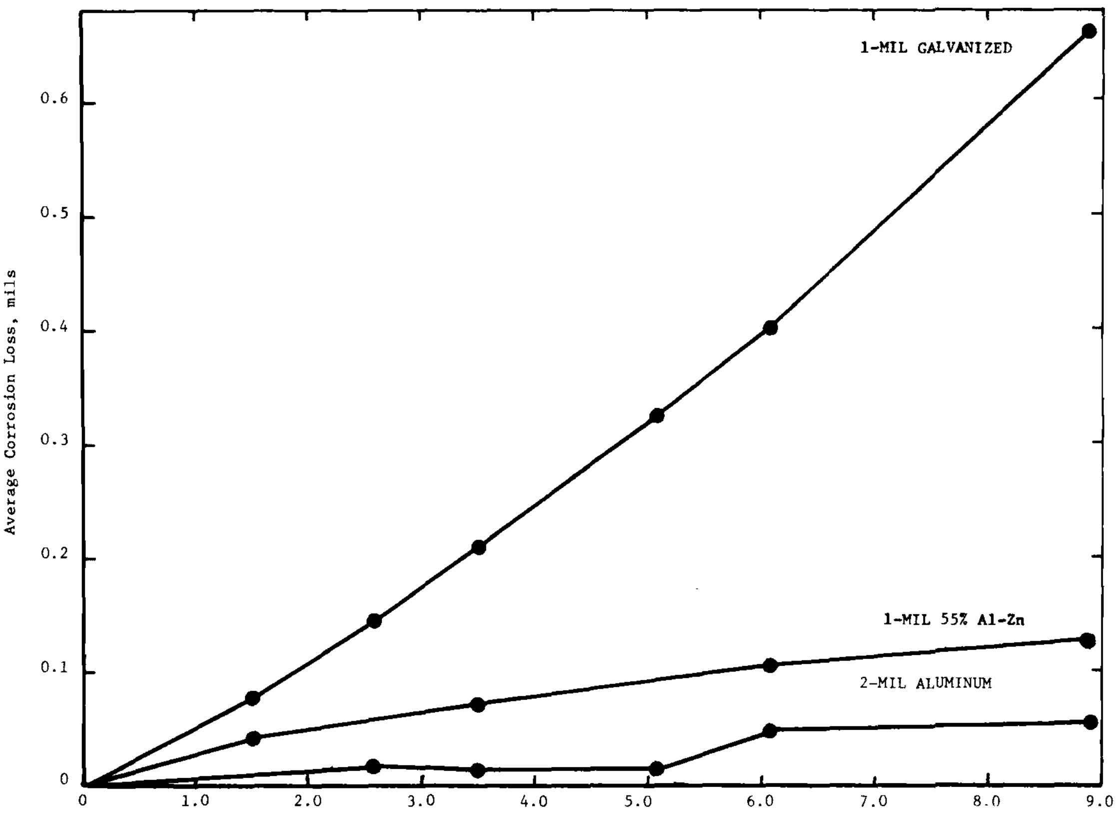

FIG. 9—*Corrosion performance of galvanized, aluminum-coated, and aluminum-zinc-coated steels in industrial atmosphere (Bethlehem, Pa.). (1 mil = 25.4 μm)*

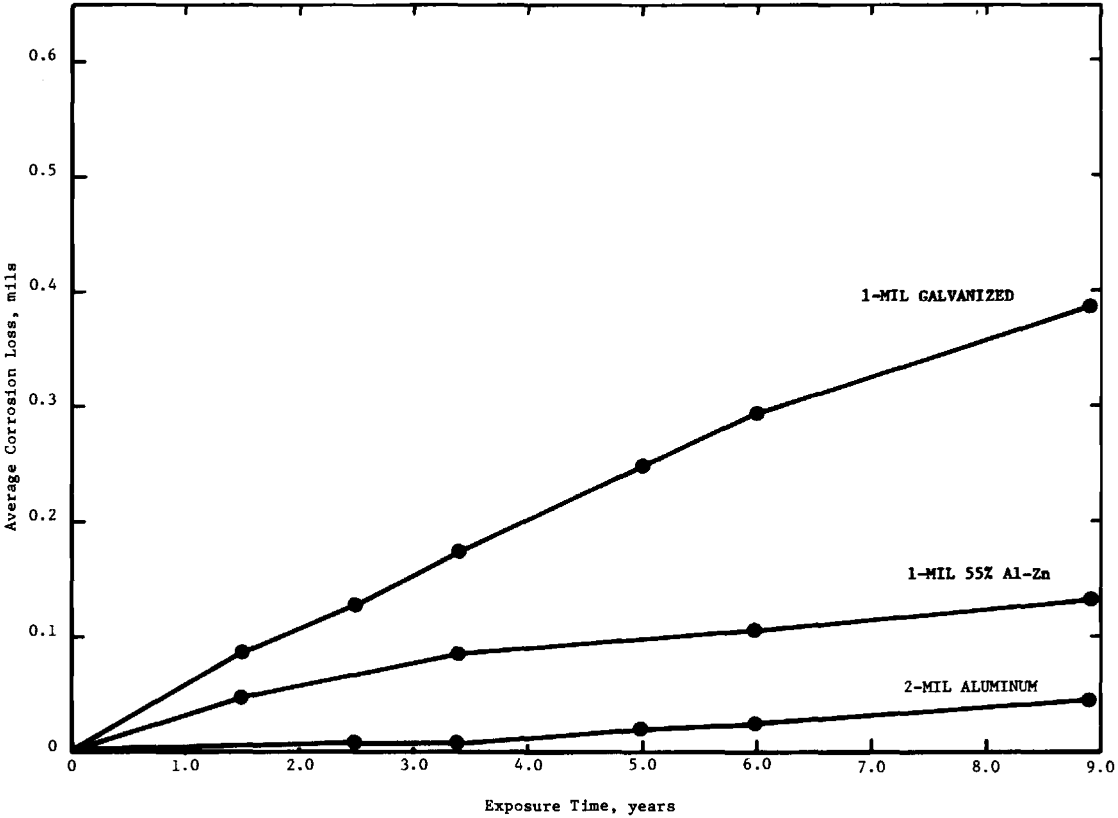

FIG 10—*Corrosion performance of galvanized, aluminum-coated, and aluminum-zinc-coated steels in rural atmosphere (Saylorsburg, Pa.). (1 mil = 25.4 μm)*

Thicknesses of commercially available coatings are typically 23 μm (0.9 mil) for G90 galvanized and 20 μm (0.8 mil) for 55 weight percent aluminum-zinc. Accordingly, we can predict that the commercially available 55 weight percent aluminum-zinc coating will outlast G90 galvanized by at least two to four times in a wide range of atmospheric environments.

The concentration of zinc in that part of the coating which has corroded (Fig. 11), is initially about 90 weight percent and decreases with time. In the rural and industrial environments, the composition of the corroded phase seems to level off after 9 years at roughly 80 weight percent zinc, while in the marine environments it continues to decrease.

Atmospheric Corrosion Mechanism

The results of the atmospheric corrosion testing, now going into the twelfth year, have demonstrated that the 55 weight percent aluminum-zinc alloy coating has excellent corrosion resistance. On the basis of these results, the commercial 20 μm (0.8-mil), 55 weight percent aluminum-zinc alloy coating is expected to last at least two to four times as long as the G90 galvanized coating (about 23 μm [0.9 mil]) in most atmospheres, and be more effective than the aluminum coating in resisting rust stain at cut edges. To account for the exceptionally good performance of the 55 weight percent aluminum-zinc coating it is useful to consider the mechanism and morphology of the corrosion process.

The time dependence of corrosion potential for 55 weight percent aluminum-zinc coatings exposed to laboratory chloride or sulfate solutions is shown schematically in Fig. 12. Subsequent to first immersion (Stage 1), the coating exhibits a corrosion potential close to that of a zinc coating exposed under identical conditions, generally about −1.0 to −1.1 V saturated calomel electrode (SCE). During Stage 1, the zinc-rich portion of the coating dissolves preferentially and the coating, like zinc, is anodic to steel. Stage 1 persists until the zinc-rich interdendritic portion of the coating is consumed, the exact time depending upon the thickness of the coating (mass of available zinc) and the severity of the environment (rate of zinc corrosion). Following depletion of the zinc-rich fraction, the corrosion potential rises and approaches that of an aluminum coating, generally about −0.7 V (SCE). During this period (Stage 2), the coating behaves like an aluminum coating, passive in sulfate environments, but anodic to steel in chloride environments.

Behavior of the 55 weight percent aluminum-zinc coating during atmospheric exposure appears to proceed in a manner analogous to that observed in laboratory solutions, although the time scale is greatly extended. We observe that the zinc-rich interdendritic portion of the coating corrodes preferentially as evidenced by the composition of the corroded phase, Fig. 11. During this period, the coating is sacrificial to steel and cut edges

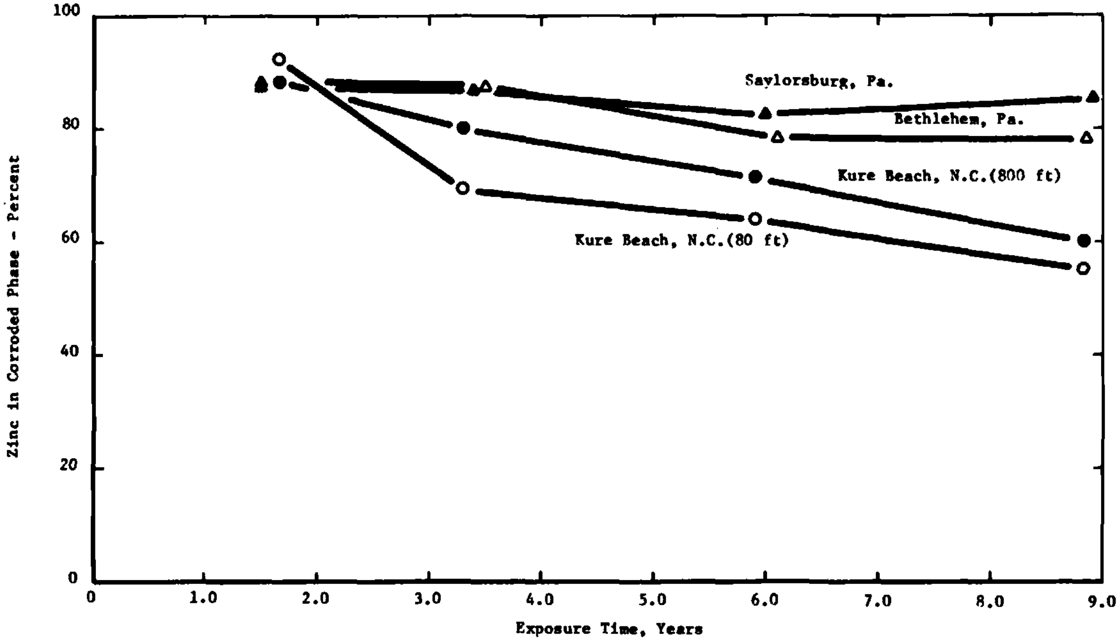

FIG. 11—*Zinc content of the corroded portion of 55 weight percent aluminum-zinc coatings for various atmospheres. (1 ft ~ 0.305 m)*

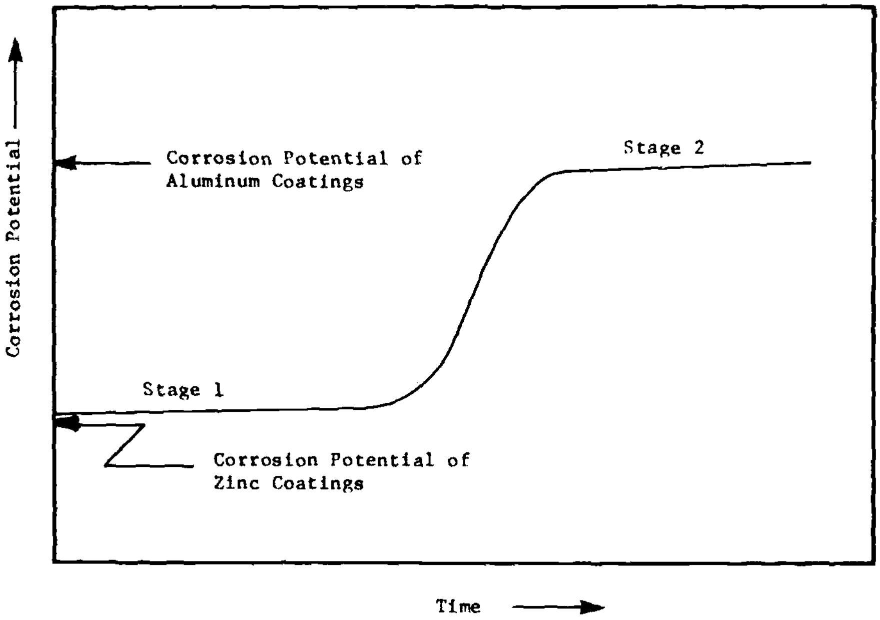

FIG. 12—*Schematic time dependence of corrosion potential of 55 weight percent aluminum-zinc coating in aqueous solution.*

of light-gage, coated steel sheet are galvanically protected. The initial overall rate of corrosion of the aluminum-zinc coating is less than that of a galvanized coating because of the relatively small area of exposed zinc.

As the zinc-rich portion of the coating is gradually corroded, the interdendritic interstices are filled with zinc corrosion products. The coating is thus transformed into a composite comprised of an aluminum-rich matrix with zinc corrosion products mechanically keyed into the interdendritic labyrinth. The zinc corrosion products should offer continued protection as a physical barrier to the transport of corrodents. In addition, as others have reported [*12*], these products may act as a cathodic inhibitor by providing continued protection at cut edges, as they are gradually leached from the coating. The decreasing corrosion rates with time in the rural and industrial environments, Figs. 9 and 10, appear to reflect a gradual change from active, zinc-like to passive, aluminum-like behavior.

The intermetallic layer is generally cathodic to the steel substrate as well as to the other components of the coating. Accordingly this layer appears to function as a barrier which prevents corrosion of the steel substrate subsequent to interdendritic corrosion of the overlay.

Conclusions

1. Of the 0 to 70 weight percent aluminum-zinc alloy coatings, the 55

weight percent coating has the best combination of salt-spray and atmospheric corrosion resistance.

2. The general corrosion resistance of the 55 weight percent aluminum-zinc alloy coating is superior to that of galvanized. Specifically, the commercial 20 μm (0.8-mil) 55 weight percent aluminum-zinc alloy-coated product should last two to four times longer than conventional galvanized of about the same coating thickness—20 μm (0.9 mil).

3. In all but the severe marine atmosphere, the best galvanic protection for cut edges is provided by the galvanized, with the 55 weight percent aluminum-zinc coating following, and the aluminum coating providing little or no protection.

To sum up, since the 55 weight percent aluminum-zinc alloy coating combines some of the best properties of both galvanized and aluminum coatings, it is inherently of great commercial importance as a new type of protective metallic coating for a wide range of sheet and other steel products.

Acknowledgment

The authors want to thank the Bethlehem Steel Corporation for permission to publish these results, the management of the Homer Research Laboratories (D. J. Blickwede, J. W. Frame, E. H. Mayer, G. F. Melloy, and J. E. Crowley) for their support and encouragement during critical periods in the development of this new material, L. Allegra and H. J. Cleary for their assistance in developing the fundamental relationships between processing, microstructure, and properties that contribute to our understanding and control of the product, numerous co-workers who have so freely given their time and effort to this development, and B. S. Mikofsky, technical editor, for his valuable assistance in the preparation and editing of our manuscript.

References

[1] Slunder, C. J. and Boyd, W. K. in *Zinc: Its Corrosion Resistance,* Zinc Institute, New York, 1971, Fig. 2.25.

[2] Kodeker, W., Peters, W., and Friehe, W., *Stahl und Eisen,* Vol. 81, 28 Sept. 1961, pp. 1313-1321.

[3] Gittings, D. O., Rowland, D. H., and Mack, J. O., "Effect of Bath Composition on Aluminum Coatings on Steel," *32nd Annual Convention of the American Society for Metals,* Chicago, Ill., 21-27 October 1950.

[4] Roe, W. P., "Improved Galvanized Coatings Through New Zinc Alloys," presented at 56th Meeting of the Galvanizer's Committee, San Francisco, Calif., 12 Oct. 1967.

[5] Sebisty, J. J. and Palmer, R. H., *Proceedings,* 6th International Conference on Hot Dip Galvanizing, Interlaken, June 1961, Zinc Development Association, London, June 1961, pp. 215-263.

[6] Wehr, E. R. and Mahlie, C. C., U.S. Patents 1,741,388 Dec. 1929, and 1,764,132 June 1930.

[7] Bablik, H., *Galvanizing (Hot-Dip),* E. & F. N. Spen Ltd., London, 34th Edition, 1950, pp. 204-223.

[*8*] Stanners, F., "Protecting Steel by Sprayed Metal Coatings," *Proceedings of Industrial Finishes Convention of First International Industrial Finishes Exhibition,* London, 8-11 May 1961.

[*9*] Hoar, T. P., *International Science and Technology,* Dec. 1963, pp. 78-85.

[*10*] Hoar, T. P. and Radovici, O., *Transactions of the Institute of Metal Finishing,* Vol. 41, 1964, pp. 88-95.

[*11*] Presnyakov, A. A., Gorban, Yu. A., and Chervyakova, V. V., *Zhurnal Fizicheskoi Khimii,* 1961, Vol. 35, No. 6, p. 1289.

[*12*] Evans, U. R. in *Metallic Corrosion, Passivity and Protection,* Edward Arnold and Son, London, Second Edition, 1946, p. 536.

Robert Baboian,[1] Gardner Haynes,[1] and Peter Sexton[2]

Atmospheric Corrosion of Laminar Composites Consisting of Copper on Stainless Steel*

REFERENCE: Baboian, Robert, Haynes, Gardner, and Sexton, Peter, "**Atmospheric Corrosion of Laminar Composites Consisting of Copper on Stainless Steel,**" *Atmospheric Factors Affecting the Corrosion of Engineering Metals, ASTM STP 646,* S. K. Coburn, Ed., American Society for Testing and Materials, 1978, pp. 185-203.

ABSTRACT: Atmospheric corrosion of laminar composites consisting of copper on stainless steels has been studied through direct exposure of copper-clad ferritic and austenitic stainless steels to provide information on galvanic effects at cut edges and pores in the copper cladding. Qualitative and quantitative results after exposure for 7.5 years are presented and environmental effects are considered. Application of electrochemical techniques for predicting galvanically induced localized corrosion are discussed and related to environmental conditions and alloy composition. Mechanisms for galvanic pitting and crevice corrosion are correlated with service performance of the copper-stainless steel couples.

KEY WORDS: corrosion, atmospheric corrosion, galvanic corrosion tests, copper, laminates, stainless steels, crevice, pitting

Copper has been used as an architectural sheet metal for many years, due to its inherent resistance to atmospheric corrosion and formation of an aesthetically pleasing layer of corrosion products (patina). In recent years, laminar composites consisting of copper on stainless steel have been used widely since they combine the surface properties of copper with the mechanical advantages of the stainless steel substrate. Although a substantial amount of data has been reported for atmospheric corrosion of copper, little information is available on the atmospheric corrosion of copper

---

*Original experimental data were measured in U.S. customary units.

[1] Manager and engineer, respectively, Electrochemical and Corrosion Laboratory, Texas Instruments Inc., Attleboro, Mass. 02703.

[2] Engineer, Research Laboratories, Allied Chemical Corp., Morristown, N.J. 07960.

clad stainless steels. This investigation was conducted to provide information on galvanic effects with the stainless steel substrates and to correlate the atmospheric corrosion of copper with that of the copper-clad stainless steels.

Corrosion of Copper

It has been established that depending on location it takes from 4 to 7 years for the initial development of the characteristic green patina on copper, with intermediate colors from brown to black having been reported [*1-4*].[3] The dark surface existing before the development of the patina is believed to be cuprite (Cu_2O) [*5*]. Basic copper carbonate is present only in small amounts in all environments and basic copper chloride predominates in marine atmospheres, while basic copper sulfate predominates in industrial environments.

Thompson has reported corrosion rates of 1.88 μm (0.0739 mils) per year after 2 years' exposure and 1.45 μm (0.0569 mils) per year after 7 years for tough-pitch copper at industrial Newark, New Jersey [*1*]. He also reported rates of 1.25 μm (0.0494 mils) per year after 2 years and 0.75 μm (0.0294 mils) per year after 7 years for tough-pitch copper at rural State

TABLE 1—*Weight loss data for 20-year exposure of phosphorized commercial copper (99.9+ copper, 0.007% phosphorus).*

Location	Weight Loss, g	Average Change Weight, %	Average Corrosion Rate: Mils Per Year[a]	Average Corrosion Rate: Milligrams Per Square Decimetres Per Day
Altoona, Pa. industrial	32.88 33.30	−6.0	0.0515	0.32
New York City industrial	31.19 31.20	−5.6	0.0476	0.30
Sandy Hook, N.J. semi-industrial-marine				
Key West, Fla. marine	12.42	−2.2	0.0198	0.12
La Jolla, Calif. marine	31.64 33.39	−5.6	0.0562	0.35
State College, Pa. rural	9.12 9.21	−1.7	0.0143	0.09
Phoenix, Ariz. arid	2.02 2.10	−0.4	0.0034	0.02

[a] 1 mil = 25.4 μm.

---

[3] The italic numbers in brackets refer to the list of references appended to this paper.

College, Pennsylvania. Table 1 shows the results reported by Copson for 20-year exposure at various test sites [*2*]. These rates represent an average value of penetration per year based on weight loss over the entire exposure period. These values do not represent the actual corrosion rate at the end of the 20th year. For example, the corrosion rate of phosphorized copper at Altoona, Pennsylvania, is listed as 1.31 μm (0.0515 mils) per year, yet the actual corrosion rate at the end of the 20-year period is much lower.

The influence of exposure time on the penetration rate of copper under atmospheric exposure was investigated by retrieving portions of copper roofing material from existing structures. Two specimens were studied: One which was in service for 22 years at Bell Laboratories, Murray Hill, New Jersey, and another exposed for 65 years at Montgomery County Courthouse, Norristown, Pennsylvania. Both areas are industrial environments and each specimen had a portion at one end which was covered with solder.

A comparison of the exposed and protected copper thickness was made by metallographic analysis. Representative photomicrographs are shown in Fig. 1. A traveling microscope at a magnification of 400 × was used to measure: (*a*) the original thickness of the copper encased in solder, (*b*) the thickness of the copper in the areas which had solder on the underside only, and (*c*) the thickness of the totally exposed copper.

The surface of all weathered areas was found to be fairly uniform on both specimens after five readings had been taken at intervals of 1.27 μm (0.050 mils.). The arithmetic mean of these five readings was used to calculate penetration or thickness loss. By comparing the average thickness of the unsoldered areas with the thickness of the areas that had solder on the unexposed side, it was determined that corrosion of the unexposed side of the copper roofing was negligible. Since the specimen exposed for 22 years included material from both sides of the soldered joint, a separate determination of the corrosion rate was made for each side. The results of these measurements are listed in Table 2.

The results show a marked reduction in average penetration (μm [mils] per year) from 22 to 65 years' exposure. Notice that after 65 years exposure the average penetration rate of copper is extremely low, 0.43 μm (0.017 mils) per year, and the total penetration is only 29.2 μm (1.15 mils). The value of 1.27 μm (0.050 mils) per year after 22 years in Sandy Hook, New Jersey is very close to the 20-year value of 1.22 μm (0.048 mils) per year found in New York City (Table 1).

The reduction in rate of penetration of copper with exposure time is probably due to the formation of adherent corrosion products on the surface. After initial development of the patina, it becomes more dense with continued exposure, thus providing a thicker, more protective coating. Figure 2 provides scanning electron microprobe photographs of the patina on specimens of copper roofing that had weathered 22 years in Murray Hill and 65 years on the Montgomery County Courthouse in Norristown. Note

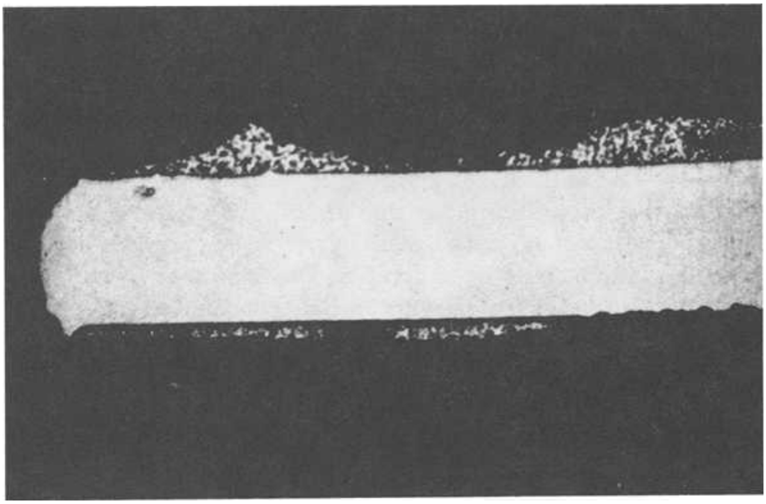

COPPER PROTECTED BY SOLDER

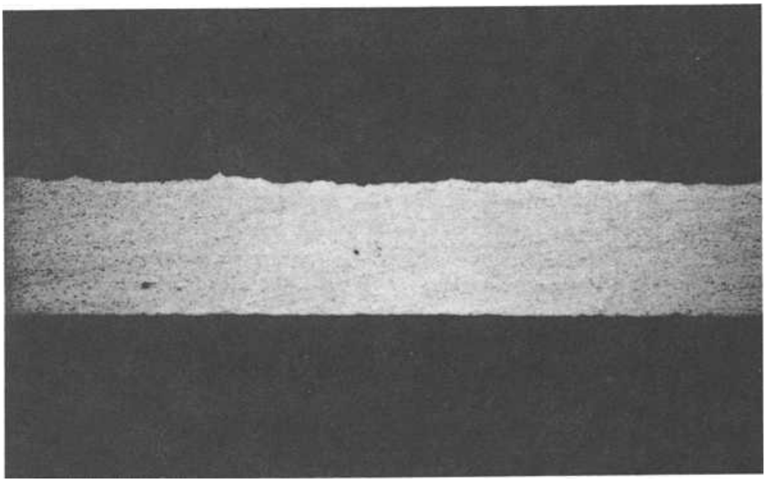

COPPER EXPOSED

FIG. 1—*Photomicrographs of cross sections (×50) of copper roofing material removed after 65 years' exposure at Norristown, Pa.*

TABLE 2—*Metallographic determination of corrosion rates of copper roofing specimens.*

Exposure Time and Location	Original Thickness (both sides soldered), mils[a]	Thickness of Unsoldered Area, mils[a]	Total Penetration, mils[a]	Average Corrosion Rate, mils per year[a]
22 years, Murray Hill, N.J.	22.40	21.30	1.10	0.050
22 years, Murray Hill, N.J.	18.50	17.40	1.10	0.050
65 years Norriston, Pa.	18.45	17.30	1.15	0.017

[a] 1 mil = 25.4 μm.

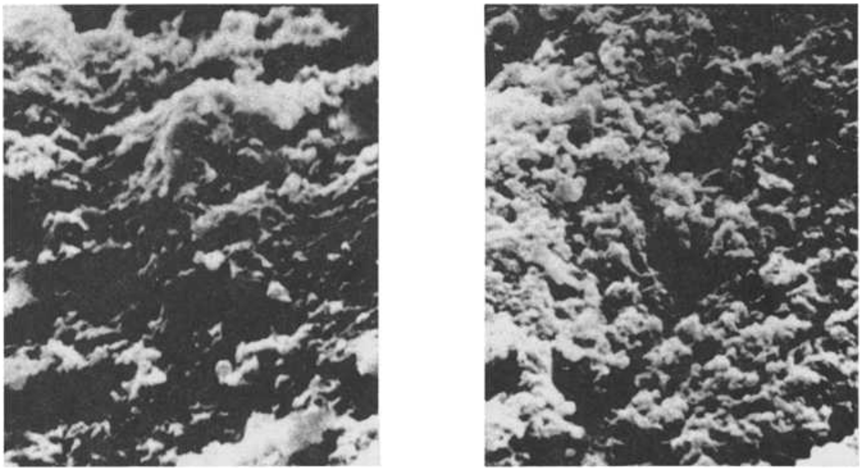

FIG. 2—*Scanning electron microprobe photographs* (×*10 000*) *of patina on copper surface. 22-year exposure* (left) *and 65-year exposure* (right).

that the longer exposure has produced a much denser corrosion product, indicating a more adherent and protective patina.

Plots of penetration versus exposure time can be constructed for copper in various environments. Based on field test exposure data, Fig. 3 provides a guide to the corrosion behavior of copper under coastal, rural-humid, and rural-dry conditions. More rapid penetration occurs in coastal environments; however, the rate is reduced after several years due to the formation of the protective patina.

The relatively low corrosion rate of copper in various atmospheric environments has led to the use of laminar composites such as copper-clad stainless steel [6]. This material combines the atmospheric corrosion resistance of copper with the mechanical properties of stainless steel.

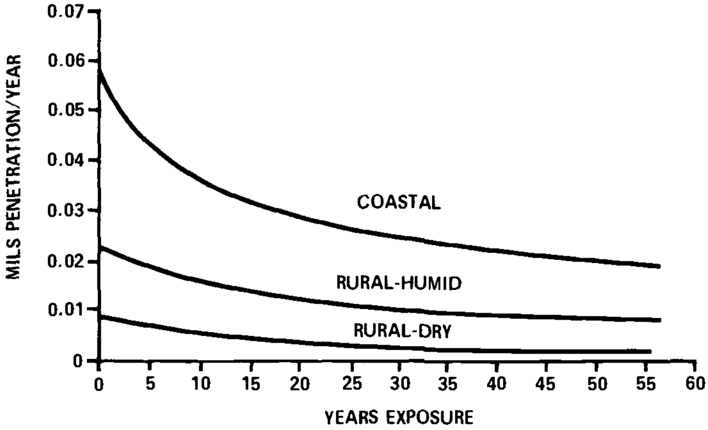

FIG. 3—*Corrosion of copper under atmospheric exposure (1 mil = 25.4 μm).*

It is the intent of this paper to provide information on the atmospheric corrosion properties of copper on stainless steel laminar composites and the galvanic effects at cut edges and pores in the copper cladding.

Atmospheric Test Procedures

Atmospheric corrosion and weathering characteristics of copper, stainless steels and copper-clad stainless steels were investigated by exposure of test panels at nine sites (Table 3) in the United States. A representative test rack at one of the atmospheric test sites is shown in Fig. 4.

TABLE 3—*Atmospheric test sites.*

Location	Type
Attleboro, Mass.	rural
Dallas, Tex.	urban industrial
Houston, Tex.	urban industrial
Anaheim, Calif.	rural
Miami, Fla. (inland)	marine
Miami, Fla. (coastal)	marine
Newark, N.J.	industrial
Kure Beach, 24-m (80-ft) lot	marine
Kure Beach, 245-m (800-ft) lot	marine

The 100 by 150-mm (4 by 6-in.) test panels were coded and marked by stamping. Each panel thickness was measured to the nearest 0.01 mm (0.001 in.) and the length and width were measured to the nearest 1 mm (0.1 in.).

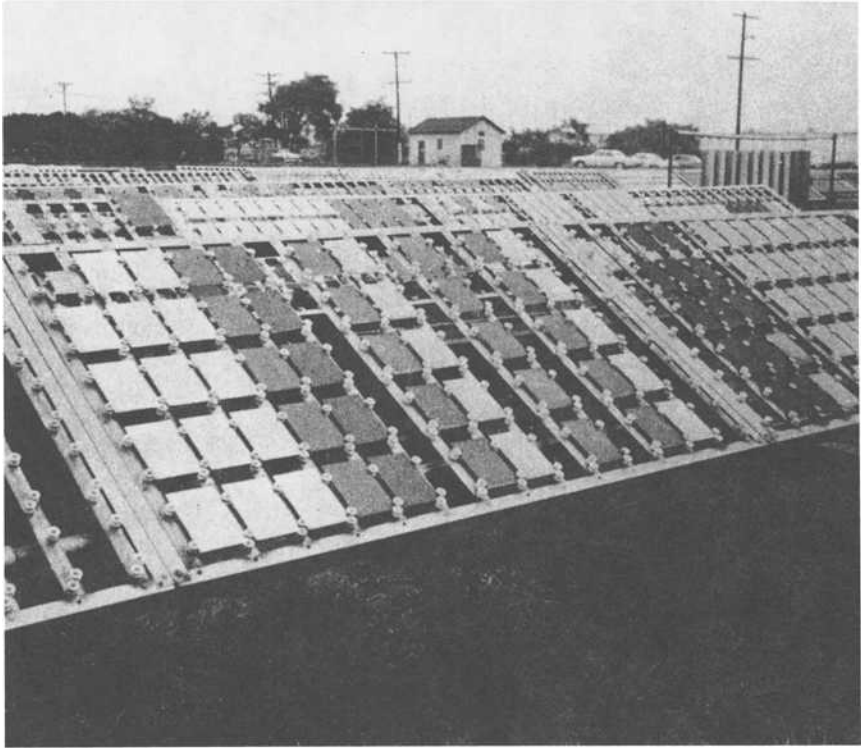

FIG. 4—*Representative test rack at atmospheric test site.*

The composition of each of the component materials was certified by the producer to be within the range specified in the ASTM Specification for Copper-Clad Stainless Steel Sheet and Strip for Building Construction (B 506-76). The copper-clad stainless steel laminates were fabricated by Texas Instruments Incorporated solid-phase roll bonding process. Cladding ratios in percent were 10/80/10 in all cases. Panels were vapor degreased and weighed prior to exposure. Multiple specimens were used at Attleboro, Massachusetts and Newark. Single specimens for each of the four time periods were used at the other sites.

After exposure, each panel was examined visually and rated for degree and type of corrosion using the 6-digit rating system which appears in Table 4. The first two digits (A and B) evaluate the bulk surface of the panels while the last four digits (C, D, E, F) rate the extent of galvanic corrosion at pores and exposed edges. The rating for tunneling (D) indicates the maximum distance of corrosion of the substrate from the exposed edge while the rating for delamination (F) indicates the distance of complete delamination of the copper cladding from the exposed edge.

TABLE 4—*Rating system for evaluation of atmospheric test panels.*

	Type of Corrosion		Ratings					
			0	1	2	3	4	5
Bulk surface	(A)	uniform	none	slight	moderate	heavy	very heavy	destruction
	(B)	pitting	none	few shallow pits	many shallow pits	few deep pits	many deep pits	destruction
Degree of galvanic attack at edges and pores	(C)	galvanic pitting	none	at identification stamp	1 to 2	3 to 5	6 to 20	destruction
	(D)	edge corrosion	none	slight	moderate	heavy	very heavy	destruction
	(E)	tunneling	none	1/16 in.[a]	1/4 in.[a]	1/2 in.[a]	1 in.[a]	3 in.[a]
	(F)	delamination	none	1/16 in.[a]	1/4 in[a]	1/2 in.[a]	1 in[a]	3 in.[a]

[a] 1 in. = 2.54 cm.

After visual evaluation each panel was cleaned and weighed. Weight changes were obtained for copper, stainless steels and the copper-clad stainless steel laminates after 0.5, 1.5, 3.5, and 7.5-year exposures.

Results

Copper

The weight losses and ratings for monolithic copper over the four exposure periods are listed in Table 5. Only the first two digits (A and B) are shown in the rating since the other four factors contributing to galvanic effects were not present. Uniform corrosion of copper occurs as indicated by the ratings. The weight losses are converted to penetration rates in Table 6. These data show that the penetration rate decreases with increasing exposure time at all of the test sites. Note that the penetration rates at the end of the 7.5-year exposure agree with values for similar environments reported by other investigators [*1*–*5*] (see Table 1).

Stainless Steels

The monolithic stainless steels included in this study are AISI Types 409, 430, and 321 stainless steels. The weight change data and ratings for the stainless steels for 3.5 and 7.5-year exposures are listed in Table 7. Shallow pitting occurred at all sites on Type 409 and at all sites except Newark on Type 430. Shallow pits were found on Type 321 at marine sites only. Weight changes were extremely small and were therefore not converted to corrosion rates due to the localized nature of corrosion.

Copper-Stainless Steel Laminates

The copper-clad stainless steel laminates in this study were composed of copper clad to both sides of stainless steel Types 409, 430, and 321. The weight loss data and ratings for these materials are listed in Tables 8 through 10. Since galvanic corrosion of the substrate (stainless steels) in the laminates can occur, weight losses can be misleading and should only be used in conjunction with the rating system. For example, the weight loss for copper-clad Type 409 at the Kure Beach 245-m (800-ft) lot is only one third the weight loss for monolithic copper (Table 5). However, as indicated by the 201330 rating, this reduction in weight loss is due to the entrapped corrosion product and does not, therefore, represent a lower overall corrosion rate. Weight losses cannot be converted to penetration rates for the copper-clad stainless steel laminates when the rating indicates that corrosion of the substrate has occurred.

TABLE 5—*Atmospheric corrosion behavior of copper.*

Site	0.5 Years		1.5 Years		3.5 Years		7.5 Years	
	Δ Weight, g	Rating, A B C D E F	Δ Weight, g	Rating, A B C D E F	Δ Weight, g	Rating, A B C D E F	Δ Weight, g	Rating, A B C D E F
Attleboro, Mass.	0.15	1 0 X X X X	0.45	2 0 X X X X	0.90	2 0 X X X X	1.52	2 0 X X X X
Dallas, Tex.	0.2	1 0 X X X X	0.10	1 0 X X X X	0.85	2 0 X X X X	1.00	2 0 X X X X
Houston, Tex.	0.2	1 0 X X X X	. . .	. . .	0.85	2 0 X X X X	. . .	. . .
Anaheim, Calif.	. . .	. . .	0.3	1 0 X X X X	0.45	2 0 X X X X	0.70	2 0 X X X X
Miami, Fla. (inland)	0.2	1 0 X X X X	0.2	1 0 X X X X	0.60	2 0 X X X X	0.72	2 0 X X X X
Miami, Fla. (coastal)	. . .	. . .	. . .	. . .	1.65	2 0 X X X X	2.40	2 0 X X X X
Newark, N.J.	. . .	. . .	0.55	2 0 X X X X	1.40	2 0 X X X X	2.00	2 0 X X X X
Kure Beach, 24-m (80-ft) lot	0.8	1 0 X X X X	1.1	2 0 X X X X	2.55	2 0 X X X X	3.10	2 1 X X X X
Kure Beach, 245-m (800-ft) lot	0.8	1 0 X X X X	1.1	2 0 X X X X	2.05	2 0 X X X X	3.10	2 1 X X X X

TABLE 6—*Corrosion rate of copper.*

Site	0.5 Years, mils per year[a]	1.5 Years, mils per year[a]	3.5 Years, mils per year[a]	7.5 Years, mils per year[a]
Attleboro	0.047	0.047	0.041	0.030
Dallas	0.062	0.01	0.038	0.020
Houston	0.062	...	0.038	...
Anaheim	...	0.031	0.020	0.014
Miami (inland)	0.062	0.02	0.027	0.015
Miami (coastal)	...	...	0.074	0.048
Newark	...	0.057	0.063	0.040
Kure Beach, 24-m (80-ft) lot	0.250	0.114	0.114	0.062
Kure Beach, 245-m (800-ft) lot	0.250	0.114	0.092	0.062

[a] 1 mil = 25.4 μm

Discussion

The two types of corrosion occurring on copper-clad stainless steel laminates were uniform corrosion of the copper cladding with no galvanic corrosion of the substrate, and uniform corrosion of the copper cladding with galvanic pitting and tunneling of the substrate. These types of corrosion are clearly demonstrated by the photomicographs of cross sections in Fig. 5 and have been described in detail previously [*7-9*].

The observed type of corrosion was found to be a function of the environment and the stainless steel substrate composition, or both. The 7.5-year exposure data listed in Table 11 show that in rural (Attleboro, Anaheim) and industrial (Houston, Newark) environments all of the copper-clad stainless steel laminates undergo uniform corrosion of the copper. Since the ratings show that no corrosion of the substrate occurs, the weight losses should be comparable to those for copper (Table 5) and the penetration rates should be similar.

In chloride-containing environments (Miami and Kure Beach, as well as Dallas, which contained chlorides resulting from industrial pollution) galvanically induced localized corrosion of the substrate occurs in copper clad Types 409 and 430, as indicated by the ratings in Table 11. Note that the weight losses differ substantially from those for monolithic copper due to the corrosion of the stainless steel substrate. Corrosion of the substrate in copper clad Type 321 does not occur in marine environments (Table 11). Thus, the weight loss data for copper clad Type 321 are similar to those for monolithic copper.

The attack observed on copper-clad Types 409 and 430 laminate can be attributed to galvanically induced localized breakdown of the passive film on the stainless steels in marine environments. Localized breakdown of the passive film on these stainless steels in chloride-containing solutions has been explained by polarization behavior [*7-12*]. Referring to the schematic polarization curve for stainless steel in sodium chloride in Fig. 6, the solid

TABLE 7—*Atmospheric corrosion behavior of stainless steels.*

Site	Type 409				Type 430				Type 321			
	3.5 Years		7.5 Years		3.5 Years		7.5 Years		3.5 Years		7.5 Years	
	Δ Weight, g	Rating, A B C D E F	Δ Weight, g	Rating, A B C D E F	Δ Weight, g	Rating, A B C D E F	Δ Weight, g	Rating, A B C D E F	Δ Weight, g	Rating, A B C D E F	Δ Weight, g	Rating, A B C D E F
Attleboro	0.1	0 2 X X X X	0.07	0 2 X X X X	0	0 1 X X X X	+0.04	0 1 X X X X	0	0 1 X X X X	+0.04	0 1 X X X X
Dallas	0.05	0 3 X X X X	0.02	0 2 X X X X	0	0 1 X X X X	+0.04	0 1 X X X X	0	0 1 X X X X	+0.04	0 1 X X X X
Houston	0.05	0 2 X X X X	0	0 2 X X X X	0	0 0 X X X X	0.01	0 0 X X X X	0	0 0 X X X X	0.01	0 0 X X X X
Anaheim	0	0 1 X X X X	0.01	0 2 X X X X	0	0 1 X X X X	+0.03	0 1 X X X X	0	0 1 X X X X	+0.03	0 1 X X X X
Miami (inland)	0.05	0 3 X X X X	0	1 2 X X X X	0	0 1 X X X X	+0.05	0 1 X X X X	0	0 1 X X X X	+0.05	0 1 X X X X
Miami (coastal)	0.05	0 4 X X X X	0.02	2 2 X X X X	0	0 2 X X X X	+0.02	0 2 X X X X	0	0 2 X X X X	+0.02	0 2 X X X X
Newark	0	0 3 X X X X	0.04	0 2 X X X X	0	0 0 X X X X	+0.01	1 0 X X X X	0	0 0 X X X X	+0.01	1 0 X X X X
Kure Beach, 24-m (80-ft) lot	0.2	1 2 X X X X	0.22	2 2 X X X X	0	0 2 X X X X	+0.01	1 2 X X X X	0	0 2 X X X X	+0.01	1 2 X X X X
Kure Beach, 245-m (800-ft) lot	0.05	1 2 X X X X	0.05	2 2 X X X X	0	0 2 X X X X	+0.06	0 2 X X X X	0	0 2 X X X X	+0.06	0 2 X X X X

TABLE 8—*Atmospheric corrosion behavior of copper-clad Type 409 stainless steel.*

Site	0.5 Years		1.5 Years		3.5 Years		7.5 Years	
	Δ Weight, g	Rating, A B C D E F	Δ Weight, g	Rating, A B C D E F	Δ Weight, g	Rating, A B C D E F	Δ Weight, g	Rating, A B C D E F
Attleboro	. . .	. . .	. . .	. . .	. . .		. . .	. . .
Dallas	. . .	. . .	0.4	1 0 0 0 0 0	0.8	2 0 0 2 1 0	0.97	2 0 0 2 2 0
Houston	. . .	. . .	0.3	1 0 1 1 0 0	0.8	2 0 0 2 2 0	. . .	. . .
Anaheim	0.25	1 0 0 0 0 0	0.25	1 0 0 0 0 0	0.45	2 0 0 0 0 0	0.70	2 0 0 0 0 0
Miami (inland)	0.2	1 0 0 0 0 0	0.25	1 0 0 1 2 0	0.45	2 0 1 2 2 0	0.66	2 0 1 2 3 0
Miami (coastal)	0.4	1 0 0 1 0 0	0.5	1 0 0 1 2 0	1.75	2 0 1 2 2 0	1.77	2 0 1 3 3 0
Newark	0.4	1 0 0 0 0 0	0.45	1 0 0 0 0 0	1.3	2 0 0 0 0 0	2.38	2 0 0 0 0 0
Kure Beach, 24-m (80-ft) lot	0.75	1 0 0 1 0 0	0.9	1 0 1 2 2 0	1.5	2 0 1 3 2 0	1.93	2 0 1 3 3 0
Kure Beach, 245-m (800-ft) lot	0.65	1 0 0 1 0 0	0.8	1 0 0 2 1 0	1.2	2 0 1 3 2 0	1.02	2 0 1 3 3 0

TABLE 9—*Atmospheric corrosion behavior of copper-clad Type 430 stainless steel.*

	0.5 Years		1.5 Years		3.5 Years		7.5 Years	
Site	Δ Weight, g	Rating, A B C D E F	Δ Weight, g	Rating, A B C D E F	Δ Weight, g	Rating, A B C D E F	Δ Weight, g	Rating, A B C D E F
Attleboro	0.4	1 0 0 0 0 0	0.4	2 0 0 0 0 0	0.8	2 0 0 1 0 0	1.4	2 0 0 1 0 0
Dallas	0.1	1 0 0 0 0 0	0.3	2 0 0 0 0 0	0.0	2 0 0 2 2 0	0.7	2 0 0 2 3 0
Houston	0.2	1 0 0 1 0 0	0.7	2 0 0 1 1 0	0.9	2 0 0 2 2 0	1.3	2 0 0 0 0 0
Anaheim	0.1	1 0 0 0 0 0	0.4	2 0 0 0 0 0	0.4	2 0 0 0 0 0	0.7	2 0 0 0 0 0
Miami (inland)	0.1	1 0 0 1 0 0	0.5	2 0 0 1 2 0	0.3	2 0 0 2 3 0	0.6	2 0 0 2 2 0
Miami (coastal)	0.3	1 0 0 2 1 0	0.6	2 0 1 2 3 0	0.5	2 0 2 3 4 1	0.5	2 0 0 3 4 3
Newark	0.2	1 0 0 0 0 0	0.7	2 0 0 0 0 0	1.3	2 0 0 0 0 0	2.4	2 0 0 0 0 0
Kure Beach, 24-m (80-ft) lot	0.5	1 0 0 1 0 0	0.9	2 0 1 2 2 0	0.9	2 0 1 3 3 1	0.6	2 0 1 3 3 0
Kure Beach, 245-m (800-ft) lot	0.5	1 0 0 1 0 0	1.0	2 0 1 2 2 0	1.2	2 0 1 2 3 0	1.4	2 0 0 2 3 0

TABLE 10—*Atmospheric corrosion behavior of copper-clad Type 321 stainless steel.*

	0.5 Years		1.5 Years		3.5 Years		7.5 Years	
Site	Δ Weight, g	Rating, A B C D E F	Δ Weight, g	Rating, A B C D E F	Δ Weight, g	Rating, A B C D E F	Δ Weight, g	Rating, A B C D E F
Attleboro	...	...	0.85	1 0 0 0 0 0	1.50	2 0 0 0 0 0	2.11	2 0 0 0 0 0
Dallas	0.20	1 0 0 0 0 0	0.40	1 0 0 0 0 0	1.00	2 0 0 0 0 0	1.33	2 0 0 0 0 0
Houston	0.20	1 0 0 0 0 0	0.60	1 0 0 0 0 0	1.00	2 0 0 0 0 0	1.41	2 0 0 0 0 0
Anaheim	0.20	1 0 0 0 0 0	0.30	1 0 0 0 0 0	0.45	1 0 0 0 0 0	0.69	2 0 0 0 0 0
Miami (inland)	0.20	1 0 0 0 0 0	0.35	1 0 0 0 0 0	0.45	1 0 0 0 0 0	0.81	2 0 0 0 0 0
Miami (coastal)	0.55	1 0 0 0 0 0	0.80	1 0 0 0 0 0	1.10	2 0 0 0 0 0	1.99	2 0 0 0 0 0
Newark	0.35	1 0 0 0 0 0	0.80	1 0 0 0 0 0	1.45	2 0 0 0 0 0	2.42	2 0 0 0 0 0
Kure Beach, 24-m (80-ft) lot	0.45	1 0 0 0 0 0	1.00	1 0 0 0 0 0	1.60	2 0 0 0 0 0	2.70	2 0 0 0 0 0
Kure Beach, 245-m (800-ft) lot	0.45	1 0 0 0 0 0	0.90	1 0 0 0 0 0	1.35	2 0 0 0 0 0	2.02	2 0 0 0 0 0

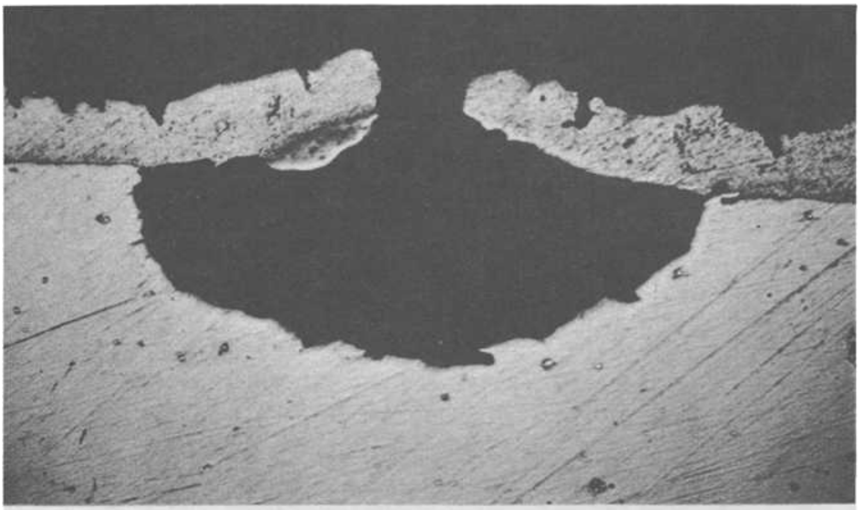

a, GALVANIC PITTING (250X)

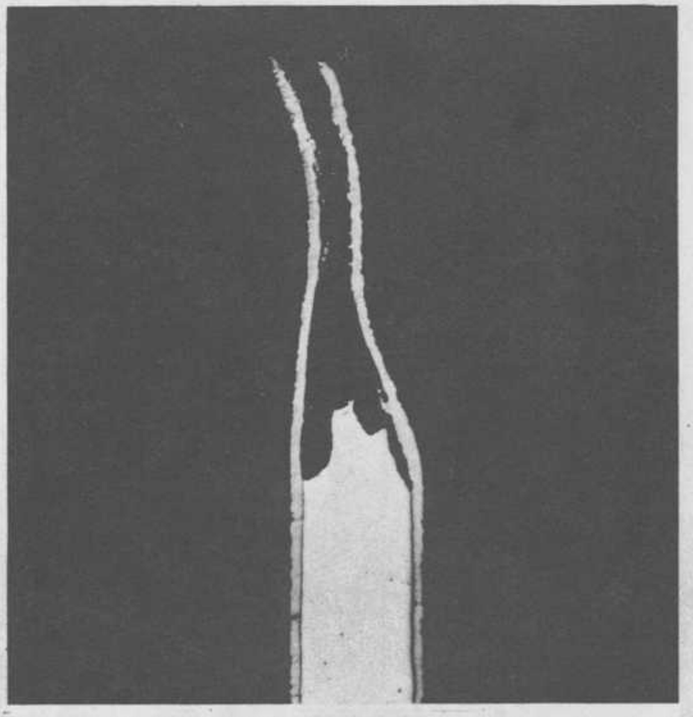

b, GALVANIC TUNNELING (50X)

FIG. 5—*Photomicrographs of cross sections showing corrosion behavior of copper-clad Type 409 stainless steel.*

TABLE 11—*Atmospheric corrosion behavior of copper-stainless steel laminates (7.5-year exposure).*

Site	Cu/409 SS/Cu							Cu/430 SS/Cu							Cu/321 SS/Cu						
	Δ Weight, g	Rating, A	B	C	D	E	F	Δ Weight, g	Rating, A	B	C	D	E	F	Δ Weight, g	Rating, A	B	C	D	E	F
Attleboro	...			...				1.43	2	0	0	1	0	0	2.11	2	0	0	0	0	0
Dallas	0.97	2	0	0	2	0	0	0.71	2	0	0	2	3	0	1.33	2	0	0	0	0	0
Houston	...			...				1.25	2	0	0	0	0	0	1.41	2	0	0	0	0	0
Anaheim	0.70	2	0	0	0	0	0	0.69	2	0	0	0	0	0	0.69	2	0	0	0	0	0
Miami (inland)	0.66	2	0	1	2	3	0	0.60	2	0	0	2	2	0	0.81	2	0	0	0	0	0
Miami (coastal)	1.77	2	0	1	2	3	0	0.44	2	0	0	2	4	3	1.99	2	0	0	0	0	0
Newark	2.38	2	0	0	0	0	0	2.37	2	0	0	0	0	0	2.42	2	0	0	0	0	0
Kure Beach, 24-m (80-ft) lot	1.93	2	0	1	3	3	0	0.57	2	0	1	2	3	0	2.70	2	0	0	0	0	0
Kure Beach, 245-m (800-ft) lot	1.02	2	0	1	3	3	0	1.40	2	0	0	2	3	0	2.02	2	0	0	0	0	0

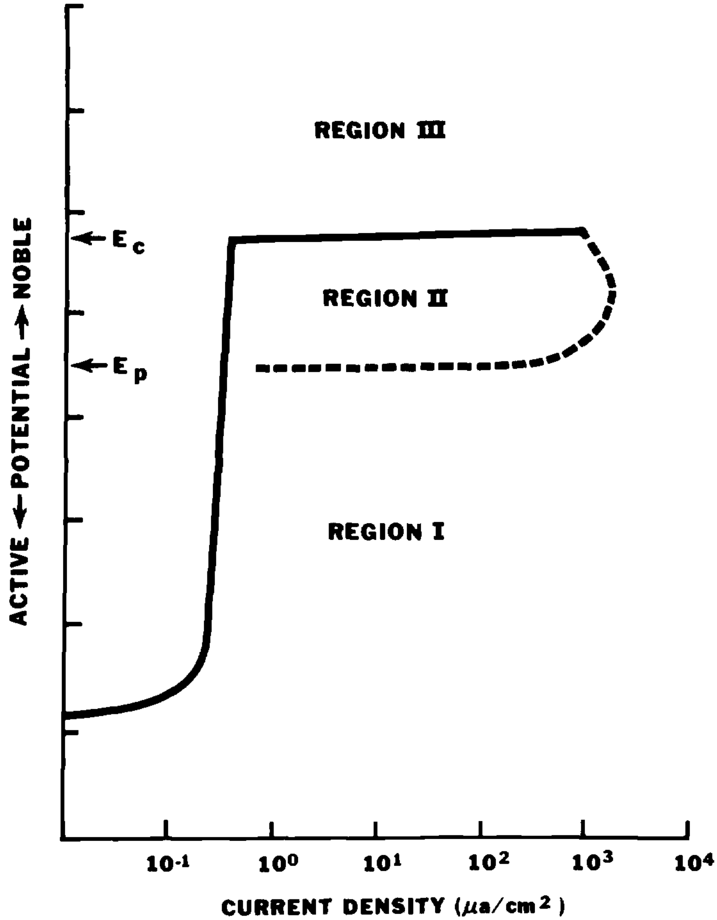

FIG. 6—*Schematic potentiodynamic polarization curve for stainless steel in 5 percent sodium chloride.*

line represents anodic potentiodynamic polarization from active to noble potentials. The dashed line represents reverse polarization back to more active potentials [*7,9*].

Polarization above the critical breakdown potential, E_c, results in a marked increase in current density due to initiation of pitting. Reverse polarization below E_c does not reduce the current density appreciably, indicating that propagation of existing pits and crevice corrosion occurs. At the critical protection potential, E_p, the current density approaches zero. Below E_p propagation of existing pits and crevice corrosion does not occur.

The corrosion behavior of stainless steels can therefore be separated into three potential regions: Region I, where protection from pit propagation and crevice corrosion is observed; Region II, where propagation of existing pits and crevice corrosion occurs; and Region III, where initiation of pitting and crevice corrosion occurs. This behavior is observed in oxygen-containing and oxygen-free electrolytes, as shown previously [7].

The atmospheric corrosion data for marine environments indicate that stainless steel Types 409 and 430 undergo localized corrosion in both monolithic and clad (with copper) configurations (Region II in their polarization curves). On the other hand, while Type 321 stainless steel pitted in the monolithic state, localized corrosion was not observed in the copper-clad laminate. Thus, Type 321 is protected from localized corrosion (Region I) in the copper-clad configuration.

Conclusions

The atmospheric corrosion rate of copper decreases with increasing exposure time due to the formation of a protective layer (patina) of corrosion products. Shallow pitting was observed on all monolithic stainless steels (Types 409, 430, and 321) in the marine atmospheres; the measured weight losses, however, were extremely small.

When localized corrosion of the substrate does not occur in copper-clad stainless steel laminates, the corrosion characteristics are similar to those of monolithic copper. In marine atmospheres, two types of corrosion of copper-clad stainless steel laminates occurred; galvanic tunneling at cut edges, and galvanic pitting at pores in the copper cladding. In rural and industrial environments penetration rates of copper-clad stainless steel laminates are similar to those of monolithic copper and the stainless steel substrates (Types 409, 430, and 321) remain passive. In chloride-containing environments copper-clad Types 409 and 430 are subject to galvanically induced localized corrosion of the substrate. Weight loss data for these couples can be misleading due to entrapped corrosion products and should only be used in conjunction with a rating system.

Although pitting of monolithic Type 321 stainless steel occurred in marine atmospheres, no localized corrosion of copper-clad Type 321 was observed in any of the atmospheres, and the penetration rate of the copper cladding was similar to that of copper.

References

[1] Thompson, D. H. in *Metal Corrosion in the Atmosphere, ASTM STP 435,* American Society for Testing and Materials, 1968, pp. 132–133.

[2] Copson, H. R., "Report of Subcommittee VI, of Committee B-3, On Atmospheric Corrosion," presented at the Symposium on Atmospheric Corrosion of Nonferrous Metals, ASTM Annual Meeting, Atlantic City, 29 June 1955.

[3] Tracy, A. W. in *Symposium on Impact Testing, ASTM STP 175,* American Society for Testing and Materials, 1956, pp. 67–76.

[4] Scholes, I. R. and Jacobs, W. R., *Journal of the Institute of Metals,* Vol. 98, 1970, p. 272.

[5] Mattsson, E. and Holm, R. in *Metal Corrosion in the Atmosphere, STP 435,* American Society for Testing and Materials, 1968, pp. 187-210.
[6] Baboian, R. and Haynes, G. S., *Materials Performance,* Vol. 14, 1975, p. 16.
[7] Baboian, R. in *Localized Corrosion—Cause of Metal Failure ASTM STP 516,* American Society for Testing and Materials, 1972, pp. 145-163.
[8] Baboian, R. and Haynes, G. S. in *Corrosion in Natural Environments, ASTM STP 558,* American Society for Testing and Materials, 1976, pp. 171-184.
[9] Baboian, R. in *Galvanic and Pitting Corrosion, ASTM STP 576,* American Society for Testing and Materials, 1976, pp. 5-19.
[10] Pourbaix, M., Klimzack-Mathieiu, L., Mertens, C., Neunier, J., Vanleugenhaghe, C., DeNuncky, L., Laverys, J., Neelemens, L., and Warzee, M., *Corrosion Science,* Vol. 3, 1963, p. 239.
[11] Pourbaix, M., *Corrosion,* Vol. 26, 1970, p. 431.
[12] Defranoux, J. M., *Corrosion Science,* Vol. 3, 1963, p. 75.

T. R. Shaw[1]

Corrosion Map of the British Isles*

REFERENCE: Shaw, T. R., "**Corrosion Map of the British Isles,**" *Atmospheric Factors Affecting the Corrosion of Engineering Metals, ASTM STP 646,* S. K. Coburn, Ed., American Society for Testing and Materials, 1978, pp. 204-215.

ABSTRACT: This paper describes a simple and reliable methodology by which the effects of atmospheric corrosion can be measured, and developed into a corrosion map. The use to which such information can be applied to provide savings in design, materials, selection of protective finishings, and maintenance expenditure of such finishings is discussed.

KEY WORDS: atmospheric corrosion, regression analysis, corrosion, grids, meteorological charts, galvanized steel, zinc, weather stations, cost analysis

In 1964, following reports of early failure of steelwork protective coatings, investigations by the Central Electricity Generating Board (CEGB) included the comments that the effects of atmospheric corrosion were more widespread than had been expected and that, near to industrial areas—particularly leeward areas—, relatively high-corrosion rates were measured in apparently rural surroundings.

This statement indicated that if these effects could be measured in a manner which would provide information that could be readily interpreted, such information would be of considerable assistance in determining the protection and long-term maintenance requirements of such steelwork. Having decided that this was practical, the method of providing this information was considered best obtained by exposing test specimen units similar to the lead peroxide method described in British Standard 1747.[2]In view of the exposure program planned, this method, which relies on a very detailed and careful stripping and analysis procedure following exposure, was considered unsatisfactory. A simpler, but equally reliable substitute was required. Reference to the work of Hudson and Stanners,[3] Schikorr

---

*Original experimental data were measured in U.S. customary units.

[1] Member, Central Electricity Generating Board, London, England.

[2] British Standard No. 1747, Part 4, "Methods for the Measurement of Air Pollution, Lead Dioxide method," British Standards Institution, London, 1969.

[3] Hudson, J. C. and Stanners, J. F., *Journal of Applied Chemistry* (*London*), Vol. 3, 1953.

and Wasserman,[4] and, of more recent date, Guttman and Sereda,[5] suggested that zinc, in a suitable quality and form, should be investigated and a pilot exercise developed to substantiate performance.

The characteristics of this material are well known as having unusually good atmospheric resistance in pure air, due to the formation of protective films. These films are prevented from forming if the surrounding atmospheric conditions decrease the amount of pure air available, which becomes particularly significant when the climatological and meteorological conditions maintain the surface of the zinc in a damp condition. The loss of the protective film and the consequent corrosion of the zinc then takes the form of a uniform metal loss.

Pilot Exercise

As the purpose of the pilot exercise was to evaluate the zinc reference method, the identification of any particular factor contributing to the cause of metal loss was ignored. Nicholson[6] had previously established good correlation from zinc in the quality and form used in the production of Size U 2 dry battery cells (see Table 1). The cells, being in the form of a can, are produced under very close material and dimensional control and are available in quantity and at low cost. Four hundred cans were obtained from a batch produced under a single production control. After receipt the cans were cleaned in a tri-chloroethylene vapor bath, washed in hot dis-

TABLE 1—*Details of Size U 2 dry battery cells.*

	SIZE
Outside diameter	31.2 to 31.5 mm
Wall thickness	0.355 mm
Length	63.5 mm
Surface area	62.5 cm^2
	COMPOSITION, %
Cadmium	0.07 (max), 0.04 (min)
Lead	1.0 (max), 0.08 (min)
Iron	0.007 (max)
Copper	0.005 (max)
Tin	0.005 (max)
Zinc	remainder

---

[4] Schikorr, G. and Wasserman, G., *Metallkind*, Vol. 2, 1949.

[5] Guttman, H. and Sereda, P. J. in *Metal Corrosion in the Atmosphere, ASTM STP 435*, 1968, pp. 326-359.

[6] Nicholson, H. L., "Measurement of Air Pollution; Corrosion Rate of Zinc Related Lead Dioxide," Publication CR. 288 (AP), Ministry of Technology, Warren Spring Laboratory, Stevenage, Herts., England, 1969.

tilled water, dried, applied with identification numbers, weighed, and packed in individual heat-sealed plastic bags. At no time were the cans contaminated by hand contact.

The sites selected for mounting the cans were nominated overhead line electricity supply support towers of angle-section galvanized steel construction. The cans, one at each corner to avoid tower screening effects, were mounted on a neoprene plug secured to a round, permanent magnet affixed to the steelwork at approximately 5 m (16 ft) above ground level (see Fig. 1). Figure 2 shows locations of exposure sites of the cans, referring to the can reference number.

The cans were placed in position at various times between December 1965 and June 1966. Retrieval commenced as soon as possible after the 12-month exposure in each case, and 382 cans were retrieved. Correlation of zinc losses for the four cans of each set was very good, and the different sets adjacent to each other or at a distance indicate the ability of the units to react to changes in a particular corrosion environment (see Table 2). Immediately following retrieval, the zinc cans were cleaned by mild agitation in a solution of 10 percent acetic acid and hot distilled water, for a period commensurate with removal of all surface contamination, dried as previously, and reweighed; results are expressed as zinc loss in mg/100 cm^2.

In addition to the foregoing, a number of selected sites with complete climatological and meteorological recording and measuring facilities were established under control conditions (Fig. 3). Results obtained were corroborated with the information provided from the transmission tower sites where similar climatological and meteorological information could be obtained and where topography and prevailing industry, or domestic conurbations, were similar.

The overall results established the zinc can as a satisfactory method of providing the information required, and confirmed the earlier report and conclusions referred to by the CEGB in 1964. Consequently, it was arranged to transfer the further development of the work, under the author's initiation, to the Construction Industry Research and Information Association as a project for providing a corrosion map of the British Isles. Obviously, the number of measuring sites would have to be increased considerably, and essential to the project was the obtaining of related climatological and meteorological information; the following describes how this was achieved.

The Corrosion Map Project

Over a number of years, stations have been established in the British Isles for the purpose of observing, recording, and measuring climatological and similar conditions. They are defined as follows, and the number of stations as of 1968 are shown in parenthesis.

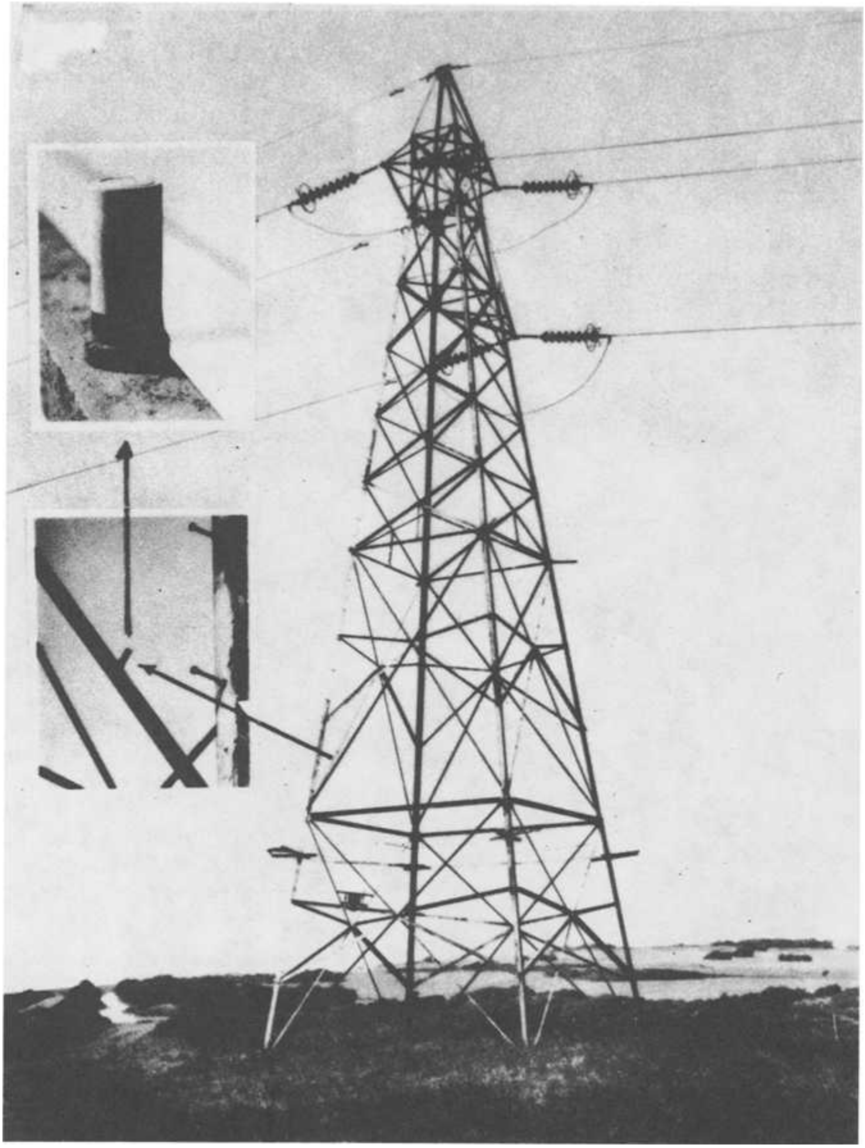

FIG. 1—*Overhead line electricity supply support tower. Bottom inset and arrow shows plug location on tower. Top inset shows position of mounted plug.*

Observatories (2)

These stations maintain continuous records of all meteorological elements and are staffed by meteorological office personnel.

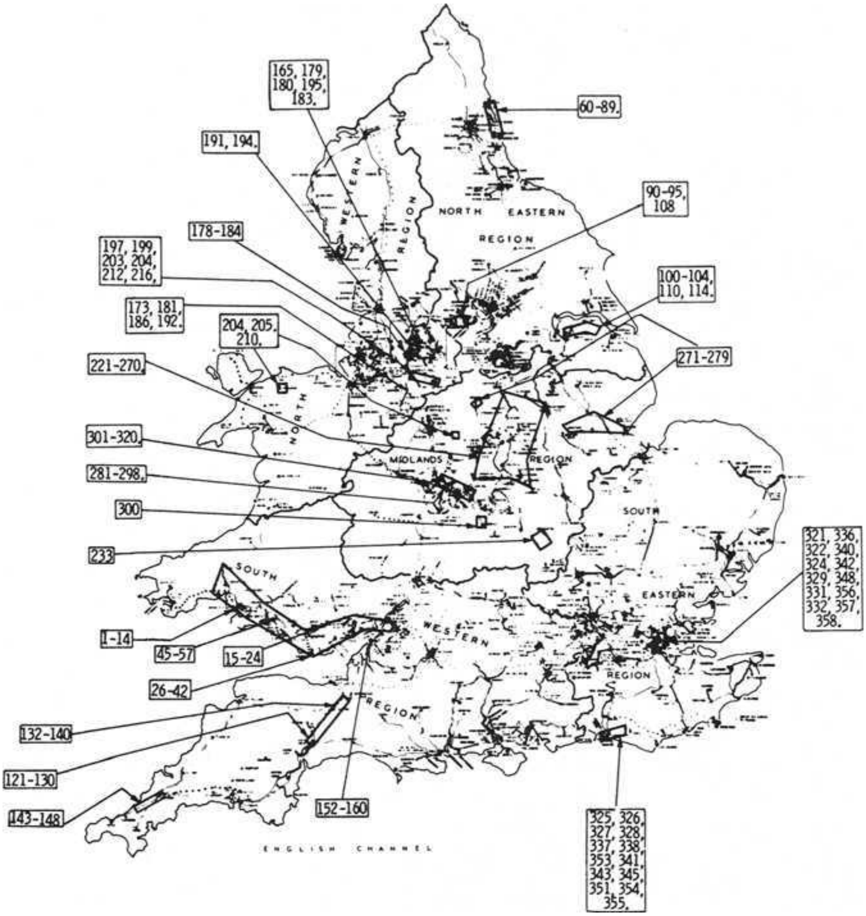

FIG. 2—*Map showing exposure site locations of towers. Reference numbers of cans at each site appear in blocks.*

Synoptic Stations (125)

The observations from these stations are primariily used in preparing synoptic charts for weather forecasting, but climatological returns are made also. These are of two types: stations manned by meteorological office personnel, and auxiliary stations manned by coastguards, lighthouse keepers, etc.

Climatological Stations (345)

These stations record observations made daily at 09.00 h GMT (and at other times also at certain stations), of maximum and minimum temper-

TABLE 2—*Standard zinc reference units—test sites.*

Serial No. of Can	Date Mounted	Preexposure Weight, g	Retrieval Date	Postexposure Weight, g	Zinc Loss, g	Site Location	National Grid Reference	Remarks
321 A through D	June 1967	15.575	12 May 1968	15.337	0.238	transmission line, PLM		
		15.864		15.634	0.230	tower no. 6		
		15.626		15.394	0.232	Northfleet, Kent		
		15.542		15.306	0.236			
132 A through D	30 Jan. 1966	16.466	1 July 1967	16.370	0.096	transmission line, E		
		16.242		16.120	0.122	(Exeter-Main)		
		15.872		15.746	0.126	tower no. 61		
		15.876		15.750	0.126	Taunton, Dorset		
90 A through D	1 March 1966	16.496	1 June 1967	15.785	0.711	transmission line, ZP		
		16.322		15.596	0.726	tower no. 46		
		15.846		15.132	0.714	Elland, South Yorkshire		
		16.242		15.520	0.722			
204 A through D	1 Jan. 1966	16.520	1 July 1967	16.038	0.482	transmission line, EA		
		16.462		15.983	0.479	tower no. 2		
		16.274		15.796	0.478	Dolgarrog, N. Wales		
		16.444		15.966	0.478			

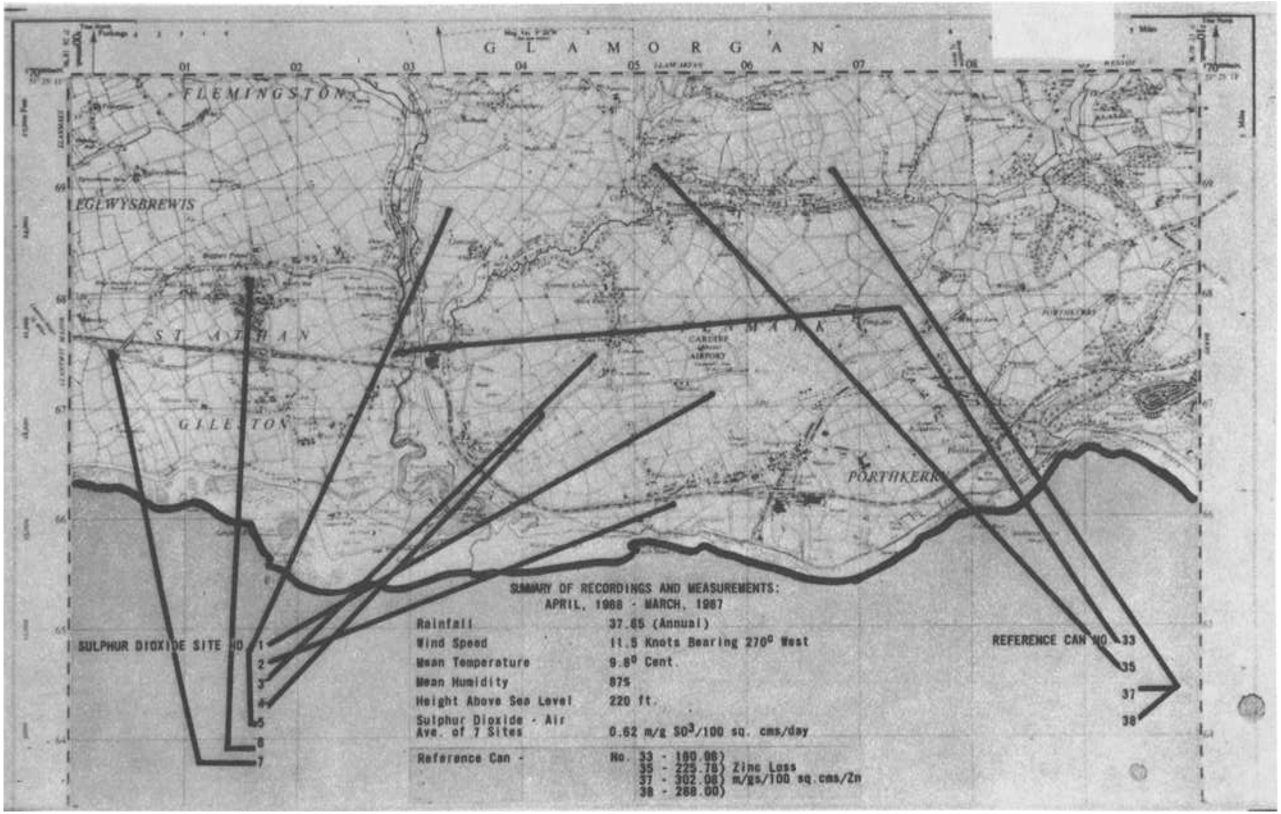

FIG. 3—*Map showing exposure sites in one of the locations selected for complete climatological and meterological observations and recordings.*

ature (wet and dry bulb), wind, cloud amount, daily rainfall, and weather. Observations of visibility and records of sunshine are commonly made at these stations as well.

Agricultural/Meteorological Stations (93)

These are climatological stations, participating in a scheme inaugurated by the Ministry of Agriculture, Fisheries, and Food and the Department of Agriculture for Scotland, in cooperation with the meteorological office.

Anemograph Stations (115)

These stations provide summaries of wind speed and direction, which are published in Table II of the monthly weather report.

Health Resort Stations (52)

These are climatological stations cooperating with the meteorological office under a health resort scheme. They make observations at 6 p.m. clock time (and also, in some places, at 9 a.m. clock time, when this differs from 09.00 GMT), and these are reported to the meteorological office for communication to the national press.

Atmospheric Pollution (629)

These stations provide daily observations of smoke and sulphur dioxide and the results are published in an annual summary for each year ending 31 March. The information processed by these stations is prepared mainly for particular purposes, and, while it is possible to relate them, they are independent of each other although, obviously, various forms of interchange of information are made.

By March 1968 a liaison had been established and the cooperation of the responsible authorities of the aforementioned recording stations obtained to expose one or more zinc can reference units in similar positions to their own recording or measuring positions. In addition, approval was obtained from other authorities, such as research centers, colleges, schools, etc.,—preferably where some form of climatological or meteorological apparatus was in use—to accept the receipt of a unit, supervise erection, and be responsible for its care and maintenance. The combined results produced 3182 measurement points, each precisely identified as to its name location as well as by its detailed national grid map reference (Fig. 4).

Sufficient zinc cans were obtained and processed in the same way as described in the pilot exercise, except that the method of mounting was altered to a flanged, unplasticized poly(vinyl chloride) cylinder of rigid

REGION	MOUNTING DATE	RETRIEVAL DATE
Midland Region	June, 1966	July, 1967

Tower Reference Line H.M. Tower 60	Reference Unit No. 253, 254 and 255	National Grid Reference 43:1.421 and 481	Pre-Exposure Weights 15.8467., 15.9012 and 15.8234 grammes Post Exposure Weights 15.6520., 15.7088 and 15.6315 grammes

Rainfall (Annual)

Measuring Point	National Grid Reference	Amount	Period
Watnall Meteorological Office	43-503-456	36.47 ins.	1966

Wind Speed and Direction

Measuring Point	Speed in Knots	Bearing	Compass Bearing
09.00 a.m. Watnall	8.02	SW	225

Height Above Sea Level	
385 ft.	Mean Temp: & Humidity: (Dry Bulb) 8.8°C. 87% Location of Meas: Point: Watnall 09.00 a.m.

Nearest Daily Lead Dioxide Gauge m/grms/SO^3/100 cms/day

Measuring Point Nottingham (Bulwell)

National Grid Reference 43-540-450

Av. Daily Mean Summer 0.8

Highest Daily 2.0 (November 1967)

Av. Daily Mean Winter 1.4

Av. Daily/Year 1.10

Topographical and General Information:

Tower No.60 on the Spondon-Annesley 132kV line, is situated North-West of Heanor, near to the A.6007 road at Loscoe. The surrounding area is undulating country, with no outstanding physical features. The area is a mining and semi-industrial region, with large engineering works at Butterley (Ripley) and Stanton Ironworks located some six miles to the South-East. Other industry consists of Nylon and Hosiery factories at Ilkeston and Heanor and a small Smelting works at Riddings.

Rainfall, wind speed and direction and temperature figures are expressed as the average for 1966, no later figures being available.

FIG. 4—*Information sheet on 1 of 3182 measurement points where zinc can reference units were mounted.*

construction. The only instruction for mounting the unit was that it should be in free air space, at a distance of 2 to 5 m (6 to 16 ft) above ground level and secure from vandalism. All cans were dispatched to exposure locations by June 1969. The initial exposure period was two years, and can withdrawal commenced in June 1971. Instructions for withdrawal included a replacement can for the next two-year period.

Results of the total four years (16 climatological/meteorological seasons) have been averaged into 10 scales of regression, the averages themselves being the individual average of each 10-km^2 area. Presentation is effected by completing an appropriate National Grid Map section as a transparency. By this means the regression values can be placed over any similar section map drawn to equal scale which itself may relate to other information, such as population densities, topography, industrial conurbations, humidity levels, rainfall, etc. This allows a comparative study and appreciation of the factors contributing to the atmospheric pollution/corrosion scenario.

Application of Information from the Corrosion Map

Following extensive investigation and research, considerable information has been made available from many sources on the corrosion effects of the atmosphere, where to reach a defined pass or failure criteria materials and surface protection systems have been exposed for differing periods at sites selected for their rigorous atmosphere and ability to provide results on a better-or-worse principle, generally expressed in terms of time.

These results only become practically useful if the environmental conditions during the time of exposure are known, and if they can be compared with similar conditions obtained elsewhere. Consequently, it is desirable to take account of the conditions prevailing at the exposure test site during the period of test. This can be done by exposing one or more zinc reference units and, at the conclusion of the tests, expressing the results in the form of zinc weight loss. Comparison of these losses, with those established by the corrosion map will indicate the suitability for service in a particular regression zone. As the corrosion map reference is limited to every 10 km^2, it may be insufficient in areas of high-density building, or where other causes of high localized environmental contamination occur. In such cases mass exposure of reference units can be made prior to the erection of the structure or building and the results assessed accordingly. A similar scheme was used in the case of the steelwork proposed to be erected for the electrification of the main line railway system between Newton-Le-Willows, Lancashire, England, and Glasgow, Scotland, some 148 km (240 miles). In this case, a reference unit was positioned at every mile post of the route and the results used to establish the relative benefits of surface-protecting the steelwork, to provide a maintenance-free period of 30 years at any part.

The economic benefits of this are considerable, when considering the recurring labor costs in the upkeep of present structures in similar duty areas. As an example, in the following section the regression value R is introduced into conventional discounting techniques for assessing the capital cost of steelwork protective systems.

Corrosion Prevention—Cost

The capital cost of protective systems and their maintenance costs are frequently assessed by discounting techniques. The net present value (N) represents the money that must be set aside now to cover both the capital and maintenance costs over the total life required. The protective system showing N to be a minimum would be normally chosen and expressed as

$$N = C + \frac{M_1}{(1 + r)^{P_1}} + \frac{M_2}{(1 + r)^{P_2}} + \ldots \qquad (1)$$

where

C = capital cost of the protective system,
M_1 = cost of maintenance in the year P_1,
M_2 = cost of maintenance in the year P_2,
r = discount rate (for example, 35 percent on capital for the CEGB, written as 0.35),
P_1 = number of years to first maintenance, and
P_2 = number of years to second maintenance.

To allow for inflation, the maintenance costs at present day value (M) should be inflated at an interest rate r_1, that is

$$N = C + \frac{M(1 + r_1)^{P_1}}{(1 + r)^{P_1}} + \frac{M(1 + r_1)^{P_2}}{(1 + r)^{P_2}} \ldots$$

For galvanized steel structures the number of years to the first maintenance (P_1) may be expressed as

$$P_1 = \frac{10\,(Z - 150)}{R} \qquad (2)$$

where

Z = galvanized coating weight of the structure (g/m^2),
150 = minimum residual level of zinc (g/m^2) before reprotection,
R = regression value (mg/100 cm^2/year), and
P_2 = P_1 + maintenance system life (protection cycle).

From Eqs 1 and 2 an increase in the galvanized coating weight (Z), although increasing the capital cost of the protective system, reduces the maintenance costs by extending the value P_1. Similarly, where other protection systems or an alternative material may offer a better P_1 value, this value should be established in the same manner as in Eq 2, and the respective N values compared.

Conclusion

It follows from the information provided that the establishment of the regression value provides an important and previously omitted value in calculations used when optimizing material and maintenance life cycle costs. It may also become important, supplementing the more conventional approach, when calculating energy economy in material manufacture, as many industrial products can nowadays be made from any one of a range of available materials. In most cases selection of materials is resolved by the appropriate design/stress loading factors; the designer may add some factor which provides for a "corrosion allowance," which in many cases is in addition to the factor of safety allowance already calculated into the design. Often the result is a severe overdesign and an accumulated misuse of materials/energy costs. The opposite does occur, and the corrosion allowance, if provided, can frequently be too little for the type of material selected, its design, and its subsequent protection. It is suggested that either of such occurrences can benefit from predictions of corrosion life style of the material. Such intelligence can be applied easily and cheaply using the method described in this paper, and is in no way different from the designer providing himself with the more conventional sort.

Acknowledgments

The author acknowledges the support given to the work involved in the establishment of the Corrosion Map of the United Kingdom by the Construction Industry Research and Information Association, London, England.

Summary

It was our thought that in assembling the papers for this Golden Anniversary Symposium, we could offer a cross section of subjects that would include the commonly used metals that see outdoor service in a variety of structural applications and environments. It was also our desire to obtain papers that would investigate means for shortening the time-consuming field exposure test, as well as papers that demonstrate a dependence upon the invaluable data already obtained by means of such tests. Finally, it was useful to include the results of a laboratory investigation to find a solution to an environmentally created corrosion problem that would ultimately function in the outdoor environment. We believe that the papers assembled herein fulfilled that criterion. Furthermore, each of the papers represents a useful building block in our attempt to understand the nature of the atmospheric corrosion process as it affects each of the metals described herein.

Sereda, of the National Research Council, Ottawa, reported that the length of time a metal is wet plays a role in the extent of its corrosion; efforts at developing instrumentation to follow this phenomenon have continued ever since. Grossman, in his attempt to utilize the instrumentation developed by Sereda, examined the phenomenon of atmospheric condensation at night as it relates to the radiation of objects warmed by the daytime sunlight. Grossman reported that the temperature of a steel panel facing the sky and supported by a polyurethane-insulated backing was some $-9°C$ (16°F) cooler than the ambient temperature. He indicated that at 70 percent relative humidity, a 10-deg difference in temperature could result in condensation of moisture on a metal surface. Grossman indicated that in Miami, Florida, the combination of sunlight, temperature, and clear nights permitted the development of useful data in two thirds the time required in more northerly locations.

To establish the significance of time-of-wetness, Grossman exposed an isolated panel of zinc on a test rack. He exposed another panel with an insulated plywood backing, 1.5 cm (½ in.) thick. A third zinc panel was made the top face of a hollow black box. Using the time-of-wetness for the isolated panel as unity, he found that the panel on the hollow box was wet 1.6 times longer than the isolated panel, and the panel with the plywood backing was wet 2.2 times longer. The significant conclusion derived from this test is that the time a metal surface is likely to be wet by atmospheric condensation is related to the type of structure to which it is attached.

By the use of regression analysis, Grossman also analyzed the time-of-wetness data obtained from an earlier ASTM exposure test performed at different locations. Relationships that called attention to the importance of sulfur oxide levels and temperature as significant contributors to the overall corrosion process were discussed.

Baboian assembled the data and prepared the report describing an ASTM-sponsored, galvanic-couple study involving magnesium alloys. This report represents the culmination of a 22-year galvanic corrosion exposure test involving the coupling of two magnesium alloys with a number of dissimilar metals and alloys. Exposures were at rural State College, Pennsylvania, the marine 240-m (800-ft) lot at Kure Beach, North Carolina, industrial New York City, and the tropical Panama Canal Zone. A unique couple design was utilized wherein two disks of the test alloy and two of the dissimilar metal, each of decreasing diameters, sandwiched one another—the whole being clamped together by an insulated stainless steel cap bolt. Some 1440 couples were prepared so that there were quadruplicate specimens of each type exposed, and enough to permit three removals. The first removal was after 30 months exposure. The test was then neglected some 20 years until 1972, when the final removal was made. Only the rural and marine exposure specimens were found.

The findings indicated that in a marine environment, both magnesium alloys were anodic to aluminum and zinc, as well as to the more noble iron, brass, nickel, and stainless steel specimens. Interestingly, the same anodic relationship was found to hold true in the rural atmosphere of State College. The order of magnitude of the losses would not suggest structural danger, should these magnesium alloys be structurally involved. Another facet uncovered was that the metals stood in the same relationship to one another as related to their inducing galvanic attack of a magnesium alloy, and as indicated by their potential measurements in seawater. Thus, development of a galvanic series was effected.

Haynie et al were engaged in a systematic study to assess the importance of a number of atmospheric variables on the corrosion rate of ferrous and nonferrous materials utilizing laboratory instrumentation. Through the construction and operation of a "controlled environmental exposure chamber," they attempted to create conditions simulating certain environmental locations. The purpose was to assess the direct and synergistic effects of certain air pollutants. The test consisted of exposing a proprietary high-strength, low-alloy steel and galvanized steel to an environment containing controlled levels of sulfur dioxide, ozone, and nitric oxide. Statistical design techniques were used in the selection of the experiments, such as high and low levels of the aforementioned gases at 50 and 90 percent relative humidity. The specimens were exposed to programmed dew/light cycles involving 20 min of light (heat) and 20 min of condensing conditions.

An empirical equation was derived on the basis of the weight loss data to account for the levels of corrosion found. The key finding was that the extent of corrosion could be related to the square root of the sulfur dioxide concentration and the square root of the time of exposure.

Examining the field data from six cities for the proprietary high-strength, low-alloy steel, and correlating it with the data from the test chamber, suggests that oxidants, such as ozone, etc., exert an inhibiting effect. The chamber data for ozone showed no influence as an accelerator nor as an inhibitor. In the study with galvanized steel, both relative humidity and sulfur dioxide were found to play significant roles.

The authors indicated this technique permitted them to identify some of the principal causes or factors responsible for the corrosion of steel through the empirical function they developed.

Smith points out that owing to their generally good resistance to attack in a variety of natural environments, it is difficult to readily evaluate the anticipated performance of new copper-base alloys. To assist in an alloy development program, an accelerated corrosion test was devised to compare new alloys with existing commercial copper-based compositions.

Using a 4 cycles/h system involving 4 min of spraying specimens that are inclined at a 30-deg angle with a 0.05 percent solution of sodium bisulfite adjusted to a pH of 4.75, followed by a drying period of 11 min using air at 50°C, he finds that in 11 days he achieved results after 1050 cycles equivalent to those developed during 3 years' exposure in New York City. Smith claims that the "rain box" he describes and the results he achieved in the way of visual, electrochemical, X-ray, Auger, and SEM measurements on new, as well as on commercially available alloys, compared well with the results obtained by exposing the same compositions in the urban industrial environment of New York City.

Normally, the protective adherent cuprous oxide films which initially form are converted to basic sulfate, basic carbonate, or oxychloride, depending upon the environment. It was proposed to insert these ions into the artificial environment to stimulate protective film formation and determine how well the new alloys perform. An important observation was made which indicates that while sulfur dioxide promotes corrosion activity, little sulfate, sulfite, or sulfide appear in the bulk film. It is believed these ions are leached out during the "rain cycle," if they are formed at all. The author indicates that the linear polarization resistance is a satisfactory measurement from which to infer atmospheric corrosion resistance and, therefore, the rain box is capable of generation of representative oxide films in a reproducible manner.

Our host at State College all of these years has been Pennsylvania State University. It was appropriate to receive a report of the results of an investigation of an unusual corrosion problem wherein the atmospheric sulfur oxides play a key role. Marx, Bittler, and Pickering reported that the corrosion of a basis metal, and the diffusion of its ions through the more noble metal overplate, is a serious problem in the miniaturization of electronic devices and components. When the ions reach the surface they react with the sulfur oxides in the atmosphere to form a metallic sulfide which increases electrical contact resistance and can result in short circuits. Intermediate films have been inserted between the substrate copper and the gold overplate to inhibit the diffusion of copper ions through the gold. Rods of copper were plated with barrier metals, such as platinum, palladium, rhodium, and chromium, as well as cobalt and nickel, and their alloys. Gold then was plated on each of these to a depth of 100 μm. Low temperature anneals at 100 to 175°C were conducted for 18 months; high temperature anneals at 400 to 550°C were conducted for 12 to 55 h. X-ray and microprobe analyses were conducted on all surfaces. The analyses show that for the 400 to 550°C range, cobalt and the cobalt-5 weight percent phosphorous alloy is the most effective barrier. At the lower temperature range it was found that diffusion of copper through the gold was dependent upon the grain size of the gold. The unusual performance of gold at these low temperatures constitutes the discovery aspect of this research.

Because of the worldwide deployment of military equipment in a diversity of environments, and the fact that electrical, structural, and other design criteria may dictate the use of dissimilar metal couples, it was necessary for the authors to initiate a study to yield information concerning the corrosion tendencies of specific metal couples in tropical atmospheres, in soil and in seawater. Pelensky and his colleagues initiated an extensive exposure test in the Panama Canal Zone involving AISI 4340 carbon and Type 316 stainless steels, together with two aluminum alloys, a magnesium alloy, brass, Monel 400, and a titanium alloy. The 5-year test involved periodic monthly removals with this interim report indicating some of the tendencies detected.

A portion of their data can be compared with those developed earlier by Southwell et al in their 16-year study in the same location. Their most significant observation is that stabilization tendencies appear to develop after the first 2-to-6-month exposure. Among other findings was the fact that when two different aluminum alloys were coupled to magnesium, one of them experienced considerable attack owing to the strong alkaline environment created as a consequence of the cathodic protective action of the magnesium. This could hardly be anticipated by design engineers familiar only with the electromotive series, nor by some corrosion engineers unfamiliar with such experimental data. The authors have shown that owing to the vagaries involved in the conduct of tests, one often cannot accept data from other published tests wherein the test conditions may not be equivalent to those from which information is desired.

German reported that in the early 1960s the Noranda Research Centre was requested by the Department of Highways of the Province of Quebec to determine why some electrogalvanized highway posts had rusted after only a short period of service. Steel test coupons were galvanized by the continuous, hot-dip, and electrogalvanizing methods. The respective coating thicknesses were 88.9, 45.7, and 25.4 μm (3.5, 1.8, and 1.0 mils). Additional coupons of carbon steel were primed and painted with 25.4 μm (1 mil) of guardrail paint. Galvanized steel coupons were painted with the same paint. The test specimens were then exposed on major highways in Ontario and Quebec, in both urban and rural environments, for periods of 5 to 7 years.

At the conclusion of the 5-year test, the 25.4-μm electrogalvanized coupons had lost almost all of their zinc. The hot-dip galvanized specimens were in good condition in both provinces. Examination of the painted carbon steel coupons revealed failure; however, the painted galvanized steel specimen continued to perform well. It was estimated that the continuous hot-dip specimens, with a zinc coating of 45.7 μm should have a service life of 9 years, and the batch-type, hot-dip coupons, with a coating thickness of 88.9 μm should serve effectively for 17 years. The thin coating that was applied by electrogalvanizing performed as expected for a film thickness of only 25.4 μm. The synergistic performance that one can expect from the painted galvanized steel coupons can result in a considerably extended service life, beyond that of the individual paint life on steel, and the zinc coating life based on film thickness. This work supplies confirmation in a Canadian environment for what has been reported from isolated ASTM tests in different environments in the United States.

Legault and Pearson evaluated the separate effects of atmospheric corrosion on the skyward and groundward surfaces of galvanized steel test specimens exposed to both a marine and an industrial environment. The purpose of this study was to isolate the effects of deposited solids, condensed moisture, and rainfall on the skyward surface, as opposed to the residual effects of condensed moisture and deposited solids on the unwashed, sheltered, groundward surface.

The authors exposed sandwiched specimens for 5 years on exposure racks inclined 30 deg to the horizontal. They found the skyward surface lost more weight than the groundward surface in both environments; however, the losses were considerably greater—sometimes twice as great—in the industrial environment. They found, too, that the skyward surface lost weight at a linear rate; this was not the case for the groundward surface. This observation was not noted by other investigators because the recorded weight loss was a combined figure.

Regression analysis of the data was utilized, as were three-dimensional graphs. The authors concluded that atmospheric corrosion can be described by the general kinetic relationship: $\Delta W = Kt^N$, wherein W is the annual weight loss, t is the exposure period in years, and K and N are empirically determined constants. Values of K and N indicate, respectively, the short- and long-term susceptibility to atmospheric attack. Such an equation permits an assessment of contributions made by alloying elements and changes in the environment. The application of such experimental techniques and empirically determined equations should assist in characterizing the relative corrosion resistance of a new alloy as well as the corrosiveness of an environment.

The report on thermal spraying by Longo and his colleague represents the results of one of the longest atmospheric exposure tests on a heretofore uncommon technique. It is anticipated, however, that with these data now available, considerable use of this technique should be forthcoming. The paper reports on a 19-year exposure test of steel panels that were thermally sprayed with several different coating thicknesses of aluminum and zinc and placed on test in a number of ASTM exposure sites around the country. The program was initiated in 1953 by the Committee on Metallizing (now the Committee on Thermal Spraying) of the American Welding Society. Some 2124 aluminum panels and an equal number of zinc panels were exposed to several different industrial and marine environments and were immersed in seawater as well. The film thicknesses ranged from 76.2 to 381 μm (0.003 to 0.015 in.). Some of the coatings were sealed with an organic formulation to protect subsurface pores. Clear vinyls, aluminum-pigmented vinyls, and a chlorinated rubber formulation were used as sealants.

It was learned that thin aluminum coatings (76.2 to 152.4 mm) both sealed and unsealed, give complete base metal protection in all environments. Unsealed zinc coatings require a 304.8-μm (0.012-in.) coating to afford complete protection in seawater. In the industrial and marine atmospheres, 228.6-μm (0.009-in.) unsealed zinc, or 76.2 to 152.4-μm sealed zinc panels, were necessary for 19-year protection. This long-term exposure test indicates that thermally-sprayed aluminum and zinc provides a new means to extend the service life of steel structures in a variety of industrial and marine environments, from mild to moderately severe.

Electroplating of zinc die castings is used extensively for atmospheric protection and for decorative purposes. Payer and Safranek recognized that automotive applications consume a considerable quantity of plated die castings and decided to evaluate experimental plating compositions under more than one type of service condition. In addition to static exposure test sites in Detroit, Michigan, and Kure Beach, North Carolina, they elected to mount specimens on trucks traveling through areas employing deicing salts and cinders. They also placed specimens on a New York Harbor tugboat to incorporate a vibration factor. The tugboat environment was rated the most severe, followed by that of the trucks; the Detroit rooftop environment was found to be mildest. The authors have been continuously engaged in these studies since 1963, and some 3000 specimens have been prepared and exposed so far.

Among the most significant findings of the current study was that application of microdiscontinuous chromium is the most influential factor for improving corrosion resistance under the most severe conditions. It produced a 30 percent reduction in nickel thickness in the intermediate coat and a thinner chromium top plate. Vibration was a useful adjunct in the testing as it was found to contribute to flaw formation in a crack-free chromium coating, which resulted in increased corrosion. The authors concluded that use of the mobile test units permitted them to obtain in 3 years results that would have required 10 years at static exposure sites.

Fitzgerald deals with aesthetic effects of the atmosphere on the appearance of copper in architectural applications. Numerous efforts have been made to accelerate patina formation. Studies begun at the University of Utah in 1966 sought reagents that would react with copper to produce the characteristic adherent, colored films seen on old copper roofs. Initially, oxidizing reagents were used to produce the initial cuprous oxide film. By adding copper sulfate, the brochantite film ($CuSO_4 \cdot 3Cu(OH)_2$) was formed. Since then the 20-day process has been reduced to 4 days. Large sheets were treated and exposed in Canada and on the East Coast of the United States. These artificially patinated surfaces do not perform well in arid climates and climates that produce acid condensate around pH 1; however, they do perform well in the more moderate urban climates.

The use of benzotriazole derivatives incorporated into a lacquer has proven quite successful, as has the use of a clear, fluorinated, polymer laminate, 25.4 μm thick. The successful weatherometer and salt spray tests have been indicative of the success attained by specimens exposed in Arizona, San Francisco, and Kure Beach, North Carolina.

In summary, the author reports that the patina chemistry of 300-year-old copper structures has been artificially duplicated so as to enhance the architectural use of copper and its alloys.

Baboian et al report that it requires from 4 to 7 years for a copper roof to develop the coloration that will remain with it. The authors review the results from ASTM tests, and from copper roofs 22 and 65 years old exposed in industrial locations. The relatively low corrosion rates noted encouraged them to develop copper-clad products called laminar composites. This combination permitted them to merge the strength of stainless steel together with the appearance and corrosion resistance of copper. Their intent was to provide information on the galvanic effects at cut edges of the composites and at pores in the copper cladding.

Test panels were exposed at nine exposure sites, with observations made periodically for up to 7.5 years. The factors observed dealt with pore formation in the cladding, galvanic pitting, and tunneling of the sandwiched stainless steel. The results indicated that the deteriorating effects were dependent upon the nature of the environment and the choice of the stainless steel composition comprising the laminar composite. It was noted that in a rural environment, only the copper cladding was attacked, and in a marine environment, only Type 321 stainless steel was unaffected. The authors reinforced these findings through polarization measurements and by establishing the regions where pitting and crevice corrosion can begin, and, thus, justified the compositions selected for their laminar composites.

Zoccola and his colleagues attempted to meld into a new coating composition the galvanic corrosion resistance offered by galvanized steel to cut edges, and the atmospheric corrosion resistance exhibted by aluminum exposed boldly in a variety of environments. The authors performed a systematic study which resulted in the selection of a composition involving 55 weight percent aluminum, 43 weight percent zinc, and the remainder, silicon, to obtain an alloy coating for which both cut-edge corrosion resistance, and a retention of the atmospheric corrosion resistance of aluminum were achieved.

The authors performed outdoor exposure tests in addition to the usual salt-spray tests. They performed potential measurements and learned from the behavior in chloride and sulfate solutions that the system had an initial potential close to that of zinc. As time went on, however, the depleted zinc surface began to approach the more noble potential of aluminum. The surface exhibited a sensitivity toward chloride ion and a passivity toward sulfate ion. On the basis of their test, the authors claim that they have been able to meld the properties of the two metals; however, further service testing and commercial distribution is underway to establish long-term performance.

Shaw indicated that because of its proximity to rural and industrial regions, the Central Electricity Generating Board in England, required an effective means for calibrating the atmospheric corrosiveness in various parts of the country toward galvanized steel structures. To do this they exposed some 3200 small zinc cans (of the type used for small dry cells) at over 1400 locations where some form of collection of weather data was being performed. A 1-year pilot test revealed the value of this technique so that it was performed on a much larger scale over a 2-year period. On the basis of the data collected, a national grid map was prepared with readings covering every 10 km^2. Various types of data were collected and placed on transparencies. By superimposing one or more sheets of data on the grid map, one could develop a variety of useful relationships.

A similar nationwide calibration of our atmospheres might prove useful. Such information available on a geographic basis could be applied to decision-making in areas such as regulation of sulfur oxide levels and fuel quality, and selection and maintenance of construction materials.

Ailor has been investigating for some time the atmospheric corrosion resistance of a variety of aluminum alloys by techniques somewhat different than those used in evaluating ferrous metals. He has recently performed a notable service by locating, describing, and referencing every large-scale corrosion test reported in the *Proceedings* of the American Society for Testing and Materials since its inception. Much of the data were generated during a period when coal was the only commercial fuel, and sulfur oxide levels were relatively high; the results revealed relatively high corrosion rates. Contemporary data will be developed under conditions of much lower levels of sulphur oxides.

Newcomers to the field of ASTM atmospheric testing are herein introduced to the variety of problems involved in initiating such large-scale, long-term tests. Because of the size and varying climates of the country, it was possible to expose specimens in a variety of environments to determine the role of geographical factors. This report brings the reader up to date with a discussion of the most recently initiated 20-year exposure test of nonferrous metals.

The totality of information accumulated since the earliest field tests is a tribute to the concept of the mutuality of interests of producer and consumer in this country. It should stand as a living testimonial to all the volunteer workers who participated in these early tests that have become a standard for future designers of such tests.

S. K. Coburn
U.S. Steel Corporation, Pittsburgh, Pa. 15230; editor

Index

ISBN-0-8031-0286-0